Muhammad Arslan | Antimicrobials in constructed wetlands can cause in planta dysbiosis

Muhammad Arslan

Antimicrobials in constructed wetlands can cause *in planta* dysbiosis

5|2019

HELMHOLTZ
CENTRE FOR
ENVIRONMENTAL
RESEARCH – UFZ

Antimicrobials in constructed wetlands can cause *in planta* dysbiosis

Der Fakultät für Mathematik, Informatik und
Naturwissenschaften der RWTH Aachen University
vorgelegte Dissertation zur Erlangung des akademischen Grades
eines Doktors der Naturwissenschaften
von

Muhammad Arslan

aus Kasur, Pakistan

Berichter:
Universitätsprofessor Dr. Rolf Altenburger
Universitätsprofessor Dr. Henner Hollert

Tag der mündlichen Prüfung: 27.06.2019

During this study, I have learned that we as humans do not have any privilege over any biome except our capability of interference.

Muhammad Arslan

ABSTRACT

Constructed wetlands (CWs) are engineered phytoremediation systems. They comprise of the two main biotic components, namely plants and bacterial community, which work synergistically to remove a wide range of pollutants from wastewater. CWs have been used as sole treatment systems or as integrated module within other types of wastewater treatment plants (WWTPs), e.g. as tertiary treatment unit. Recent investigations have shown that WWTPs are typically not able to remove low concentrations of certain pollutants, known as organic micropollutants (OMPs). This class of pollutant is of emerging concern for ecotoxicologists because of their unknown toxic effects. A prominent category among OMPs comprises antimicrobials whose presence in the wastewater may disturb plant-microbe interplay in CWs due to the active biological nature of the compounds.

Antimicrobials are inhibitors of bacterial growth hence may inhibit the beneficial bacterial endophytes in planta.

To date, nothing is known about what consequences can arise for the plant-associated bacterial communities, mainly endophytes, upon exposure of antimicrobials. Endophytic bacteria are described as being analogous to the gut bacteria that provide health benefits to the host, i.e. phytohormones production, stress alleviation, and defense against pathogens. Therefore, any disturbance in the endophytic community that may affect the performance of plants is a subject of interest. This dissertation strives to illuminate the response of endophytic bacteria **(Chapter 2)** and *Juncus effusus* **(Chapter 3)** upon exposure of two antimicrobials, namely sulfamethoxazole (SMX) and trimethoprim (TMP). *J. effusus* (soft or common rush) is a model wetland plant and has been extensively used in phytoremediation studies; whereas, SMX and TMP are commonly found antimicrobials in European wastewaters whose harmful effects are still unknown to the *in planta* bacterial community.

This dissertation addresses response of endophytic community and Juncus effusus *to two antimicrobials.*

In two studies, repeated exposures of antimicrobials were found to decrease plant fitness in the model wetlands (tested through visual and physiological observations). Subsequently, microbiological analyses were carried out to see if the decrease in plant fitness resulted due to changes in plant microflora. In the first study, initial high concentrations of antimicrobials (10 and 100 µg/L of SMX and TMP, respectively) caused a drop in evapotranspiration (a surrogate for plant fitness) within a few days. Evapotranspiration recouped after omitting the antimicrobials, albeit to the lower values than prior exposure. After

several exposures at lower concentrations, plants became infested with insects, evapotranspiration was almost zero, and plant tissue turned necrotic. The response of the endophytic bacterial community was therefore recorded through cultivation-dependent and cultivation-independent analyses.

Culture-dependent and independent approaches revealed substantial changes in community composition, which were particularly pronounced in the roots.

Cultivation-dependent analysis illustrated an increase of the bacterial community in the post-exposure period. This increase was significantly higher in the exposed roots than the exposed shoots. *In vitro* biochemical characterization was conducted to see if there were any bacterial strains possessing plant growth promoting (PGP) characteristics. Assays confirmed that many of the isolated strains possessed a stress alleviation trait [i.e., 1-aminocyclopropane-1-carboxylate (ACC) deaminase activity], whereas some of the strains also exhibited other PGP characteristics, i.e., phosphorus solubilization, siderophore production, and indole acetic acid (IAA) formation. Cultivation-independent analysis through quantitative PCR (qPCR) revealed an at least 8-fold increase of endophytic bacteria in exposed roots as compared to the community present in un-exposed roots. Taxon-specific observations, made via both cultivation-dependent and independent analysis, revealed that Gammaproteobacteria was the dominant group, followed by Firmicutes and Actinobacteria. To test whether this new community was accepted by the plant itself or not, a study on production of reactive oxygen species (ROS) and reactive nitrogen species (RNS) was carried out in the post-exposure period when there were no antimicrobials in the system for at least three months. High ROS and RNS were detected in the exposed roots, which suggested an invasion of detrimental bacteria or opportunistic behavior of the pre-existing community. Concomitantly, fluorescent *in situ* hybridization (FISH) confirmed that Gammaproteobacteria and Firmicutes were intensively colonizing the plant root interior as biofilms were found along the inner walls of the conducting elements and aerenchyma. To develop a further understanding about the community structure, 16S rRNA gene amplicon sequencing was carried out. Results indicated that before exposure, the community composition was similar for both roots and shoots, however, the post-exposure period exhibited drastic changes, i.e., the pre-exposure community was replaced with a new community. These changes occurred mainly in the exposed roots but less in exposed shoots.

Invasion of pervasive bacteria was indicated by intensive production of reactive oxygen species (ROS) and reactive nitrogen species (RNS).

To understand how plant and bacterial community responded temporally to the presence of the antimicrobials, a second study was carried out with different experimental conditions. Concentrations of antimicrobials were increased in a step-wise manner and plant fitness was evaluated in terms

of evapotranspiration, chlorophyll fluorescence, and visual inspections. No significant change in evapotranspiration was seen until plants were exposed to 50 and 17 μg/L of SMX and TMP, respectively. Then, chlorophyll fluorescence was reduced and plants roots started turning porous and blackish. The further increase in concentrations resulted in insect infestation on exposed plant shoots. The cultivation-independent analysis (16S amplicon sequencing) revealed a dose-dependent effect on the root endophytic community. A decline in Fisher's alpha diversity index was observed up to the concentration of 50 μg/L SMX and 17 μg/L TMP. Further increase in concentrations resulted in regain in the diversity, however, coordinate analyses revealed that this improvement was not due to the recovery of the previous microbiome but rather that a new community took over the system. Thus, a change in microbial community appeared before the physiological and morphological changes of the plants. Finally, at concentrations of 100 μg/L SMX and 33 μg/L TMP, changes in the endophytic community structure were highly significant for the roots, and they were in accordance to the results of 16S amplicon sequencing made in the first experiment. Additionally, it was shown that the rhizospheric community did not change significantly. Apparently, the endophytic community is more prone to face dysbiosis as compared to the rhizospheric community.

Temporal study elucidated that endophytic community was inhibited first and then new community took over the system.

Next, to advance our understandings on plant defense/stress response in the post-exposure period, the first genomic database of *J. effusus* was developed **(Chapter 3)**. The *de novo* transcriptome assembly was previously prepared by sequencing the transcriptome of 19 genotypes of *J. effusus.* The accuracy of the assembly was tested through functional analysis with closer phylogenetic relatives of *J. effusus*. After confirming the high quality of the assembly via computational, statistical, and manual analyses, targeted investigations on specific genes involved in plant defense were carried out. It was revealed that the KEGG pathway for "plant-pathogen interaction" was almost complete, including expressed genes related to "hypersensitive response", "defense-related gene induction", and "programmed cell death". The developed database was further tested in preliminary metaproteomics, which was performed on a subset of exposed and un-exposed plant tissues. The extraction of proteins from plants in the post-exposure period were less efficient, nevertheless, pre-exposure proteins were identified to be involved in typical plant processes such as photosynthesis, biosynthesis of polyphenol compounds, and others were related to general metabolic processes such as glycolysis, citric acid cycle, cell division, oxidative

Genes involved in stress response for J. effusus *were identified for plant-pathogen interactions pathway.*

pentose phosphate pathway. The bacterial proteins matching in the post-exposure period were mostly related to the bacteria involved in oxidation of one-carbon (C_1) compounds. This observation was in accordance to the finding established at genomics scale, i.e. flux of C_1 compounds was increased in the post-exposure period. Archaeal proteins, likely from ammonium oxidizers, were only identified in the exposed roots. Although insignificant observations were made for the metaproteomics analyses, they do confirm the observations made at genomics level. Nevertheless, a major strength of this work is high quality of the database which shares extensive information on functional descriptions of several genetic features including genes involved in the plant-defence. This database is expected to open new opportunities for future *omics* studies on this plant.

ZUSAMMENFASUNG

Pflanzenkläranlagen (PKs) sind weit verbreitete Phytoremediationssysteme. Sie enthalten die beiden wichtigten biotischen Komponenten, nämlich Pflanzen und Bakteriengemeinschaft, die synergistisch arbeiten, um ein breites Spektrum an Schadstoffe aus dem Abwasser zu entfernen. PKs können als Einzelbehandlungssysteme oder als integriertes Modul in anderen Abwasseraufbereitungsanlagen eingesetzt werden, z.B. als tertiäre Behandlungseinheit. Jüngste Untersuchungen haben gezeigt, dass Kläranlagen in der Regel nicht in der Lage sind, geringe Konzentration bestimmter Schadstoffe, so genannter organischer Mikroschadstoffe (OMSs), zu entfernen. Diese Schadstoffklasse ist für Ökotoxikologen aufgrund ihrer oftmals unbekannten toxischen Wirkungen von zunehmender Bedeutung. Eine wichtige Kategorie unter den OMSs sind antimikrobielle Substanzen, deren Anwesenheit im Abwasser aufgrund der aktiven biologischen Natur der Verbindungen das Zusammenspiel zwischen Pflanze und Mikrobe in PKs stören könnte.

Antimikrobielle Mittel sind Inhibitoren des Bakterienwachstums und können daher die nützlichen bakteriellen Endophyten in der Plantage hemmen.

Bislang ist nicht bekannt, welche Folgen dies für die pflanzenassoziierten Bakteriengemeinschaften, vor allem Endophyten, nach der Exposition von antimikrobiellen Substanzen haben kann. Die bakterielle Endophyten wird als analog zu den Darmbakterien beschrieben, die dem Wirt gesundheitliche Vorteile bieten, d.h. Phytohormonproduktion, Stressabbau und Verteidigung gegen Krankheitserreger. Daher ist jede Störung in der endophytischen Gemeinschaft, die die Leistung von Pflanzen beeinträchtigen kann, ein Thema von Interesse. Diese Dissertation zielt darauf ab, die Reaktion von endophytischen Bakterien **(Kapitel 2)** und *Juncus effusus* **(Kapitel 3)** bei Exposition von zwei antimikrobiellen Substanzen, nämlich Sulfamethoxazol (SMX) und Trimethoprim (TMP), aufzuklären. *J. effusus* (Flatterbinse) ist eine Modell-Feuchtgebietspflanze, die in Phytosanierungsstudien umfassend eingesetzt wurde; SMX und TMP werden häufig in europäischen Abwässern gefunden, deren schädliche Auswirkungen der *in planta* bakteriellen Gemeinschaft noch unbekannt sind.

Diese Dissertation befasst sich mit der Reaktion der endophytischen Gemeinschaft und Juncus effusus auf zwei antimikrobielle Mittel.

In zwei unabhängigen Experimenten wurde festgestellt, dass eine wiederholte Zugabe antimikrobieller Mittel die Pflanzenfitness in den PKs des Modells herabsetzten, welches mithilfe visuellen, und physiologischen Beobachtungen getestet wurde. Anschließend wurden mikrobiologische Analysen durchgeführt, um festzustellen, ob die Abnahme der Pflanzenfitness auf Veränderungen der Pflanzenmikroflora zurückzuführen ist. Im ersten Experiment führten erhöhte Konzentrationen antimikrobieller Substanzen (10 und 100 µg/L von SMX bzw. TMP) innerhalb weniger Tage zu einem Rückgang der Evapotranspiration, welches als Indikator für Pflanzenfitness fungiert. Nach Beendigung der Exposition durch die antimikrobiellen Mittel fand eine teilweise Regeneration der Evapotranspiration statt. Weitere Expositionen mit geringerer Konzentration führte zu Insektenbefall, beinahe vollständigem Verlust der Evapotranspiration und nekrotischem Pflanzengewebe. Die Reaktion der bakteriellen Gemeinschaft wurde durch kulturabhängige und kultivierungsunabhängige Analysen aufgezeichnet.Letztere zeigte eine Zunahme der Bakteriengemeinschaft in der Zeit nach der Exposition. *In vitro* wurden biochemische Charakterisierungen durchgeführt, um festzustellen, ob es Stämme mit pflanzenwachstumsfördernden Eigenschaften (PGP) gab. Die Untersuchungen bestätigten, dass viele der isolierten Stämme über ein Stressabbau-Merkmal verfügten [1-aminocyclopropane-1-carboxylate (ACC) Deaminase-Aktivität], während einige der Stämme auch andere PGP-Merkmale aufwiesen, d.h. Phosphor-Solubilisierung, Siderophorproduktion und Indolessigsäure (IAA)-Bildung. Die kultivierungsunabhängige Analyse durch quantitative PCR (qPCR) bestätigte, dass der Anstieg der endophytischen Bakterien in den exponierten Wurzeln mindestens 8-fach höher war als in den nicht exponierten Wurzeln. Die taxonspezifische Aufzählung endophytischer Bakterien ergab, dass die Wurzeln von Gamma-Proteobakterien dominiert wurden, gefolgt von Firmicuten und Actinobakterien. Um die zugrundeliegende Annahme zu testen, dass die neu entwickelte Bakteriengemeinschaft der Pflanze selbst keinen Schaden zufügt, wurde eine Studie über die Produktion von reaktiven Sauerstoffspezies (ROS) und reaktiven Stickstoffspezies (RNS) in der Zeit nach der Exposition durchgeführt, in der mindestens drei Monate lang keine antimikrobiellen Stoffe im System vorhanden waren. Es wurden hohe ROS und RNS Signale in den exponierten Wurzeln nachgewiesen, was auf eine mögliche Invasion von Bakterien hindeutete. Gleichzeitig bestätigte die fluoreszierende in situ Hybridisierung (FISH), dass Gamma-

Kulturabhängige und unabhängige Ansätze zeigten erhebliche Veränderungen in der Gemeindezusammensetzung, die in den Wurzeln besonders ausgeprägt waren.

Proteobakterien und Firmicutes das Innere der Pflanzenwurzeln intensiv kolonisierten, während entlang der Innenwände der leitenden Elemente Schlieren oder Biofilme gefunden wurden. Um ein weiteres Verständnis über die Gemeinschaftsstruktur zu entwickeln, wurde die 16S rRNA-Genamplikon-Sequenzierung durchgeführt. Die Ergebnisse zeigten, dass die Zusammensetzung der Gemeinschaft vor der Exposition sowohl für Wurzeln als auch für Triebe ähnlich war, jedoch zeigte die Zeit nach der Exposition drastische Veränderungen, d.h. die Gemeinschaft vor der Exposition wurde durch eine neue Gemeinschaft ersetzt. Diese Veränderungen wurden hauptsächlich für die freiliegenden Wurzeln, aber kaum für die freiliegenden Triebe beobachtet.

Die Invasion von durchdringenden Bakterien wurde durch die intensive Produktion von reaktiven Sauerstoffspezies (ROS) un reaktiven Stickstoffspezies (RNS) angezeigt.

Um zu verstehen, wie Pflanzen und Bakteriengemeinschaften zeitlich auf das Vorhandensein der antimikrobiellen Substanzen reagieren, wurde ein zweites Experiment mit unterschiedlichen Versuchsbedingungen durchgeführt. Die Konzentrationen antimikrobieller Mittel wurden kontinuierlich erhöht und die Fitness der Pflanze hinsichtlich Evapotranspiration, Chlorophyllfluoreszenz und visueller Inspektionen bewertet. Es wurde keine signifikante Veränderung der Evapotranspiration festgestellt, bis die Pflanzen 50 und 17 µg/L von SMX bzw. TMP ausgesetzt waren. Dann wurde die Chlorophyllfluoreszenz reduziert und die Pflanzenwurzeln begannen, porös und dunkelbraun zu werden. Der weitere Anstieg der Konzentrationen führte zu einem Insektenbefall an exponierten Pflanzenschösslingen. Die kultivierungsunabhängige Analyse (16S Amplikon-Sequenzierung) ergab einen dosisabhängigen Effekt auf die Wurzelendophytengemeinschaft. Ein allmählicher Rückgang der Alpha-Diversität (Fisher's alpha diversity) wurde bis zur Konzentration von 50 µg/L SMX und 17 µg/L TMP beobachtet. Weitere Konzentrationsanstiege führten zu einer Zunahme der Alpha-Diversität. Hauptkomponentenanalysen ergaben jedoch, dass diese Verbesserung nicht die Wiederherstellung des vorherigen Mikrobioms war, sondern dass eine neue Gemeinschaft das System übernahm. So zeigte sich eine Veränderung in der mikrobiellen Gemeinschaft vor den physiologischen und morphologischen Veränderungen bei Pflanzen. Schließlich waren bei Konzentrationen von 100 µg/L SMX und 33 µg/L TMP Veränderungen in der endophytischen Gemeinschaftsstruktur für die Wurzeln von großer Bedeutung, und sie entsprachen den Ergebnissen der 16S Amplikon-Sequenzierung im ersten Experiment. Darüber hinaus wurde in diesem Teil der Studie gezeigt, dass sich die rhizosphärische

Zeitliche Studien erhellten, dass die endophytische Gemeinschaft zuerst gehemmt wurde und dann eine neue Gemeinschaft das System übernahm.

Gemeinschaft nicht wesentlich verändert hat. Anscheinend ist die endophytische Gemeinschaft anfälliger für Dysbiose als die rhizosphärische Gemeinschaft.

Um unsere Erkenntnisse über Pflanzenabwehr und Stressreaktion in der Zeit nach der Exposition voranzubringen, wurde eine erste genomische Datenbank von *J. effusus* entwickelt **(Kapitel 3)**. Eine *de novo* Transkriptomanordnung wurde zuvor durch Sequenzierung des Transkriptoms von 19 Genotypen von *J. effusus* hergestellt. Die Genauigkeit der Anordnung wurde durch Funktionsanalyse mit näheren phylogenetischen Verwandten von *J. effusus* getestet. Nach der Bestätigung der hohen Qualität der Anordnung durch rechnerische, statistische und manuelle Analysen wurden gezielte Untersuchungen an spezifischen Genen durchgeführt, die an der Pflanzenabwehr beteiligt sind. Es wurde festgestellt, dass fast alle Gene im KEGG-Pfad für die "Pflanzen-Pathogen-Interaktion" exprimiert wurden, sowie die mit "hypersensibler Reaktion", "abwehrbezogener Geninduktion" und "programmiertem Zelltod" zusammenhängenden Gene. Basierend auf diesen Beobachtungen wurde die entwickelte Datenbank auf ihre Eignung als Nukleinsäuredatenbank für Metaproteomik getestet, die an einer Teilmenge von exponiertem und unexponiertem Pflanzengewebe durchgeführt wurde. Die Extraktion von Proteinen aus Pflanzen in der Nachbelichtungsphase war weniger effizient, dennoch wurden Proteine identifiziert, die an typischen pflanzlichen Prozessen wie Photosynthese, Biosynthese von Polyphenolverbindungen beteiligt waren; und andere waren mit allgemeinen Stoffwechselprozessen wie Glykolyse, Zitronensäurezyklus, Zellteilung, oxidativer Pentosephosphatweg verbunden. Die Bakterienproteine, die aus der Zeit nach der Exposition isoliert und identifiziert werden konnten, waren hauptsächlich mit den Verbindungen verbunden, die am One-Carbon Metabolism (C_1)-Pfad beteiligt sind; diese Beobachtung entsprach dem auf der Genomikskala etablierten Befund, d.h. der Fluss der C_1-Verbindungen wurde in der Zeit nach der Exposition erhöht. wurden Proteine von Archaea, wahrscheinlich von Ammonium-Oxidierern wurden nur in den exponierten Wurzeln identifiziert. Obwohl für die Metaproteomanalysen unbedeutende Beobachtungen gemacht wurden, bestätigen sie doch die Beobachtungen auf genomischer Ebene. Dennoch ist eine große Stärke dieser Arbeit ist die hohe Qualität der Datenbank, die umfangreiche Informationen über funktionelle Beschreibungen verschiedener

Gene, die an der Stressreaktion auf J. effusus *beteiligt sind, wurden für den Pflanzen-Pathogen-Interaktionsweg identifiziert.*

genetischer Merkmale, einschließlich der an der Pflanzenabwehr beteiligten Gene, teilt. Diese Datenbank soll neue Möglichkeiten für zukünftige *Omics*-Studien an dieser Anlage eröffnen.

CONTENTS

LIST OF FIGURES

LIST OF TABLES

ABBREVIATIONS

1-aminocyclopropane-1-carboxylate deaminase	ACC deaminase
Analysis of similarity	ANOSIM
Benchmarking Single-Copy Ortholog genes	BUSCO
Biochemical oxygen demand	BOD
Chemical oxygen demand	COD
Chrome azurol S	CAS
Clusters of orthologous gene	COG
Confocal laser scanning electron microscope	CLSM
Constructed Wetlands	CWs
Database for annotation, visualization and integrated discovery	DAVID
Enzyme commission	EC
European Union	EU
Fluorescent *in situ* hybridization	FISH
Gene ontology	GO
Gene set enrichment analysis	GSEA
hypersensitive response	HR
Indole acetic acid	IAA
KEGG automatic annotation server	KAAS
KEGG orthology	KO
Kyoto Encyclopedia of Genes and Genomes	KEGG
National Environmental Quality Standards	NEQS
Negative control probe	NONEUB
Non-metric multidimensional scaling	nMDS
para-aminobenzoic acid	PABA
Permutational multivariate analysis of variance	PERMANOVA
Plant growth promoting	PGP
Planted fixed-bed reactors	PFRs
Quantitative PCR	qPCR

Reactive nitrogen species	RNS
Reactive oxygen species	ROS
Ribosomal Database Project	RDP
Single-directional best-hit	SBH
Sulfamethoxazole	SMX
Trimethoprim	TMP
Wastewater treatment plants	WWTPs
Web gene ontology annotation plot	WEGO

BACKGROUND AND MOTIVATION

1

One of the major challenges faced by modern societies is to maintain their water resources. Wastewater generated from municipal activities contains a wide range of pollutants among which antimicrobials are of significant concern (Arslan et al., 2014). These antimicrobials, despite their small concentrations, are able to affect non-target bacterial communities as well as other organisms (Grenni et al., 2018). The main source of antimicrobials to the environment is the excretion by humans or animals (Marshall and Levy, 2011; Zhang et al., 2014). According to a survey, approximately 100,000 – 200,000 tons of antimicrobials are consumed every year worldwide (Van Boeckel et al., 2015); and in Germany alone, more than 250 types are used as human and veterinary medicine (Kümmerer and Henninger, 2003).

Antimicrobials are administered to prevent (prophylaxis) or treat infections without affecting the host cells (Kümmerer, 2008)). Many of the antimicrobials remain stable within the animal body, which results into excretion of a major fraction (40–90%) in its parent form (Marshall and Levy, 2011; Zhang et al., 2014). Those which are

excreted in the form of residual metabolites may also transform back to the parent compound upon excretion (Arslan et al., 2017b; Langhammer, 1989). Hence, most of the administered antimicrobials reach wastewater treatment plants (WWTPs).

Problem: Constructed wetlands are exposed to the low concentration of antimicrobials which could affect phytoremediation efficiency.

There are numerous reports available about the presence of antimicrobials in WWTPs: while in some countries, their concentrations have been detected up to a few µg/l (Barbosa et al., 2016; Batt et al., 2007; Botitsi et al., 2007; Hernández et al., 2007; Michael et al., 2013; Xu et al., 2007). The conventional treatment processes at WWTPs are insufficient to remove these pollutants because of their minute concentrations (Lishman et al., 2006); therefore, subsequent treatment via constructed wetlands (CWs) exposes plants to low concentrations of these antimicrobials.

1.1 Constructed wetlands

CWs are engineered phytoremediation systems which are extensively used for the treatment of wastewater. They have been used as sole treatment systems or as an integrated module within other types of WWTPs, e.g. as tertiary treatment unit. The term "constructed wetland" is derived from the German word *"Pflanzenkläranlage"* as these systems were first established and reported from Germany. In principle, CWs are the innovative product of 'sewage field' (German: *Rieselfeld*) which were first used in 1891 by German social reformers. In *Rieselfeld,* domestic wastewater is trickled over a large surface of water-permeable soil and during seeping, the waste material is mechanically trapped and/or degraded by microorganisms (Bjarsch, 1997). In the mid of 1950s, a German limnologist Dr. Käthe Seidel (Max Planck Hydrobiologische Anstalt, Krefeld-Hülserberg, Germany) developed a similar system to treat wastewater that contained filtering media as well as vegetation (i.e., lakeshore bulrush, *Schoenoplectus lacustris*) (Bally and Bittner, 2009; Seidel, 1955). These systems had one vertical and several horizontal seepage beds, which were filled with gravel and grown with marsh plants. Initially, Dr. Seidel thought that the marsh plants were responsible for the purification effect; however, later observations revealed that most of the purifying action was performed by the microorganisms living on the roots and gravel substrate. This experimentation was expanded by another German

Wetlands are being used for wastewater treatment since the 20th century.

scientist Dr. Reinhold Kickuth (Göttingen University) who in cooperation with Dr. Seidel optimized the system using clayey soil as a substrate bed while maintaining the water flow in a horizontal manner. Dr. Kickuth presumed that plants can introduce atmospheric oxygen into the root zone, which would enhance rapid aerobic transformation of pollutants. Furthermore, root growth would keep this zone permeable and the large contact area of the fine soil particles as well as long horizontal flow routes could further improve the clean-up process (Bally and Bittner, 2009). Thus, water purification is enhanced in the rhizosphere of CWs, and the process has hence been termed as Root Zone Method (German: *Wurzelraumverfahren*) (Brix, 1987; Kickuth, 1980). Initially, the application of CWs was limited to treat domestic and municipal wastewater. However, recent developments in ecological engineering have enabled us to use this technology for the treatment of wastewater of multiple origins, e.g., sewage, stormwater, industrial wastewater, agricultural runoff, mine drainage, landfill leachates, and polluted river water (Brix, 1994; Hoffmann et al., 2011; Wu et al., 2015). Figure 1.1 displays a schematic representation of CW and the application of a CW as an integrated module at a WWTP.

Several variants of CWs are engineered to treat wastewater of multiple origins.
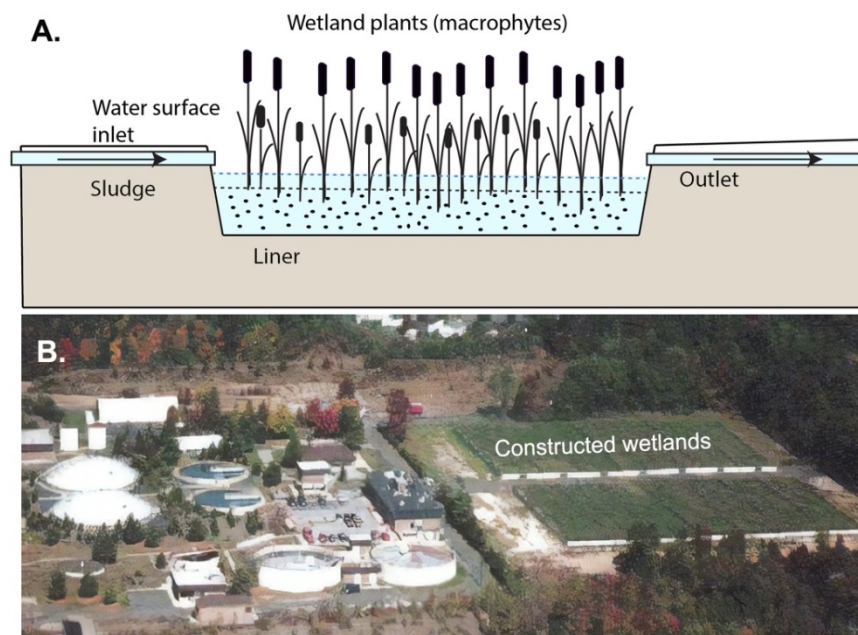
CWs can be used as a stand-alone system as well as tertiary treatment systems

Figure 1.1: (A) The schematic representation of a general CW system, and (B) CWs installed at wastewater treatment plant as an integrated module in the United States. In typical CWs, wastewater is fed from one side of the wetland whereas treated water is collected on the other side. Between inlet and outlet, vegetation and physical processes result into cleaning of the wastewater.
[source (A): own drawing; (B): http://www.constructedwetlandsgroup.com/ReedBeds/wastewater-treatment-plants/]

As of today, more than 50,000 field-scale CWs are in operation in Europe and more than 10,000 in North America (Vymazal and Kröpfelová, 2011; Wu et al., 2015). They are also employed in other parts of the world including developed and developing countries. A major reason behind the successful application of CWs technology is their strong capability in removing organic and inorganic compounds at comparably low costs from a wide range of wastewater (Coleman et al., 2001; Kadlec, 2009; Vymazal, 2007). In developed countries, mostly with small treatment plants, these systems are often used to minimize chemical oxygen demand (COD) and biochemical oxygen demand (BOD) of already treated wastewater for final return to the freshwater resources (Lee et al., 2009; Schwartz and Boyd, 1994; Vymazal, 2010, 2013). In developing countries, similar systems are employed as a complete wastewater treatment approach at large-scale (Afzal et al., 2019; Hussain et al., 2018a, b) or as a decentralized wastewater treatment system (Behrends et al., 2007; Parkinson and Tayler, 2003).

NIBGE signed a MoU with Water and Sanitation Agency (WASA) to treat city's wastewater.

Case Study: In this section, I briefly describe my activities on the field-scale operation of CWs during my Ph.D. time frame. This study is directly linked to the importance of CWs in wastewater treatment. The work was done in collaboration with my home country institute "National Institute for Biotechnology and Genetic Engineering (NIBGE), Faisalabad, Pakistan". To this end, floating wetlands with a total area of ~1,858 m^2 were installed over the stabilization ponds that receive sewage and industrial wastewater of Faisalabad city in Pakistan. Faisalabad is the third most populous city of Pakistan (3.2 million people) whose wastewater receives only primary treatment. The primary aim was to provide a practical, cost-effective, and long-term remediation solution before the city's wastewater is discharged to the surface drains. The wetlands operation was studied for a period of three

The findings of the case stdy are accepted for publication in Nature Sustainability journal. (c.v. for details)

years. We found that wetlands application promoted a substantial improvement of all recorded water quality parameters [dissolved oxygen (DO) chemical oxygen demand (COD), biochemical oxygen demand (BOD), total dissolved solids (TDS), total suspended solids (TSS), nitrates, sulfates, total phosphorous (TP)], and attenuation of trace metal concentrations in the outflow compared to the inflow. The maximum removal capacities of the system were 78.8% of COD, 88.2% of BOD, and 64.9% of TDS. The performance was optimal in the second and third year of operation during which about 60 million

m^3 per year of wastewater was treated at a cost of $ 0.00026 per m^3. This work concluded that wetlands are an appropriate ecotechnology for large-scale cleanup of sewage and industrial wastewater and have great potential for the countries with economic constraints such as Pakistan (Afzal et al., accepted).

1.2.1 Plant-bacteria partnership in CWs

The efficiency of CWs in the removal of pollutants depends on several parameters among which the plant-bacteria partnership is vitally important (Hussain et al., 2018a, b). In this partnership, plants and bacteria support each other to perform degradation services synergistically (Stottmeister et al., 2003b). Principally, plants provide nutrients and residency to the bacterial communities (Saleem et al., 2018), whereas bacteria in return protect their host by degrading toxic compounds (Afzal et al., 2014). Additionally, various bacteria help plants to thrive in harsh environments by providing phytohormones, alleviating (a)biotic stresses, and protecting against pathogen invasion (Arslan et al., 2017a). This partnership is established in the rhizosphere and endosphere depending upon the environmental niches and type of plant and bacterial species (Ijaz et al., 2016). As per the classical definition, plant-rhizobacteria partnership is the relationship between plant and rhizospheric bacterial communities (Afzal et al., 2011), whereas plant-endophyte interaction is the associations of plant and those bacteria that reside inside the plant without causing pathogenicity (Afzal et al., 2014).

Plant and bacteria support each other in a way that their performance is increased multifold as compared to their individual performances.

In CWs, the role of rhizobacteria in pollutant transformation has been well documented (Afzal et al., 2013; Glick, 2010; Weyens et al., 2009). Oxygen leaks from the roots of wetland plants, which results in the development of an oxidized zone in the close vicinity of the roots. Rhizospheric heterotrophic bacteria may then use oxygen as a terminal electron acceptor and mineralize organic content, and nitrifying bacteria may oxidize ammonia to nitrate. At some distance from the root surface, oxygen is depleted and anoxic conditions develop. In this zone, degradation of organic content is achieved by e.g. denitrifying bacteria that convert nitrate to dinitrogen. In the absence of suitable electron acceptors other than protons, organic matter may be degraded anaerobically into methane and carbon dioxide. This interaction of

Rhizobacteria are the main contributor of rhizoremediation.

rhizospheric community and plant roots in oxic and anoxic zones positively influence the degradation of organic matter and nutrients in CWs (Brix, 1987). Additionally, various rhizospheric bacteria can act as plant growth promoting (PGP) bacteria because they favor the growth of plant by solubilizing inorganic phosphorus, producing siderophores, and forming indole acetic acid (Glick, 2014). A general scheme on the role of rhizospheric bacteria in CWs is shown in Figure 1.2 (Al-Baldawi et al., 2017; Button et al., 2015; Edwards et al., 2006).

Log K_{ow} values for most of the sulphonamides and quinolones antimicrobial drugs lies within the range 0.5-3.0.
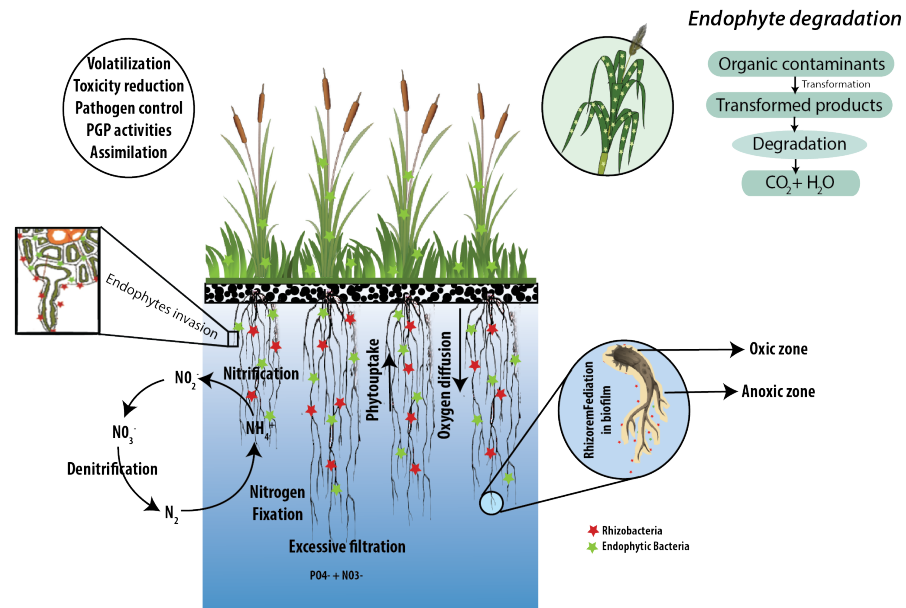
Figure 1.2: Schematic representation of the functioning of rhizo- and endophytic bacteria. Rhizobacteria may carry out degradation of the pollutants or nutrients present in the rhizosphere whereas endophytic bacteria may degrade those pollutants which are taken up by plants (modified from Rehman et al., 2019).

Endophytic bacteria degrade pollutants which are taken up by the plant without being attacked by rhizobacteria.

Endophytic bacteria that enter the plant interior through lateral root junctions or stomata can also play a major role for *in planta* pollutant degradation in CWs (Afzal et al., 2014). Usually, they have the advantage of being protected from the high-stress environment (Sturz and Nowak, 2000). During the operation of CW, organic contaminants with lipophilicity Log K_{ow} ranging between $0.5 - 3.0$ may enter the root xylem before the rhizospheric bacteria can degrade them. In this case, endophytic bacteria are the primary candidates to mineralize the pollutants and reduce phytotoxicity (Weyens et al., 2009). Typically, plants did not evolve pathways for mineralization of organic pollutants but rather endophytic bacteria co-evolved inside the plant for respective functioning (Figure 1.2) (Burken, 2003; Gerhardt et al., 2009).

1.3 Insights on how bacterial communities respond to antimicrobials

To date, nothing is known about the effect of antimicrobials on plant-microbe interactions mainly endophytes. Hence, in order to elucidate how exposure of antimicrobials can affect the bacterial community structure within plants, it might be helpful to understand how microbial communities respond to the presence of antimicrobials in the environment, and other host-microbiome systems, e.g. the animal gut.

Antimicrobials act as ecological factors that regulate microbial community in the environment.

1.3.1 Response of bacterial communities in the environment

In the environment, all basic nutrient cycles such as those of carbon, nitrogen, and oxygen depend on microbial metabolism. Therefore, the presence of antimicrobials in the environment may alter the functioning of these cycles. Although only a few studies have attempted to address it (Katipoglu-Yazan et al., 2015; Kotzerke et al., 2008; Liu et al., 2016; Roose-Amsaleg and Laverman, 2016), the topic is gaining serious attention worldwide. It is a fact that antimicrobials' concentrations are low in most ecosystems; nevertheless, specific bacterial responses might be triggered even at these concentrations due to the active biological nature of the compounds (Linares et al., 2006; Yim et al., 2006a; Yim et al., 2006b; Yim et al., 2007).

Antibiotics are made to kill bacteria without affecting the host cells.

Antimicrobials are also regarded as ecological factors because they regulate community structure based on their chemical nature (Aminov, 2009). A stressor at high concentration will have a high impact on the overall community composition (Abeles et al., 2016; Cleary et al., 2016). However, each species has a characteristic level of susceptibility to a specific antimicrobial. This means that for any given concentration of antimicrobials, the most susceptible members of the bacterial community will be inhibited while other members may get a competitive advantage and their abundance may increase, cf. concept of intrinsic resistance (Cox and Wright, 2013; Girgis et al., 2009; Olivares et al., 2014). Thus, low antimicrobial concentrations may allow growth of taxa whose presence was minor before the stress (Zhang et al., 2015). Such a change may influence ecological functioning of that particular micro-ecosystem (Kotzerke et al., 2008; Thiele-Bruhn and Beck, 2005).

Exposure of antimicrobials confers imbalance in beneficial microbial community and potential opportunists.

Multiple studies have attempted to rationalize these changes in different environmental settings, e.g. host-microbiome, and interactions in the marine environment and soil ecosystem (Apprill, 2017; Bosch and Miller, 2016; Egan and Gardiner, 2016; Mendes et al., 2011). These studies reported microbial imbalance upon antimicrobial treatment. The microbial imbalance is a state in which a beneficial microbiome is replaced with pathological microbiome or pathobionts (Figure 1.3).
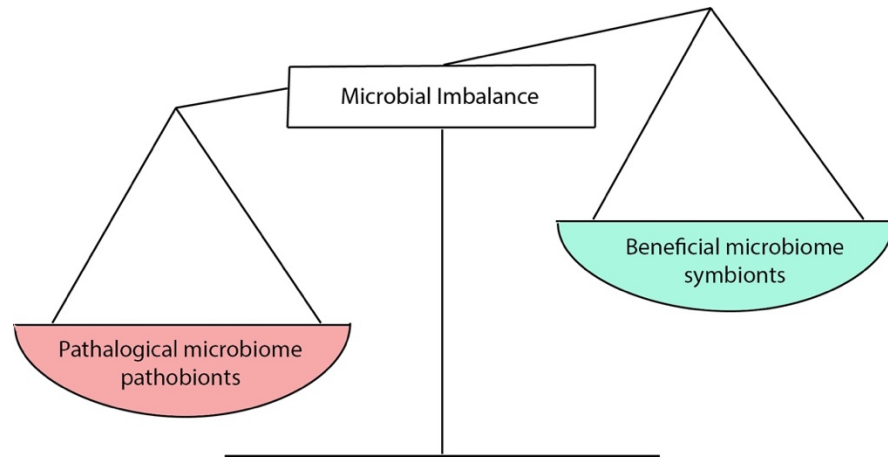
Figure 1.3: Microbial imbalance after treatment with antimicrobials. Imbalance leads to a situation where the beneficial microbiome or symbionts are reduced in proportion and pathological microbiome or pathobionts are increased [modified from Mazmanian and Lee, (20114)].

Once treatment ends, the composition of the microbiome may see partial recovery after some time; nevertheless, the fine structure of microbial community is not always similar to the original community (Raymond et al., 2016). This indicates that antimicrobials can pose lasting effects on microbial community even after they disappeared from an exposed environment. In terms of host-microbiome interactions, the animal gut microbiome is comparably well investigated (Jernberg et al., 2010; Looft and Allen, 2012; Robinson and Young, 2010). Below I discuss how microbial community responds in the animal gut upon antimicrobials exposures and what consequence can arise if a disbalance occurs in the microflora. This comparison is based on the analogy that gut microbiome behaves similarly as of root-microbiome which is already being discussed in recent literature (Ramírez-Puebla et al., 2013).

1.3.2 Response of bacterial community in the animal gut

The animal gut is a semi-open system with a large surface area that helps bacteria to colonize the interior (Ong et al., 2018). These bacteria are typically derived from the diet (Ley et al., 2008). Collectively, they have been recognized as "gut microbiome" or "secondary genome". This secondary genome is vital for the host as it performs important metabolic functions, which the host cannot carry out on its own (Gill et al., 2006). This includes the acquisition of certain nutrients, immune system modulation, synthesis of essential amino acids and vitamins, and protection against pathogens (Jandhyala et al., 2015; Mendes and Raaijmakers, 2015).

In addition to the diet, medical interventions are recognized as the main regulators of shaping the structure of gut microbiome. About 30% of the total community in the gut is disturbed with a single dose of antimicrobials treatment (Dethlefsen et al., 2008; Dethlefsen and Relman, 2011). This condition, where microbial community is disturbed, was coined as dysbiosis by Metchnikoff (Metchnikoff, 1907; Thevaranjan et al., 2017). The population structure is altered qualitatively and/or quantitatively where beneficial bacteria are replaced with opportunistic bacteria or pathogenic bacteria (Holzapfel et al., 1998; Mazmanian and Lee, 2014). These alterations could be long-lasting, spanning for months or even years (Dethlefsen and Relman, 2011; Jernberg et al., 2010).

The microbial community in the gut is shaped by food or drugs which animals take up.

The dysbiotic microbiome may not be able to perform appropriate metabolic functions for their host (Mendes and Raaijmakers, 2015; Ramírez-Puebla et al., 2013). In humans, these perturbations have been linked to several ailments such as luminal diseases (Ferreira et al., 2014), metabolic diseases (Ferreira et al., 2014), cardiovascular diseases (Carding et al., 2015) and immune system disorders (Nawrocki et al., 2014). A good example is the disturbances in the ratio of Firmicutes to Bacteroidetes in the animal gut which leads to obesity (Turnbaugh et al., 2006), and likewise, a reduction in microbiome diversity has been found to cause inflammatory bowel diseases (Khoruts et al., 2010). The dysbiotic microbiome also affects the host's defense and immune system which functions for protection against pathogen invasion and colonization (Carding et al., 2015). The general

It is argued that disturbed microbiome is never recovered completely in the whole life of the host.

response of the gut microbiome in disease and health of their host is presented in Figure 1.4.
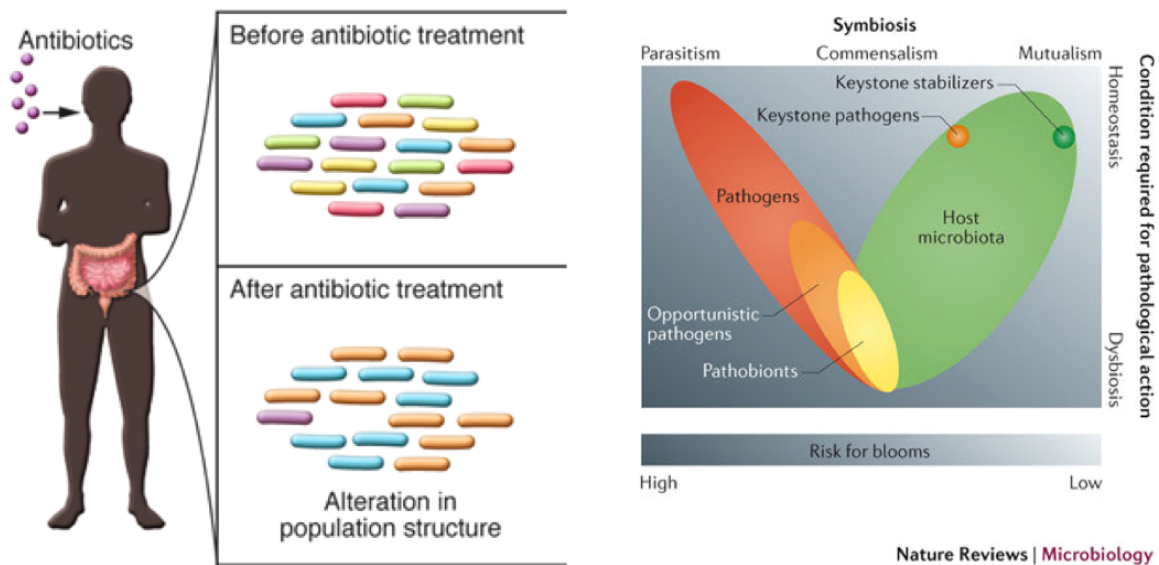
Figure 1.4: Effect of antimicrobials to the gut microbiome in humans. (A) Gut microbial community before exposure is diverse whereas exposure of antimicrobials results into alterations in population structure especially decreases in diversity. (B) Venn diagram illustration about health risks for the host during mutualism, commensalism, and parasitism. (source: Stecher et al., (2013).

1.3.3 Plant and gut microbiome commonalities

Plant and gut microbiome regulate gene expression of their host. They provide metabolic capabilities and essential nutrients; and confers protection against pathogen attack.

The idea that gut and plant microbiome behave similarly has gained substantial attention in recent years (Mendes and Raaijmakers, 2015; Ramírez-Puebla et al., 2013). Both systems have large surface areas and are inhabited by trillions of bacteria (Mendes and Raaijmakers, 2015; Ramírez-Puebla et al., 2013). These bacteria are generally recruited based on their beneficial services to their host (Rudrappa et al., 2008; Thursby and Juge, 2017). Based on its structure and function, the rhizosphere has been described as "the gut inside out" (Ramírez-Puebla et al., 2013) while the endosphere is analogized to the gut interior (Fitzpatrick et al., 2018). In this regard, several arguments have been made while comparing the behavior of microbiome in both ecosystems. These are:

1. Gut and plant microbiomes are generally recruited from the environment (Kikuchi et al., 2008; Ramírez-Puebla et al., 2013). In animals, food is the main source of the gut microbiome (De Filippo et al., 2010) whereas the plant microbiome is most likely attracted by chemotaxis from the soil (Rudrappa et al., 2008). The microbiome may also be transferred vertically from mothers to the progenies during or after birth (Jost et al., 2014) but it is also being debated that transmission can occur before birth as well (Jiménez et al., 2008; Mshvildadze et al., 2010). Likewise, in plants endophytic bacteria which are present in the seeds, mainly in the kernels, can colonize the rhizosphere or endosphere after germination (Johnston-Monje and Raizada, 2011; López-López et al., 2010).

2. Gut and plant microbiome enhance the metabolic capacity of their host by producing indispensable amino acids and vitamins that are exclusive products of prokaryotes (Bäckhed et al., 2005; Ramírez-Puebla et al., 2013). Likewise, the gut microbiome appears to regulate animal behavior (Macfarlane and Macfarlane, 2003) whereas the plant microbiome produces phytohormones that impact the growth of the host (Ortíz-Castro et al., 2009). Gut and plant microbiome also help the host in detoxification and degradation of pollutants which the host cannot perform by its own (Arslan et al., 2017b; Ramírez-Puebla et al., 2013). For example, the gut microbiome can transform/degrade medical drugs in humans (Haiser and Turnbaugh, 2012; Sousa et al., 2008), and the plant microbiome can degrade a variety of organic compounds through rhizoremediation and/or endophytic degradation (Arslan et al., 2017b). Similarly, gut bacteria are found to be rich in sugar hydrolases (Flint et al., 2008) and other catabolic genes such as those for transformation of tannin (Osawa et al., 2000), cholesterol (Gérard et al., 2007), or mucin (gut glycosylated proteins) (Derrien et al., 2008); whereas rhizospheric bacteria are capable to degrade e.g. polysaccharides, polyphenols (Calvaruso et al., 2006; López-López et al., 2010; Rodriguez et al., 2004).

Comparison of plant and gut microbial communities are a key to understand better both ecosystems in an analogous manner.

3. Gut and plant microbiome help their host to defend against pathogen attack. Once the balance of beneficial microbiome is disturbed, both systems are prone to the invasion of pathogenic bacteria (Friesen et al., 2011; Kane et al., 2011). The practice of

inoculating bacteria to a diseased or stressed plant has been found equivalent to the use of probiotics where a disturbed microflora can be replaced with beneficial microflora, i.e., rebiosis (Mendes and Raaijmakers, 2015). This practice can also be correlated with the faecal transplantation method where the microbiome is transferred from a donor to the patient to re-establish the beneficial microbial community in the gut (Khoruts et al., 2010).

It is argued that despite of two seemingly different ecosystems, both gut and plant shares several analogies in the structure and function of their microbiome (Ramírez-Puebla et al., 2013).

1.4 Motivation

Exposure of antimicrobials in CWs can impact plant growth and development (Fatta-Kassinos et al., 2011). However, it is unclear whether, at wastewater relevant concentrations, negative effects can arise from direct damages to the plant tissues or through disturbances in plant microbiome interactions (Grassi et al., 2013). Thus far, only a few studies have been conducted to track plant response (Brain et al., 2008) and bacterial communities present in the wetlands (Fatta-Kassinos et al., 2011; Weber et al., 2011; Yan et al., 2017); however, nothing is known in terms of the bacterial communities residing within the plants (endophytes). Weber et al., (2010) studied the effects of ciprofloxacin on the development, function, and stability of bacterial communities in the interstitial water of CWs planted with *Phragmites australis*. They reported that the antimicrobial exposure could lead to a temporary decrease in the catabolic capabilities which play an important role in the assimilation of anthropogenic carbon-based compounds. Although the effect was transitory because bacterial communities returned to normal functionalities in 2-5 weeks after the exposure; however, plants did not adapt the environment and faced a reduction in evapotranspiration. Nevertheless, in this system, focus was given to the rhizospheric microbial community whereas no specific observations or plant-endophyte interactions were made. In later years, Fatta-Kassinos et al. (2011) reviewed the literature on effect of antimicrobials to agroecological environment and they argued that exposure of antimicrobials can disrupt microbial communities in the soil, mainly close vicinity of plant roots, that results in lack of feed for the fauna, i.e., protozoa, micro-arthropods, and nematodes. This could influence

Earlier studies are conducted to track the response of rhizobacteria to antimicrobials whereas nothing is known in terms of disturbances in plant-endophyte interactions due to antimicrobials.

the biological cycles such as decomposition of plant residues gets slower and nutrients recycling is weakened (Fatta-Kassinos et al., 2011; Jjemba, 2002). Despite that, the available literature on plant-bacteria interactions in response to antimicrobials is scarce. Recently, Koskella et al., (2017) suggested that changes in endophytic community that correlates to the decrease in alpha diversity are in line to human microbiome studies and hence could be regarded as "dysbiosis in plants". This dysbiosis may also affect the performance of CWs treating wastewater. Therefore, investigations on the response of the endophytic communities to the antimicrobials are timely.

1.5 Aims and objectives

As discussed above, the biologically active nature of antimicrobials allows us to hypothesize various possibilities of disturbances in terms of plant-endophyte interplay in CWs. These changes, if occurring significantly, may also weaken the system's performance. To this end, this dissertation aims to understand the response of bacterial endophytes to antimicrobials, and to develop a genomic resource of *Juncus effusus* for subsequent studies on (a)biotic stress responses. Briefly, the objectives established are explained below:

The nature of antimicrobials allows us to speculate all possibilities of disturbance in endophytic community.

Objective #1: Elucidating the response of the endophytic bacterial community in the model plant *J. effusus* to antimicrobials in CWs.

This objective aimed to address fundamental questions relating to the response of the endophytic community upon exposure of antimicrobials, i.e., cotrimoxazole in this study (see section 2.1 of Chapter 1 for details). This is timely because CWs are being used to control pharmaceuticals including antimicrobials in wastewater without knowing much about the bacterial communities that are involved in these processes. Therefore, in this study, several approaches were adapted covering classical methods of microbiology to the modern tools of microbial ecology, i.e. cultivation dependent analysis, cultivation independent analysis, and confocal laser scanning microscopy observations. The results from this objective were based on two independent experiments which attempt to address basic and fundamental questions for the ongoing debate on "*dysbiosis in plants*". In the first experiment, plants were exposed to the concentrations

1ˢᵗ objective tracks response of bacterial communities in J. effusus *upon exposure of cotrimoxazole.*

higher than natural levels depicting what consequences can be arisen for the systems treating antimicrobials in particular; whereas, in the second experiment, exposure was started from environmentally relevant concentrations and then increased up to moderately high concentrations to elucidate the impact at effective concentrations. The detailed outcomes of the objective are presented in **Chapter 2**.

Objective #2: Developing benchmark resources to study stress response in *J. effusus*

2ⁿᵈ objective establishes first molecular database of J. effusus, which was tested for plant stress response upon exposure of cotrimxazole. This objective further aims to guide future research on natural and engineered wetland ecosystem functioning and evolutionary studies on the Poales.

The main rationale behind this objective was to extend the picture of stress response at the plant level. This was a necessary step because several plant-specific questions originated during investigation of the 1ˢᵗ objective. Thus, the primary task was to develop the genomic resource (database) of *J. effusus*, which can provide information on specific genes and proteins involved in stress response. Hence, RNA-Seq analyses were carried out by annotating transcriptome assembly of *J. effusus*. The results were compared with previously well-annotated transcriptomes of three phylogenetic relatives, namely *Sorghum bicolor*, *Oryza sativa*, and *Zea mays* for quality control purposes. Targeted investigations on the presence of genes involved in plant defense were studied via (Kyoto Encyclopedia of Genes and Genomes) KEGG analysis, specifically studying the KEGG pathway "*plant-pathogen interactions*". Finally, the developed database was tested for proteomics study on a subset of antimicrobials-exposed plant tissues (studied in objective 1). The outcomes of this research objective are summarized in **Chapter 3**.

1.5 Study parameters

1.5.1 Cotrimoxazole

This study investigates the effects of cotrimoxazole, which is a combination of two antimicrobials, namely Sulfamethoxazole (SMX) and Trimethoprim (TMP), on *J. effusus* at low to moderate concentrations, i.e., 10 ng/L to 100 μg/L. They are mostly prescribed together for the treatment of various bacterial infections in humans and animals, for instance, bronchitis, pneumonia, bacillary diarrhea, and infections related to urinary tract, middle ear, and intestines. Their

optimal ratio for potential synergy has been determined to be 20 parts of SMX to 1 part of TMP (Bushby, 1975; Bushby, 1973). They have been very popular in many countries of the European Union (EU) including Germany. Adriaenssens et al., (2011) reported that across the EU from 1997 to 2009, the consumption rate of SMX differed by 35-fold and the highest consumption was estimated for Germany. On the other hand, consumption of TMP differed 226-fold nationwide and the maximum consumption was seen in France (Johnson et al., 2015). This consumption rates, however, were not stable throughout the year as high consumption was found during winter (Suda et al., 2014) (Suda et al., 2014). As a consequence, both SMX and TMP are frequently detected at WWTPs of many countries of the EU including Germany (Loos et al., 2013; Nikolaou et al., 2007). Loos et al., (2013) conducted an EU-wide survey on WWTP effluents in 2010 for which they reported percentile frequency of detection for 161 compounds. According to the survey, TMP and SMX ranked at 93% and 83%, respectively, and the maximum concentration of SMX was recorded to be 1.7 μg/L. Johnson et al., (2015) modeled the average annual concentrations of SMX and TMP in the surface waters of EU, based on drug consumption parameters, location, and size of the human population, and their association with sewage treatment plants. The spatial variation of modeled concentrations of SMX and TMP are shown in Figure 1.5.

Cotrimoxazole is comprised of approximately 10% of total antimicrobial load in the European wastewaters.
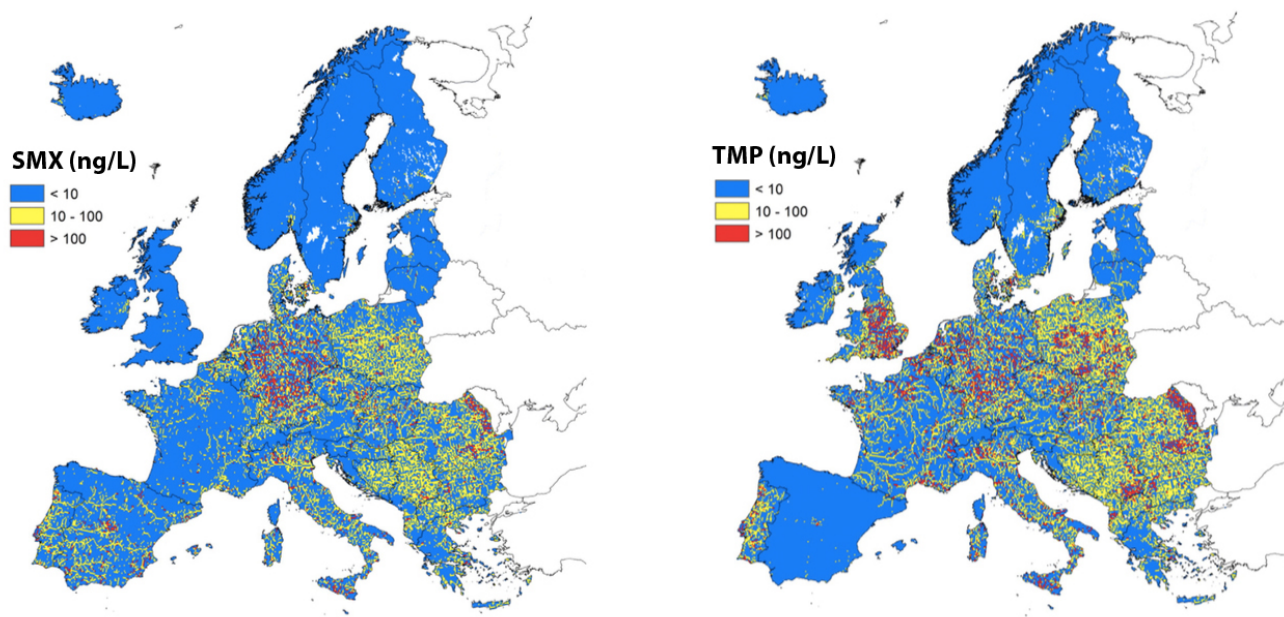
Figure 1.5: Predicted annual average concentrations of SMX and TMP in the surface waters of European Union (Johnson et al., 2015). The maps were made by using global water availability assessment (GWAVA) model. The effluent's concentrations from sewage treatment plants were incorporated with other natural and artificial flows into the hydrological model. The maps show that SMX is very popular in Germany.

A significant proportion of both drugs is excreted unchanged via the urine. This is particularly true for TMP, which is metabolized between 10–30% into an inactive form, whereas the remaining fraction is excreted in the parent form. By contrast, due to better metabolization of SMX in the liver, only 30% of it is excreted unchanged. An important metabolite of SMX is N^4-acetylsulfamethoxazole that accounts for approximately 50% of the administered dose. Half-lives of both parent compounds in healthy individuals range between 8-14 hours. Upon excretion, these compounds may enter WWTPs and are adsorbed on to the solid materials or dissolved in liquid effluent (Batt et al., 2007; Brown et al., 2006; Ryan et al., 2011). Additionally, their metabolites can be re-transformed to the parent compound during wastewater treatment processes (Göbel et al., 2005). For instance, in Switzerland, the concentration of SMX was detected up to 570 ng/L in the raw influent, which was increased to 640 ng/L in the primary effluent, 840 ng/L in the secondary effluent, and 860 ng/L in the tertiary effluent. From there, CWs are exposed to the wastewater containing similar concentrations of the antimicrobials (Göbel et al., 2005).

1.6.1 *J. effusus*

Linnaeus first described *J. effusus* (common or soft rush) in 1753. It is an almost cosmopolitan monocotyledonous C_3 plant that can grow abundantly in temperate wetlands, riparian strips, and other damp or wet terrestrial habitats (Kirschner, 2002). In fact, it is an indicator species (German: *kennzeichnende Art*) for damp and terrestrial environments and has been extensively studied for its impact on wetland functions. The species is well studied in respect to its autecology (Ervin and Wetzel, 1997; Lazenby, 1955a, b; Yoon et al., 2011). The morphological traits of the plant can vary across its worldwide distributional range leading to the description of several subspecies (Born and Michalski, 2017). In Europe, only *J. effusus* ssp. *effusus* is known to occur but at least two genetically distinct cryptic lineages within the taxa have been found recently (Michalski and Durka, 2012).

The plant grows in dense tufts and is able to reproduce by producing abundant seeds which are easily dispersed as well as via rhizomes, rendering the species an efficient colonizer (Richards and Clapham, 1941). The rhizomes, as well as the shoots of this plant, are characterized by forming aerenchyma for channeling air into the roots. This structural feature allows *J. effusus* to thrive in waterlogged environments (Visser and Bögemann, 2006; Vymazal, 2014; Vymazal and Březinová, 2016). The release of oxygen in the rhizosphere creates a cone-shaped oxic zone around the root tips. The plant has thus multifarious effects on major element cycles in wetlands (Wiessner et al., 2008).

Autecology is the ecological study of a particular species.

Interactions of *J. effusus* with microbial communities as well as co-occurring plant species are exploited in ecotechnological applications such as CWs (Stottmeister et al., 2003a). Based on these characteristics, *J. effusus* has been extensively employed as a model plant in addressing fundamental and applied research questions on wetland ecosystems (Agethen and Knorr, 2018; Martínez-Lavanchy et al., 2015; Wiessner et al., 2008).

References

Abeles, S.R., Jones, M.B., Santiago-Rodriguez, T.M., Ly, M., Klitgord, N., Yooseph, S., Nelson, K.E., Pride, D.T., 2016. Microbial diversity in individuals and their household contacts following typical antibiotic courses. Microbiome 4, 39.

Afzal, M., Khan, Q.M., Sessitsch, A., 2014. Endophytic bacteria: Prospects and applications for the phytoremediation of organic pollutants. Chemosphere 117, 232-242.

Afzal, M., Khan, S., Iqbal, S., Mirza, M.S., Khan, Q.M., 2013. Inoculation method affects colonization and activity of *Burkholderia phytofirmans* PsJN during phytoremediation of diesel-contaminated soil. International Biodeterioration & Biodegradation 85, 331-336.

Afzal, M., Rehman, K., Shabir, G., Tahseen, R., Ijaz, A., Hashmat, A.J., Brix, H., 2019. Large-scale remediation of oil-contaminated water using floating treatment wetlands. npj Clean Water 2, 3.

Afzal, M., Yousaf, S., Reichenauer, T.G., Kuffner, M., Sessitsch, A., 2011. Soil type affects plant colonization, activity and catabolic gene expression of inoculated bacterial strains during phytoremediation of diesel. Journal of Hazardous Materials 186, 1568-1575.

Agethen, S., Knorr, K.-H., 2018. *Juncus effusus* mono-stands in restored cutover peat bogs–Analysis of litter quality, controls of anaerobic decomposition, and the risk of secondary carbon loss. Soil Biology and Biochemistry 117, 139-152.

Al-Baldawi, I., Abdullah, S., Anuar, N., Mushrifah, I., 2017. Bioaugmentation for the enhancement of hydrocarbon phytoremediation by rhizobacteria consortium in pilot horizontal subsurface flow constructed wetlands. International journal of environmental science and technology 14, 75-84.

Aminov, R.I., 2009. The role of antibiotics and antibiotic resistance in nature. Environmental Microbiology 11, 2970-2988.

Apprill, A., 2017. Marine Animal Microbiomes: Toward Understanding Host–Microbiome Interactions in a Changing Ocean. Frontiers in Marine Science 4.

Arslan, M., Afzal, M., Amin, I., Iqbal, S., Khan, Q.M., 2014. Nutrients Can Enhance the Abundance and Expression of Alkane Hydroxylase CYP153 Gene in the Rhizosphere of Ryegrass Planted in Hydrocarbon-Polluted Soil. PLOS ONE 9, e111208.

Arslan, M., Imran, A., Khan, Q.M., Afzal, M., 2017a. Plant–bacteria partnerships for the remediation of persistent organic pollutants. Environmental Science and Pollution Research 24, 4322-4336.

Arslan, M., Ullah, I., Müller, J.A., Shahid, N., Afzal, M., 2017b. Organic Micropollutants in the Environment: Ecotoxicity Potential and

Methods for Remediation, in: Anjum, N.A., Gill, S.S., Tuteja, N. (Eds.), Enhancing Cleanup of Environmental Pollutants: Volume 1: Biological Approaches. Springer International Publishing, Cham, pp. 65-99.

Bäckhed, F., Ley, R.E., Sonnenburg, J.L., Peterson, D.A., Gordon, J.I., 2005. Host-Bacterial Mutualism in the Human Intestine. Science 307, 1915-1920.

Bally, A., Bittner, K., 2009. Pflanzenkläranlagen–Die ökologische Alternative zur technischen Kleinkläranlage. Ingenieurbiologie/Genie Biologique 4, 80-85.

Barbosa, M.O., Moreira, N.F.F., Ribeiro, A.R., Pereira, M.F.R., Silva, A.M.T., 2016. Occurrence and removal of organic micropollutants: An overview of the watch list of EU Decision 2015/495. Water Research 94, 257-279.

Batt, A.L., Kim, S., Aga, D.S., 2007. Comparison of the occurrence of antibiotics in four full-scale wastewater treatment plants with varying designs and operations. Chemosphere 68, 428-435.

Behrends, L.L., Bailey, E., Jansen, P., Houke, L., Smith, S., 2007. Integrated constructed wetland systems: design, operation, and performance of low-cost decentralized wastewater treatment systems. Water Science and Technology 55, 155-161.

Bjarsch, B., 1997. 125 Jahre Berliner Rieselfeld-Geschichte. Wasser und Boden 49, 45-48.

Born, J., Michalski, S.G., 2017. Strong divergence in quantitative traits and plastic behavior in response to nitrogen availability among provenances of a common wetland plant. Aquatic Botany 136, 138-145.

Bosch, T.C., Miller, D.J., 2016. Bleaching as an obvious dysbiosis in corals, The holobiont imperative. Springer, pp. 113-125.

Botitsi, E., Frosyni, C., Tsipi, D., 2007. Determination of pharmaceuticals from different therapeutic classes in wastewaters by liquid chromatography–electrospray ionization–tandem mass spectrometry. Analytical and Bioanalytical Chemistry 387, 1317-1327.

Brain, R.A., Ramirez, A.J., Fulton, B.A., Chambliss, C.K., Brooks, B.W., 2008. Herbicidal Effects of Sulfamethoxazole in *Lemna gibba*: Using p-Aminobenzoic Acid As a Biomarker of Effect. Environmental Science & Technology 42, 8965-8970.

Brix, H., 1987. Treatment of wastewater in the rhizosphere of wetland plants–the root-zone method. Water Science and Technology 19, 107-118.

Brix, H., 1994. Functions of macrophytes in constructed wetlands. Water Science and Technology 29, 71-78.

Brown, K.D., Kulis, J., Thomson, B., Chapman, T.H., Mawhinney, D.B., 2006. Occurrence of antibiotics in hospital, residential, and dairy effluent, municipal wastewater, and the Rio Grande in New Mexico. Science of The Total Environment 366, 772-783.

Burken, J., 2003. Uptake and metabolism of organic compounds: green-liver model. Phytoremediation: transformation and control of contaminants 59, 59-84.

Bushby, S.R., 1975. Synergy of trimethoprim-sulfamethoxazole. Canadian Medical Association journal 112, 63-66.

Bushby, S.R.M., 1973. Trimethoprim-Sulfamethoxazole: *In Vitro* Microbiological Aspects. The Journal of Infectious Diseases 128, S442-S462.

Button, M., Nivala, J., Weber, K.P., Aubron, T., Müller, R.A., 2015. Microbial community metabolic function in subsurface flow constructed wetlands of different designs. Ecological Engineering 80, 162-171.

Calvaruso, C., Turpault, M.-P., Frey-Klett, P., 2006. Root-Associated Bacteria Contribute to Mineral Weathering and to Mineral Nutrition in Trees: a Budgeting Analysis. Applied and Environmental Microbiology 72, 1258-1266.

Carding, S., Verbeke, K., Vipond, D.T., Corfe, B.M., Owen, L.J., 2015. Dysbiosis of the gut microbiota in disease. Microbial Ecology in Health and Disease 26, 26191.

Cleary, D.W., Bishop, A.H., Zhang, L., Topp, E., Wellington, E.M.H., Gaze, W.H., 2016. Long-term antibiotic exposure in soil is associated with changes in microbial community structure and prevalence of class 1 integrons. FEMS Microbiology Ecology 92, fiw159-fiw159.

Coleman, J., Hench, K., Garbutt, K., Sexstone, A., Bissonnette, G., Skousen, J., 2001. Treatment of Domestic Wastewater by Three Plant Species in Constructed Wetlands. Water, Air, and Soil Pollution 128, 283-295.

Cox, G., Wright, G.D., 2013. Intrinsic antibiotic resistance: Mechanisms, origins, challenges and solutions. International Journal of Medical Microbiology 303, 287-292.

De Filippo, C., Cavalieri, D., Di Paola, M., Ramazzotti, M., Poullet, J.B., Massart, S., Collini, S., Pieraccini, G., Lionetti, P., 2010. Impact of diet in shaping gut microbiota revealed by a comparative study in children from Europe and rural Africa. Proceedings of the National Academy of Sciences 107, 14691-14696.

Derrien, M., Collado, M.C., Ben-Amor, K., Salminen, S., de Vos, W.M., 2008. The Mucin degrader Akkermansia muciniphila is an abundant resident of the human intestinal tract. Applied and environmental microbiology 74, 1646-1648.

Dethlefsen, L., Huse, S., Sogin, M.L., Relman, D.A., 2008. The Pervasive Effects of an Antibiotic on the Human Gut Microbiota, as Revealed by Deep 16S rRNA Sequencing. PLOS Biology 6, e280.

Dethlefsen, L., Relman, D.A., 2011. Incomplete recovery and individualized responses of the human distal gut microbiota to repeated antibiotic perturbation. Proceedings of the National Academy of Sciences 108, 4554-4561.

Edwards, K.R., Čižková, H., Zemanová, K., Šantrůčková, H., 2006. Plant growth and microbial processes in a constructed wetland planted with *Phalaris arundinacea*. Ecological Engineering 27, 153-165.

Egan, S., Gardiner, M., 2016. Microbial dysbiosis: rethinking disease in marine ecosystems. Frontiers in microbiology 7, 991.

Ervin, G.N., Wetzel, R.G., 1997. Shoot:root dynamics during growth stages of the rush *Juncus effusus* L. Aquatic Botany 59, 63-73.

Fatta-Kassinos, D., Meric, S., Nikolaou, A., 2011. Pharmaceutical residues in environmental waters and wastewater: current state of knowledge and future research. Analytical and Bioanalytical Chemistry 399, 251-275.

Ferreira, C.M., Vieira, A., Thomaz, l., Vinolo, M.A.R., Oliveira, F.A., Curi, R., Martins, F.d.S., 2014. The Central Role of the Gut Microbiota in Chronic Inflammatory Diseases. Journal of Immunology Research 2014, 12.

Fitzpatrick, C.R., Copeland, J., Wang, P.W., Guttman, D.S., Kotanen, P.M., Johnson, M.T.J., 2018. Assembly and ecological function of the root microbiome across angiosperm plant species. Proceedings of the National Academy of Sciences 115, E1157-E1165.

Flint, H.J., Bayer, E.A., Rincon, M.T., Lamed, R., White, B.A., 2008. Polysaccharide utilization by gut bacteria: potential for new insights from genomic analysis. Nature Reviews Microbiology 6, 121.

Friesen, M.L., Porter, S.S., Stark, S.C., von Wettberg, E.J., Sachs, J.L., Martinez-Romero, E., 2011. Microbially mediated plant functional traits. Annual Review of Ecology, Evolution, and Systematics 42, 23-46.

Gérard, P., Lepercq, P., Leclerc, M., Gavini, F., Raibaud, P., Juste, C., 2007. Bacteroides sp. strain D8, the first cholesterol-reducing bacterium isolated from human feces. Applied and environmental microbiology 73, 5742-5749.

Gerhardt, K.E., Huang, X.-D., Glick, B.R., Greenberg, B.M., 2009. Phytoremediation and rhizoremediation of organic soil contaminants: Potential and challenges. Plant Science 176, 20-30.

Gill, S.R., Pop, M., DeBoy, R.T., Eckburg, P.B., Turnbaugh, P.J., Samuel, B.S., Gordon, J.I., Relman, D.A., Fraser-Liggett, C.M., Nelson, K.E.,

2006. Metagenomic analysis of the human distal gut microbiome. Science 312, 1355-1359.

Girgis, H.S., Hottes, A.K., Tavazoie, S., 2009. Genetic Architecture of Intrinsic Antibiotic Susceptibility. PLOS ONE 4, e5629.

Glick, B.R., 2010. Using soil bacteria to facilitate phytoremediation. Biotechnology Advances 28, 367-374.

Glick, B.R., 2014. Bacteria with ACC deaminase can promote plant growth and help to feed the world. Microbiological Research 169, 30-39.

Göbel, A., Thomsen, A., McArdell, C.S., Joss, A., Giger, W., 2005. Occurrence and sorption behavior of sulfonamides, macrolides, and trimethoprim in activated sludge treatment. Environmental science & technology 39, 3981-3989.

Grassi, M., Rizzo, L., Farina, A., 2013. Endocrine disruptors compounds, pharmaceuticals and personal care products in urban wastewater: implications for agricultural reuse and their removal by adsorption process. Environmental Science and Pollution Research 20, 3616-3628.

Grenni, P., Ancona, V., Caracciolo, A.B., 2018. Ecological effects of antibiotics on natural ecosystems: A review. Microchemical Journal 136, 25-39.

Haiser, H.J., Turnbaugh, P.J., 2012. Is It Time for a Metagenomic Basis of Therapeutics? Science 336, 1253-1255.

Hernández, F., Sancho, J.V., Ibáñez, M., Guerrero, C., 2007. Antibiotic residue determination in environmental waters by LC-MS. TrAC Trends in Analytical Chemistry 26, 466-485.

Hoffmann, H., Platzer, C., Winker, M., von Muench, E., 2011. Technology review of constructed wetlands: Subsurface flow constructed wetlands for greywater and domestic wastewater treatment. Deutsche Gesellschaft für Internationale Zusammenarbeit (GIZ) GmbH, Eschborn, Germany, 11.

Holzapfel, W.H., Haberer, P., Snel, J., Schillinger, U., Huis in't Veld, J.H.J., 1998. Overview of gut flora and probiotics. International Journal of Food Microbiology 41, 85-101.

Hussain, Z., Arslan, M., Malik, M.H., Mohsin, M., Iqbal, S., Afzal, M., 2018a. Integrated perspectives on the use of bacterial endophytes in horizontal flow constructed wetlands for the treatment of liquid textile effluent: Phytoremediation advances in the field. Journal of Environmental Management 224, 387-395.

Hussain, Z., Arslan, M., Malik, M.H., Mohsin, M., Iqbal, S., Afzal, M., 2018b. Treatment of the textile industry effluent in a pilot-scale vertical flow constructed wetland system augmented with bacterial endophytes. Science of The Total Environment 645, 966-973.

Ijaz, A., Imran, A., Anwar ul Haq, M., Khan, Q.M., Afzal, M., 2016. Phytoremediation: recent advances in plant-endophytic synergistic interactions. Plant and Soil 405, 179-195.

Jandhyala, S.M., Talukdar, R., Subramanyam, C., Vuyyuru, H., Sasikala, M., Nageshwar Reddy, D., 2015. Role of the normal gut microbiota. World journal of gastroenterology 21, 8787-8803.

Jernberg, C., Löfmark, S., Edlund, C., Jansson, J.K., 2010. Long-term impacts of antibiotic exposure on the human intestinal microbiota. Microbiology 156, 3216-3223.

Jiménez, E., Marín, M.L., Martín, R., Odriozola, J.M., Olivares, M., Xaus, J., Fernández, L., Rodríguez, J.M., 2008. Is meconium from healthy newborns actually sterile? Research in Microbiology 159, 187-193.

Jjemba, P.K., 2002. The potential impact of veterinary and human therapeutic agents in manure and biosolids on plants grown on arable land: a review. Agriculture, Ecosystems & Environment 93, 267-278.

Johnson, A.C., Keller, V., Dumont, E., Sumpter, J.P., 2015. Assessing the concentrations and risks of toxicity from the antibiotics ciprofloxacin, sulfamethoxazole, trimethoprim and erythromycin in European rivers. Science of The Total Environment 511, 747-755.

Johnston-Monje, D., Raizada, M.N., 2011. Conservation and Diversity of Seed Associated Endophytes in Zea across Boundaries of Evolution, Ethnography and Ecology. PLOS ONE 6, e20396.

Jost, T., Lacroix, C., Braegger, C.P., Rochat, F., Chassard, C., 2014. Vertical mother–neonate transfer of maternal gut bacteria via breastfeeding. Environmental Microbiology 16, 2891-2904.

Kadlec, R.H., 2009. Comparison of free water and horizontal subsurface treatment wetlands. Ecological Engineering 35, 159-174.

Kane, M., Case, L.K., Kopaskie, K., Kozlova, A., MacDearmid, C., Chervonsky, A.V., Golovkina, T.V., 2011. Successful Transmission of a Retrovirus Depends on the Commensal Microbiota. Science 334, 245-249.

Katipoglu-Yazan, T., Merlin, C., Pons, M.-N., Ubay-Cokgor, E., Orhon, D., 2015. Chronic impact of tetracycline on nitrification kinetics and the activity of enriched nitrifying microbial culture. Water Research 72, 227-238.

Khoruts, A., Dicksved, J., Jansson, J.K., Sadowsky, M.J., 2010. Changes in the composition of the human fecal microbiome after bacteriotherapy for recurrent Clostridium difficile-associated diarrhea. Journal of clinical gastroenterology 44, 354-360.

Kickuth, R., 1980. Abwasserbehandlung im Wurzelraumverfahren. Wlb 'wasser, luft und betrieb 11, 21-24.

Kikuchi, Y., Hosokawa, T., Fukatsu, T., 2008. Diversity of bacterial symbiosis in stinkbugs. Nova Science Publishers, Inc: New York, USA.

Kirschner, J., 2002. Juncaceae. Australian Biological Resources Study.

Koskella, B., Meaden, S., Crowther, W.J., Leimu, R., Metcalf, C.J.E., 2017. A signature of tree health? Shifts in the microbiome and the ecological drivers of horse chestnut bleeding canker disease. New Phytologist 215, 737-746.

Kotzerke, A., Sharma, S., Schauss, K., Heuer, H., Thiele-Bruhn, S., Smalla, K., Wilke, B.-M., Schloter, M., 2008. Alterations in soil microbial activity and N-transformation processes due to sulfadiazine loads in pig-manure. Environmental Pollution 153, 315-322.

Kümmerer, K., 2008. Pharmaceuticals in the environment: sources, fate, effects and risks. Springer Science & Business Media.

Kümmerer, K., Henninger, A., 2003. Promoting resistance by the emission of antibiotics from hospitals and households into effluent. Clinical Microbiology and Infection 9, 1203-1214.

Langhammer, J.-P., 1989. Untersuchungen zum Verbleib antimikrobiell wirksamer Arzneistoffe als Rückstände in Gülle und im landwirtschaftlichen Umfeld.

Lazenby, A., 1955a. Germination and establishment of *Juncus effusus* L.: II. The interaction effects of moisture and competition. The Journal of Ecology, 595-605.

Lazenby, A., 1955b. Germination and establishment of *Juncus effusus* L.: the effect of different companion species and of variation in soil and fertility conditions. The Journal of Ecology, 103-119.

Lee, C.g., Fletcher, T.D., Sun, G., 2009. Nitrogen removal in constructed wetland systems. Engineering in Life Sciences 9, 11-22.

Ley, R.E., Lozupone, C.A., Hamady, M., Knight, R., Gordon, J.I., 2008. Worlds within worlds: evolution of the vertebrate gut microbiota. Nature Reviews Microbiology 6, 776.

Linares, J.F., Gustafsson, I., Baquero, F., Martinez, J.L., 2006. Antibiotics as intermicrobial signaling agents instead of weapons. Proceedings of the National Academy of Sciences 103, 19484-19489.

Lishman, L., Smyth, S.A., Sarafin, K., Kleywegt, S., Toito, J., Peart, T., Lee, B., Servos, M., Beland, M., Seto, P., 2006. Occurrence and reductions of pharmaceuticals and personal care products and estrogens by municipal wastewater treatment plants in Ontario, Canada. Science of The Total Environment 367, 544-558.

Liu, A., Cao, H., Yang, Y., Ma, X., Liu, X., 2016. Combinational effects of sulfomethoxazole and copper on soil microbial community and

function. Environmental Science and Pollution Research 23, 4235-4241.

Looft, T., Allen, H.K., 2012. Collateral effects of antibiotics on mammalian gut microbiomes. Gut Microbes 3, 463-467.

Loos, R., Carvalho, R., António, D.C., Comero, S., Locoro, G., Tavazzi, S., Paracchini, B., Ghiani, M., Lettieri, T., Blaha, L., Jarosova, B., Voorspoels, S., Servaes, K., Haglund, P., Fick, J., Lindberg, R.H., Schwesig, D., Gawlik, B.M., 2013. EU-wide monitoring survey on emerging polar organic contaminants in wastewater treatment plant effluents. Water Research 47, 6475-6487.

López-López, A., Rosenblueth, M., Martínez, J., Martínez-Romero, E., 2010. Rhizobial Symbioses in Tropical Legumes and Non-Legumes, in: Dion, P. (Ed.), Soil Biology and Agriculture in the Tropics. Springer Berlin Heidelberg, Berlin, Heidelberg, pp. 163-184.

Macfarlane, S., Macfarlane, G., 2003. Food and the large intestine. Gut flora, nutrition, immunity and health, 24-51.

Marshall, B.M., Levy, S.B., 2011. Food Animals and Antimicrobials: Impacts on Human Health. Clinical Microbiology Reviews 24, 718-733.

Martínez-Lavanchy, P., Chen, Z., Lünsmann, V., Marin-Cevada, V., Vilchez-Vargas, R., Pieper, D., Reiche, N., Kappelmeyer, U., Imparato, V., Junca, H., 2015. Microbial toluene removal in hypoxic model constructed wetlands occurs predominantly via the ring monooxygenation pathway. Applied and Environmental Microbiology, AEM. 01822-01815.

Mazmanian, S.K., Lee, Y.K., 2014. Interplay between intestinal microbiota and host immune system. Journal of Bacteriology and Virology 44, 1-9.

Mendes, R., Kruijt, M., de Bruijn, I., Dekkers, E., van der Voort, M., Schneider, J.H.M., Piceno, Y.M., DeSantis, T.Z., Andersen, G.L., Bakker, P.A.H.M., Raaijmakers, J.M., 2011. Deciphering the Rhizosphere Microbiome for Disease-Suppressive Bacteria. Science 332, 1097-1100.

Mendes, R., Raaijmakers, J.M., 2015. Cross-kingdom similarities in microbiome functions. The Isme Journal 9, 1905.

Metchnikoff, E., 1907. The Prolongation of Life: Optimistic Studies. G. P. Putnam's Sons.

Michael, I., Rizzo, L., McArdell, C.S., Manaia, C.M., Merlin, C., Schwartz, T., Dagot, C., Fatta-Kassinos, D., 2013. Urban wastewater treatment plants as hotspots for the release of antibiotics in the environment: A review. Water Research 47, 957-995.

Michalski, S.G., Durka, W., 2012. Identification and characterization of microsatellite loci in the rush *Juncus effusus* (Juncaceae) 1. American journal of botany 99, e53-e55.

Mshvildadze, M., Neu, J., Shuster, J., Theriaque, D., Li, N., Mai, V., 2010. Intestinal Microbial Ecology in Premature Infants Assessed with Non–Culture-Based Techniques. The Journal of Pediatrics 156, 20-25.

Nawrocki, E.P., Burge, S.W., Bateman, A., Daub, J., Eberhardt, R.Y., Eddy, S.R., Floden, E.W., Gardner, P.P., Jones, T.A., Tate, J., 2014. Rfam 12.0: updates to the RNA families database. Nucleic acids research 43, D130-D137.

Nikolaou, A., Meric, S., Fatta, D., 2007. Occurrence patterns of pharmaceuticals in water and wastewater environments. Analytical and Bioanalytical Chemistry 387, 1225-1234.

Olivares, J., Álvarez-Ortega, C., Martinez, J.L., 2014. Metabolic Compensation of Fitness Costs Associated with Overexpression of the Multidrug Efflux Pump MexEF-OprN in *Pseudomonas aeruginosa*. Antimicrobial Agents and Chemotherapy 58, 3904-3913.

Ortíz-Castro, R., Contreras-Cornejo, H.A., Macías-Rodríguez, L., López-Bucio, J., 2009. The role of microbial signals in plant growth and development. Plant Signaling & Behavior 4, 701-712.

Osawa, R., Kuroiso, K., Goto, S., Shimizu, A., 2000. Isolation of Tannin-Degrading Lactobacilli from Humans and Fermented Foods. Applied and Environmental Microbiology 66, 3093-3097.

Parkinson, J., Tayler, K., 2003. Decentralized wastewater management in peri-urban areas in low-income countries. Environment and Urbanization 15, 75-90.

Ramírez-Puebla, S.T., Servín-Garcidueñas, L.E., Jiménez-Marín, B., Bolaños, L.M., Rosenblueth, M., Martínez, J., Rogel, M.A., Ormeño-Orrillo, E., Martínez-Romero, E., 2013. Gut and Root Microbiota Commonalities. Applied and Environmental Microbiology 79, 2-9.

Raymond, F., Déraspe, M., Boissinot, M., Bergeron, M.G., Corbeil, J., 2016. Partial recovery of microbiomes after antibiotic treatment. Gut Microbes 7, 428-434.

Rehman, R., Ijaz, A., Arslan, M., Afzal, M., 2019. Floating treatment wetlands as biological buoyant filters for wastewater reclamation, International Journal of Phytoremediation, DOI: 10.1080/15226514.2019.1633253

Richards, P., Clapham, A., 1941. *Juncus Effusus* L.(*Juncus Communis β effusus* E. Mey). Journal of Ecology 29, 375-380.

Robinson, C.J., Young, V.B., 2010. Antibiotic administration alters the community structure of the gastrointestinal microbiota. Gut Microbes 1, 279-284.

Rodriguez, H., Gonzalez, T., Goire, I., Bashan, Y., 2004. Gluconic acid production and phosphate solubilization by the plant growth-promoting bacterium Azospirillum spp. Naturwissenschaften 91, 552-555.

Roose-Amsaleg, C., Laverman, A.M., 2016. Do antibiotics have environmental side-effects? Impact of synthetic antibiotics on biogeochemical processes. Environmental Science and Pollution Research 23, 4000-4012.

Rudrappa, T., Czymmek, K.J., Paré, P.W., Bais, H.P., 2008. Root-Secreted Malic Acid Recruits Beneficial Soil Bacteria. Plant Physiology 148, 1547-1556.

Ryan, C.C., Tan, D.T., Arnold, W.A., 2011. Direct and indirect photolysis of sulfamethoxazole and trimethoprim in wastewater treatment plant effluent. Water Research 45, 1280-1286.

Saleem, H., Rehman, K., Arslan, M., Afzal, M., 2018. Enhanced degradation of phenol in floating treatment wetlands by plant-bacterial synergism. International Journal of Phytoremediation 20, 692-698.

Schwartz, M.F., Boyd, C.E., 1994. Effluent Quality during Harvest of Channel Catfish from Watershed Ponds. The Progressive Fish-Culturist 56, 25-32.

Seidel, K., 1955. Die Flechtbinse Scirpus lacustris L.

Sousa, T., Paterson, R., Moore, V., Carlsson, A., Abrahamsson, B., Basit, A.W., 2008. The gastrointestinal microbiota as a site for the biotransformation of drugs. International Journal of Pharmaceutics 363, 1-25.

Stecher, B., Maier, L., Hardt, W.-D., 2013. Blooming in the gut: how dysbiosis might contribute to pathogen evolution. Nature Reviews Microbiology 11, 277.

Stottmeister, U., Wießner, A., Kuschk, P., Kappelmeyer, U., Kästner, M., Bederski, O., Müller, R., Moormann, H., 2003a. Effects of plants and microorganisms in constructed wetlands for wastewater treatment. Biotechnology advances 22, 93-117.

Stottmeister, U., Wießner, A., Kuschk, P., Kappelmeyer, U., Kästner, M., Bederski, O., Müller, R.A., Moormann, H., 2003b. Effects of plants and microorganisms in constructed wetlands for wastewater treatment. Biotechnology advances 22, 93-117.

Sturz, A.V., Nowak, J., 2000. Endophytic communities of rhizobacteria and the strategies required to create yield enhancing associations with crops. Applied Soil Ecology 15, 183-190.

Suda, K.J., Hicks, L.A., Roberts, R.M., Hunkler, R.J., Taylor, T.H., 2014. Trends and Seasonal Variation in Outpatient Antibiotic Prescription Rates in the United States, 2006 to 2010. Antimicrobial Agents and Chemotherapy 58, 2763-2766.

Thevaranjan, N., Puchta, A., Schulz, C., Naidoo, A., Szamosi, J.C., Verschoor, C.P., Loukov, D., Schenck, L.P., Jury, J., Foley, K.P., Schertzer, J.D., Larché, M.J., Davidson, D.J., Verdú, E.F., Surette, M.G., Bowdish, D.M.E., 2017. Age-Associated Microbial Dysbiosis Promotes Intestinal Permeability, Systemic Inflammation, and Macrophage Dysfunction. Cell Host & Microbe 21, 455-466.e454.

Thiele-Bruhn, S., Beck, I.-C., 2005. Effects of sulfonamide and tetracycline antibiotics on soil microbial activity and microbial biomass. Chemosphere 59, 457-465.

Thursby, E., Juge, N., 2017. Introduction to the human gut microbiota. The Biochemical journal 474, 1823-1836.

Turnbaugh, P.J., Ley, R.E., Mahowald, M.A., Magrini, V., Mardis, E.R., Gordon, J.I., 2006. An obesity-associated gut microbiome with increased capacity for energy harvest. Nature 444, 1027.

Van Boeckel, T.P., Brower, C., Gilbert, M., Grenfell, B.T., Levin, S.A., Robinson, T.P., Teillant, A., Laxminarayan, R., 2015. Global trends in antimicrobial use in food animals. Proceedings of the National Academy of Sciences 112, 5649-5654.

Visser, E.J.W., Bögemann, G.M., 2006. Aerenchyma formation in the wetland plant Juncus effusus is independent of ethylene. New Phytologist 171, 305-314.

Vymazal, J., 2007. Removal of nutrients in various types of constructed wetlands. Science of The Total Environment 380, 48-65.

Vymazal, J., 2010. Constructed wetlands for wastewater treatment. Water 2, 530-549.

Vymazal, J., 2013. Emergent plants used in free water surface constructed wetlands: a review. Ecological engineering 61, 582-592.

Vymazal, J., 2014. Constructed wetlands for treatment of industrial wastewaters: a review. Ecological Engineering 73, 724-751.

Vymazal, J., Březinová, T., 2016. Accumulation of heavy metals in aboveground biomass of Phragmites australis in horizontal flow constructed wetlands for wastewater treatment: A review. Chemical Engineering Journal 290, 232-242.

Vymazal, J., Kröpfelová, L., 2011. A three-stage experimental constructed wetland for treatment of domestic sewage: First 2 years of operation. Ecological Engineering 37, 90-98.

Weber, K.P., Mitzel, M.R., Slawson, R.M., Legge, R.L., 2011. Effect of ciprofloxacin on microbiological development in wetland mesocosms. Water Research 45, 3185-3196.

Weyens, N., van der Lelie, D., Taghavi, S., Vangronsveld, J., 2009. Phytoremediation: plant–endophyte partnerships take the challenge. Current Opinion in Biotechnology 20, 248-254.

Wiessner, A., Kuschk, P., Jechorek, M., Seidel, H., Kästner, M., 2008. Sulphur transformation and deposition in the rhizosphere of Juncus effusus in a laboratory-scale constructed wetland. Environmental pollution 155, 125-131.

Wu, H., Zhang, J., Ngo, H.H., Guo, W., Hu, Z., Liang, S., Fan, J., Liu, H., 2015. A review on the sustainability of constructed wetlands for wastewater treatment: design and operation. Bioresource technology 175, 594-601.

Xu, W., Zhang, G., Li, X., Zou, S., Li, P., Hu, Z., Li, J., 2007. Occurrence and elimination of antibiotics at four sewage treatment plants in the Pearl River Delta (PRD), South China. Water Research 41, 4526-4534.

Yan, Q., Min, J., Yu, Y., Zhu, Z., Feng, G., 2017. Microbial community response during the treatment of pharmaceutically active compounds (PhACs) in constructed wetland mesocosms. Chemosphere 186, 823-831.

Yim, G., de la Cruz, F., Spiegelman, G.B., Davies, J., 2006a. Transcription Modulation of *Salmonella enterica* Serovar Typhimurium Promoters by Sub-MIC Levels of Rifampin. Journal of Bacteriology 188, 7988-7991.

Yim, G., Huimi Wang, H., Davies, J., 2006b. The truth about antibiotics. International Journal of Medical Microbiology 296, 163-170.

Yim, G., Wang, H.H., Frs, J.D., 2007. Antibiotics as signalling molecules. Philosophical Transactions of the Royal Society of London B: Biological Sciences 362, 1195-1200.

Yoon, J.-H., Kim, H.-T., Nam, J.-M., Kim, J.-G., 2011. Optimal environmental range for Juncus effusus, an important plant species in an endangered insect species (*Nannopya pygmaea*) habitat in Korea. Journal of Ecology and Environment 34, 223-235.

Zhang, X., Li, Y., Liu, B., Wang, J., Feng, C., Gao, M., Wang, L., 2014. Prevalence of Veterinary Antibiotics and Antibiotic-Resistant Escherichia coli in the Surface Water of a Livestock Production Region in Northern China. PLOS ONE 9, e111026.

Zhang, Y., Tian, Z., Liu, M., Shi, Z.J., Hale, L., Zhou, J., Yang, M., 2015. High Concentrations of the Antibiotic Spiramycin in Wastewater Lead to High Abundance of Ammonia-Oxidizing Archaea in Nitrifying Populations. Environmental Science & Technology 49, 9124-9132.

RESPONSE OF ENDOPHYTIC BACTERIAL COMMUNITIES TO COTRIMOXAZOLE

2

_____

Context

The work described in this chapter was originated from earlier observations made by a master degree student at the UFZ, Marcello Santoni (Erasmus student from the – University of Rome, Italy). He was studying the degradation of cotrimoxazole in a model wetland system planted with *Juncus effusus*, which is a common wetland plant. Instead of successful phytoremediation, he noticed that plant fitness was compromised, as judged by a substantial decrease in evapotranspiration and plant shoot infestation with insects. The present study was therefore designed to investigate if plant health was affected due to the antimicrobial action of cotrimoxazole on the endophytic community in *J. effusus*. In general, many endophytic bacteria have been previously

suggested to be beneficial for the host due to their stress alleviation and plant growth promoting activities.

2.1 Introduction

Endophytic bacteria are efficient colonizers of the plant interior. These microorganisms are classified as obligate or facultative endophytes depending on their mode of infection (Hardoim et al. 2008). Obligate endophytes are derived from the seeds and cannot thrive in the open environment whereas facultative endophytes can survive within or without the host depending upon the environmental conditions (Liu et al. 2017). Typically, facultative endophytes infect their host through lateral root junctions, stomata, or epidermal junctions of stem, leaves, and flowers (Bulgari et al. 2014, Compant et al. 2010). Once inside the plant, they either localize to the specific plant tissue or proliferate/colonize the whole plant by active migration through the plant's conducting elements, depending on the plant and bacterial species (Bulgari et al. 2014). These endophytic bacteria are believed to provide beneficial services to the host plant such as stress alleviation, plant growth promotion, and pollutant degradation without causing pathogenicity (Afzal et al. 2014).

Plant provides protection and residency to the endophytic bacteria whereas they, in return, produce plant growth hormones.

To understand the impact of cotrimoxazole on endophytic bacteria, it is important to consider the chemical nature and mode of action of both compounds, i.e., SMX and TMP. Briefly, SMX is a sulfonamide drug whereas TMP is pyrimidine inhibitor of dihydrofolate reductase. Both drugs are antifolate agents that can block synergistically the synthesis of tetrahydrofolic acid (Fig. 2.1). Tetrahydrofolic acid is a necessary cofactor during the synthesis of purine, thymidine, and thus nucleic acids. SMX is a structural analogue of the tetrahydrofolic acid precursor, *para*-aminobenzoic acid (*p*ABA). It competes with *p*ABA in the dihydrofolic acid synthetase reaction, hence, ultimately reducing the formation of tetrahydrofolic acid. TMP is the structural analogue of the pteridine portion of dihydrofolic acid, and competes with the physiological substrate dihydrofolic acid in the synthesis of tetrahydrofolic acid. Those bacteria that synthesize folate *de novo* cannot obtain tetrahydrofolic acid from their environment, thus the double blockade of two enzymes in the folate biosynthesis pathway causes inhibition of many gram-positive and gram-negative bacteria (Figure 2.1) (Acar 2012).

TMP and SMX are bacteriostatic individually, but when present together, they may become bactericidal; Bactericidal = kill bacteria, Bacteriostatic = reduce growth or reproduction.
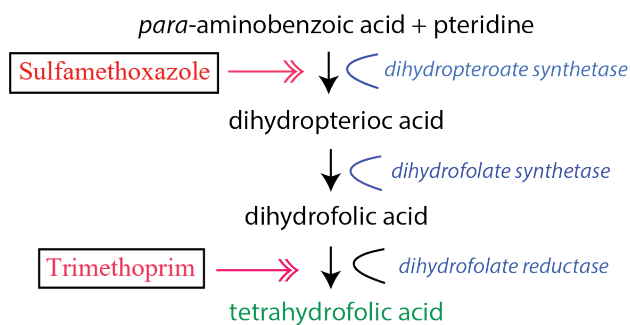
Figure 2.1: Synthesis of folate and mode of action for sulfamethoxazole and trimethoprim. Sulfamethoxazole competes with *para*-aminobenzoic acid to inhibit the synthesis of dihydrofolic acid whereas trimethoprim binds with dihydrofolate reductase and prevents the formation of tetrahydrofolic acid. Both antimicrobials act sequentially and inhibit the synthesis of tetrahydrofolic acid, which is an important cofactor in the anabolism of nucleic acids and amino acids. While humans and many other eukaryotes take up folate with their diet, many bacteria are obligate folate synthesizers and are hence affected by cotrimoxazole.

Both drugs blocks two consecutive steps in the biosythesis of nucleic acids and proteins which are essential for the bacterial growth.

The octanol-water partition coefficient (K_{ow}) for SMX and TMP is 0.89 and 0.91, respectively; therefore, both compounds can be taken up by the plant easily. Thereon, the endophytic community within the plant is prone to disturbances due to the antibacterial nature of cotrimoxazole. Nevertheless, no information is available on this topic at wastewater relevant concentrations of cotrimoxazole. This chapter addresses the response of the plant-endophytic community at low to moderate concentrations of SMX and TMP, i.e. 0.1 µg/L to 100 µg/L. Following the initial observation of a decline in plant fitness after cotrimoxazole exposure, this research addressed first the following questions:

Cotrimoxazole's mode of action makes it likely to affect in planta bacterial community.

1. How did cotrimoxazole exposure affect the endophytic bacterial community in *J. effusus*? Did the exposure eliminate beneficial endophytic bacteria?

2. What was the physiological response of *J. effusus* throughout the exposure and in the post-exposure period?

In this regard, a hypothesis was formulated in analogy of animal gut dysbiosis, which states that "*exposure with antimicrobials can inhibit beneficial bacterial endophytes that play an important role in defining host health*".

2.2 Methods

2.2.1 Experimental design and system operation

Continuous-flow Planted Fixed-bed Reactors (PFRs) were used as constructed model systems (three controls, four cotrimoxazole treated PFRs) (Kappelmeyer et al. 2002). Each PFR comprised a cylindrical glass vessel (30 × 30 cm) with a metal basket inside (height: 28 cm, diameter: 26 cm) filled with gravel (20 kg, diameter of 2–4 mm). PFRs were established by planting healthy shoots of *J. effusus*, previously grown in an uncontaminated environment. The schematic representation and a photograph of the model system are shown in Figure 2.2.

PFRs are model wetland systems and previously established as universal test system to study processes in CWs.

The PFRs were run in a continuous manner and the inflow to the systems comprised distilled water, trace metal solution, SMX and TMP, and constituents of artificial wastewater (Table 2.1). A plunger pump (ISMA-TEC, REGLO-CPF) and a syringe pump (KDS 200; DK Scientific, Inc., USA) were used to control the flow rate. The pore water volume of PFRs was maintained at ~8 liters with a continuous internal circulation flow (ISMA-TEC-MCP) and water level control system (Kappelmeyer et al. 2002).
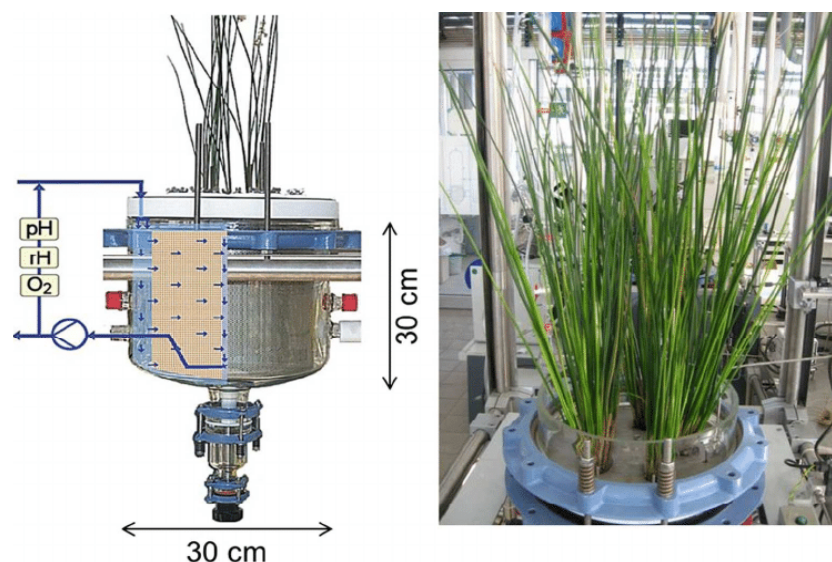
Figure 2.2: Schematic representation and photograph of the experimental system − Planted Fixed-bed Reactor (PFR). PFRs were planted with *J. effusus,* which was grown in tap water prior planting in the PFRs.

Table 2.1: The composition of artificial wastewater and trace mineral solution.

Type	Compound	Amount (mg/L)
Artificial wastewater	CH_3COONa	204.9
	C_6H_5COONa	107.1
	$K_2HPO_4 \times 3H_2O$	36.7
	NaCl	7
	NH_4Cl	118
	$MgCl_2 \times 6H_2O$	3.4
	$CaCl_2 \times 2H_2O$	4
	Na_2SO_4	222
	Trace mineral solution	1 ml/L
Trace mineral solution	EDTA-Na	0.1
	$FeSO_4 \times 7H_2O$	0.1
	$MnCl_2 \times 4H_2O$	0.1
	$CoCl_2 \times 5H_2O$	0.17
	$CaCl_2 \times 6H_2O$	0.1
	$ZnCl_2$	0.1
	$CuCl_2 \times 5H_2O$	0.02
	$NiCl_2 \times 6H_2O$	0.03
	H_3BO_3	0.01
	$Na_2MoO_4 \times 2H_2O$	0.01
	H_2SeO_3	0.001
	HCl	3 ml/L

(Wiessner et al. 2008)

Artificial wastewater was used in PFRs to mimic the conditions of natural wetlands treating wastewater.

In order to address the first research objective "*elucidating the response of endophytic bacterial community in a model wetland plant* Juncus effusus *to cotrimoxazole*", two studies were carried out.

In the aforementioned Master's thesis by Marcello Santoni on the fate of cotrimoxazole in CWs, two PFRs were initially exposed to 100 μg/L TMP and 10 μg/L SMX. These concentrations were chosen largely due to analytical reasons at that time. Furthermore, the high concentration of TMP was supposed to have negligible phytotoxicity because the compound is 50,000 to 100,000 times more active against bacterial dihydrofolate reductase than the eukaryotic enzyme (studied in humans).

Also, no toxicity of TMP is reported to several plant species up to concentrations greater than 10,000 µg/L (Hillis et al. 2011). By contrast, the concentration of SMX might be slightly phytotoxic as described earlier (Brain et al. 2008, Yan et al. 2017). For the experimental design, six phases were followed. In Phase I, plants were grown in the presence of artificial wastewater without TMP/SMX. In Phase II, the exposure was given (100 µg/L TMP and 10 µg/L SMX) and omitted to study the plant response. Thereon, three further phases (Phase III-V) of lower concentration exposure (i.e. 1 µg/L of TMP and 0.1 µg/L of SMX, respectively) were followed. The entire study was run for 12 months: exposure for Phase I and Phase II for 3 months each, and Phase III-V of 1 month each. There were no differences in the exposure regime for Phase III-V except that the pulse was given and omitted to monitor plant recovery in term of evapotranspiration rate (discussed in the paragraph below). In Phase VI, there were no antimicrobials in the system. Instead of observing pollutant transformation in PFRs, plant health was drastically reduced. This was not expected. Therefore, at the beginning of the present thesis, a study was designed and carried out to investigate the endophytic community in the plants (*J. effusus*) during the "post-exposure period". The hypothesis here was that the compromised plant health status was due to loss of beneficial endophytic bacteria. For this study, plant root and shoot samples were taken at the end of the study and compared with un-exposed plant tissues (growing in the natural environment). Questions 1 and 2 phrased at the end of Chapter 2.1 were mainly addressed during this study.

In the first study, instead of seeing successful phytoremediation of SMX and TMP, plant fitness was compromised.

The performance of PFRs and experimental conditions were regularly observed through online sensors fixed on the PFRs (Supplementary Table A.7 and A.8). Root and shoot status were monitored through visual observations. Additionally, evapotranspiration and number of green shoots were counted as surrogate parameters of plant health. The evapotranspiration rate was calculated twice a week as per the inflow and outflow volumes, whereas the number of healthy shoots was determined every three months. A complete illustration of the experimental design is shown in Figure 2.3.

A.

Control: Plants grown in natural environment.

Wastewater

Phase I: 3 PFRs treated in the absence of SMX and TMP.
Pre-exposure observations were made.
Evapotranspiration recorded to be higher than 7 ml/h.

Wastewater +
SMX + TMP

Phase II: PFRs treated with antimicrobials.
Experiment started with high concentrations.

Wastewater +
SMX + TMP

Phase III-V: PFRs treated with antimicrobials.
Concentrations were reduced. Each phase was similar.
Exposure pulse was given for short time and then omitted
to see the recovery of plants.

Wastewater

Phase VI: PFRs treated in the absence of SMX and TMP.
Post-exposure observations were made.
Evapotranspiration dropped to approximaltey 3 ml/h.

B.

	Phase I	**Phase II**	**Phase III**	**Phase IV**	**Phase V**	**Phase VI**
Concentration exposure	SMX: 0 TMP: 0 (µg/L)	SMX: 10 TMP: 100 (µg/L)	SMX: 1 TMP: 1 (µg/L)	SMX: 1 TMP: 1 (µg/L)	SMX: 1 TMP: 1 (µg/L)	SMX: 0 TMP: 0 (µg/L)

C.

Figure 2.3: (A) Experimental design describing the nature of exposure regime and primary observations, (B) details on exposure design for cotrimoxazole – sulfamethoxazole (SMX) and trimethoprim (TMP), and (C), response of plant recorded in terms of evapotranspiration in the un-exposed (Phase I) and post-exposure periods (Phase VI). Phase III-V were similar as a pulse was given and omitted to monitor plant recovery in term of evapotranspiration rate. PFR – planted fixed bed reactor; PFRa–c – treated with wastewater.

2.2.2 Cultivation dependent analysis

Isolation and characterization of bacterial endophytes from un-exposed and exposed plant tissues

To study if exposure of cotrimoxazole had eliminated endophytic bacteria, bacterial strains were isolated from un-exposed and exposed plant tissues after surface sterilization. Previously, isolation of bacteria after surface sterilization was reported as a recommended method for the

study of bacterial endophytes (Yousaf et al. 2011). For this purpose, un-exposed and exposed plant root and shoot sections were washed for 2 minutes in the sterilized distilled water. Thereon, root sections were placed in 70% ethanol for 10 min and shoots for 5 min. This was followed by 1 min rinse in 1% sodium hypochlorite (NaOCl) solution containing 0.01% Tween 20 solution. Next, plant tissues were washed thrice in sterilized distilled water. As a quality control step, absence of culturable bacteria of the last rinse was assessed by spreading 1 ml of the last rinse on nutrient-rich agar medium and incubation for 48 h (Afzal et al. 2011). Approximately 5 g of the plant tissues from each sample was grounded in a mortar in the presence of 0.9% NaCl (10 ml, w/v). The grounded plant tissues were agitated in a shaker for an hour at $30°C$. Serial dilutions up to 10^{-3} of the agitated solution were plated on solid Luria broth (LB) medium. The plates were then incubated for 48 h at $30°C$. There were 62 morphotypes identified based on the cell morphology; each distinguishable bacterial colony was purified by re-streaking at least thrice. Subsequently, two colonies from each morphotype were picked randomly and subjected to PCR amplification. For this, 16S rRNA gene was targeted using universal primers 27F (5′-AGAGTTTGATCCTGGCTCAG-3′) and 1492R (5′-TACGGYTACCTTGTTACGACTT-3′) (Weisburg et al., 1991). PCR products were then cleaned and sent to commercial service provider Macrogen (Amsterdam, Netherlands) for sequencing with the 27F primer. For characterization, obtained sequences were identified by performing nucleotide BLAST available at NCBI (http://blast.ncbi.nlm.nih.gov/Blast.cgi). The sequences were submitted to GenBank with the accession numbers ranging between KX885489 – KX885549.

Endophytic bacteria were isolated after surface sterilization of plant tissues.

Determination of plant growth-promoting properties of the isolated bacteria

In vitro assessment of plant growth promoting traits is an indirect way of studying bacterial behaviour in situ.

The isolated bacteria were tested for the four well-studied plant growth-promoting (PGP) traits, i.e., 1-aminocyclopropane-1-carboxylate (ACC) deaminase activity, production of indole acetic acid (IAA) and siderophore, and phosphorous solubilization. These traits are previously recognized as key parameters of endophytic bacteria that play a major role in defining the health of the host plant (Afzal et al. 2011, Andria et al. 2009, Ijaz et al. 2016). For this purpose, well-established methods

were adapted as explained previously (Naveed et al. 2014, Yousaf et al. 2011). Briefly, ACC deaminase activity of the isolated bacteria was assessed on minimal media containing 0.7 g ACC L^{-1} as a sole nitrogen source; IAA production was evaluated using Salkowski reagent, siderophore production was studied on Chrome Azurol S (CAS) agar medium, and phosphate solubilization was tested on Pikovskaya's agar medium (Naveed et al. 2014).

2.2.3 Plant stress response investigation

Production of reactive oxygen and reactive nitrogen species

The plant stress response was assessed to investigate if the endophytic community in the post-exposure period (Phase VI) was adopted by the plant or if the host was stressed due to the invasion of unwanted bacteria. For this purpose, molecular probes were used to detect reactive oxygen species (ROS), and reactive nitrogen species (RNS). CellROX® orange reagent (Life Technologies, USA) was used for ROS whereas 4-amino-5-methylamino-2',7'-difluorofluorescein diacetate (DAF-FM DA) was used for RNS (Life Technologies, USA). Earlier studies suggest that high ROS and RNS can be associated with the presence of pathogenic microbes, or at least the localization of un-wanted microorganisms (Torres et al. 2006), and was therefore used as a biomarker in this study. Confocal laser scanning electron microscope (CLSM) (SP5X, Leica, Germany), provided with a super continuum light source, was used to detect signal intensity at excitation / emission settings at 644/665 nm for ROS and 495/515 nm for RNS.

Production of reactive oxygen and nitrogen species is an indication of compromised plant basal defence system.

2.2.4 Cultivation independent analysis

Cultivation independent analyses were carried out to support the findings made via cultivation dependent analysis. It is a well-established fact that cultivation dependent analyses are subject to cultivation bias, which questions the accuracy of the results (Ellis et al. 2003). Thus, this study attempted to overcome possible biases in order to develop a comprehensive picture towards a better understanding of the plant-endophyte interplay during cotrimoxazole exposure. For this purpose, the following steps were carried out.

Cultivation independent analysis were carried out to eliminate any bias related to the cultivation of bacteria.

DNA Extraction

Genomic DNA was extracted from un-exposed and exposed roots and shoots of *J. effusus* by using the PowerSoil Kit, MoBio, Germany. Prior to that, the plant tissues were surface sterilized in order to target only the endophytic bacterial community (discussed in section 2.2.2). The roots and shoots samples were selected by a ranked set sampling procedure (Mehmood et al. 2014) in which thin tissue slices (1-2 mm) from the tip, middle, and base of the plants were prepared in order to represent the homogeneity of the studied specimen. Extraction was performed in triplicates and the DNA concentration in each extract was measured using NanoDrop (Thermo Fisher Scientific, Waltham, Massachusetts, EUA).

Quantitative PCR enumeration of bacterial endophytes and taxon-specific phyla

Quantification of desired gene via qPCR is one of the most reliable approach among all cultivation independent methods.

To enumerate the endophytic community within exposed and un-exposed plant tissues (roots and shoots), quantitative PCR (qPCR) was performed for total bacteria as well as taxon-specific groups, i.e., Gammaproteobacteria, Alphaproteobacteria (phylum Proteobacteria), Firmicutes, and Actinobacteria. The qPCR reactions were performed by targeting the respective 16S rRNA gene and were in accordance with established protocols (Bacchetti De Gregoris et al. 2011, Dorn-In et al. 2015). The primer sequences and efficiencies for the qPCR reaction are shown in Table 2.2. Primer efficiency indicates the PCR amplification efficiency of an amplicon when using a particular set of primers.

The qPCR assays were performed on a 7300 Real-Time PCR System (Applied Biosystems). Each reaction mixture contained 6.25 µL of SYBR Green (Kapa Biosystems), 4.25 µL of H_2O, and 0.25 µl of each 200 nM primer, and 1 µL of template DNA (a total of 12 µL). The thermocycling program included an initial denaturation at 95 °C for 10 min, following 40 cycles of 95 °C annealing and 1 min of elongation at 60°C. The standards were prepared from the PCR-amplified product of a pure colony of *Escherichia coli* for total bacteria, *Bacillus pumilus* for Firmicutes, *Micrococcus aloeverae* for Actinobacteria, *Pseudomonas putida* for Gammaproteobacteria, and *Rhizobium pseudoryzae* for Alphaproteobacteria. Standard curves over the dilution range of 10^8 to

10^1 copies of the target gene were linear and showed a detection limit of 10^1 copies. The samples were run in triplicates and the amplification efficiency was calculated by $10^{-1/slope}$.

Table 2.2: Nucleotide sequences (primers) used in the qPCR assays. Efficiency of the primers for each qPCR reaction is presented in the last column.

Name	Primer Sequence (5'- 3')	Taxon Target	Strand	Primer efficiency (%)
Com1	CAGCAGCCGCGGTAATAC	Bacteria	Forward	81.2
769R	ATCCTGTTTGMTMCCCVCRC	Bacteria	Reverse	
928Ffirm	TGAAACTYAAAGGAATTGACG	Firmicutes	Forward	92.2
1040FirmR	ACCATGCACCACCTGTC	Firmicutes	Reverse	
Act920F3	TACGGCCGCAAGGCTA	Actinobacteria	Forward	90.8
Act1200R	TCRTCCCCACCTTCCTCCG	Actinobacteria	Reverse	
1080γF	TCGTCAGCTCGTGTYGTGA	Gammaproteobacteria	Forward	87.7
γ1202R	CGTAAGGGCCATGATG	Gammaproteobacteria	Reverse	
α682F	CIAGTGTAGAGGTGAAATT	Alphaproteobacteria	Forward	88.9
908αR	CCCCGTCAATTCCTTTGAGTT	Alphaproteobacteria	Reverse	

(Bacchetti De Gregoris et al. 2011, Dorn-In et al. 2015)

To ensure that changes in the endophytic community were due to antimicrobial exposure and not because of natural variations, root and shoot samples were tested from nine additional wetland plants (controls). These plants were previously grown in the natural environment and controlled environment, i.e., PFRs without any exposure. The abundance values of bacterial endophytes generated by qPCR were plotted by using package "ggplot2" in R computational language (Wickham 2016). Additionally, the nonparametric statistics Wilcoxon–Mann–Whitney U rank-sum test (alternative to two sample *t*-test) was used to check the significant differences ($p < 0.05$). The test was applied using the `wilcox.test` function in R.

Fluorescent in situ *hybridization analysis*

To develop a better understanding of spatial colonization by endophytic bacteria in the pre- and post-exposure period, plant roots and shoots were subjected to fluorescent *in situ* hybridization (FISH) analysis. The plant tissues were cut into small parts (0.3 – 0.5 cm in depth) and put immediately in a 4% paraformaldehyde solution (4% in PBS, pH 7) for overnight fixation at 4 °C. The fixed plant tissues were washed twice in sterile phosphate-buffered saline (PBS) for 5-10 min followed by 10 min treatment with lysozyme solution (1 mg mL^{-1} in PBS) at 37 °C. Afterward, dehydration was performed in an ethanol series (25 to 99.9%; 15 min each step). The dehydrated plant tissues were then sliced into thin sections (approximately 2 – 5 mm) with a sterilized sharp edge blade (Gillette Platinum-Plus), and a minimum of 10 slices was fixed onto the pre-washed hybridization slide with ethanol 70%. Thereon, FISH analyses were carried out using group-specific probes (i.e., Firmicutes, Actinobacteria, Alphaproteobacteria, and Gammaproteobacteria) labeled with CY3 and Alexa488 dyes, while a negative control probe (NONEUB) was used as an internal control (Table 2.3).

Although semi-quantitative in nature, FISH is a power technique to visualize in situ *colonization of bacterial cells.*

For FISH analysis, hybridization was performed on each plant sample in the presence of 10-20 μL solution (0.9 M NaCl, 20 mM Tris-HCl at pH 8.0, 0.01% w/v SDS, probe specific formamide concentration, and 10 ng μL^{-1} of each probe) at 46 °C for 2 hours. The slides were then placed in a 50 mL moist chamber along with a tissue paper already moisturized with 5 mL hybridization buffer (40 mM ethanesulfonic acid, 0.1% polyvinylpyrrolidine 10 K, 0.1% Ficoll 4000, 140 mM NaCl, pH 7.8). Subsequently, plant tissues were washed at 48 °C for 30 min with pre-warmed solution (post-FISH) comprising 0.01% (w/v) SDS, 20 mM Tris-HCl (pH 8.0), 5 mM EDTA (pH 8.0), and NaCl at a concentration corresponding to formamide concentration (Supplementary Table A.1). Following post-hybridization, samples were rinsed twice with sterile distilled water and then air-dried for 24 h in the dark. After hybridization, plant tissues were observed under a CLSM system running the LEICA confocal software v 2.4.1 Build 1537 (Leica, Germany). The settings for excitation and emission/detection for CY3 gene probes were set at 560 – 610 and for Alexa488 at 510 – 610 nm. Images were convoluted in the IMARIS software for improved presentation.

Table 2.3: Names, sequences, and accession numbers of FISH probes used to study the spatial localization of Gammaproteobacteria, Firmicutes, and Actinobacteria via microscopic investigations.

Probe names	Sequence	Accession Number at probeBase	Target	Dye
GAM42a	GCCTTCCCACATCGTTT	pB-174	Gammaproteobacteria	CY3
LGC354A	TGGAAGATTCCCTACTGC	pB-195	Firmicutes	Alexa488
HGC69A	TATAGTTACCACCGCCGT	pB-182	Actinobacteria	Alexa488
NONEUB	ACTCCTACGGGAGGCAGC	pB-243	Control probe	CY3

(Alm et al. 1996, Compant et al. 2011); http://probebase.csb.univie.ac.at/

Illumina 16S rRNA Gene Amplicon Sequencing

Total DNA was extracted from plants in both studies and the endophytic community characterized by sequencing the V1-V2 region of the 16S rRNA gene using Illumina MiSeq. For the first study, DNA was extracted after the exposures when plant tissues turned necrotic and evapotranspiration was almost zero. For the second study, DNA was extracted every time when added concentrations of SMX and TMP were changed. Total DNA was also extracted from the pore water samples to study the response of the rhizospheric bacterial community during and after the cotrimoxazole exposure. PCR amplification of 20 cycles was performed using the 27F and 338R primers, followed by generation of amplicon libraries by targeting the hypervariable region V1-V2 of the 16S rRNA and then sequenced on a MiSeq (2×250 bp, Illumina, California, USA).

The 16S gene in bacteria contains nine hypervariable regions (V1-V9).

In order to generate operational taxonomic unit (OTU) tables, bioinformatics analyses were carried out. Briefly, raw reads were merged by using Ribosomal Database Project (RDP) assembler (Cole et al. 2013). MOTHUR pipeline was used to align the sequences which uses SILVA reference database (gotoh algorithm). The sequences were pre-clustered to yield so-called phylotypes, which were filtered for a sequence length of ≥250 bp and the average abundance of ≥ 0.02% before analysis. Data sets with overly abundant chloroplasts-derived sequences were excluded from the analysis part. Phylotypes were taxonomically assigned using the naïve Bayesian RDP classifier with a

16S amplicon sequencing is the standard approach for in depth investigations of microbial community structure.

pseudo-bootstrap threshold of 80% (Wang et al. 2007). A phylotype was assigned to a genus name when gene fragments of 16S rRNA of the previously described isolates belonging to that genus and 16S rRNA gene fragments originating from uncultured representatives of that genus showed only up to two mismatches (Schulz et al. 2018). The actual phylotypes abundance data was used to generate a dysbiosis fingerprint (heatmap with detrended correspondence analysis), rank-abundance curves, diversity indices, and abundance histograms in the package "phyloseq" (McMurdie &Holmes 2013) and ampvis2 (Skytte Andersen et al. 2018) in R computational language. The multivariate analysis non-metric multidimensional scaling (nMDS) with Bray-Curtis algorithm was performed on relative abundances of phylotypes (in percentage) using PRIMER-E (V.7.0.11, Plymouth Marine Laboratory, UK). The significant differences between sample groups were further evaluated by using analysis of similarity (ANOSIM) and permutational multivariate analysis of variance (PERMANOVA). Samples groups were considered significantly different when p-value was higher than 0.01.

Phyloseq is a bioinformatics tool to graphically analyze the microbiological sequencing data that has already been clustered into operational taxonomic units.

Function prediction based on 16S amplicon data

Function prediction based on 16S data is less effective but still a used strategy. The effectiveness mainly depends on the accuracy of database and citing literature.

Function prediction was carried out for the endophytic community detected from the plant roots using a manual approach. For the manual analysis, the top 25 most abundant taxa of the microbial community were selected, normalized with qPCR abundance data, and compared with the literature to extract biological information on the role of newly developed bacterial communities in *J. effusus*. Here, the main emphasis was given on the question "what these bacteria are feeding on to maintain their high abundance in the post-exposure period". The results of abundant taxa were plotted in the form of heatmap using ampvis2 in R computational language (Skytte Andersen et al. 2018).

2.2.5 Analytical measurements

Detecting the concentration of SMX and TMP in the pore water

The concentration of SMX and TMP were measured from the porewater using High Performance Liquid Chromatography-Tandem Mass Spectrometry (HPLC-MS-MS). For this purpose, 250 mL of water

samples were filtered (0.45 mesh) through a glass fiber filter (GE Healthcare, Buckinghamshire, UK). Subsequently, solid phase extraction (SPE) with Oasis HLB sorbent (200 mg, Waters, Milford, USA) was carried out. Before applying the filtered sample, the SPE sorbent was conditioned with methanol (Biosolve, Dieuze, France) and Milli-Q water. The sorbent was dried under a gentle stream of inert gas for 30 min, and the analytes were eluted with 10 mL methanol. The eluates were then concentrated to 0.5 mL by evaporating the methanol (TurboVap II, Biotage, SWE). Thereon, 5 µL of the prepared sample extract (HPLC solvent, water, and 5mM NH4ac) was injected into an HPLC-MS-MS system (Agilent 1260 HPLC instrument, Agilent Technologies, Waldbronn, Germany, and a triple stage quadrupole mass spectrometer, "QTrap 5500", SCIEX, Darmstadt, Germany). An Ascentis Express C18" column (10 cm × 3 mm id and 2.7 µm particle size, Supelco, Seelze, Germany) was used to perform chromatographic separation. Water with formic acid (0.1%, solvent A) and methanol with formic acid (0.1%, solvent B) were used to elute SMX and TMP at the flow rate of 300 µL min^{-1} and following a linear gradient (1 min 95% A, to 15 min 10% A, from 20 – 25 min 95 %A). The column oven temperature was set at 30 °C. Electrospray ionization was operated at positive mode with 5.5 kV spray voltage. Mass analysis at *multiple reactions monitoring mode* used the analyte-specific ion transitions listed in Supplementary Table A.2.

2.3 Results

2.3.1 First study

In the first study, observations on endophytic bacterial communities were made in the post-exposure period and then compared with the communities from un-exposed plant tissues. The outcomes of these sections aim to address the question raised in Chapter 2.1.

Fitness of J. effusus *declined after several exposures*

The fitness of *J. effusus* was assessed by visual inspections, counting green shoots, and monitoring of evapotranspiration, which is a key parameter to evaluate plant health status. A significant drop in

In the first study, the initial high concentration of cotrimoxazole caused a significant drop in evapotranspiration which recovered slightly upon omitting the exposure.

evapotranspiration was observed at the end of Phase II, whereas omitting TMP and SMX resulted in a partial recovery of the evapotranspiration albeit to lower values than prior the exposure. Further exposures at low concentrations (1 µg/L of SMX and TMP each) in Phase III to Phase V permanently reduced the evapotranspiration and plant shoots started becoming infested with insects. The number of green shoots increased to 354 in the absence of cotrimoxazole; however, later exposure reduced their number to 140 at the end of Phase VI (Figure 2.4). In the last phase (Phase VI), evapotranspiration was lower than 1 ml/h and the roots turned necrotic. The plant visual status before and after the exposure is presented in Figure 2.5.
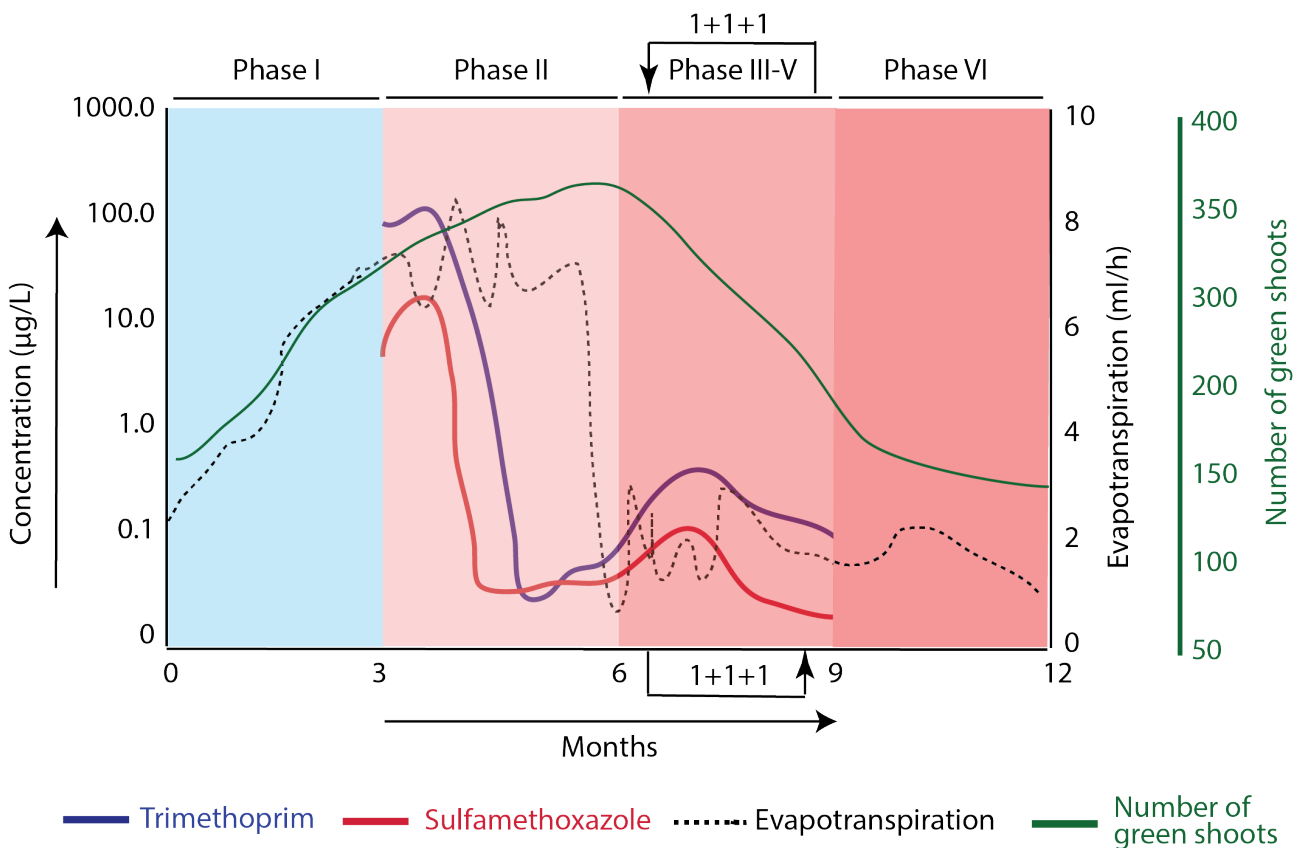
Figure 2.4: Exposure design for the first study depicting a drop of evapotranspiration upon initial high impulse exposure of sulfamethoxazole (SMX) and trimethoprim (TMP). Evapotranspiration is presented in the form of a dotted line; measured concentrations of SMX and TMP are presented with red and blue symbols; Phase VI represents the period when evapotranspiration rate was nearly 1 ml/h at the end and plant shoots were infested by insects. The level of SMX and TMP was not measured in Phase VI. The values presented are from 1 PFR; the other PFR essentially behaved similar (data not shown).
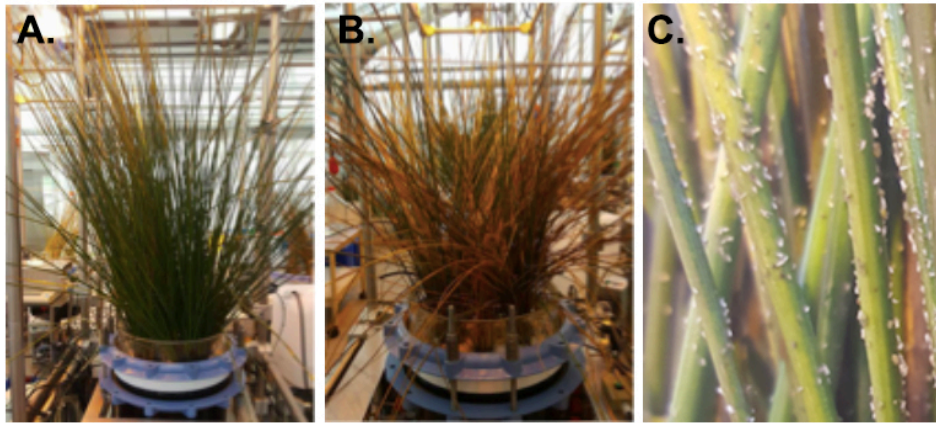
Figure 2.5: Plant status before and after cotrimoxazole's exposure in PFRs, (A) shoots of *J. effusus* were greenish before the exposure, (B) shoots of *J. effusus* started turning brownish during the exposure regime [the picture was taken in Phase VI], and (C) infestation of shoots with insects after the exposure. PFR: Planted Fixed-bed Reactor

Endophytes were present at increased abundances in the post-exposure period:

Cultivation dependent analysis

Tissues (root and shoot samples) were collected from exposed plants and comparisons were made with plants growing in the natural environment. Results revealed that abundance and diversity of the endophytic bacteria were increased in the exposed plant tissues. Colony Forming Units (CFUs) analysis revealed that this increase in endophytic bacteria was at least 10-fold from exposed roots and 6-fold from the exposed shoots (Figure 2.6).
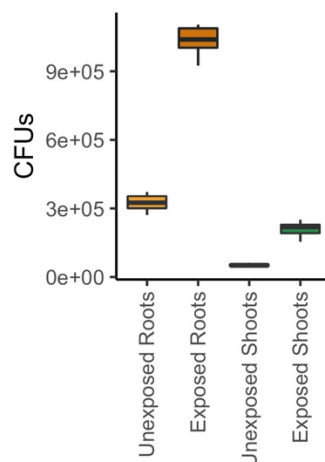
Cultivation dependent analyses revealed increased abundance of bacterial endophytes in the exposed plants tissues.

Figure 2.6: Comparison of the colony forming units (CFUs) in un-exposed and exposed plant roots and shoots. The total abundance of endophytic bacteria was increased 10-fold in the exposed roots.

In total, 26 bacterial species were identified from exposed plants, among which 15 inhabited roots and 11 were harbored by shoots. By contrast, only 15 species were identified from un-exposed plants, comprising 8 species from roots and 7 species from shoots (Table 2.4). The genus level taxonomy revealed the presence of *Bacillus* and *Rhizobium* species and their closer relatives *Paenebacillus*, *Fictibacillus* and *Agrobacterium* in the roots of un-exposed plants. The exposure of SMX and TMP resulted in the appearance of other genera including *Achromobacter*, *Pseudomonas*, *Microbacterium*, *Micrococcus*, *Enterobacter*, *Pandoraea*, *Leifsonia*, *Comamonas*, and *Stenotrophomonas*. Un-exposed shoots were inhabited with *Bacillus*, *Paenibacillus*, *Chryseobacterium*, *Brevundimonas*, *Buttiauxella*, and *Pseudomonas*, whereas exposed shoots harbored *Micrococcus*, *Pantoea,* and *Pseudomonas* in addition to *Bacillus*, *Paenibacillus*, and *Buttiauxella*. The relative proportion of *Bacillus*, *Paenibacillus*, and *Buttiauxella* was high in the shoots of exposed plants but the results were less substantial as compared to the roots. Most isolates from the un-exposed roots belonged to the Firmicutes and Alphaproteobacteria whereas exposed roots were mainly inhabited by Gammaproteobacteria*,* Betaproteobacteria*,* and Firmicutes (Figure 2.7)*.*
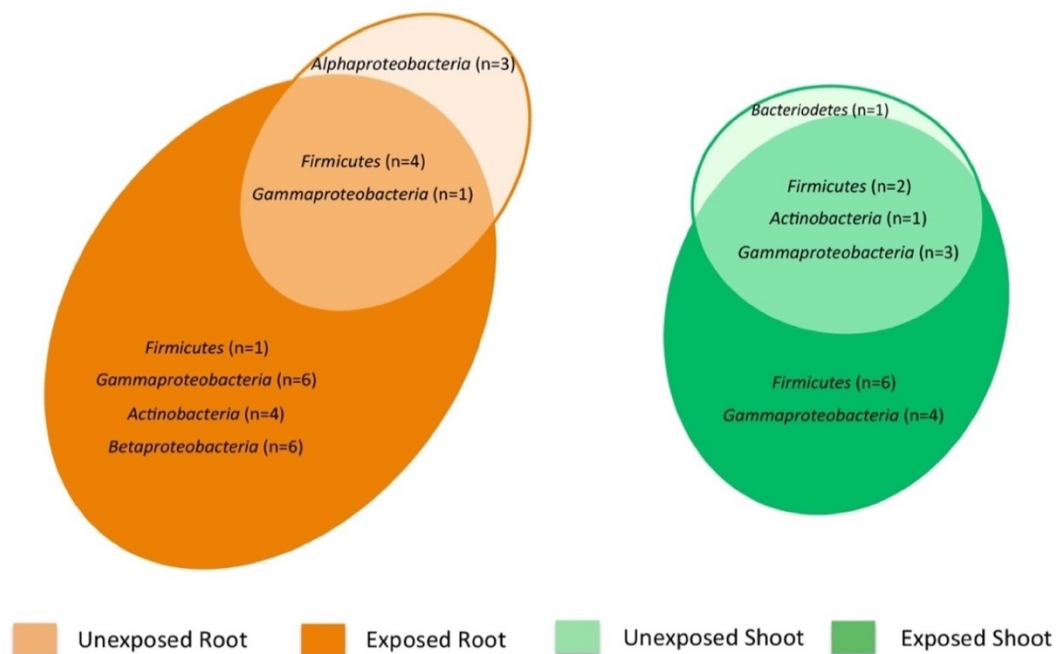
Figure 2.7: Venn diagram representing relative distribution of bacterial endophytes (taxonomy: phyla) before and after the exposure. The total abundance of the endophytic community increased in both roots and shoots after cotrimoxazole exposure.

Table 2.4: Isolated endophytic bacteria from un-exposed and exposed plant tissues.

	Species	Phylum / Class*
Un-exposed Root	*Bacillus pumilus*	Firmicutes
	Bacillus toyonensis	Firmicutes
	Fictibacillus phosphorivorans	Firmicutes
	Paenibacillus turicensis	Firmicutes
	Agrobacterium vitis	Alphaproteobacteria*
	Rhizobium pseudoryzae	Alphaproteobacteria*
	Rhizobium subbaraonis	Alphaproteobacteria*
	Pseudomonas cuatrocienegasensis	Gammaproteobacteria*
Exposed Root	*Bacillus pumilus* (n=3)	Firmicutes
	Bacillus toyonensis	Firmicutes
	Microbacterium azadirachtae	Actinobacteria
	Micrococcus yunnanensis	Actinobacteria
	Micrococcus aloeverae	Actinobacteria
	Leifsonia naganoensis	Actinobacteria
	Comamonas thiooxydans	Betaproteobacteria*
	Achromobacter animicus (n=2)	Betaproteobacteria*
	Achromobacter denitrificans	Betaproteobacteria*
	Achromobacter insuavis	Betaproteobacteria*
	Pandoraea pnomenusa	Betaproteobacteria*
	Enterobacter asburiae (n=2)	Gammaproteobacteria*
	Pseudomonas monteilii	Gammaproteobacteria*
	Pseudomonas putida (n=3)	Gammaproteobacteria*
	Stenotrophomonas maltophilia	Gammaproteobacteria*
Un-exposed Shoot	*Bacillus vietnamensis*	Firmicutes
	Paenibacillus amylolyticus	Firmicutes
	Chryseobacterium ginsenosidimutans	Bacteroidetes
	Brevundimonas vesicularis	Alphaproteobacteria*
	Buttiauxella izardii	Gammaproteobacteria*
	Buttiauxella noackiae	Gammaproteobacteria*
	Pseudomonas cuatrocienegasensis	Gammaproteobacteria*
Exposed Shoot	*Bacillus pumilus* (n=3)	Firmicutes
	Bacillus toyonensis (n=2)	Firmicutes
	Paenibacillus amylolyticus (n=3)	Firmicutes
	Micrococcus aloeverae	Actinobacteria
	Burkholderia contaminans	Betaproteobacteria*
	Buttiauxella gaviniae (n=2)	Gammaproteobacteria*
	Buttiauxella izardii	Gammaproteobacteria*
	Buttiauxella noackiae (n=3)	Gammaproteobacteria*
	Buttiauxella warmboldiae	Gammaproteobacteria*
	Pantoea rwandensis	Gammaproteobacteria*
	Pseudomonas chlororaphis	Gammaproteobacteria*

"n" represents number of isolated strains

Bacterial species in the post-exposure period were different than the species detected in un-exposed plant tissues. A suspected plant pathogen, *Pantoea rwandensis*, was detected after the exposure whereas the frequency of isolation of other potential opportunists such as *Bacillus pumilus* increased as well. Previously, *P. rwandensis* was isolated from Eucalyptus with symptoms of bacterial blight and die-back (Brady et al. 2012), whereas some strains of *B. pumilus* were found to be pathogenic (Yuan &Gao 2015). The increased abundance of endophytic bacteria in the post-exposure period (Fig. 2.6) together with the presence of suspected pathogens made questionable whether the decline in plant fitness after the exposure with cotrimoxazole was indeed primarily due to the elimination of beneficial endophytic bacteria as hypothesized at the beginning of this thesis. Therefore, a question was raised, "was the newly developed endophytic community playing a beneficial role for the host or was this community comprised of opportunistic or pathogenic bacterial species?" To address this question, two experiments were carried out. The bacterial community in the post-exposure period was tested for plant growth promoting (PGP) activities as well as plant stress response was assessed in terms of production of reactive oxygen species (ROS) and reactive nitrogen species (RNS). Analyzing stress response was used as a surrogate for querying for pathogenicity of the isolates as that would have been too time-consuming while having an uncertain outcome (e.g. it is far from trivial to identify an opportunistic pathogen as such). The results of these analyses are discussed in the sections below.

Detection of suspected plant pathogen raised several concerns over in situ *performance of the newly developed endophytic community.*

Some endophytes exhibited plant growth promoting traits: Cultivation dependent characterization

The PGP activities of the isolated strains were tested *in vitro* because there is no direct method established for the *in situ* measurements of these traits. Interestingly, the majority of strains displayed one or more PGP activities. Briefly, 33 strains displayed 1-aminocyclopropane-1-carboxylate (ACC) deaminase activity, 22 strains exhibited phosphorous solubilization potential, 20 strains showed production of indole-3-acetic acid (IAA), and 18 strains were capable of producing siderophores (Figure 2.8; Table 2.5). Only three strains from shoot did not exhibit any of the tested PGP activities. This led to the hypothesis that "cotrimoxazole allowed the growth of antimicrobial-insensitive bacteria that were opportunistic or pathogenic in nature".

In vitro *assessment of plant growth promoting activities revealed presence of beneficial traits in newly developed community.*
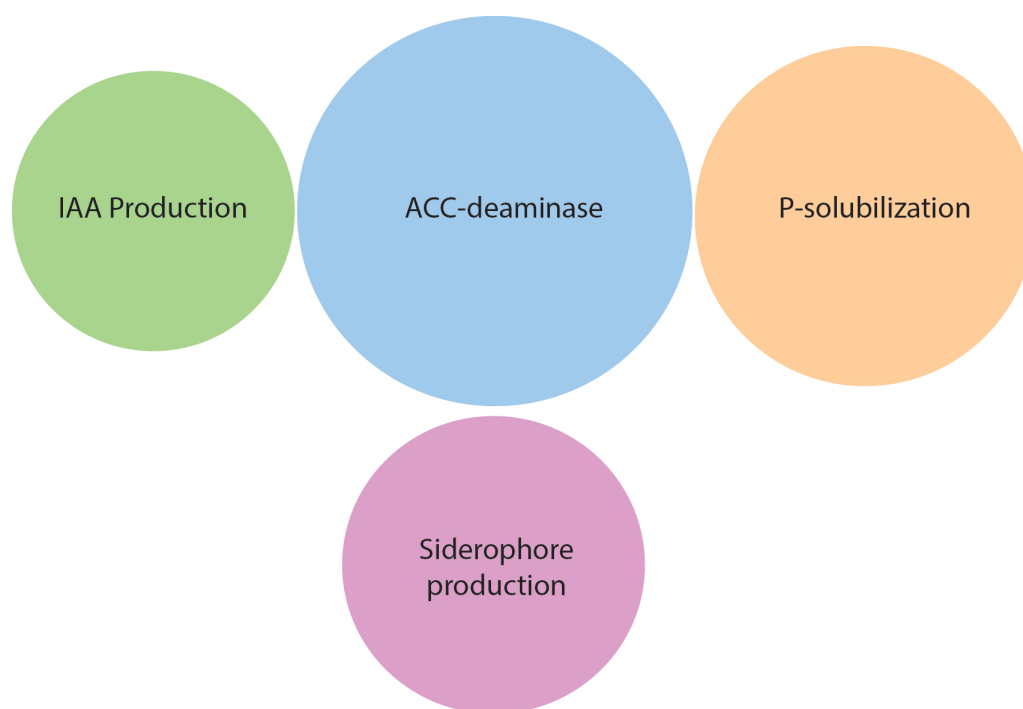
Figure 2.8: Proportional ellipses illustrating plant growth promoting (PGP) activities for the endophytic bacteria isolated from exposed plant tissues [IAA: indole acetic acid (IAA) production, ACC-deaminase: 1-aminocyclopropane-1-carboxylate deaminase, P-solubilization: phosphorus solubilization]. Area of the ellipses represents relative proportion of endophytic bacteria possessing the specific trait.

Table 2.5: Isolated endophytic bacteria exhibiting *in vitro* plant growth-promoting activities (ACC-deaminase, phosphorus solubilization, auxin production, siderophore production) from exposed plants.

	Bacterial strains	ACC-deaminase	P-solubilization	IAA production	Siderophore production
Endophytic bacteria in exposed roots	*Microbacterium resistens*	+	-	++	-
	Micrococcus yunnanensis	+	-	-	+
	Micrococcus yunnanensis	+	+	-	-
	Comamonas testosteroni	-	-	-	-
	Achromobacter insuavis	+	-	-	-
	Bacillus pumilus	+	-	-	+
	Achromobacter aegrifaciens	+	-	-	+
	Bacillus toyonensis	-	++	-	+
	Pseudomonas putida	+	-	++	-
	Leifsonia naganoensis	-	+	-	-
	Enterobacter asburiae	+	+	++	-
	Enterobacter asburiae	+	+	++	-
	Achromobacter insuavis	+	+	-	-
	Pseudomonas putida	+	++	++	-
	Pseudomonas putida	+	++	++	-
	Bacillus pumilus	+	++	-	+
	Achromobacter insuavis	+	-	-	-

RESPONSE OF ENDOPHYTIC BACTERIA

Bacillus amyloliquefaciens	+	+	-	++
Bacillus pumilus	+	-	-	+
Achromobacter insuavis	+	+	+	+
Stenotrophomonas maltophilia	-	+	-	+
Enterobacter asburiae	+	+	++	+
Stenotrophomonas maltophilia	+	++	+	+
Bacillus pumilus	+	++	++	+
Pandoraea pnomenusa	+	+	-	-
Achromobacter insuavis	+	++	++	+
Pseudomonas putida	+	+	-	+
Burkholderia contaminans	+	-	-	++
Buttiauxella warmboldiae	+	+	+	-
Buttiauxella gaviniae	-	++	+	-
Buttiauxella gaviniae	-	-	+	-
Buttiauxella gaviniae	+	+	+	-
Buttiauxella warmboldiae	+	-	+	-
Pantoea rwandensis	-	-	-	-
Pseudomonas fluorescens	+	+	++	+

Endophytic bacteria in exposed shoots

Buttiauxella warmboldiae	+	-	-	-
Buttiauxella warmboldiae	+	-	+	-
Buttiauxella warmboldiae	+	-	+	-
Bacillus cereus	+	-	-	-
Bacillus pumilus	+	-	-	+
Paenibacillus amylolyticus	+	-	++	-
Bacillus pumilus	+	-	-	+
Bacillus toyonensis	-	-	-	-

Verification of increased abundance of endophytic bacteria:
Cultivation independent analysis

In order to confirm that the increase in abundance of endophytic bacteria in the post-exposure period was not due to the cultivation bias, cultivation-independent analyses were carried out. For this purpose, abundance of total endophytic community as well as the abundant bacterial groups, i.e. Gammaproteobacteria, Firmicutes, Actinobacteria, were enumerated via qPCR. For the enumeration of total endophytic community, caution was taken regarding the selection of primers that amplify only bacterial DNA and avoid binding with the 16S rRNA gene chloroplasts and mitochondria (viz. endosymbiont theory) (Dorn-In et al. 2015). Quantification of Alphaproteobacteria and Betaproteobacteria was not possible due to methodological reasons. Briefly, qPCR-enumeration of Alphaproteobacteria gave higher counts than for total bacteria. This was likely due to cross-hybridization of primers with the 16S ribosomal RNA gene of mitochondria. Betaproteobacteria were not enumerated because no specific primer sequences usable in qPCR are available (Bacchetti De Gregoris et al. 2011). Results of qPCR confirmed that the total abundance of endophytic bacteria was at least 8-times higher in exposed plant roots as compared to the community present in the un-exposed plant roots. To test if this increase in abundance was statistically significant, non-parametric statistics were applied. The numbers of total endophytic bacteria from both studies were found to be statistically different for the roots [Mann–Whitney U test, p = 0.00004], whereas insignificant differences were seen for the shoots [Mann–Whitney U test, p = 0.2581] before and after the exposure. Taxon-specific qPCR analyses indicated that Gammaproteobacteria was the dominating group in the exposed roots among the tested ones, closely followed by Firmicutes. Actinobacteria was the least abundant phylum among the tested ones, nevertheless differences among un-exposed and exposed plant tissues were significant (Figure 2.9; Supplementary Table A3).

Cultivation independent analysis verified increased abundance of bacterial endophytes in the exposed plant roots.

The microbiome abundance among healthy individuals can have several yet un-explainable variations (Bäckhed et al. 2012). Therefore, to avoid any bias due to these natural un-explained variations, additional qPCRs reactions were carried out on plant root and shoot samples obtained from the natural and controlled un-contaminated

environment. At least nine biological replicates were used. Once again, results of qPCR were in accordance with the earlier observations made for the un-exposed PFRs, i.e. variation in the abundance of total and taxon-specific groups was within the normal range (Figure 2.11, Supplementary Table A.3). This analysis provided further evidence that the observed increase in endophytic community was not due to natural variations but rather a consequence of the exposure with cotrimoxazole.
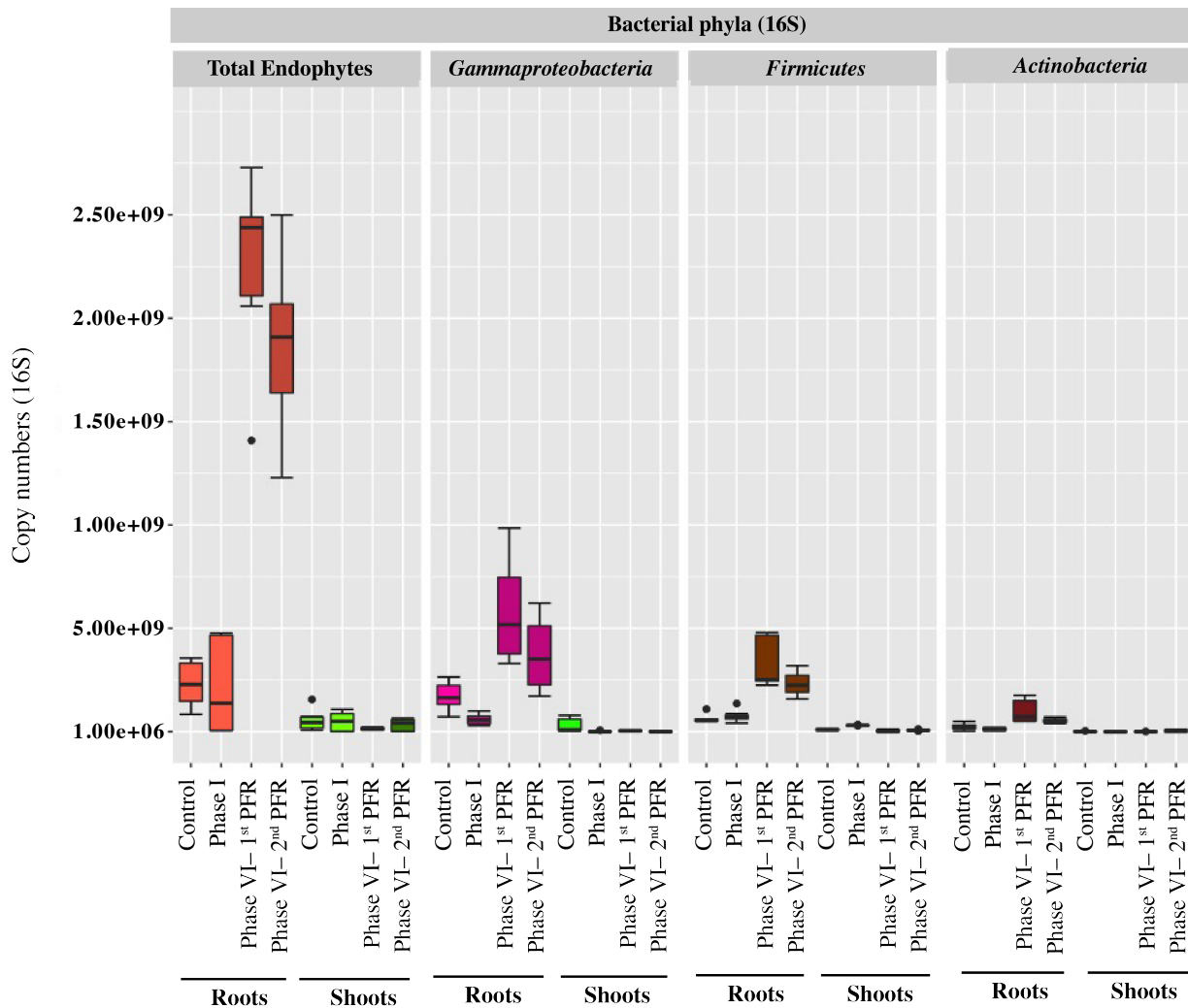
Figure 2.9: Quantitative PCR showing relative distribution of bacterial endophytes in terms of gene copy number (16S rRNA gene) from the plants growing in natural environment (Control), Phase I, and Phase V1. Abundance of endophytic bacteria was increased 8-fold in the exposed roots whereas Gammaproteobacteria was the dominating group.
PFR: Planted Fixed bed Reactor.

Plant defense was activated in the post-exposure period:
Microscopic analysis

To test if the newly developed endophytic community was opportunistic or pathogenic, plant stress response was measured by hybridizing molecular probes for ROS and RNS detection (Torres et al., 2006), and visualized under CLSM (see section 2.2.3 for details). The observations were made in the post-exposure period (approximately three months after the last exposure) and compared with the un-exposed plant tissues. This experiment was conducted to elucidate if the plant defense system was still activated even when no cotrimoxazole were in the system.

Study of ROS and RNS is a well-adapted method to test the invasion of potential pathogens.

Figure 2.10 displays the cross-sectional anatomy of the root interior of un-exposed *J. effusus* as background information for the results on CLSM investigations of stress response.
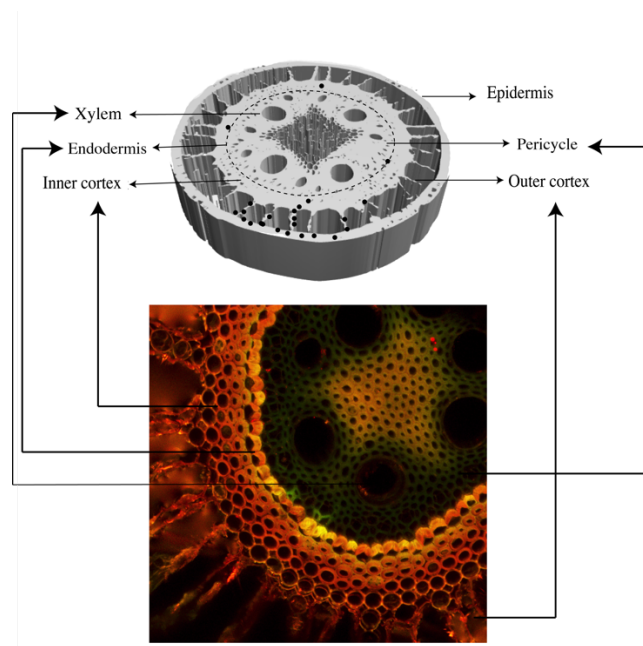
Figure 2.10: *J. effusus* root anatomy: single-celled epidermal layer surrounds the inner structure; cortex comprises radiating plates of cells separated by air spaces (also known as lacunae); cortex is subdivided into two parts, outer cortex – a layer of three to nine cells, inner cortex – a layer of three to eight cells; endodermis is one cell in thickness; the pericycle is one to three cells in thickness and occurs immediately after the endodermis; the conducting vessels or phloem occur in mature roots as inconspicuous patches pressed against the pericycle (Eleuterius 1976) (own drawing and own taken CLSM picture).

Increased production of ROS was recorded in the stressed roots, which was intense in the root center and reduced towards the periphery (Figure 2.11A,B). RNS production was evenly detected in the whole plant root (Figure 2.11C,D). Moderate ROS production was also observed in exposed shoots (Supplementary Figure A.1).

Increased in situ production of reactive oxygen and nitrogen species elucidated activation of plant defence.
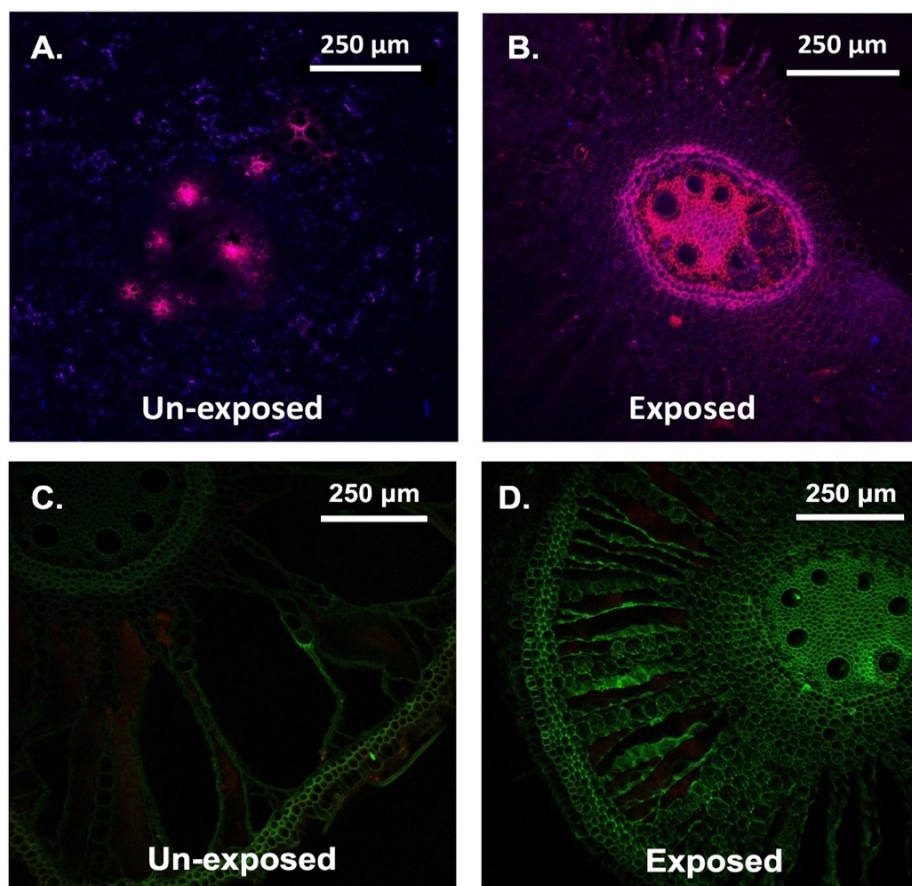
Figure 2.11: Micrographs representing the production of reactive oxygen species (ROS) and reactive nitrogen species (RNS) in plant roots before and after the cotrimoxazole exposure. (A, C) un-exposed roots exhibit lower production of ROS and RNS, (B, D) exposed plant roots shows high production. ROS production was more centralised whereas RNS production was distributed in the whole root interior.

New community excessively colonized plant root interior

Based on the aforementioned observations, a new question was raised, i.e. how the endophytic bacterial communities were spatially localized *in planta* before and after cotrimoxazole exposure? Specifically, did the regions of highest HR correspond with bacterial colonization pattern? To address this question, the abundant phyla were visualized through

fluorescent *in situ* hybridization (FISH) in order to study the spatial colonization of endophytic community in the post-exposure period (Phase VI) and in un-exposed plant tissues (Control). The visualization could be made with roots, while a high autofluorescence signal in the shoot samples resulted in artifacts and thus poor visualization. For the root's endophytic community, individual microbial cells were observed in the un-exposed roots, whereas thick colonies and smears, presumably microbial biofilms, were recorded from the exposed roots (Figure 2.12).

Thick colonies of bacteria were detected within the plant roots in the post-exposure period.
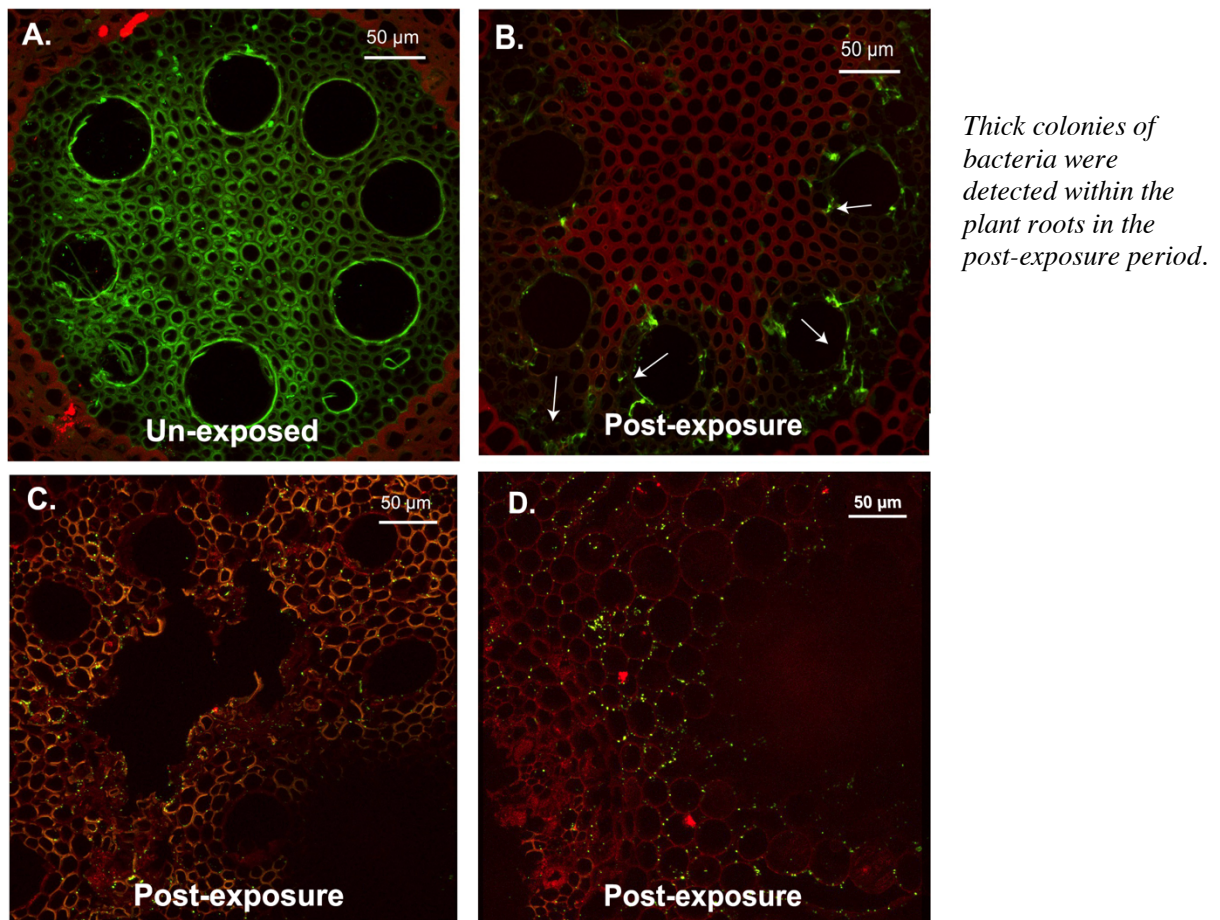
Figure 2.12: Microscopic visualizations of colonies of endophytic bacteria detected via SYBR Green I within the plant interior at two stages of cotrimoxazole exposure: (A) plant root before exposure of cotrimoxazole display compact root structures without any significant colonization of the endophytic bacteria, (B) plant root after the exposure (Phase VI) illustrates development of biofilms (shown with arrows) in the endodermis and phloem, (C) plant root in the post-exposure reveals damages within plant roots which are presumably the result of high ROS and RNS production, and (D) some unicellular bacteria colonizing the endodermis in the post-exposure period (Phase VI) (see below).

Moreover, colonization of endophytic bacteria was strongly influenced by the plant anatomical structures. For instance, more colonization was observed in the inner structures (endodermis, phloem, and pericycle) as compared to the outer structures (cortex, and epidermis) (Figure 2.10).

By performing probe specific FISH analysis, an important observation was made. In the post-exposure period (Phase VI), substantial colonization with Gammaproteobacteria was observed mostly along the inner walls of the phloem, which were essentially empty of stained microbial cells in the un-exposed plant roots (Control) (Figure 2.13). By visualizing in 3-dimensional space, it was further revealed that this group of bacteria was proliferating along the length of the phloem tubes. It is a possibility that bacterial growth in the phloem restricted transport of photosynthesis products into the roots. By contrasts, no such observations were made for the un-exposed plant roots (Control).

Substantial colonization of Gammaproteobacteria *was observed along the inner walls of the phloem.*
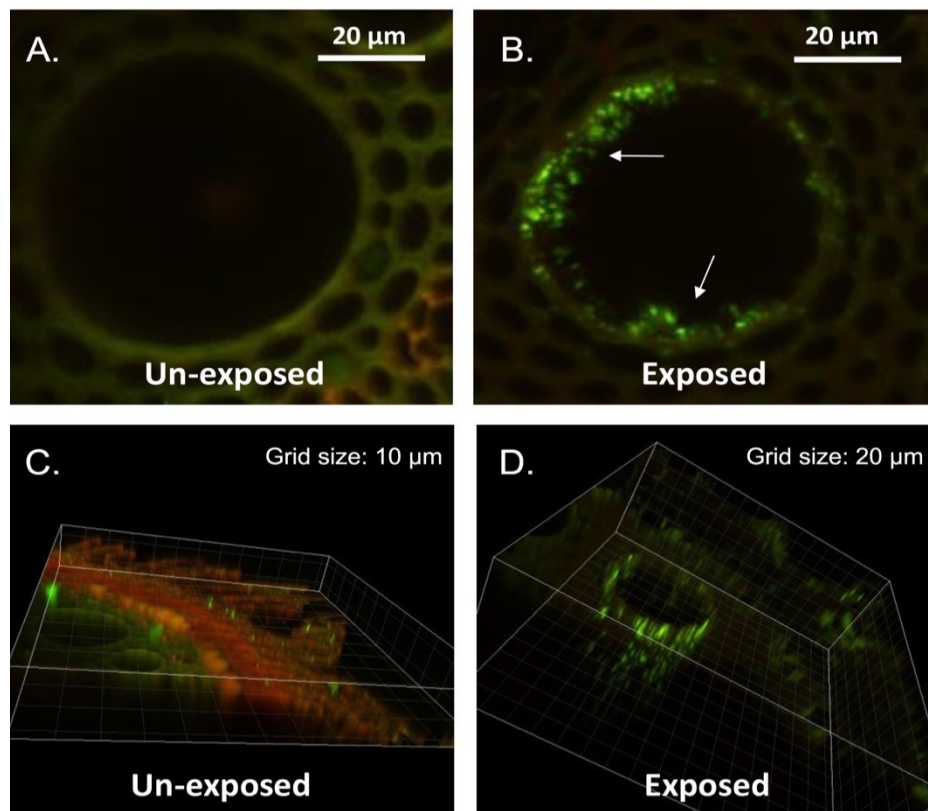
Figure 2.13: Colonization of Gammaproteobacteria in the phloem of the plant root before and after cotrimoxazole's exposure. Less colonization was observed in un-exposed root interior (A & C) as compared to the exposed root interior (B & D).

Similar results were observed for the outer root structures. Gammaproteobacteria were found to colonize the outer structures as well, i.e. inner and outer cortex, and epidermis (Figure 2.14). The pericycle and radiating cells of the cortex were colonized by bacterial biofilms whereas only a few bacterial cells were observed on these structures of un-exposed plant roots.
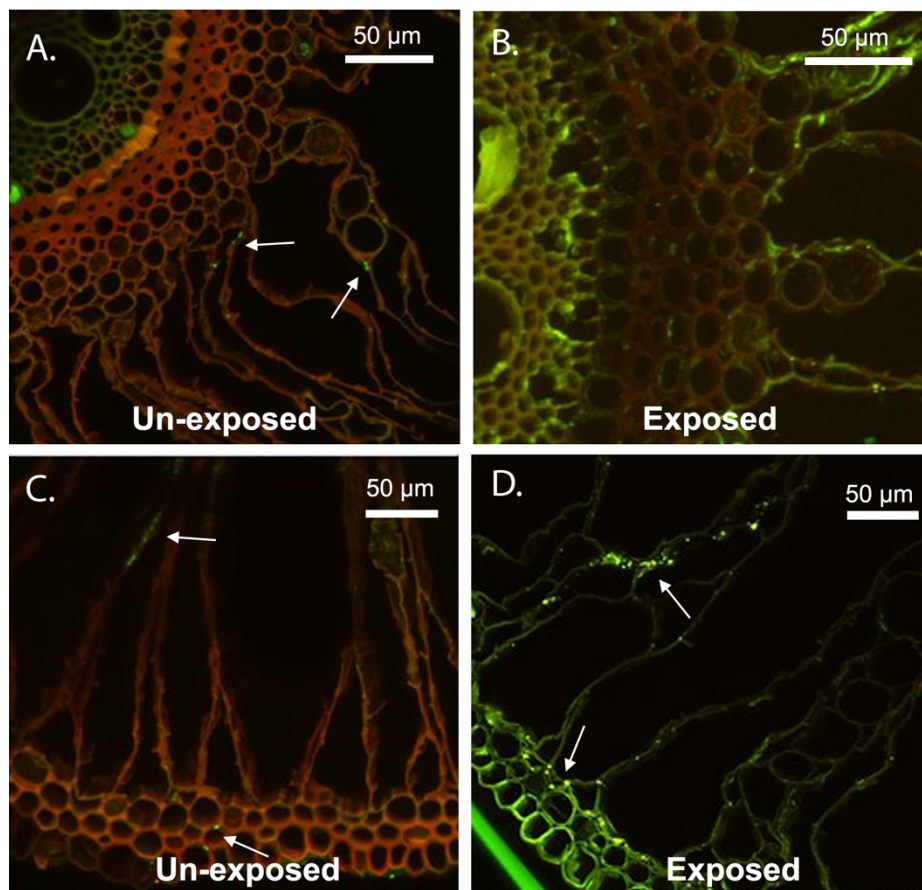
Endophytic bacteria formed thick colonies in the inner and outer cortex, and inner wall of epidermis.

Figure 2.14: Colonization of Gammaproteobacteria in the inner and outer cortex, and epidermis of the plant root before and after cotrimoxazole's exposure. Less colonization was observed in the un-exposed plant interior as compared to the exposed plant interior. In the un-exposed roots, a smaller number of endophytic bacteria were detected in the inner structures (endodermis, pericycle, and phloem) as compared to the outer structures (cortex and epidermis) (A,C); however, in the exposed roots, endophytic bacteria were ubiquitously colonizing both inner and outer structures (B,D).

Similar observations were made for the Firmicutes; however, non-specific binding of the probe resulted in poor quality micrographs (for details, see Supplementary Figure A.2). FISH analysis was also carried out to study the colonization of Actinobacteria. Results confirmed that

Actinobacteria was the least colonizing group among the studied phyla, for which slight or no differences were seen in the un-exposed roots and exposed roots (Supplementary Figure A.3). This finding confirmed the earlier observations made via cultivation dependent analysis, qPCR analysis.

FISH analysis for shoots was not successful due to a high autofluorescence signal.

New endophytic communities were different in terms of diversity, composition, and function:
Cultivation independent analysis

Major changes in the relative abundances of bacterial taxa were seen for the members of Proteobacteria.

In order to study the in-depth response of endophytic bacterial communities, 16S rRNA gene based amplicon sequencing was carried out for the exposed (Phase VI) and un-exposed plant tissues (Control). Here, over 1200 phylotypes were observed at the 97% sequence similarity level, which comprised >400 genera and >20 phyla. Proteobacteria, Bacteroidetes, Actinobacteria, Firmicutes, Acidobacteria, Spirochaetes, and Gemmatimonadetes were dominating the overall community in both exposed and un-exposed plant tissues (~95% of all reads). However, major changes were seen in the relative abundances of the members of Proteobacteria, i.e. mainly Alphaproteobacteria, Betaproteobacteria, Gammaproteobacteria, and Epsilonproteobacteria. Briefly, Betaproteobacteria were decreased in exposed plant roots and shoots whereas Alphaproteobacteria and Gammaproteobacteria were increased upon exposure (Supplementary Figure A.4). Epsilonproteobacteria were only detected from un-exposed plant tissues, and Deltaproteobacteria were evenly present in all samples. The relative abundance of *Acidobacteria* was increased in the exposed shoots. The relative read numbers affiliated with Alphaproteobacteria, Betaproteobacteria and Gammaproteobacteria matched the earlier findings on abundances made via cultivation dependent and qPCR analysis.

The main aim behind performing 16S amplicon sequencing was to observe changes in plant endophytic at lower ranks, e.g. genus level taxonomy. Hence, the data of the top twenty-five most abundant OTUs

(reflecting bacterial genera at 97% similarity, see section 2.2.4 for details) was manually analyzed by comparing with the literature. Here, three important observations were made for the plant roots (data on the top 25 most abundant OTUs is presented as Supplementary Table A.4). These were: (1) there was a vigorous iron cycle in the exposed roots, (2) abundance of one carbon C_1-oxidizing bacteria was increased, and (3) abundance of sulfur oxidizers was decreased after antimicrobials exposure.

More precisely, some iron oxidizers such as *Sideroxydans* were present in the un-exposed plant roots; however, in the post-exposure period, the relative abundances of both iron oxidizers, as well as iron reducers, were increased, e.g. *Ferritrophicum*, *Sideroxydans*, *Geothrix,* and *Geofilum*. We know that catabolic iron transformations yield only little metabolic energy per reaction run (Benz et al. 1998, Blake et al. 1993); hence, to run an iron cycle within roots, respective members of the endophytic community have to turn-over a substantial amount of iron to synthesize enough ATP for growth. Here, ferrous iron is presumably generated by ferric iron reduction by members of the genera *Geothrix* and *Geofilum* (Supplementary Table A.4). Such a cycle could operate at oxic-anoxic interfaces, indicating that those niches developed within the root. The electron donors for such a cycle were probably derived from the plant tissue since we assume that photosynthesis decreased and plant tissues started degrading due to intensive ROS/RNS production.

Post-exposure deductions on community profile reveal vigorous iron cycle, the flux of C_1 compounds, and a decrease in sulfur oxidizers

Secondly, the flux of one-carbon (C_1) compounds was apparently increased in the exposed roots as deduced from an increased abundance of *Methylocystis* and other C_1-oxidizing bacteria after the exposure. Members of the genus *Methylocystis* can use methane, methanol and to a minor extent other carbon compounds as catabolic substrate (Belova et al. 2013). In order to test whether methane was generated *in planta*, presence of methanogenic Archaea was queried for by PCR. PCR products were obtained with primers targeting total Archaea as well as with primers targeting ammonium-oxidizing Archaea but not for methanogens. This result suggests that methane was not generated at high rates, at least not *in planta*, and that the increased proportion of C_1-oxidizing bacteria inside root was due to the production of methanol stemming from the degradation of hemicellulose and/or pectin. High

ROS production may have contributed to this degradation process (discussed above).

Thirdly, sulfur oxidizers such as *Sulfuritalea* and *Sulfuricum* were highly abundant in the un-exposed plant roots but their proportion decreased significantly in the post-exposure period. In that period, phylotypes affiliated with the genus *Thiobacillus*, which is also a sulfur oxidizer, were abundant. To the best of my knowledge, such a high abundance of sulfur oxidizers was never reported in the literature for any other plant including *J. effusus*. At this stage of the study, it was unclear what the role of sulfur oxidizers was and what might have been the source of reduced sulfur such as sulfide or elemental sulfur in the plant roots. Sequences derived from sulfate-reducing bacteria were not found in the root endosphere and were only of very low abundance in the rhizosphere, the presence of which would have suggested a source of hydrogen sulfide in the plant interior. Maybe there was a high turnover of organosulfonates such as sulfoquinovose [accounting for approximately 1% of dry weight of leave tissue (Heinz 1993)] in *J. effusus*.

Computing diversity indices is an indirect way to assess the ecosystem stability and robustness.

In order to statistically interpret the changes within the endophytic communities after cotrimoxazole exposure, species diversity, evenness, and richness analyses were carried out. These analyses served as a starting point to understand how much stable were the endophytic communities before and after the cotrimoxazole's exposure (Shade 2016). In this regard, Shannon, Chao1, and Fisher's alpha diversity indices were measured. Briefly, Chao1 is a richness-based estimator for a community, Shannon's index combines evenness and richness in a single measure, and Fisher's alpha diversity analysis describes the mathematical relationship between the number of species and the number of individuals in those species. Results showed that in the post-exposure period (Phase VI), both richness and the evenness of the community increased in the roots but decreased in the shoots as indicated via Shannon's index. The values for Chao1 were increased in the roots and decreased in the shoots upon exposure. Fisher's alpha diversity index revealed that the diversity was similar for the exposed and un-exposed roots, whereas a decrease was found for the shoots in the post-exposure period (Figure 2.15).
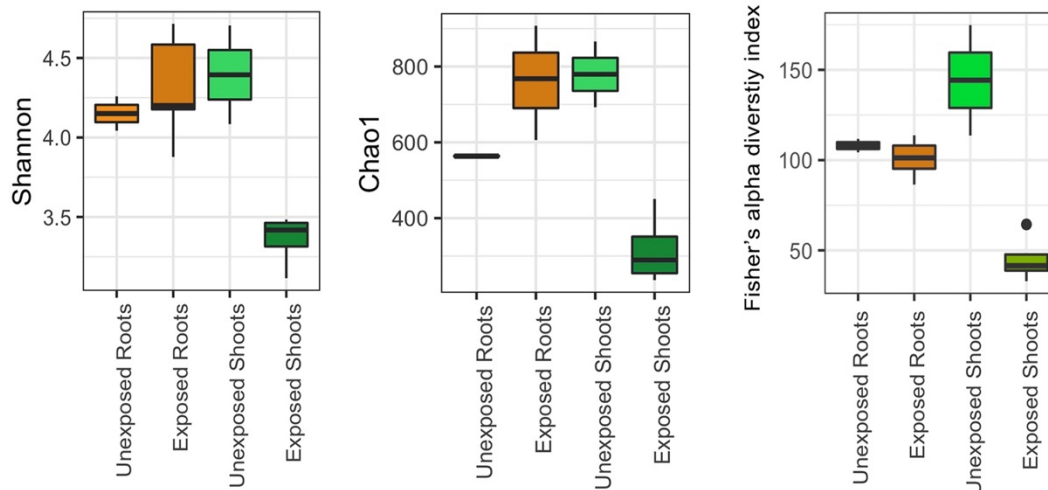
Figure 2.15: Box-and-Whisker plots illustrating diversity (Shannon and Fisher's alpha diversity indices) and richness (Chao1 index) of the endophytic communities. Diversity and richness were increased in the exposed roots, while exposed shoots displayed a decrease of these indices.

Together with genus-level information, these indices reflected that the endophytic community was changed in terms of diversity, composition, and function. This may have affected the robustness of this micro-ecosystem. Hence, in a follow-up data analysis, diversity patterns among exposed and un-exposed plant tissues were computed. Previously, it was stated that common patterns represent high level of similarity in ecological processes (Shade 2016). To this end, a non-metric multidimensional scaling (nMDS) test was performed based on Bray–Curtis dissimilarities. Briefly, nMDS is an indirect gradient analysis which produces an ordination diagram of the tested samples (Kruskal, 1964), whereas Bray–Curtis dissimilarity is a well-adapted statistic used for the quantification of the compositional dissimilarity between two different sites (Bray &Curtis 1957). The method has been very popular among human microbiome studies for the study of "healthy" and "dysbiotic" microbiomes (Castaño-Rodríguez et al. 2017, Chen et al. 2016). Results of nMDS showed that endophytic communities in the post-exposure period (Phase VI) clustered differently from the un-exposed community (Control) [based on the OTU level)]. Specifically, communities from un-exposed roots and shoots behaved similarly as they were clustered together in the nMDS plot; however, exposure of SMX and TMP resulted in significant changes in the community as shown in the form of distinct clusters in

Diversity patterns were computed to explain the functional similarities in different ecosystem.

the plot (test statistics = 0.91; 1 for complete separation and 0 for no separation) (Fig. 2.16).
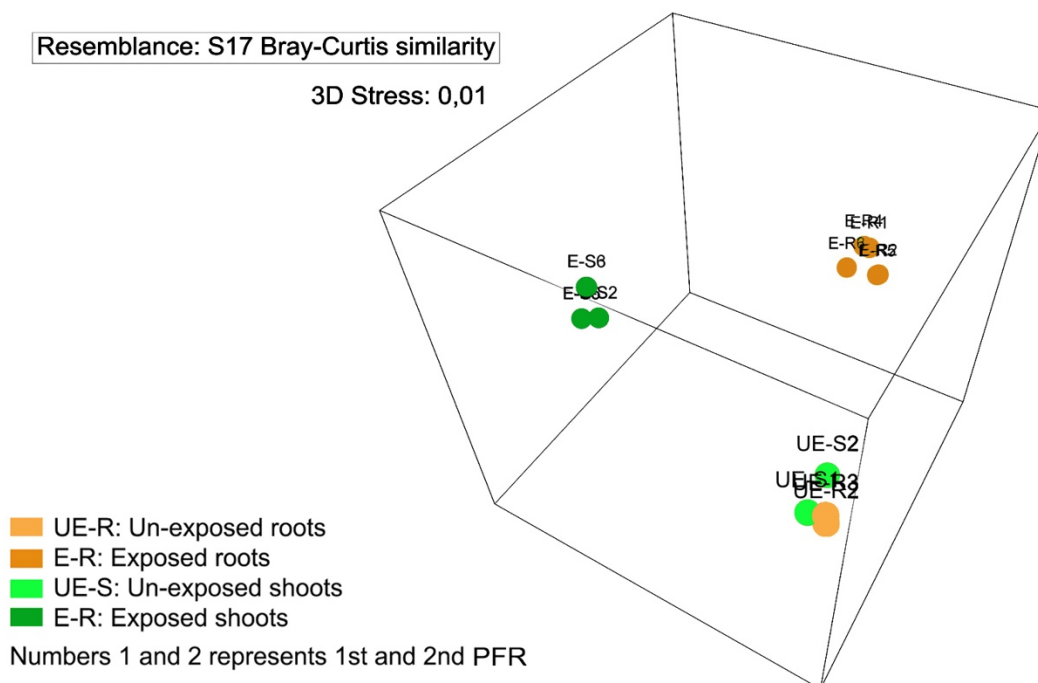
Figure 2.16: Non-metric multidimensional scaling (nMDS) ordination of endophytic bacteria in un-exposed and exposed plant tissues. Un-exposed roots and shoots are clustered together whereas communities in the exposed plant roots and shoots were significantly different from the un-exposed community (control). The community in the exposed roots was also significantly different from the community in the exposed shoots.

For further statistical validation of the above results, analysis of similarities (ANOSIM) and Permutational MANOVA were performed. These analyses supported the findings that the sample groups in the whole community differ significantly except for un-exposed roots and shoots (PERMANOVA, p=0.001) (Supplementary Table A.5 and A.6).

Further, for the visualization of OTUs data before and after the exposure, fractional abundances of OTUs were plotted in the form of a heatmap (based on detrended correspondence analysis) (Figure 2.17). Here, an additional advantage was to see if the change in the endophytic communities was related to the disappearance of indigenous

community (community before exposure) or appearance of new genera. Results were in favour of the hypothesis that the endophytic community from un-exposed plant tissues disappeared in the plant roots (Groups 1 and 3) whereas a new community proliferated after the exposure (Groups 2a,b and 4). These observations were prominent for the root endophytic community. Likewise, a fraction of the un-exposed community (control) in the shoots also disappeared but the appearance of new genera was not as strong as it was for the roots. These results correspond to the Fisher's alpha diversity analysis as reported above, i.e. diversity remained similar in the roots but decreased significantly in the shoots (see Figure 2.15).
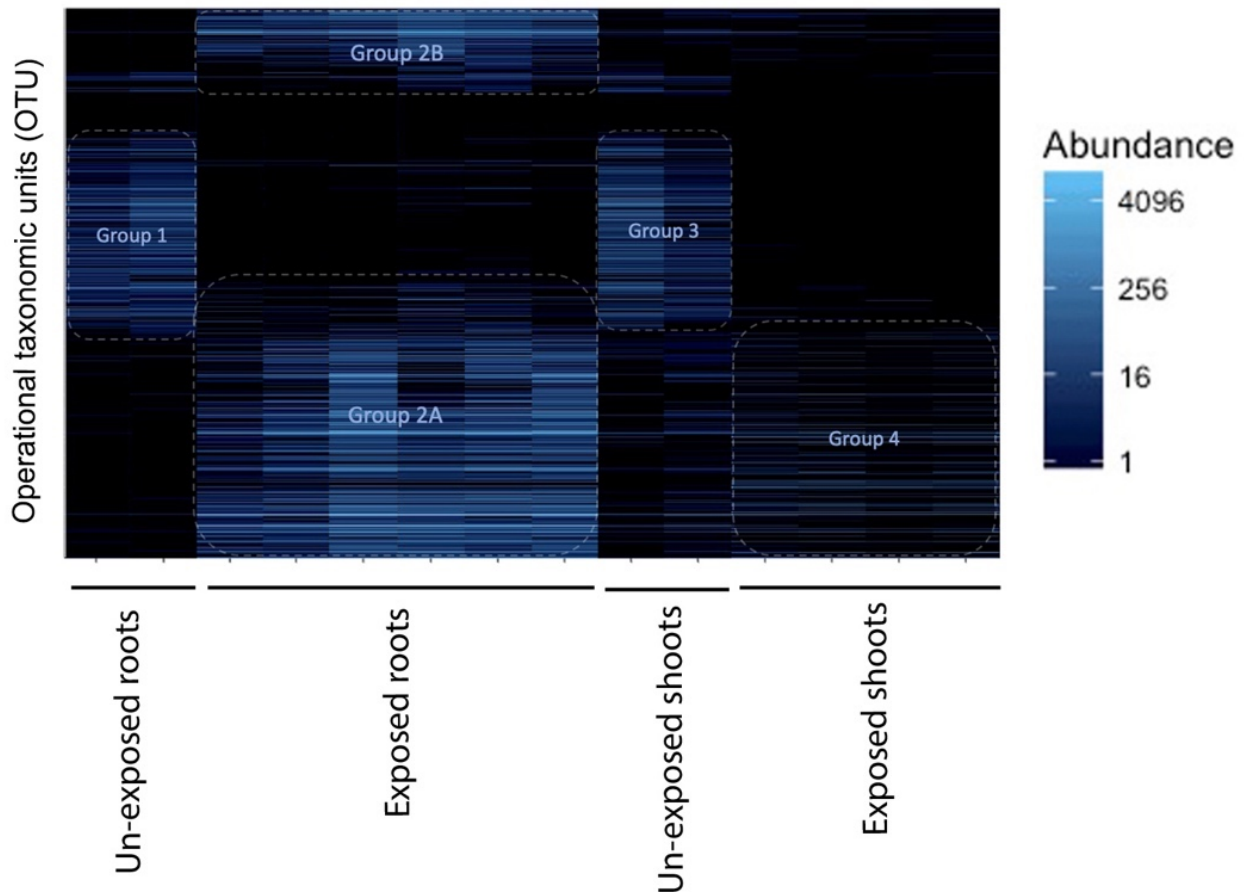
Figure 2.17: Heatmap illustrating of genus-level OTUs distribution and abundance for the exposed and unexposed plant tissues. Root endophytic community in the un-exposed period [Group 1] was replaced by a new community after the exposure [Group 2a,b]. Likewise, a fraction of indigenous shoot endophytic community was also inhibited [Group 3] while a new community proliferated in the post-exposure period [Group 4]. The heatmap was generated in an ordination-organized method based on detrended correspondence analysis.

2.3.3 Second study

In the first study, it was found that the endophytic community structure in *J. effusus* underwent major disturbances in terms of diversity and composition after cotrimoxazole exposure. This elicited further questions relating to the temporal changes in the endophytic bacterial community during the exposure regime.

Second study was carried out to answer questions related to the effective concentrations of cotrimoxazole for the bacterial community in J. effusus. *Additionally, plant physiological response was studied in a temporal fashion.*

1. Which temporal changes of the endophytic community structure occur upon step-wise increases in cotrimoxazole concentration? Which concentrations of cotrimoxazole were effective against the endophytic bacteria?

2. What is the response of the endophytic community in terms of diversity and composition at low to moderate concentrations of cotrimoxazole? Can we use the changes in endophytic community structure as a proxy of dysbiosis in plants?

3. Was there any role of the rhizospheric bacterial community in shaping the endophytic community structure upon exposure? Did the rhizospheric bacterial community experience similar changes as in the endospheric communities?

4. What was the physiological response of the plant to cotrimoxazole? At which phase does a decrease in plant health parameters become apparent?

To address these questions, the second study was carried out detailing with temporal changes in endophytic and well as rhizospheric community structure along with recording plant fitness parameters during the course of the study. After a phase without cotrimoxazole addition, exposure was started with the lowest concentration (i.e. 0.1 and 0.03 μg/L of SMX and TMP in the first phase), which were then step-wise increased to 10 μg/L of SMX and 3 μg/L of TMP in the second phase, 50 μg/L of SMX and 17 μg/L of TMP in the third phase, and lastly 100 μg/L of SMX and 33 μg/L of TMP in the fourth phase. Here, the concentration of SMX was always three times higher than of TMP in order to represent actual concentration ratios of cotrimoxazole in the wastewater (Göbel et al. 2005). This study lasted for 9 months. The plant tissues (roots and shoots), as well as pore water samples, were taken at each exposure concentration (Phase I–VI). Phase VI was

subdivided into two phases because of the changes recorded in terms of visual observations.

For this study, performance of PFRs and experimental conditions were also monitored through online sensors fixed on the PFRs (Supplementary Table A.7 and A.8). Likewise, root and shoot status were monitored through visual observations and evapotranspiration, and number of green shoots were counted temporally to record the plant fitness and growth. Additionally, for this study, plant fluorescence was recorded via a MINI-PAM-II fluorometer as an additional plant fitness parameter. The experimental design for the study is shown in Figure 2.18 whereas a description of the system's performance is presented in the following sections.

Fitness of J. effusus *declined during step-wise concentration increase of cotrimoxazole*

The observations on fitness of *J. effusus* for the second study were similar as for the first study, i.e. plant evapotranspiration was decreased in the post-exposure period, roots turned porous and necrotic, shoots became infested with insects, and the numbers of green shoots decreased. Additionally, the impact of concentration on system's performance was tracked more precisely. Briefly, a gradual decrease in evapotranspiration was seen for the 1st PFR while concentrations of 50 µg/L of SMX and 17 µg/L of TMP (Phase IV) brought a significant drop during Phase V; whereas, for the 2nd PFR, decrease in evapotranspiration was not prominent until plants were exposed to 100 µg/L of SMX and 33 µg/L of TMP (Phase V) (Figure 2.18). The plant roots remained intact (strong and light brownish) till the middle of Phase IV; however further exposure caused them to become dark brownish, porous and necrotic in Phase VI-a, and finally blackish in Phase VI-b. Likewise, the insect attack started by the end of Phase III for 1st PFR and middle of Phase IV for the 2nd PFR. In the post-exposure period (Phase VI), plant health status decreased despite of the fact that no antimicrobials (SMX and TMP) were present in the system. Based on the progression of the decrease as well root appearance, Phase VI is further divided into two sub-phases, i.e. Phase VI-a and Phase VI-b. This study was stopped when evapotranspiration was reduced to 2 ml/h of water transpired at the end of the Phase VI-b for

In the second study, decline in the fitness of J. effusus was similar to the first study despite of different exposure design.

1st PFR and 4 ml/h for the 2nd PFR. The number of green shoots decreased from 316 to 93 for the 1st PFR and 353 to 149 for the 2nd PFR. Total organic carbon (TOC) increased from 6.44 to 19.1 for the 1st PFR and from 7.75 to 17.2 for the 2nd PFR during Phase V and then started decreasing again. In the control reactors, TOC was recorded in the range of 8.1 to 10.0 mg/L. These observations are summarized in Figure 2.18.
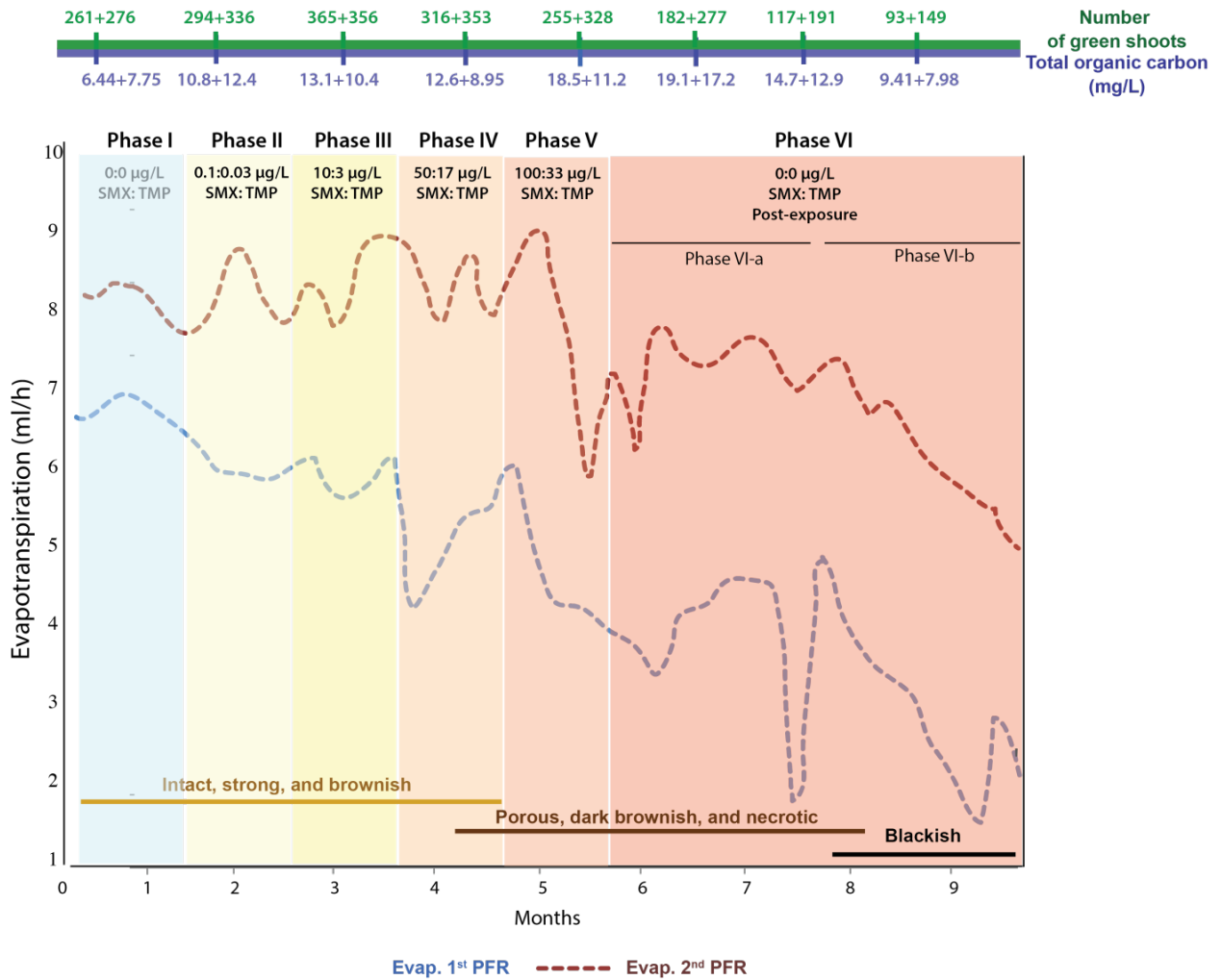
Figure 2.18: Exposure design and observations recorded for the second study. The study depicts a drop in evapotranspiration after an increase of cotrimoxazole concentrations. Evapotranspiration is presented in the form of dotted lines for the 1st (blue) and 2nd (red) PFRs; root status was evaluated based on visual observations (presented at the bottom); green line above represents number of shoots and blue line represents Total Organic Carbon content in the pore water for both PFRs (1st and 2nd values represent 1st and 2nd PFR respectively). PFR: Planted Fixed-bed Reactor

This increase in TOC is most likely derived from plant tissues because the inflow of acetate and benzoate remained constant (147.5 mg/L for acetate and 90 mg/L for benzoate), whereas the concentration of benzoate in the pore water remained below the limit of detection (LOD: 0.1 mg/L) and of acetate was occasionally < 1.2 mg/L but mostly below LOD (0.3 mg/L) throughout the experiment (Supplementary Table A.7 and A.8).

During this study, the level of chlorophyll fluorescence, which is a measure of photosystem II activity (PSII, F_v), was recorded. It provides an estimation of plant response to environmental stressors, whereas the high sensitivity of this technique is advantageous for the on-site analysis purposes (Murchie &Lawson 2013). Results on F_v/F_m indicated that the inhibitory effects of cotrimoxazole on PSII activity were not prominent until Phase IV, i.e. 50 µg/L of SMX and 17 µg/L of TMP (Table 2.6). This observation is in accordance with the observations made in terms of evapotranspiration which was recorded in parallel.

A sharp decline in chlorophyll fluorescence was recorded in Phase IV. These results were concomitant to the other plant health parameters.

Table 2.6: Measuring the chlorophyll fluorescence signal at different exposure concentrations.

Exposure	SMX and TMP concentration	F_v 1st PFR	F_v 2nd PFR
Phase I	0 and 0	357 (28)	386 (47)
Phase II	0.1 and 0.03	394 (35)	414 (54)
Phase III	10 and 3	370 (63)	406 (6)
Phase IV	50 and 17	251 (51)	332 (58)
Phase V	100 and 33	217 (27)	298 (55)
Phase VI-a	0 and 0	162 (59)	204 (64)
Phase VI-b	0 and 0	125 (17)	178 (39)

Each value is the mean of 10 values measured after 6 days of the respective increase to higher cotrimoxazole concentrations. Standard deviations are presented in parenthesis. PFR: Planted Fixed bed Reactor

Change in endophytic community was a dose-dependent phenomenon

For the second study, similar observations on the endophytic community structure were made as during the first study, i.e. the abundance of endophytic bacteria increased in the post-exposure period. These results were initially tested via qPCR (Supplementary Figure A.5). Nevertheless, since this study was conducted to reveal how the endophytic community behaved at different concentrations of cotrimoxazole and if the change occurred abruptly or whether happened in a slow but continuous manner. Thus, 16S rRNA gene amplicon sequencing was performed for the root samples targeting endophytic bacterial communities. Here, we had the advantage of the step-wise increase in the concentration of cotrimoxazole, which elucidated the changes in a temporal fashion. To address the question of temporal change in diversity, results of amplicon sequencing were first subjected to Fisher's alpha diversity analysis. Here, the hypothesis was, "exposure of cotrimoxazole could have inhibited the endophytic bacteria leading to decrease in diversity". As mentioned earlier, such a decrease in alpha diversity has been well-recognized as a dysbiosis in animals. However, the commonalities in plant kingdom are still under debate (see section 1.6). The results confirmed that in the 1st PFR, alpha diversity was decreased gradually with an increase in the cotrimoxazole concentrations until Phase V. In later phases, a regain in diversity was seen. For the 2nd PFR, diversity was decreased in Phase IV but recovered in later phases (Figure 2.19). These changes in diversity are in accordance to the changes observed for plant health parameters for both PFRs.

Decrease in alpha diversity was similar to the earlier studies reporting dysbiosis in animal gut.

Figure 2.19: Box-and-Whisker plots depicting Fisher's alpha diversity index for both PFRs. In the 1st PFR, diversity decreased with the increase of cotrimoxazole concentration until Phase V whereas, in the 2nd PFR, drop in diversity was observed in Phase IV. In later Phases, a regain in diversity was observed. Phase VI-a and Phase VI-b represent samples taken in the middle and at the end of Phase VI (evapotranspiration was further dropped in Phase VI-b).

Decrease in alpha diversity is in accordance to basic criteria of dysbiosis in animal kingdom.

Next, the pattern of endophytic diversity in the plant roots was studied via principle component analysis in order to establish the host-microbiome signatures for *J. effusus* during cotrimoxazole exposure. Based on the earlier observation, this analysis was performed to address two further questions: (1) does the change in endophytic community between Phase I and Phase IV for both PFRs was similar at community level? and (2) if the regain in bacterial diversity after Phase IV was related to the recovery of the endophytic disturbed community or whether it was a new community? First, although the reduction in diversity was prominent only for 1st PFR until Phase IV (the significant decrease was seen in Phase IV for the 2nd PFR), results of principal component analysis illustrated endophytic community in both PFRs

was still similar. Secondly, distinct clustering was seen for the endophytic communities. Three clusters were obtained: (A) the first cluster comprised the communities of the Control, Phase I, Phase II, and Phase III; (B) the second cluster comprised the communities from Phase IV, Phase V, and Phase VI-a; and (C) the third cluster comprised the community from Phase VI-b (Figure 2.20). This part confirmed that the regain in alpha diversity was not due to the recovery of the initial microbiome but rather that a new community took over the system.

Changes in endophytic communities were lasting because regain in endophytic diversity was not related to recovery of indigenous microbiome.
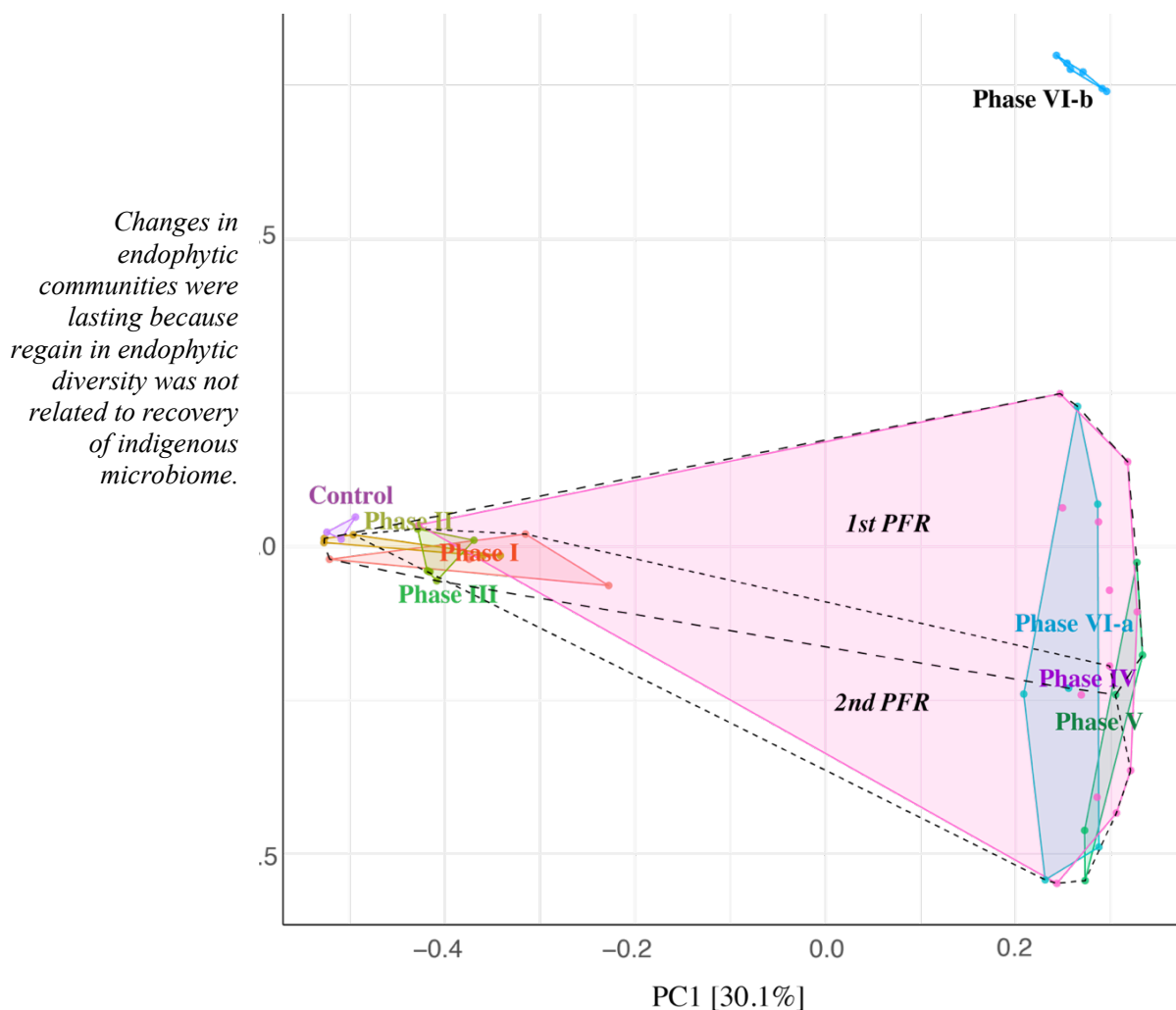
Figure 2.20: Principle component analysis illustrating dose-dependent effect of cotrimoxazole on endophytic community structure *in J. effusus*. The communities displayed three distinct clusters. The first cluster comprised of communities from Control, Phase I, Phase II, and Phase III; the second cluster representing communities from Phase IV, Phase V, and Phase VI-a; and the third cluster for the communities from Phase VI-b only.

In order to further understand the results of principle component analysis, network analysis was carried out. Recently, microbiome network analysis (based on network theory) is proposed as an exciting holistic methodology that can enhance our understanding of microbiome in terms of microbe-microbe and microbe-host interactions (Layeghifard et al. 2017). Therefore, in-depth observations were made for root and shoot endophytic communities in different phases. Once again, distinct but clearer clustering was seen for different phases and less significant differences were observed between both PFRs. Briefly, root and shoot endophytic communities were similar for Control, and Phase I-III (Figure 2.21). However, in Phase IV to Phase VI-a, a separate cluster was observed. For Phase VI-b, the endophytic community structure was different for both roots and shoots. This observation was similar to the findings made during the first study (cf. nMDS plot, Figure 2.16).
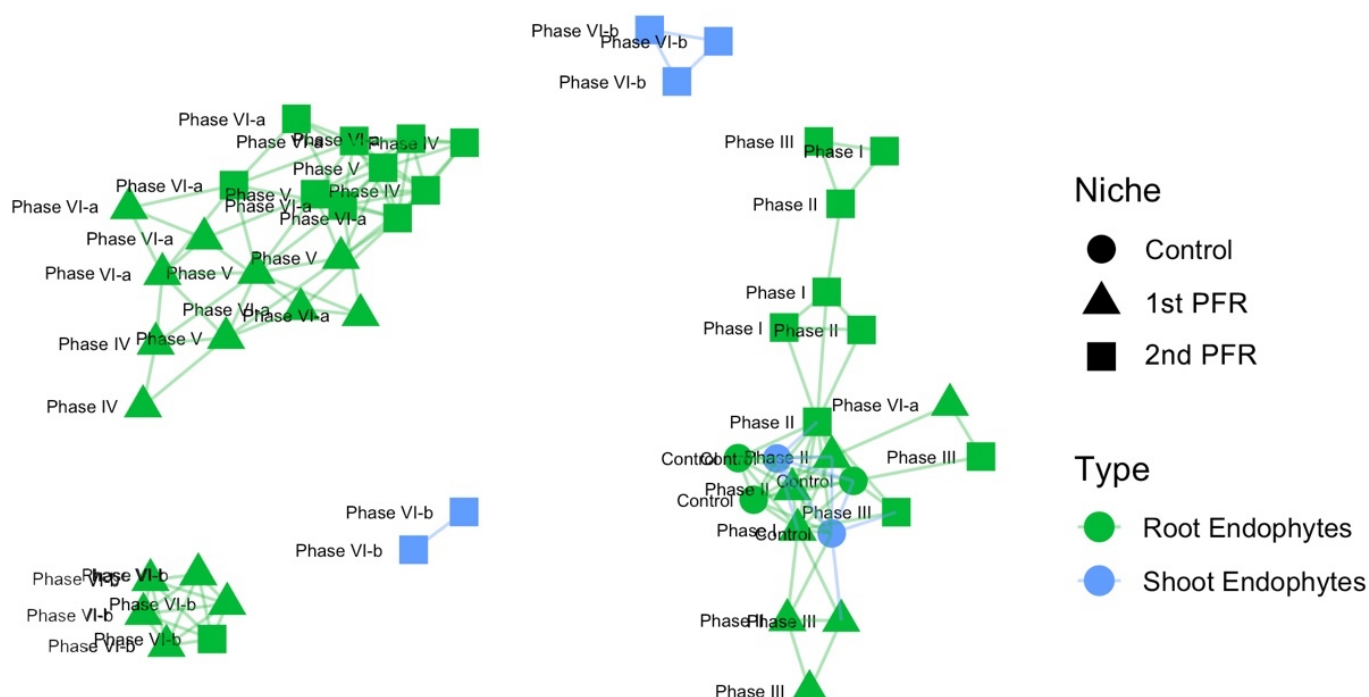
Figure 2.21: Network analysis confirmed the dose-dependent effect of cotrimoxazole to the endophytic community. The root endophytic community for Control, Phase I, Phase II and Phase III were clustered together; the communities for Phase IV, Phase V, and Phase VI-a were clustered together; and the community from Phase VI-b was different from any of the community structures from earlier time points. Shoot endophytic community for control (plants grown in natural environment) displayed close clustering with root endophytic community of Control. Upon exposure, shoot endophytic community exhibited a separate clustering in for both Phase VI-a and Phase VI-b.

In addition to these overall community-level changes, response of endophytic communities was also looked at the genus level to interpret the previously made observations on flux of C_1 compounds, iron cycle, and sulfur oxidizers (Figure 2.22). The results confirmed these observations as well as provided an extended overview of changes in bacterial genera in different phases. First of all, it became clearer that the flux of C_1 compounds was increased significantly in Phase IV (50 µg/L of SMX and 17 µg/L of TMP). For example, *Methylocystis* became abundant up to 5% of the total bacterial community in Phase IV. As discussed for the first study these microbes may have grown on plant cell wall-derived methanol. Secondly, a similar observation was made for iron cycle as the abundance of *Geothrix* increased from ~2% up to 10% in Phase IV. The members of *Geothrix* link the iron and carbon cycles under strictly anaerobic conditions. They can oxidize organic compounds all the way to carbon dioxide coupled to the reduction of ferric to ferrous iron. The increased abundance of strict anaerobes such as *Geothrix* suggests that the development of oxic-anoxic niches within roots (discussed above) likely happened in Phase IV (Figure 2.22). In the same phase, the abundance decreases of aerobes such as *Kineococcus*, *Rhizobacter*, *Gemmatimonas*, *Aquabacterium*, *Ideonella*, and *Hydrogenophaga* also supported the idea that conditions in at least in some root patches started turning anoxic upon cotrimoxazole's exposure (Figure 2.22). Thirdly, phylotypes affiliated with sulfur oxidizers (e.g. *Sulfuritalea*, *Sulfuricurvum*) were highly abundant up till Phase III but their relative proportion decreased drastically in Phase IV onward. Previously, *Sulfuritalea* was reported as a facultative autotroph that is present in fresh water whereas *Sulfuricurvum* is a facultatively anaerobic and chemolithoautotrophic bacterium (Kodama and Watanabe, 2004).

Additionally, *Treponema* was found to be a highly abundant genus from Phase IV onwards (Figure 2.22). While this genus comprises prominent human pathogens, nothing specific is known about its function and life style in plant-based habitats. It was detected previously in wetlands (Yan et al. 2017) and in rice roots (Bertani et al. 2016), and it has been recently reported that the absolute abundance of this genus increased in CWs treating pharmaceutically active compounds such carbamazepine, sulfamethoxazole, ofloxacin, and androxithromycin (Yan et al., 2017). Furthermore, it was shown that members of the Spirochaetes family can grow as acetogens using

Temporal investigations on 16S amplicons not only confirmed the observations made in the first study, but also provided an extended overview of the development and functioning of new endophytic communities.

hydrogen as an electron donor or various organic compounds as substrates (Chouari et al. 2005, Dong et al. 2018), as well as scavenging of detrital biomass (Dong et al. 2018).
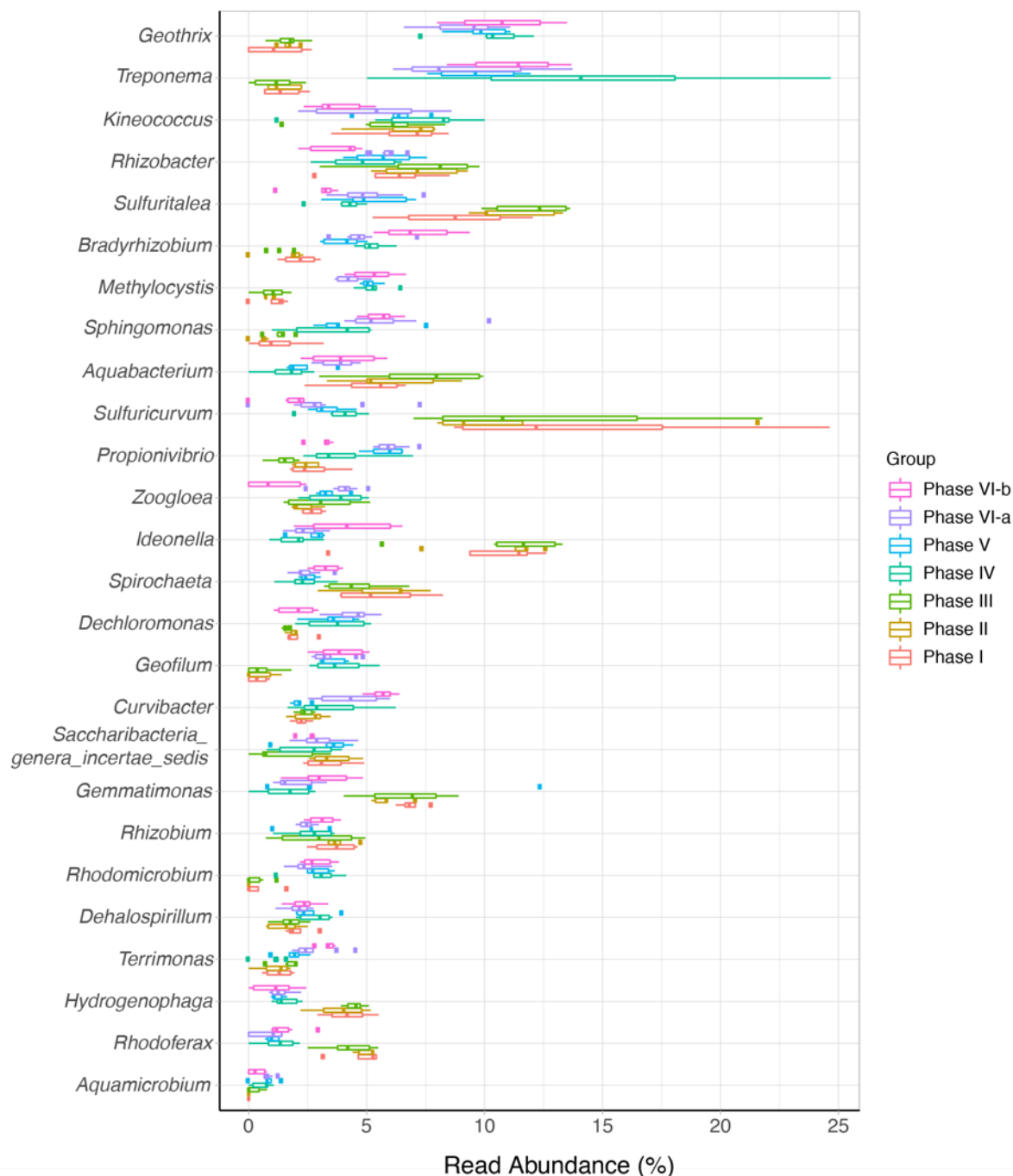
Figure 2.22: Quantitative PCR normalized abundance data of the top twenty-five OTUs in the exposed plant roots in different phases. None of the detected bacteria were previously reported as known plant pathogens. Major changes at genus level taxonomy for the bacteria became prominent in the Phase IV.

Response of rhizospheric bacterial communities to cotrimoxazole

As discussed earlier, another aim of the second study was to investigate the response of pore water bacterial community in terms of (1) how the abundances in rhizospheric bacterial community changed during the exposure regime, and (2) if rhizobacteria played any role in shaping the endophytic community upon cotrimoxazole exposure.

Results of qPCR indicated no major differences in the absolute abundances of rhizospheric communities during the exposure regime.

To address the first part, qPCR-based enumerations as with the endophytic communities were carried out. Results of qPCR revealed that, in contrast to the endophytic community, the rhizospheric community did not show any abundance pattern at different exposure concentrations. Furthermore, abundances from both reactors varied by an order of magnitude through the course of the study, which renders it difficult to detect whether there was a dosage effect of cotrimoxazole on the abundance of rhizospheric bacteria (Figure 2.23).
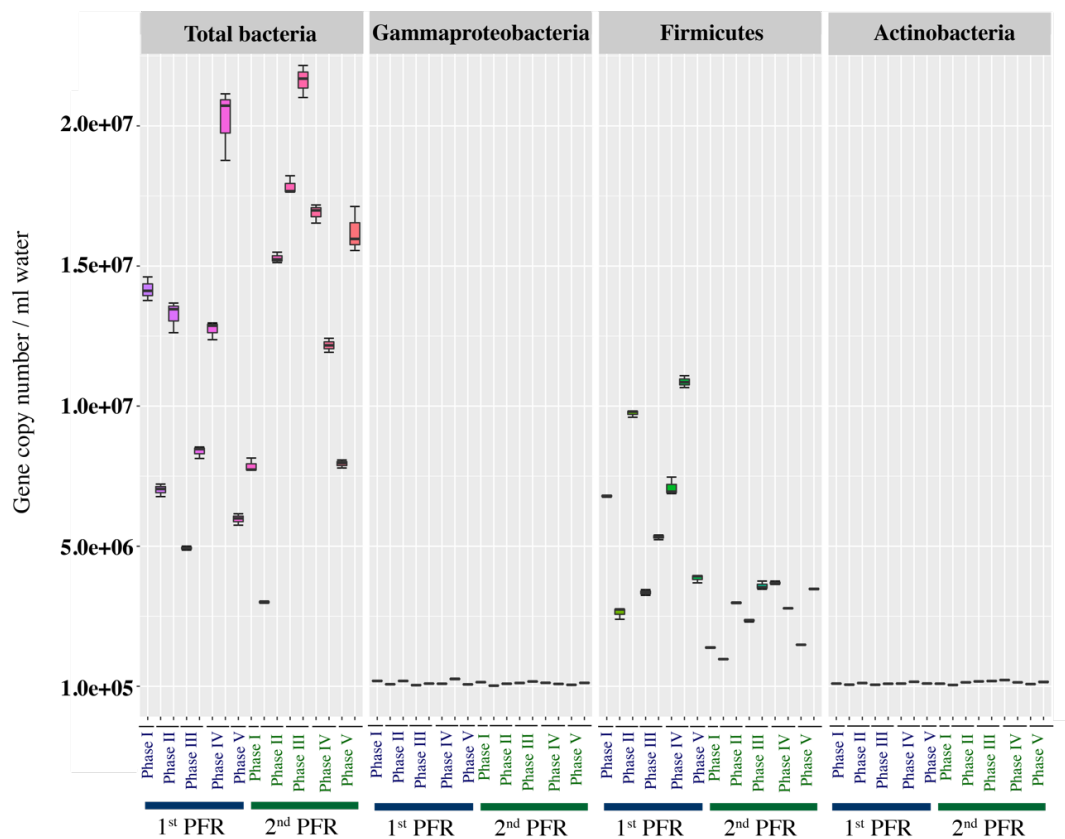
Figure 2.23: Quantitative PCR enumeration of the pore water bacterial community (rhizospheric) during the second study. Firmicutes was the most abundant phylum among the the studied groups. The bacterial community from both PFRs did not undergo any specific abundance changes during the exposure regime.

For the second part, towards revealing the influence of rhizobacteria in shaping endophytic community structure, 16S amplicon sequencing was carried out. Thereon, results were merged with the endophytic community's datasets and plotted in the form of principal coordinate analysis. A separate clustering was observed for the rhizospheric bacterial communities showing that there were only very few similarities with the endophytic communities (Figure 2.24). In addition to revealing that the communities were distinct, this showed also that the endophytic DNA as isolated was essentially free of contamination with rhizospheric DNA.
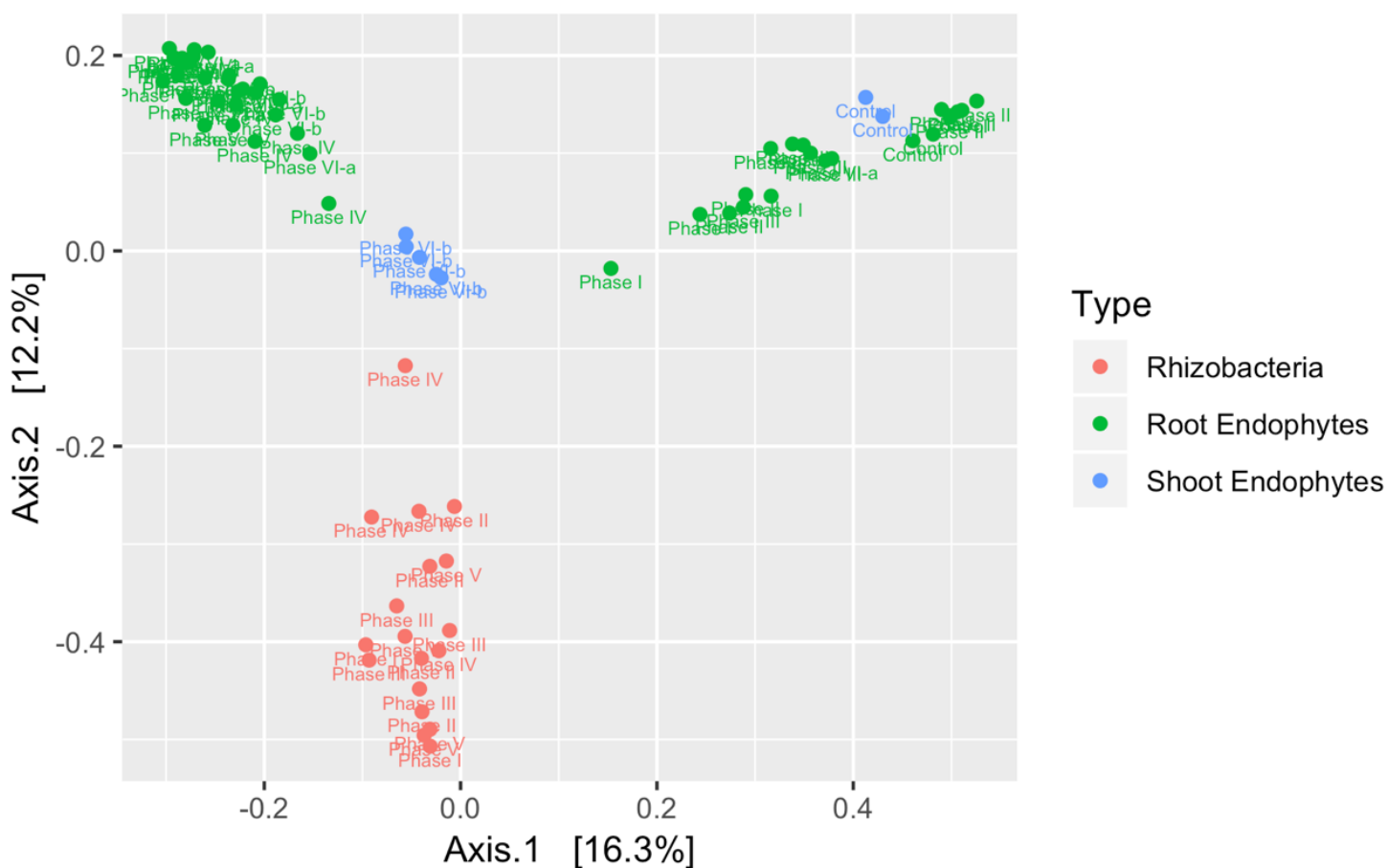
Figure 2.24: Principle coordinate analysis reveals that rhizospheric bacterial community was distinct from the endophytic bacterial community. Endophytic community displayed two clusters for different phases (dose-dependent effect) whereas rhizospheric community remained least influenced by the concentration of cotrimoxazole.

Results of qPCR indicated no major differences in the absolute abundances of rhizospheric communities during the exposure regime.

Next, to advance our understandings on *in situ* role of rhizospheric bacteria, we manually looked at the genus level taxonomy for both rhizo- and endophytic bacteria. It was found that the bacterial communities in the rhizosphere were dominated by anaerobic bacteria such as members of the Bacteroides and Firmicutes, which were mostly obligates, and could be fermenting the plant-derived complex organic matter. Many of these taxa have been previously reported from the human gut (Khan et al. 2012, Ley 2016, Yuan et al. 2011) where they may carry out essentially the same metabolic reactions in the anaerobic environment. Here, changes in community structure were significantly different for Phase IV (Figure 2.25). It seems less likely that these changes were the result of the antimicrobial nature of cotrimoxazole since many of the identified anaerobes (e.g. members of the Bacteroides) are apparently not susceptible to SMX at these concentrations, i.e. full inhibition occurs at low mg/L concentrations (Rosenblatt &Stewart 1974, Wüst &Wilkins 1978). A more likely reason behind these changes could be the result of changes in radial loss of oxygen in Phase IV and/or changes in flux and chemical nature of the root exudates, i.e., also indicated via increased TOC concentrations (Armstrong &Armstrong 2001, Bodelier 2003, Li &Wang 2013, Wang et al. 2015).

The high abundance of sulfur oxidizers in the beginning was due to the aerobic oxidation of molecular hydrogen which was diffused from the rhizosphere.

Additionally, the presence of many fermenting bacteria in the rhizosphere suggests high fluxes of molecular hydrogen (H_2), which is a common fermentation product (Li &Fang 2007, Shin et al. 2004). Some of that hydrogen probably diffused into the root where it could have fuelled aerobic H_2-oxidation by endophytes. Since *Sulfuricurvum, Sulfuritalea, Hydrogenophaga*, and *Ideonella* can use H_2 as an electron donor (Handley et al., 2014; Kojima and Fukui, 2011), this could be the reason that these genera were highly abundant in the beginning, i.e. ~50% of the total endophytic community. Many of these bacteria are previously described as capable of autotrophic growth using H_2 as energy source. The exposure of cotrimoxazole apparently changed the environmental conditions, while the activity of these H_2-oxidizers might have been partially replaced by *Treponema,* at least in anoxic regions (Graber et al. 2004).

	Phase I		Phase II		Phase III		Phase IV		Phase V	
	1st PFR	2nd PFR	1st PFR	2nd PFR	1st PFR	2nd PFR	1st PFR	2nd PFR	1st PFR	2nd PFR
Bacteroidaceae; Bacteroides	26.7	17.1	11.5	19.1	28.9	24.9	10.8	13	24.6	11
Prevotellaceae; Prevotella	7.3	5.2	0.6	10.3	1.9	2.1	1.1	2	9.1	12.6
Pseudomonadaceae; Pseudomonas	0.1	0.2	38.5	1.1	0.2	0.1	0	0	0.3	2.5
Kineosporiaceae; Kineococcus	1	17.8	0.7	1.4	1.4	6.9	1.7	6.6	0.2	3.1
Lachnospiraceae; Lachnospiracea_incertae_sedis	4.1	3.2	1.1	4.7	4.1	2.4	0.4	2.2	5.1	3.8
Bradyrhizobiaceae; Bosea	0	1.6	2.6	1.5	0.4	0.2	0	8.5	0	11.4
Ruminococcaceae; Faecalibacterium	3.4	2.4	0.4	2.8	3.8	3.1	1.9	2.6	2.7	3.1
Oceanospirillaceae; Litoribrevibacter	5.7	0	4.3	0.4	1.6	0	6	0.3	1.8	5.8
Propionibacteriaceae; Propionibacterium	0.5	0.8	1.8	2	0.3	2.5	3.2	0.3	1.3	5.7
Staphylococcaceae; Staphylococcus	0.4	0.5	0.1	2.9	0.2	2.6	0.9	3	2.6	4.4
Rikenellaceae; Alistipes	2.3	2.2	0.7	2.3	1.2	2.9	1.7	0	2.9	1.3
Coriobacteriaceae; Collinsella	3.4	0.4	0.4	1.4	2.9	1.9	0.8	1.5	2.6	0.5
Lachnospiraceae; Fusicatenibacter	4.1	1.4	0.1	1.6	1.9	0.7	2	0	1.2	2.1
Lachnospiraceae; Roseburia	2.2	2.9	1	1.3	1.9	1.7	0.4	1	2.2	0.1
Porphyromonadaceae; Parabacteroides	1.5	0.1	0.1	2.5	1.9	2.1	1	0.2	2.3	0.8
Lactobacillaceae; Lactobacillus	0.6	1.6	0.9	1.3	0.6	2.8	0	0.9	1.3	1.1
Bifidobacteriaceae; Bifidobacterium	2	1.1	0.1	1.7	0.5	2.6	0	0.4	2.7	0.4
Lachnospiraceae; Ruminococcus2	0.5	1.9	0	0.7	2.1	2.2	1.7	0.8	0.7	0.1
Acidaminococcaceae; Succinispira	0	0.2	1.5	0	1.4	0	5.4	0	0.6	0.5
Syntrophaceae; Desulfomonile	0	1.1	0.5	0.2	0.9	0.7	2.1	3.1	0.9	0.6
Erysipelotrichaceae; Holdemanella	0.9	0.7	1.3	0.3	1.1	0.9	1	0.4	0.5	2.7
Microbacteriaceae; Leucobacter	1.1	1.9	2.9	1	0	1.3	0	1.2	0.1	0.3
Ruminococcaceae; Butyricicoccus	1.1	1	0.7	0.8	1.3	0.2	1.2	0.3	0.8	1.4
Corynebacteriaceae; Corynebacterium	0.7	0.4	0.3	1	0	0.4	0.6	1.9	0.5	2.1
Lachnospiraceae; Blautia	1.4	0.5	0.9	1	1.1	1	0.9	0.2	1	0.3
Microbacteriaceae; Microbacterium	2.9	1.5	3.1	0.1	0.1	0.1	0	0.5	0.2	1
Saccharibacteria_genera_incertae_sedis	0.1	1	1.7	2.7	1.1	0	0.6	0	0.1	0.1
Lachnospiraceae; Clostridium XlVa	0.7	0	0.9	0.2	1.7	0	0.6	0	0.6	1.6
Sphingobacteriaceae; Nubsella	0	0	0.5	0	1.7	0	3.6	0	0	0
Hyphomicrobiaceae; Ancalomicrobium	0	0	0	0.2	0.8	0	2.4	1.2	0.1	0.6
Holophagaceae; Holophaga	0	0	0.6	0.3	0.1	0	0.7	3.5	0	0
Brucellaceae; Ochrobactrum	0	0	0	0.2	1.3	0.5	0	2.1	0.1	0.8
Streptococcaceae; Streptococcus	0.6	1.3	0.5	0.9	0.1	1.1	0	0.4	0.8	0.2
Veillonellaceae; Dendrosporobacter	0	0	0	0	1.2	0	3.7	0	0.1	0
Ruminococcaceae; Subdoligranulum	0.5	0.2	0	0.4	0.7	0.8	0	0.9	0.7	1.1
Porphyromonadaceae; Barnesiella	1.6	0.5	0	1.3	0.5	0	0.3	0	1.3	0.4
Comamonadaceae; Curvibacter	0	0	0	0	1.7	0	2.4	0.7	0.1	0
Intrasporangiaceae; Phycicoccus	0	5.9	0	0.6	0.1	0.5	0	0.2	0.1	0
Clostridiaceae 1; Clostridium sensu stricto	0.2	0	0	0.5	0.7	0.3	2.3	0	0.4	0
Lachnospiraceae; Dorea	0.7	0.3	0	0.5	0.5	0.3	0	0.4	0.7	1.3
Burkholderiaceae; Ralstonia	0	0	0.1	0.6	0	0.4	1.8	1.2	0	0
Lachnospiraceae; Coprococcus	0.8	0	1	0.9	0.2	0.5	0	0	1	0
Legionellaceae; Legionella	0.2	0	0.3	0.9	0	0	0	2.3	0	0.3
Sutterellaceae; Parasutterella	0.3	0.4	0.1	0.6	0.9	0.4	0.7	0.3	0.5	0
Clostridiaceae 1; Proteiniclasticum	0	0	0	0	0.9	0	2.8	0	0	0
Veillonellaceae; Pelosinus	0	0	0.5	0.1	0.8	0.1	2	0.2	0	0
Ruminococcaceae; Ruminococcus	0.7	0.7	0	0.2	0.8	0.9	0	0.1	0.5	0.2
Anaeroplasmataceae; Asteroleplasma	2.2	0.1	0	0.1	0.4	0	0	0.3	1.3	0.1
Ectothiorhodospiraceae; Spiribacter	0	0	0	0	0.2	0	3.3	0	0	0
Sutterellaceae; Sutterella	0.4	0.7	0.1	1	0.6	0	0	0	0.7	0.5

Figure 2.25: Heatmap illustration of the top 50 phylotypes identified via 16S amplicon sequencing for the rhizospheric bacterial communities. Major changes in community structure were seen during Phase IV; nevertheless, the behavior of both PFRs in terms of overall composition was different.

Some of the rhizospheric bacteria might have entered plant interior upon weakening of its health status.

Lastly, we also looked if some rhizospheric genera specifically colonized the interior of *J. effusus* upon weakening of its health status (c.f. newly developed endophytic community). Some of the rhizospheric bacteria such as *Rhizomicrobium*, *Rhodomicrobium*, and *Tepidamorphus* (members of Rhizobiales) had a very small abundance in the plant endosphere till Phase III. However, in Phase IV and Phase V, these three genera together had relative abundances of 3.5% and 8.6%, respectively (Supplementary Figure A.6). In total, the total abundance of Rhizobiales was increased from 3.7% in Phase III to 21.1% in Phase IV (Supplementary Figure A.7). On the other hand, their abundance in the rhizospheric community was low throughout the study. Thus, we can argue that they could be potential opportunists that entered the plant endosphere when *in planta* conditions for them become favorable.

The dose-dependent responses were visualized for the rhizospheric bacterial communities by principal component analysis. Results showed that only Phase IV was different during different concentration exposures. However, this finding was based on 22.3% of total inertia for the first two components whereas 77.8% of the data variance remained unexplained. Hence, there could have been several other factors responsible for the change in rhizospheric community other than the influence of cotrimoxazole, e.g. seasonal variations, light intensity, and availability of plant-derived organic carbon and changes in oxygen flux into the rhizosphere (Figure 2.26).

Rhizospheric bacterial communities did not show any diversity pattern during the exposure regime.

Lastly, Fisher's alpha diversity index for rhizospheric community did not reveal any pattern as it was found for the endophytic community. Values for Fisher alpha diversity index ranged between 12.8 to 57.7 for the 1st PFR and 7.66 to 44.8 for the 2nd PFR. In the first two phases, the range of diversity index was low but increased in the later exposures. The graphical representation is presented as Supplementary Figure A.8.
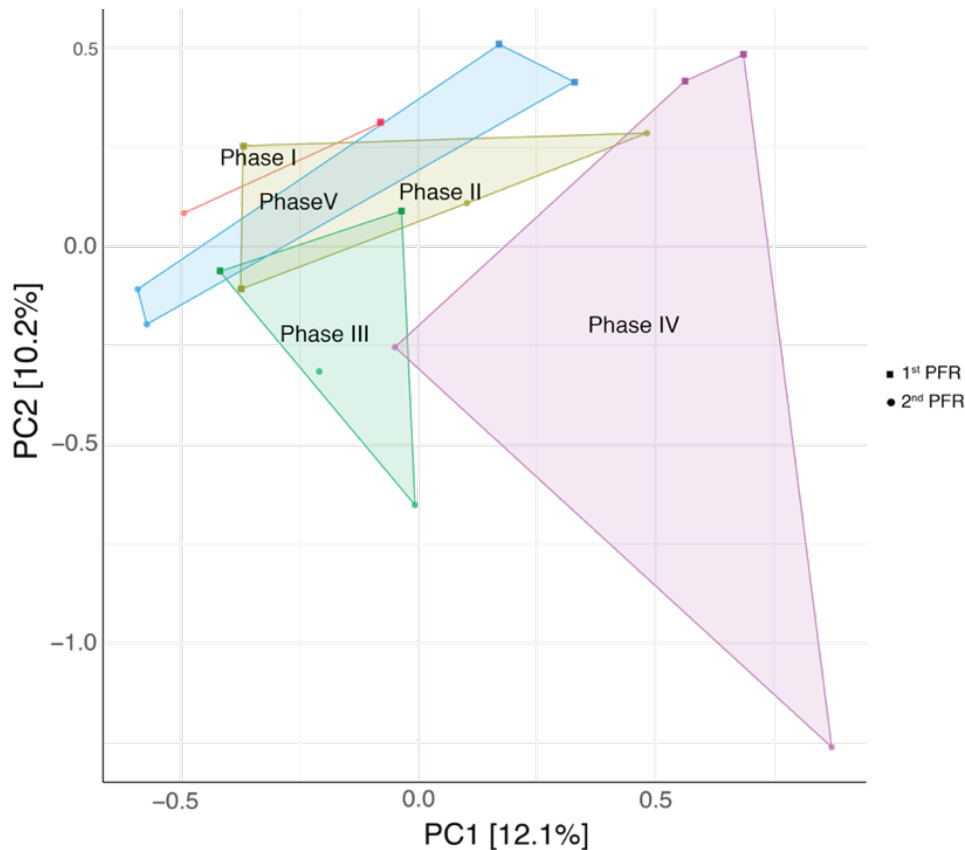
Figure 2.26: Ordination analysis shows that the rhizospheric community from Phase IV was different than the communities from other phases. Nevertheless, overall inertia of ~22.3% remained insignificant to explain the data variations due to antimicrobials influence.

2.4 Discussion

CWs harbor microbiological communities that play a major role in wetland ecosystem services such as degradation of the contaminants and recycling of the nutrients (Kadlec 2009, Stottmeister et al. 2003, Wynn &Liehr 2001). However, the stability of these communities is subject to several stressors present in the environment. Among them, antimicrobials could be a prominent category even though they have gained less attention until today. Interestingly, CWs are being used to remediate antimicrobials without looking at the changes in microbial communities that are prone to disturbances due to their mode of action. Thus, research into understanding these changes particularly in terms of community density and diversity, both spatially and temporally, could help understand better the health, stability, and robustness of the system in addition to the ongoing improvement and future design of CWs

(Faulwetter et al. 2009, Nivala et al. 2018, Weber &Legge 2009). Here, the response of microbial communities (rhizo- and endophytic bacteria) was investigated for *J. effusus* in the presence of cotrimoxazole, which is a commonly found drug in European wastewater.

First study

Exposure of cotrimoxazole was found to have a pronounced effect on the endophytic community because the absolute, as well as relative abundances of some phylotypes, were increased significantly in the post-exposure period. This observation was not supporting the hypothesis formulated at the beginning of this thesis: "*exposure to cotrimoxazole can inhibit beneficial endophytic bacterial community in CWs*". The appearance of new endophytic communities led us to query for their potential role considering two possibilities: (i) the newly developed community might have been beneficial to the plant, or (ii) there was an invasion of pathobionts in the compromised plant system (Lindow &Brandl 2003). The assumptions were tested via *in vitro* biochemical characterization of the isolated bacteria for possible PGP activities as well as *in situ* production of ROS and RNS in the post-exposure period. Both of these approaches have been previously adopted to study the beneficial services of endophytic bacteria (Khan et al., 2015) or stress induction by plant in the presence of pathogens (Liebthal &Dietz 2017). Many of the isolated bacteria displayed at least one of the tested PGP activities. This suggests that they were beneficial *in planta*, but it is not proven because PGP assays were carried out *in vitro*. Till today, there is no straightforward method available to estimate PGP activities of the endophytic bacteria *in situ*, hence PGP potential of endophytic bacteria are carried out *in vitro* (Afzal et al. 2011, Andria et al. 2009, Khan et al. 2013, Yousaf et al. 2011). Therefore, to test the second possibility, *in situ* production of ROS and RNS was carried out by CLSM. Results were in agreement with the activation of plant hypersensitive response (HR) in the post-exposure period. It is a well-established fact that plants use HR to prevent the spread of infection by pathobionts (Freeman &Beattie 2008). Opportunistic or pathogenic bacteria are always present on the plant surface (known as epiphytes) that sporadically enter the endosphere if environmental conditions become favorable for them (Dickinson 2012). In such conditions, the first defense line is to confine their action by

HR of the host (Salguero-Linares &Coll 2019). Since the detection of HR was made after three months of omitting the antimicrobials, it was less likely that the ROS/RNS production was due to a direct effect of cotrimoxazole on *J. effusus* but rather that the new community was proliferating due to an increase in available plant-derived nutrients. This observation led us to confront the classical definition of endophytes stating, "endophytes reside inside the plant without causing pathogenicity" (Andria et al. 2009). By contrasts, this study argues that endophytic bacteria could be of any nature ranging from mutualism to pathogenesis depending upon the environmental conditions. This revision in definition has also been suggested recently by other authors as well (Brader et al. 2017).

In general, four phyla have been found to dominate the bacterial endophytic community, i.e., Proteobacteria followed by Firmicutes, Actinobacteria, and Bacteroidetes (Bulgarelli et al. 2013, Vorholt 2012). Our results on endophytic community structure of *J. effusus* were also consistent with these findings. However, upon exposure to cotrimoxazole, their absolute abundances were greatly increased. This observation is analogous to human gut microbiome studies which reported that members of Proteobacteria were particularly enriched after the treatment with antibiotics (Antonopoulos et al. 2009). Within the phylum Proteobacteria, Gammaproteobacteria was a highly abundant class and managed to proliferate and survive significantly better than the other groups. This might be due to the fact that members of this class have adopted several mechanisms to survive and proliferate in stressed environment (Hardoim et al. 2015). Additionally, their ecological relationships range from mutualism to pathogenesis, which allows them to adapt to various environments easily. This is mainly true for the members of genera *Enterobacter, Pseudomonas, Pantoea,* and *Stenotrophomonas* (Hardoim et al. 2013, Hardoim et al. 2015). All of these genera were observed in this study either via cultivation dependent or cultivation independent analysis.

Members of Gammaproteobacteria *are opportunistic as well they possess abilities to survive in the presence of oxidative stress.*

The production of ROS and RNS might have further caused anatomical damages within plant roots (Zurbriggen et al. 2010) leading to the uncontrolled release of plant metabolites that helped in proliferation of opportunistic bacteria (Zhou et al. 2015). Previously, several members of Gammaproteobacteria and Firmicutes are reported as latent

phytopathogens (Bull et al. 2012, Bull et al. 2010, Hardoim et al. 2015). This means that they can be either neutral or beneficial to the host when the host defense is strong, however, they become pathogenic upon weakening of host health (Kloepper &Ryu 2006). Also, it was argued that the same species or even strain can be beneficial or pathogenic for the host depending upon the environmental conditions (Hardoim et al. 2015). These bacteria could also degrade the plant material for its own growth (Singer et al. 2003). Additionally, the activation of hypersensitive response in *J. effusus* in the post-exposure period may have been due to the presence of bacteria such as the suspected plant pathogen, *P. rwandensis*, as well as members of the order *Xanthomonadales* (Class: Gammaproteobacteria), affiliated mainly with the genus *Dyella* (Supplementary Figure A.6). Members of *Xanthomonadales* are previously recognized as the largest group of bacterial phytopathogens (Naushad &Gupta 2013) although no information on the pathogenic role of *Dyella* in plants is available in the literature.

Endophytic bacteria are not necessarily always beneficial for the plant. They can be latent opportunists, or pathogens that behave according to the environmental conditions.

Second study

One of the most important observations made in the second study was the dose-dependent effect of cotrimoxazole on the root endophytic community. A decrease in alpha diversity was concomitant with the concentration increase of cotrimoxazole up to 50 µg/L of SMX and 17 µg/L of TMP. It has been argued previously that community diversity has a positive effect on the ecosystem functioning whereas a decrease in diversity is negatively correlated for the respective functioning (Hooper et al., 2005). Therefore, such a decrease is an indirect indication of weakened performance of *J. effusus*. Weber et al., (2011) also reported that ciprofloxacin can reduce the bacterial diversity and functions in wetland mesocosms, thus affecting the metabolic capabilities of the system (Weber et al. 2011).

Interestingly, with further increase in cotrimoxazole's concentration, a raise of diversity was observed. This recovery in diversity might be attributed to the two phenomena: (A) the antagonistic potential of beneficial endophytes could have been compromised, which led to the invasion of pervasive, opportunist, or pathogenic bacteria with less susceptibility to cotrimoxazole (Atkinson &Urwin 2012, Grassi et al.

2013, Ramegowda &Senthil-Kumar 2015), or (B) excessive availability of plant-derived nutrients could have allowed the opportunists to proliferate *in planta*. The latter is mainly true for facultative endophytes that consume plant-derived nutrients and reduce the ecological fitness of the host (Hardoim et al. 2015, Hardoim et al. 2008).

The results of dose-dependent effects of cotrimoxazole are a step forward to the *in planta* dysbiosis debate. From human microbiome studies, a common indication of dysbiosis is the observation that alpha diversity is decreased (de Paiva et al. 2016, Manichanh et al. 2006). For the plant kingdom, it was argued previously that distinguishing a 'healthy' microbiome from a 'diseased' microbiome is a difficult procedure mainly due to unexplained microbiome variations across 'healthy' individuals (Bäckhed et al. 2012). In our results, we found that the natural community was similar both in composition and diversity whereas exposure of cotrimoxazole brought major changes.

Endophytic diversity was drastically reduced after 3rd and 4th concentrations regimes. The observation is analogous to "dysbiosis" in the animal kingdom.

By contrast, the pore water community representing rhizospheric bacterial communities was relatively stable throughout the exposure period which did not show any decrease in alpha diversity or bacterial abundance. Previously, Mendes et al., (2011) reported that the condition of dysbiosis rarely satisfies for the plant rhizosphere. Similar observations were made in other systems such as corals (Roder et al. 2014). Moreover, since reported minimum inhibitory concentrations of SMX and TMP are higher than the concentrations used in this study (http://www.antimicrobe.org/d20tab.htm; Kirven and Thornsberry, 1978; Czekalski et al., 2012); it is argued that *in planta* community is prone to disturbances more than the rhizospheric community. This might be related to their direct association with the host whose compromising health provides lesser chances for the indigenous community to recover. By contrast, rhizospheric communities are comparatively thriving in an open system where environmental conditions are continuously changing depending upon the presence/absence of external stressors. In an earlier study, it was reported that bacterial communities in the wetland interstitial water recovered in a 2–5 weeks period after omitting the antimicrobial exposure, nevertheless, plants did not adapt to the antibiotic presence and eventually died (Weber et al., 2011).

Rhizobacteria are less prone to face dysbiosis as compared to endophytic bacteria.

Response of *J. effusus* to cotrimoxazole

Although cotrimoxazole was designed to disrupt the folate biosynthetic pathway in bacteria, it can inhibit this pathway in plants, too (Eguchi et al., 2004; Brain et al., 2008; Liu et al., 2009; García-Galán et al., 2009). In plants, folate is synthesized in three subcellular compartments, i.e. cytosol, plastids, and mitochondria (Basset et al., 2004). Briefly, pteridine is synthesized in the cytosol and *p*ABA is synthesized in plastids. These metabolic precursors are then transported to the mitochondrial matrix where subsequent reactions synthesize folate. Out of the two compounds in cotrimoxazole, SMX is apparently much more phytotoxic than TMP (Hillis et al., 2011). The reasons for that are unclear. The concentration at which SMX becomes phytotoxic varies substantially between plants. With *Daucus carota* (carrot), root length was affected by SMX with an EC_{50} of 60 μg/L. Similarly, fresh weight and frond number of *Lemna gibba* (duckweed) were affected by SMX exposure with EC_{50} of 100 μg/L 30 μg/L, respectively (Brain et al. 2004). In contrast, with *Lactuca sativa* (lettuce), and *Medicago sativa* (alfalfa) TMP did not produce a significant observable adverse effect up to the maximum concentration tested (10,000 μg/L) (Hillis et al., 2011). Thus, the concentration of 50 μg SMX/L at which a decrease of plant vitality parameters were observed in the present study is at the low concentration end of the EC_{50} range reported in the literature, and higher than the concentration at which we observed the first changes in the endophytic bacterial communities (10 μg/L).

The physiological response of plant to cotrimoxazole was more prominent after that major changes in endophytic community seen already.

However, Brain et al., (2008) found that exposure of *L. gibba* to SMX resulted in an increased content *in planta* of *p*ABA, indicating its reduced usage in the folate pathway due to inhibition of dihydropteroate synthase. They computed an EC_{50} for significant *p*ABA increase of 3.36 μg/L (Hanson and Roje, 2001). We expected a similar *p*ABA response for *J. effusus*, which might have caused changes in lignin secondary metabolite biosynthesis. These *in planta* changes might have allowed the compromised endophytic community to proliferate in the plant interior.

Based on these observations, this study proposes that it might not even matter whether SMX/TMP was effective first as an antimicrobial or as phytotoxic agent given the intricacy of the partnership. Lastly, the

decline in plant fitness parameters could be the results of increased production of ROS and RNS that caused anatomical damages within plant. Previously, Kummerová et al., (2016) reported that high ROS and RNS production can lead to the degradation of plant material and affect plant performance.

2.5 Concluding remarks and future outlook

In summary, this chapter provides an in-depth analysis of the response of the endophytic community after exposure to various aqueous concentrations of cotrimoxazole. The fitness of *J. effusus* was decreased upon multiple exposures of SMX and TMP. These effects were enhanced over time in all PFRs exposed to cotrimoxazole. The results on bacterial community structure indicated a pronounced effect of community shift in the exposed plant roots. It was observed that the indigenous microbiome could be replaced due to antimicrobial exposure and that a new bacterial community took over the system in upon cotrimoxazole exposure. These results can be considered similar to various observations made for the human gut where antibiotics can cause dysbiosis. Nevertheless, the notable effects were observed at concentrations which are typically above that what is found in the WWTPs, so wastewaters contaminated with antimicrobials are likely to be remediated through processes occurring in CWs. In the end, it is suggested that further studies on metagenomics and proteomics can provide an extended view on functional description of the community upon cotrimoxazole exposure. Moreover, further studies about the direct impact of sulfonamides on plant biochemistry, and other antimicrobials such as β-lactams that are less likely to have any direct impact on plant, might also be investigated.

References

Acar JF (2012): Inhibition of Folate Metabolism in Chemotherapy: the origins and uses of Co-trimoxazole, 64. Springer Science & Business Media

Afzal M, Yousaf S, Reichenauer TG, Kuffner M, Sessitsch A (2011): Soil type affects plant colonization, activity and catabolic gene expression of inoculated bacterial strains during phytoremediation of diesel. Journal of Hazardous Materials 186, 1568-1575

Afzal M, Khan QM, Sessitsch A (2014): Endophytic bacteria: Prospects and applications for the phytoremediation of organic pollutants. Chemosphere 117, 232-242

Alm EW, Oerther DB, Larsen N, Stahl DA, Raskin L (1996): The oligonucleotide probe database. Applied and environmental microbiology 62, 3557-3559

Andria V, Reichenauer TG, Sessitsch A (2009): Expression of alkane monooxygenase (alkB) genes by plant-associated bacteria in the rhizosphere and endosphere of Italian ryegrass (Lolium multiflorum L.) grown in diesel contaminated soil. Environmental Pollution 157, 3347-3350

Antonopoulos DA, Huse SM, Morrison HG, Schmidt TM, Sogin ML, Young VB (2009): Reproducible Community Dynamics of the Gastrointestinal Microbiota following Antibiotic Perturbation. Infection and Immunity 77, 2367-2375

Armstrong J, Armstrong W (2001): Rice and Phragmites: effects of organic acids on growth, root permeability, and radial oxygen loss to the rhizosphere. American Journal of Botany 88, 1359-1370

Atkinson NJ, Urwin PE (2012): The interaction of plant biotic and abiotic stresses: from genes to the field. Journal of Experimental Botany 63, 3523-3543

Bacchetti De Gregoris T, Aldred N, Clare AS, Burgess JG (2011): Improvement of phylum- and class-specific primers for real-time PCR quantification of bacterial taxa. Journal of Microbiological Methods 86, 351-356

Bäckhed F, Fraser Claire M, Ringel Y, Sanders Mary E, Sartor RB, Sherman Philip M, Versalovic J, Young V, Finlay BB (2012): Defining a Healthy Human Gut Microbiome: Current Concepts, Future Directions, and Clinical Applications. Cell Host & Microbe 12, 611-622

Belova SE, Kulichevskaya IS, Bodelier PLE, Dedysh SN (2013): Methylocystis bryophila sp. nov., a facultatively methanotrophic bacterium from acidic Sphagnum peat, and emended description of the genus Methylocystis (ex Whittenbury et al. 1970) Bowman et al. 1993. International Journal of Systematic and Evolutionary Microbiology 63, 1096-1104

Benz M, Brune A, Schink B (1998): Anaerobic and aerobic oxidation of ferrous iron at neutral pH by chemoheterotrophic nitrate-reducing bacteria. Archives of Microbiology 169, 159-165

Bertani I, Abbruscato P, Piffanelli P, Subramoni S, Venturi V (2016): Rice bacterial endophytes: isolation of a collection, identification of beneficial strains and microbiome analysis. Environmental Microbiology Reports 8, 388-398

Blake R, Shute E, Greenwood M, Spencer G, Ingledew W (1993): Enzymes of aerobic respiration on iron. FEMS Microbiology Reviews 11, 9-18

Bodelier PLE (2003): Interactions Between Oxygen-Releasing Roots and Microbial Processes in Flooded Soils and Sediments. In: de Kroon H , Visser EJW (Editors), Root Ecology. Springer Berlin Heidelberg, Berlin, Heidelberg, pp. 331-362

Brader G, Compant S, Vescio K, Mitter B, Trognitz F, Ma L-J, Sessitsch A (2017): Ecology and genomic insights into plant-pathogenic and plant-nonpathogenic endophytes. Annual review of phytopathology 55, 61-83

Brady CL, Cleenwerck I, van der Westhuizen L, Venter SN, Coutinho TA, De Vos P (2012): *Pantoea rodasii* sp. nov., *Pantoea rwandensis* sp. nov. and *Pantoea wallisii* sp. nov., isolated from Eucalyptus. International Journal of Systematic and Evolutionary Microbiology 62, 1457-1464

Brain RA, Johnson DJ, Richards SM, Sanderson H, Sibley PK, Solomon KR (2004). Effects of 25 pharmaceutical compounds to Lemna gibba using a seven-day static-renewal test. Environmental Toxicology and Chemistry: An International Journal. 23(2):371-82.

Brain RA, Ramirez AJ, Fulton BA, Chambliss CK, Brooks BW (2008): Herbicidal effects of sulfamethoxazole in Lemna gibba: using p-aminobenzoic acid as a biomarker of effect. Environmental Science & Technology 42, 8965-8970

Bray JR, Curtis JT (1957): An ordination of the upland forest communities of southern Wisconsin. Ecological monographs 27, 325-349

Bulgarelli D, Schlaeppi K, Spaepen S, van Themaat EVL, Schulze-Lefert P (2013): Structure and Functions of the Bacterial Microbiota of Plants. Annual Review of Plant Biology 64, 807-838

Bulgari D, Casati P, Quaglino F, Bianco PA (2014): Endophytic bacterial community of grapevine leaves influenced by sampling date and phytoplasma infection process. BMC Microbiology 14, 198

Bull C, De Boer S, Denny T, Firrao G, Saux MF-L, Saddler G, Scortichini M, Stead D, Takikawa Y (2010): Comprehensive list of names of plant pathogenic bacteria, 1980-2007. Journal of Plant Pathology, 551-592

Bull C, De Boer S, Denny T, Firrao G, Fischer-Le Saux M, Saddler G, Scortichini M, Stead D, Takikawa Y (2012): List of new names of plant pathogenic bacteria (2008-2010). Journal of Plant Pathology 94, 21-27

Castaño-Rodríguez N, Goh K-L, Fock KM, Mitchell HM, Kaakoush NO (2017): Dysbiosis of the microbiome in gastric carcinogenesis. Scientific Reports 7, 15957

Chen J, Chia N, Kalari KR, Yao JZ, Novotna M, Paz Soldan MM, Luckey DH, Marietta EV, Jeraldo PR, Chen X, Weinshenker BG, Rodriguez

M, Kantarci OH, Nelson H, Murray JA, Mangalam AK (2016): Multiple sclerosis patients have a distinct gut microbiota compared to healthy controls. Scientific Reports 6, 28484

Chouari R, Le Paslier D, Dauga C, Daegelen P, Weissenbach J, Sghir A (2005): Novel major bacterial candidate division within a municipal anaerobic sludge digester. Applied and Environmental Microbiology 71, 2145-2153

Cole JR, Wang Q, Fish JA, Chai B, McGarrell DM, Sun Y, Brown CT, Porras-Alfaro A, Kuske CR, Tiedje JM (2013): Ribosomal Database Project: data and tools for high throughput rRNA analysis. Nucleic acids research 42, D633-D642

Compant S, Clément C, Sessitsch A (2010): Plant growth-promoting bacteria in the rhizo- and endosphere of plants: Their role, colonization, mechanisms involved and prospects for utilization. Soil Biology and Biochemistry 42, 669-678

Compant S, Mitter B, Colli-Mull JG, Gangl H, Sessitsch A (2011): Endophytes of Grapevine Flowers, Berries, and Seeds: Identification of Cultivable Bacteria, Comparison with Other Plant Parts, and Visualization of Niches of Colonization. Microbial Ecology 62, 188-197

de Paiva CS, Jones DB, Stern ME, Bian F, Moore QL, Corbiere S, Streckfus CF, Hutchinson DS, Ajami NJ, Petrosino JF, Pflugfelder SC (2016): Altered Mucosal Microbiome Diversity and Disease Severity in Sjögren Syndrome. Scientific Reports 6, 23561

Dickinson CH (2012): Microbiology of aerial plant surfaces. Elsevier

Dong X, Greening C, Brüls T, Conrad R, Guo K, Blaskowski S, Kaschani F, Kaiser M, Laban NA, Meckenstock RU (2018): Fermentative Spirochaetes mediate necromass recycling in anoxic hydrocarbon-contaminated habitats. The Isme Journal 12, 2039-2050

Dorn-In S, Bassitta R, Schwaiger K, Bauer J, Hölzel CS (2015): Specific amplification of bacterial DNA by optimized so-called universal bacterial primers in samples rich of plant DNA. Journal of Microbiological Methods 113, 50-56

Eguchi K, Nagase H, Ozawa M, Endoh YS, Goto K, Hirata K, Miyamoto K, Yoshimura H (2004): Evaluation of antimicrobial agents for veterinary use in the ecotoxicity test using microalgae. Chemosphere 57, 1733-1738

Eleuterius LN (1976): Vegetative morphology and anatomy of the salt marsh rush, *Juncus roemerianus*. Gulf and Caribbean Research 5, 1-10

Ellis RJ, Morgan P, Weightman AJ, Fry JC (2003): Cultivation-Dependent and -Independent Approaches for Determining Bacterial Diversity in Heavy-Metal-Contaminated Soil. Applied and Environmental Microbiology 69, 3223-3230

Faulwetter JL, Gagnon V, Sundberg C, Chazarenc F, Burr MD, Brisson J, Camper AK, Stein OR (2009): Microbial processes influencing performance of treatment wetlands: A review. Ecological Engineering 35, 987-1004

Freeman BC, Beattie GA (2008): An overview of plant defenses against pathogens and herbivores. The Plant Health Instructor

García-Galán MJ, Silvia Díaz-Cruz M, Barceló D (2009): Combining chemical analysis and ecotoxicity to determine environmental exposure and to assess risk from sulfonamides. TrAC Trends in Analytical Chemistry 28, 804-819

Göbel A, Thomsen A, McArdell CS, Joss A, Giger W (2005): Occurrence and sorption behavior of sulfonamides, macrolides, and trimethoprim in activated sludge treatment. Environmental science & technology 39, 3981-3989

Graber JR, Leadbetter JR, Breznak JA (2004): Description of Treponema *azotonutricium* sp. nov. and *Treponema primitia* sp. nov., the First Spirochetes Isolated from Termite Guts. Applied and Environmental Microbiology 70, 1315-1320

Grassi M, Rizzo L, Farina A (2013): Endocrine disruptors compounds, pharmaceuticals and personal care products in urban wastewater: implications for agricultural reuse and their removal by adsorption process. Environmental Science and Pollution Research 20, 3616-3628

Hanson AD, Roje S (2001). One-carbon metabolism in higher plants. Annual review of plant biology.52(1):119-37.

Hardoim PR, van Overbeek LS, Elsas JDv (2008): Properties of bacterial endophytes and their proposed role in plant growth. Trends in Microbiology 16, 463-471

Hardoim PR, Nazir R, Sessitsch A, Elhottová D, Korenblum E, van Overbeek LS, van Elsas JD (2013): The new species Enterobacter oryziphilus sp. nov. and *Enterobacter oryzendophyticus* sp. nov. are key inhabitants of the endosphere of rice. BMC Microbiology 13, 164

Hardoim PR, van Overbeek LS, Berg G, Pirttilä AM, Compant S, Campisano A, Döring M, Sessitsch A (2015): The Hidden World within Plants: Ecological and Evolutionary Considerations for Defining Functioning of Microbial Endophytes. Microbiology and Molecular Biology Reviews 79, 293-320

Heinz E (1993): Recent investigations on the biosynthesis of the plant sulfolipid. Sulfur Nutrition and Assimilation in Higher Plants., 163-178

Hillis DG, Fletcher J, Solomon KR, Sibley PK (2011): Effects of Ten Antibiotics on Seed Germination and Root Elongation in Three Plant

Species. Archives of Environmental Contamination and Toxicology 60, 220-232

Ijaz A, Imran A, Anwar ul Haq M, Khan QM, Afzal M (2016): Phytoremediation: recent advances in plant-endophytic synergistic interactions. Plant and Soil 405, 179-195

Kadlec RH (2009): Comparison of free water and horizontal subsurface treatment wetlands. Ecological Engineering 35, 159-174

Kappelmeyer U, Wießner A, Kuschk P, Kästner M (2002): Operation of a Universal Test Unit for Planted Soil Filters – Planted Fixed Bed Reactor. Engineering in Life Sciences 2, 311-315

Khan MT, Duncan SH, Stams AJM, van Dijl JM, Flint HJ, Harmsen HJM (2012): The gut anaerobe Faecalibacterium prausnitzii uses an extracellular electron shuttle to grow at oxic–anoxic interphases. The Isme Journal 6, 1578

Khan S, Afzal M, Iqbal S, Khan QM (2013): Plant–bacteria partnerships for the remediation of hydrocarbon contaminated soils. Chemosphere 90, 1317-1332

Kloepper JW, Ryu C-M (2006): Bacterial Endophytes as Elicitors of Induced Systemic Resistance. In: Schulz BJE, Boyle CJC, Sieber TN (Editors), Microbial Root Endophytes. Springer Berlin Heidelberg, Berlin, Heidelberg, pp. 33-52

Kummerová M, Zezulka Š, Babula P, Tříska J (2016): Possible ecological risk of two pharmaceuticals diclofenac and paracetamol demonstrated on a model plant *Lemna minor*. Journal of Hazardous Materials 302, 351-361

Layeghifard M, Hwang DM, Guttman DS (2017): Disentangling Interactions in the Microbiome: A Network Perspective. Trends in Microbiology 25, 217-228

Ley RE (2016): Gut microbiota in 2015: Prevotella in the gut: choose carefully. Nature reviews Gastroenterology & hepatology 13, 69

Li C, Fang HHP (2007): Fermentative Hydrogen Production From Wastewater and Solid Wastes by Mixed Cultures. Critical Reviews in Environmental Science and Technology 37, 1-39

Li Y, Wang X (2013): Root-induced changes in radial oxygen loss, rhizosphere oxygen profile, and nitrification of two rice cultivars in Chinese red soil regions. Plant and Soil 365, 115-126

Liebthal M, Dietz K-J (2017): The fundamental role of reactive oxygen species in plant stress response, Plant Stress Tolerance. Springer, pp. 23-39

Lindow SE, Brandl MT (2003): Microbiology of the Phyllosphere. Applied and Environmental Microbiology 69, 1875-1883

Liu F, Ying G-G, Tao R, Zhao J-L, Yang J-F, Zhao L-F (2009): Effects of six selected antibiotics on plant growth and soil microbial and enzymatic activities. Environmental Pollution 157, 1636-1642

Liu H, Carvalhais LC, Crawford M, Singh E, Dennis PG, Pieterse CM, Schenk PM (2017): Inner plant values: Diversity, colonization and benefits from endophytic bacteria. Frontiers in Microbiology 8, 2552

Manichanh C, Rigottier-Gois L, Bonnaud E, Gloux K, Pelletier E, Frangeul L, Nalin R, Jarrin C, Chardon P, Marteau P, Roca J, Dore J (2006): Reduced diversity of faecal microbiota in Crohn's disease revealed by a metagenomic approach. Gut 55, 205-211

McMurdie PJ, Holmes S (2013): phyloseq: An R Package for Reproducible Interactive Analysis and Graphics of Microbiome Census Data. PLOS ONE 8, e61217

Mehmood R, Riaz M, Does RJMM (2014): Quality Quandaries: On the Application of Different Ranked Set Sampling Schemes. Quality Engineering 26, 370-378

Mendes R, Kruijt M, de Bruijn I, Dekkers E, van der Voort M, Schneider JHM, Piceno YM, DeSantis TZ, Andersen GL, Bakker PAHM, Raaijmakers JM (2011): Deciphering the Rhizosphere Microbiome for Disease-Suppressive Bacteria. Science 332, 1097-1100

Murchie EH, Lawson T (2013): Chlorophyll fluorescence analysis: a guide to good practice and understanding some new applications. Journal of Experimental Botany 64, 3983-3998

Naushad HS, Gupta RS (2013): Phylogenomics and Molecular Signatures for Species from the Plant Pathogen-Containing Order *Xanthomonadales*. PLOS ONE 8, e55216

Naveed M, Mitter B, Yousaf S, Pastar M, Afzal M, Sessitsch A (2014): The endophyte Enterobacter sp. FD17: a maize growth enhancer selected based on rigorous testing of plant beneficial traits and colonization characteristics. Biology and fertility of soils 50, 249-262

Nivala J, Neale PA, Haasis T, Kahl S, König M, Müller RA, Reemtsma T, Schlichting R, Escher BI (2018): Application of cell-based bioassays to evaluate treatment efficacy of conventional and intensified treatment wetlands. Environmental Science: Water Research & Technology 4, 206-217

Ramegowda V, Senthil-Kumar M (2015): The interactive effects of simultaneous biotic and abiotic stresses on plants: Mechanistic understanding from drought and pathogen combination. Journal of Plant Physiology 176, 47-54

Roder C, Arif C, Daniels C, Weil E, Voolstra CR (2014): Bacterial profiling of W hite P lague Disease across corals and oceans indicates a conserved and distinct disease microbiome. Molecular ecology 23, 965-974

Rosenblatt JE, Stewart PR (1974): Combined Activity of Sulfamethoxazole, Trimethoprim, and Polymyxin B Against Gram-Negative Bacilli. Antimicrobial Agents and Chemotherapy 6, 84-92

Salguero-Linares J, Coll NS (2019): Plant proteases in the control of the hypersensitive response.

Schulz C, Schütte K, Koch N, Vilchez-Vargas R, Wos-Oxley ML, Oxley AP, Vital M, Malfertheiner P, Pieper DH (2018): The active bacterial assemblages of the upper GI tract in individuals with and without Helicobacter infection. Gut 67, 216-225

Shade A (2016): Diversity is the question, not the answer. The Isme Journal 11, 1

Shin H-S, Youn J-H, Kim S-H (2004): Hydrogen production from food waste in anaerobic mesophilic and thermophilic acidogenesis. International Journal of Hydrogen Energy 29, 1355-1363

Singer AC, Crowley DE, Thompson IP (2003): Secondary plant metabolites in phytoremediation and biotransformation. Trends in Biotechnology 21, 123-130

Skytte Andersen KS, Kirkegaard RH, Karst SM, Albertsen M (2018): ampvis2: an R package to analyse and visualise 16S rRNA amplicon data. bioRxiv, 299537

Stottmeister U, Wießner A, Kuschk P, Kappelmeyer U, Kästner M, Bederski O, Müller RA, Moormann H (2003): Effects of plants and microorganisms in constructed wetlands for wastewater treatment. Biotechnology advances 22, 93-117

Torres MA, Jones JD, Dangl JL (2006): Reactive oxygen species signaling in response to pathogens. Plant Physiology 141, 373-378

Vorholt JA (2012): Microbial life in the phyllosphere. Nature Reviews Microbiology 10, 828

Wang Q, Garrity GM, Tiedje JM, Cole JR (2007): Naive Bayesian classifier for rapid assignment of rRNA sequences into the new bacterial taxonomy. Applied and Environmental Microbiology 73, 5261-5267

Wang Q, Xie H, Zhang J, Liang S, Ngo HH, Guo W, Liu C, Zhao C, Li H (2015): Effect of plant harvesting on the performance of constructed wetlands during winter: radial oxygen loss and microbial characteristics. Environmental Science and Pollution Research 22, 7476-7484

Weber KP, Legge RL (2009): One-dimensional metric for tracking bacterial community divergence using sole carbon source utilization patterns. Journal of Microbiological Methods 79, 55-61

Weber KP, Mitzel MR, Slawson RM, Legge RL (2011): Effect of ciprofloxacin on microbiological development in wetland mesocosms. Water Research 45, 3185-3196

Wickham H (2016): ggplot2: elegant graphics for data analysis. Springer

Wiessner A, Kuschk P, Jechorek M, Seidel H, Kästner M (2008): Sulphur transformation and deposition in the rhizosphere of Juncus effusus in a laboratory-scale constructed wetland. Environmental pollution 155, 125-131

Wüst J, Wilkins TD (1978): Susceptibility of Anaerobic Bacteria to Sulfamethoxazole/Trimethoprim and Routine Susceptibility Testing. Antimicrobial Agents and Chemotherapy 14, 384-390

Wynn TM, Liehr SK (2001): Development of a constructed subsurface-flow wetland simulation model. Ecological Engineering 16, 519-536

Yan Q, Min J, Yu Y, Zhu Z, Feng G (2017): Microbial community response during the treatment of pharmaceutically active compounds (PhACs) in constructed wetland mesocosms. Chemosphere 186, 823-831

Yousaf S, Afzal M, Reichenauer TG, Brady CL, Sessitsch A (2011): Hydrocarbon degradation, plant colonization and gene expression of alkane degradation genes by endophytic *Enterobacter ludwigii* strains. Environmental Pollution 159, 2675-2683

Yuan J, Zeng B, Niu R, Tang H, Li W, Zhang Z, Wei H (2011): The Development and Stability of the Genus Bacteriodes from Human Gut Microbiota in HFA Mice Model. Current Microbiology 62, 1107-1112

Yuan Y, Gao M (2015): Genomic analysis of a ginger pathogen Bacillus pumilus providing the understanding to the pathogenesis and the novel control strategy. Scientific Reports 5, 10259

Zhou S, Lou Y-R, Tzin V, Jander G (2015): Alteration of Plant Primary Metabolism in Response to Insect Herbivory. Plant Physiology 169, 1488-1498

Zurbriggen MD, Carrillo N, Hajirezaei M-R (2010): ROS signaling in the hypersensitive response. Plant Signaling & Behavior 5, 393-396

Authors contribution statement

Title: Antimicrobials in constructed wetlands can cause *in planta* root dysbiosis.

Authors: Arslan, M., Santoni, M., Wiessner, A., Schmidt-Jansen, M., Neu, T.R., Pieper, D., Müller, J.A.

Muhammad Arslan
- Planned the study.
- Run the planted fixed bed reactors (PFRs)
- Performed microbiological analysis.
- Conducted statistical analyses for biological interpretation.
- Wrote the chapter / manuscript.

Marcello Santoni
- Initiated and operated the PFR in the first study.
- Made initial observations on plant physiology in the first study.

Arndt Wiessner
- Helped in operation of PFRs including solving technical problems.

Mechthild Schmidt-Jansen
- Helped in study design and interpretation.

Thomas R. Neu
- Helped in performing microscopic analysis such as FISH, ROS, and RNS detection.

Dietmar Pieper
- Performed 16S amplicon sequencing.
- Generated OTU table with Mothur pipeline

Jochen A. Müller
- Planned/supervised the study.
- Helped in the interpretation of the data and extracting biological information especially in 16S amplicon sequencing.

Monika Möder

- HPLC-MS-MS analysis

DEVELOPING A GENOMIC RESOURCE TO STUDY STRESS
RESPONSE IN *J. EFFUSUS*

3

_____

Context

Chapter 2 elucidated in depth the response of endophytic bacteria to cotrimoxazole. However, it remained less clear whether there was an indeed a pathogen attack after the exposure since no known plant pathogens were seen despite of the fact that ROS and RNS production was high in the post-exposure period. This raised further questions regarding the stress response in *J. effusus*. To this end, targeted investigations on stress-related genes in *J. effusus* and metaproteomics analysis on un-exposed and exposed plant tissues could provide an extended insight. When I began my research, there was no genomic database available for *J. effusus*. However, at that time, Dr. Stefan Michalski (UFZ, Halle) was working on a description of SNPs variation in transcriptome of *J. effusus*. I used this opportunity and obtained the transcriptome assembly for the development of *J. effusus* database which could be used to study stress response. To this end, I

assessed the quality of assembly, performed annotation, conducted functional analysis, and compared the results with previously well-annotated transcriptome of phylogenetic closer relatives of *J. effusus* for quality control purposes. The database was then tested on a subset of cotrimoxazole exposed root and shoot samples of *J. effusus* (chapter 2) and compared with un-exposed plant tissues. Now, the finished transcriptome database with detailed information on its genomic features is publicly available in the Mendeley repository for future *omics* studies (DOI:10.17632/cx7k2v38m7.3).

Plants respond to stressors by upregulating the genes involved in plant defence.

3.1 Introduction

Plants are sessile organisms. They cannot escape from the stressed environment but rather they try to cope with the stressors (Hirayama and Shinozaki, 2010). Therefore, the study of plant defense in response to external stimuli, mainly pathogen invasion, is an important topic in plant research. However, one of the major limitations in these studies is a comprehensive understanding of stress-induced genes (Kreps et al., 2002). Major progress in this area has come through the application of molecular biology. In the past, a common practice was to isolate the stress-inducible genes whose functions were then characterized in transgenic plants (Hirayama and Shinozaki, 2010; Kreps et al., 2002). However, in recent years, next-generation sequencing (NGS) and quantitative proteomics techniques have enabled us to reveal insights into physiological and metabolic changes at the transcriptome and protein level (Low and Heck, 2016; Unamba et al., 2015). A major advantage in using these approaches is their usefulness for both model and non-model organisms (Armengaud et al., 2014; Garg and Jain, 2013).

An importance application of NGS technologies is the sequencing of messenger RNA (RNA-Seq)

RNA-Seq analysis has been extensively used to study stress response in both model and non-model organisms.

RNA-Seq analysis – also known as whole transcriptome shotgun sequencing – is one of these extensively adapted NGS methodologies. It generates large-scale transcriptomic data that reveals the presence of expressed genetic elements in a given biological sample (Mahdavi Mashaki et al., 2018). Resultantly, it has been effectively used to study stress response (He et al., 2012). Additionally, it allows developing a transcriptome database which could serve as a useful resource in *omics* studies, e.g. metaproteomics (Wang et al., 2015a; Wu et al., 2014). Several studies reported successful application of RNA-Seq towards the study of stress response in *Oryza sativa* (He et al., 2015), *Sorghum*

bicolor (Dugas et al., 2011; Fracasso et al., 2016), and *Brassica juncea* (Bhardwaj et al., 2015). Accordingly, studies have reported the usefulness of (meta)proteomics for stress response in marsh plants including *Aeluropus lagopoides* (Sobhanian et al., 2010), *Cakile maritime* (Debez et al., 2012), *Salicornia europaea* (Fan et al., 2011; Wang et al., 2009a), *Suaeda aegyptiaca* (Askari et al., 2006), and *Thellungiella halophila* (Wang et al., 2013).

To date, there are only a few molecular insights in *J. effusus*. The species is diploid ($2n = 42$) and has a relatively small genome with a measured DNA 1C-value of 0.3 pg (Michalski and Durka, 2012). Plastome sequence data are available (Bennett and Leitch, 2005). With the available information on *J. effusus*, and considering the results of **Chapter 2**, this study aimed to achieve three objectives:

1. Annotating the transcriptome assembly of *J. effusus* to generate the first report on its genomic elements. Here, functional analysis, orthologs comparison, and gene enrichment analysis were carried out. Results were compared with the three phylogenetic relatives, namely *S. bicolor*, *O. sativa*, and *Zea mays*. This part served also to evaluate the quality of the assembled transcriptome.

Database of J. effusus *was a necessary step to pursue further for stress response stud.*

2. Targeted investigations on the presence of genes involved in plant defense. Here, we manually looked at the genes typical to plant-pathogen interactions, as well as transcript abundances of peroxidases and superoxide dismutase.

3. Testing the developed database for metaproteomics analysis on a subset of plant tissues which were previously exposed to cotrimoxazole in order to study the stress response of *J. effusus* during the exposure regime (discussed in **Chapter 2**).

These research goals aim to benefit future studies on the performance of wetland ecosystems carrying *J. effusus* as a model plant as well as extend the observations on plant response to cotrimoxazole stress in CWs.

3.2 Methods

3.2.1 Plant materials and RNA isolation

Plant tissues (roots and shoots) were harvested from individuals at the vegetative developmental stage. In total 18 genotypes that were raised from seeds collected in the field were used. The geographical distribution of the sampled locations is presented in Supplementary Figure B.1. The obtained plant tissues were frozen in liquid nitrogen and kept at −80°C until processing. Total RNA was extracted from roots and shoots separately using the RNeasy Plant Mini Kit as per manufacturer's guidelines (Qiagen, Hilden, Germany). In order to represent a wide range of expressed genotypic variability within individuals and the species, extracts were then pooled with the final mix containing approximate equal contributions of each genotype and tissue type.

3.2.2 Transcriptome sequencing and assembly

Assembly preparation refers to the aligning and merging of smaller nucleotide sequences to generate a longer yet accurate sequence.

Standard library preparation and sequencing of total RNA using one lane of an Illumina HiSeq (2 x 100 bp paired-end) and two runs of Roche 454 Titanium were done at the Duke Center for Genomic and Computational Biology (Durham, USA) yielding 249 million Illumina paired-end reads and 2.8 million 454 reads. After removing sequencing adaptors, quality-controlled reads were processed using two different *de novo* transcriptome assemblers. Illumina reads were assembled using Trinity version 20130225 (Grabherr et al., 2011), and 454 reads were assembled using Mira version 3.9.15, (Chevreux et al., 2004; Chevreux et al., 1999). Both assemblers were run with default parameters. The software TransRate (Smith-Unna et al., 2016), which enables reference-free quality evaluations of *de novo* transcriptome assemblies, was used for analysis of Trinity assembly. Mira and Trinity assemblies were combined and CD-HIT version 4.5.7 (Chevreux et al., 2004; Grabherr et al., 2011) was used to remove redundant sequences. The assembly is available at GenBank under accession no. PRJNA345287.

De novo transcriptome assembly refers to the creation of assembly without the aid of reference genome.

3.2.3 Functional annotation

In this research, Camille Scott's *dammit!* annotation pipeline was used to annotate the transcriptome assembly (https://github.com/camillescott/dammit). Within the pipeline, annotation begins by building gene models with TransDecoder v2.0.1 (Haas et al., 2013a). Subsequently, it utilizes multiple databases for annotating the transcriptome: protein domains in PfamA v29.0, Rfam v12.0 to find non-coding RNAs (Nawrocki et al., 2014), the execution of a LAST search for known proteins in the OrthoDB database (Finn et al., 2016; Sonnhammer et al., 1997), ortholog matches in the Benchmarking Universal Single-Copy Orthologs (BUSCO) database (Simão et al., 2015), and orthology searches in OrthoDB (Kriventseva et al., 2014). The pipeline was further provided with the previously finished transcriptome of *S. bicolor* as a reference genome based on the fact that phylogenetic position of *J. effusus* is closer to *S. bicolor* (Figure 3.1) (Givnish et al., 2010) and its transcriptome is also well-annotated (Dugas et al., 2011; Olson et al., 2014).

Transcriptome annotation is the process of characterizing genetic elements in the assembly for putative functioning.

According to the plastome data, S. bicolor *was a suitable closer relative of* J. effusus *based on its well-finished transcriptome annotation history among other members of Poales.*
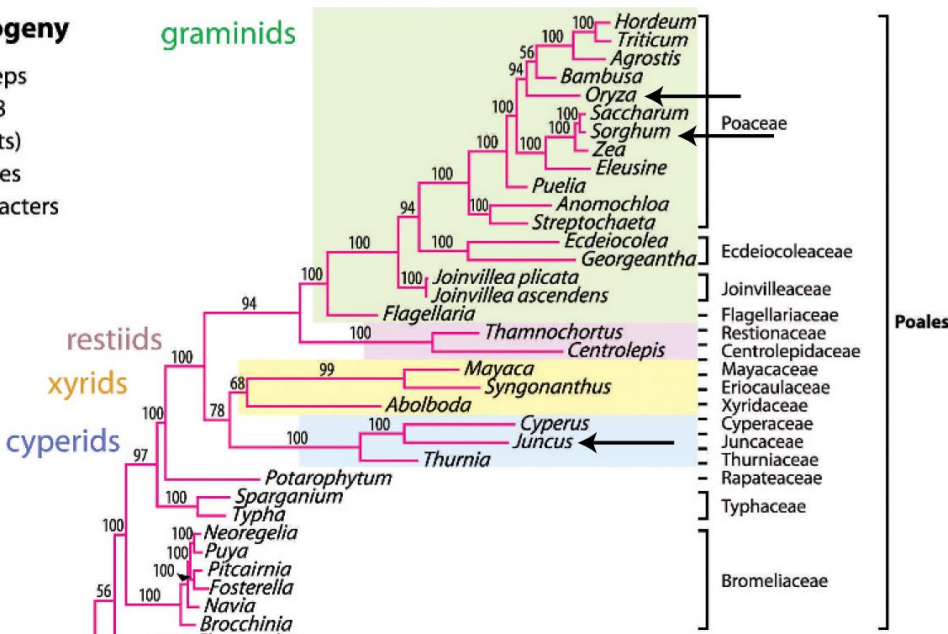
Figure 3.1: Phylogenetic tree for Poales based on the plastome data. Black arrows highlight studied members of the Poales and their phylogenetic relationship. (Source: Givnish et al., 2010). MP: maximum parsimony.

The assembly quality and annotation completeness were assessed using BUSCO v3, which supports interpretation of assembly coverage based on the presence of single-copy orthologous genes (Simão et al., 2015). To compare the assembly results of *J. effusus*, BUSCO was also run with transcriptomes of *O. sativa* subsp. japonica and *S. bicolor* (http://plants.ensembl.org/info/website/ftp/index.html). All annotation files incl. Supplementary Tables are available at Mendely under the DOI:10.17632/cx7k2v38m7.3.

Mandely repository is a cloud to upload and share scientific data. It assigns DOI to each submitted data.

3.2.4 Functional classification

Gene ontology (GO) analyses were carried out on predicted protein sequences using InterProScan v.5.26-65.0, available as virtual machine image on Jetstream cloud (https://use.jetstream-cloud.org/application/images/586). The GO annotations were then plotted using the BGI-WEGO program (http://wego.genomics.org.cn/cgi-bin/wego/index.pl) (Ye et al., 2018) together with *O. sativa* and *S. bicolor* to elucidate relative distribution of Molecular Function, Cellular Components, and Biological Processes (Ashburner et al., 2000a). Afterward, predicted protein sequences were mapped to the reference canonical Kyoto Encyclopedia Genes and Genomes (KEGG) pathways as additional approach for functional annotation and categorization. The predicted protein sequences were then submitted to KEGG automatic annotation server (KAAS) (http://www.genome.jp/tools/kaas/) with the single-directional best-hit (SBH) method selected for pathway mapping. Finally, gene set enrichment analysis (GSEA) was performed on non-redundant gene sequences using the GO-based enrichment tool DAVID (Database for Annotation, Visualization, and Integrated Discovery) (Huang et al., 2007). DAVID provides ranking of KEGG pathways on the basis of Benjamini corrected *p* values. The number of genes shared between *J. effusus* and the members of the Poaceae *S. bicolor*, *O. sativa*, and *Z. mays* was assessed by OrthoVenn, a web platform that identifies COGs clusters by comparing the predicted proteins sequences with the database (Wang et al., 2015b). Default parameters were used for protein similarity comparisons.

GO project aims to maintains the vocabulary of gene products as well as provide annotation.

KEGG is the collection of databases covering information about genomes, biological pathways, diseases, and chemical substances.

GSEA analysis were carried out to study whether genes enriched in J. effusus and its closer relatives are similar.

3.2.5 Genes potentially involved in plant-stress response

J. effusus, being a helophyte plant, has evolved various regulatory and metabolic mechanisms to cope with environmental stresses (Flowers and Colmer, 2008). To study such stress response, KEGG identified genes were characterized with regard to the biochemical pathway "plant-pathogen interaction" for hypersensitive response (HR), programmed cell death, pathogen-associated molecular pattern (PAMP) triggered immunity and defense-related gene induction. Additionally, I also looked for peroxidases and superoxide dismutase in the Pfam database that are previously recognized as an important role in plant defense especially the production and scavenging of ROS (Yazawa et al., 2013). To restrict the search, only plant peroxidases with a Pfam peroxidase domain "PF00141" (http://pfam.sanger.ac.uk) were queried for.

Assembly annotation is usually integrated with metabolic pathways construction using KEGG database.

3.2.6 Metaproteomics: response of *J. effusus* to cotrimoxazole

The metaproteomics study was carried out on four samples, i.e., exposed and un-exposed roots and shoots. These samples were collected from the PFRs treated with cotrimoxazole (see section 2.2.1 of Chapter 2). Here, the main idea was to see whether the developed database was a useful resource for the metaproteomics study. We aimed to extend this study if protein extraction was efficient enough to obtain valuable biological information for this study. The protocols used for the extraction of proteins were previously established by the proteomics group, Environmental Biotechnology Department, UFZ, Germany, for soil samples.

Metaproteomics analysis were carried out to test the database efficiency and to support results of Chapter 2.

For this purpose, 5 g of root and shoot samples were subjected to protein extraction. The plant tissues were transferred to 2-ml tubes, which already had two spatula tips of zirconium beads (0.1 mm diameter, Biospec) for the protein extraction according to Lünsmann et al., (2016). After proteolytic cleavage using in-gel digestion, the peptide lysates were desalted with SOLAμ™ SPE plates (Thermo Scientific). Peptide lysates were reconstituted in 15 µL 0.1% formic acid and peptide concentrations were determined using Nanodrop (NanoDrop2000, Thermo Fisher Scientific). For each LC-MS run, 1 µg of peptides were injected into a Nano-HPLC (UltiMate 3000, Dionex,

Thermo Fisher Scientific). Peptides were first trapped for 3 min on a C18-reverse phase trapping column (Acclaim PepMap® 100, 75 µm x 2 cm, particle size 3 µm, nanoViper, Thermo Fisher Scientific), followed by separation on a C18-reverse phase analytical column (Acclaim PepMap® 100, 75 µm x 25 cm, particle size 3 µm, nanoViper, Thermo Fisher Scientific) using a two-step gradient (90 min from 4 % to 30 % B, then 30 min from 30 % to 55 % B ; A: 0.1 % formic acid in MS-grade water; B: 80 % acetonitrile, 0.1 % formic acid in MS-grade water) with a solvent flow-rate of 300 nL/min and a column temperature of 35°C. Eluting peptides were ionized by a nano ion source (Advion TriVersa Nanomate, Ithaca, NY, USA) and measured using a Q Exactive HF mass spectrometer (Thermo Fisher Scientific) with the following settings: MS resolution 120,000, MS automatic gain control (AGC) target 3,000,000 ions, maximum injection time for MS 80 ms, intensity threshold for MS/MS of 17,000 ions, dynamic exclusion 30 sec, TopN =20, isolation window 1.6 m/z, MS/MS resolution 15,000, MS/MS AGC target 50,000 ions, maximum injection time for MS/MS 120 ms.

Proteome Discoverer (v2.0, Thermo Fisher Scientific) software was used to process LC-MS/MS files. MS spectra were searched against three databases. (1) For plant proteins, the database developed in this study was used. (2) For bacterial proteins, an additional database was developed to target only those bacterial species which were previously identified through 16S rRNA gene amplicon sequencing (see section 2.3.7 of Chapter 2). This included proteins sequences from all the species belonging to identified 414 genera available at NCBI (cf. section 2.3.7 of chapter 2). The sequences were merged to generate a single protein (fasta) file. (3) The publicly available SILVA archaeal database was used. The SEQUEST HT algorithm was used for matching purposes. Enzyme specificity was selected to trypsin with up to two missed cleavages allowed using 10 ppm MS tolerance and 0.02 Da MS/MS tolerances. Oxidation (methionine) and acetylation (lysine) were set as dynamic modifications; carbamidomethlyation (cysteine) was selected as a fixed modification. Peptide spectrum matches (PSMs) were validated using percolator with a false discovery rate (FDR) less than 1% and quality filtered for only rank 1 peptides with XCorr ≥2.25 [+2] and ≥2.5 [+3]. Protein quantification was carried out using the precursor ion area detector (2 ppm mass precision) of Proteome Discoverer. Lastly, identified peptides from each plant

In addition to the plant database, database of bacterial endophytes was also developed. These endophytic bacteria were previously identified through 16S amplicon sequencing (Chapter 2).

sample (un-exposed and exposed roots and shoots) were plotted using phyloseq package in R.

3.3 Results

3.3.1 Transcriptome assembly and analysis scheme

The overall process of transcriptome sequencing, assembly, annotation, ortholog comparison and validation of the assembly is summarized in Figure 3.2.

Illumina and 454 sequencing generated 108,600,750 clean reads comprising a total of 47 Gb, which was considered as good transcriptome coverage of the estimated genome size of around 270 Mbp. The reads were *de novo* assembled using Trinity (Haas et al., 2013b) and Mira (Chevreux et al., 2004; Chevreux et al., 1999). Quality analysis of the Trinity assembly with the software TransRate computed an optimized score of 0.34, which was better than the score for about 50% of 155 sampled *de novo* assembled transcriptomes (Gore et al., 2009). CD-HIT was used to remove redundant sequences, which resulted in 158,591 contigs with lengths ranging between 200 bp to 18.5 kbp. The average contig length was 780 bp, and N50 was 255 bp.

As a first quality control, BUSCO v3 was run on the *J. effusus* assembly as well as on previously assembled and annotated transcriptomes of *O. sativa* and *S. bicolor* to determine whether the genome coverage was sufficiently high to allow for comprehensive analyses. BUSCO results for the three species were very similar. Out of 429 single copy ortholog genes common to the Eukaryota lineage there were 81%, 82%, and 78% complete single-copy BUSCOs, 42%, 26%, and 24% duplicated BUSCOs, 8.8%, 4.1%, and 6% fragmented BUSCOs, and 9.5%, 12%, and 15% missing BUSCOs respectively for *J. effusus*, *S. bicolor* and *O. sativa*.

BUSCO results indicated that transcriptome assembly was reliable and can be used for downstream analysis and database development.
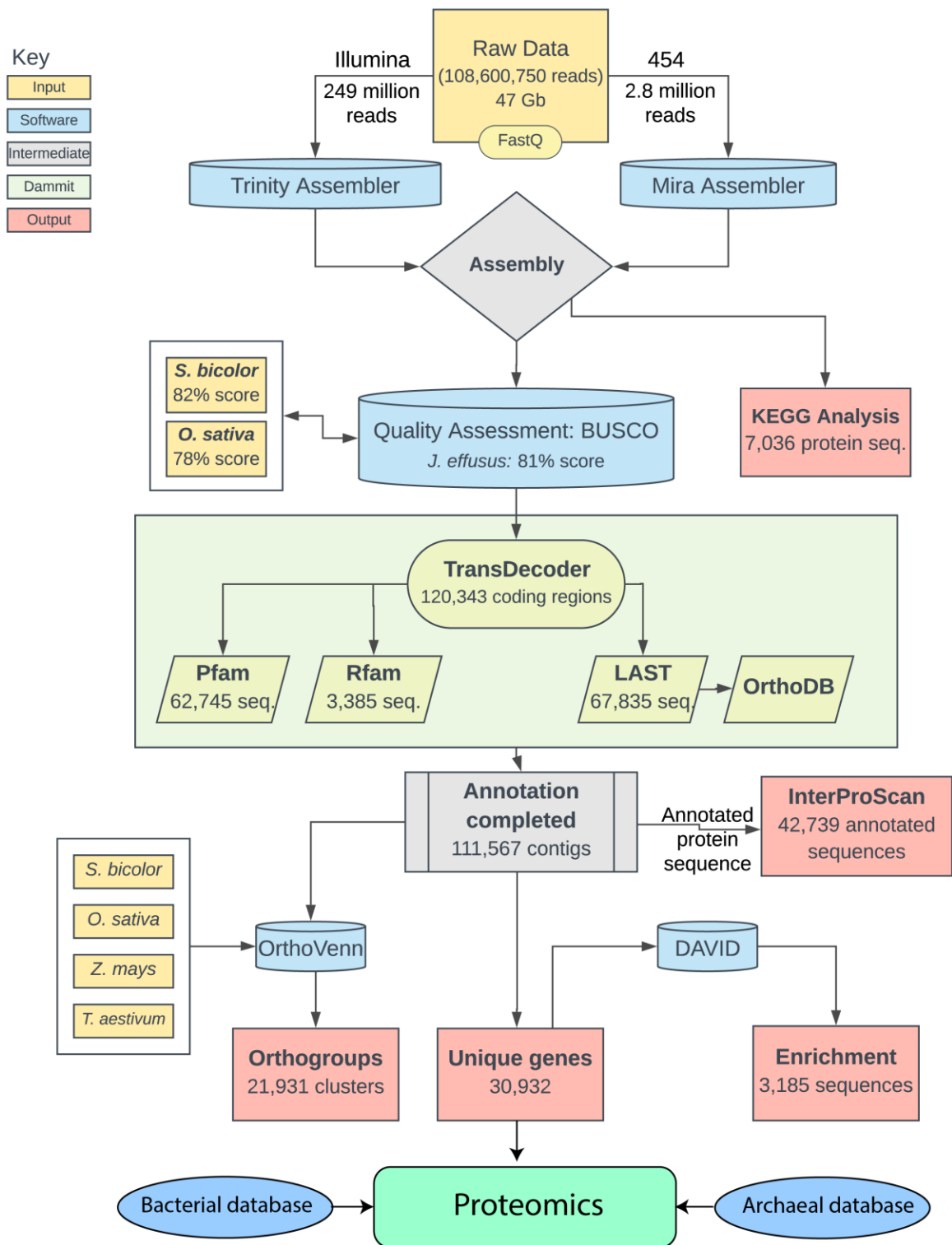
Figure 3.2: The overall process of transcriptome assembly, functional annotation, GO enrichment, orthologs clustering, and validation. In total, 30,932 genes were used in the proteomics study.

3.3.2 Constructing and annotating gene models

The assembled transcripts were annotated using Camille Scott's *dammit!* annotation pipeline (https://github.com/camillescott/dammit). Gene model building using Transdecoder (Fu et al., 2012) predicted 120,343 likely coding regions (75.8% of all contigs) among which 79,203 (49.4%) contained a stop codon. There were 62,745 (39.6%) predicted coding regions that matched to the protein family database Pfam (Haas et al., 2013a), whereas the LAST search found that 67,835 predicted coding regions (42.8%) matched to the OrthoDB database (Kriventseva et al., 2007; Kriventseva et al., 2014; Waterhouse et al., 2010). In addition, 3,385 predicted coding regions (2.13%) matched to the Rfam database for non-coding RNAs. In total, 111,567 contigs (70.3%) were annotated when combining the results of all searches. The annotation features included putative nucleotide and protein matches, five- and three-prime UTRs, exons, mRNA, as well as start and stop codons.

Gene model is the genetic element with information on transcript features such as exon, intron, splice sites, UTRs, etc.

To ensure further that the assembly was of high quality, genomic features were compared both statistically and manually with previously well-annotated transcriptomes of *S. bicolor* and *O. sativa* (second quality control step). Annotated transcripts were classified into different functional groups via Gene Ontology (GO) analysis by InterProScan. A total of 42,739 sequences (38.3% of all annotated contigs) were GO annotated out of the categories Molecular Functions, Cellular Components, and Biological Processes. The WEGO (web gene ontology annotation plot) plot for GO terms revealed that Molecular Functions was the dominant category (50.7% of all GO-annotations) followed by Biological Processes (35.7%) and Cellular Components (13.6%). Highly represented GO terms within Molecular Functions were 'binding' (GO:0005488) and 'catalytic activity' (GO:0003824); in the Biological Processes ontology group it were 'cells' (GO:0005623), 'cellular process' (GO:0009987), and 'biological regulation' (GO:0065007); and 'cellular parts' (GO:0044464) and 'organelles' (GO:0043226) in the Cellular Components ontology. The GO terms of the assembled transcriptome were compared with those of *S. bicolor* and *O. sativa* (Figure 3.3).

The GO project aims to unify the information about gene products and its attributes across all species.
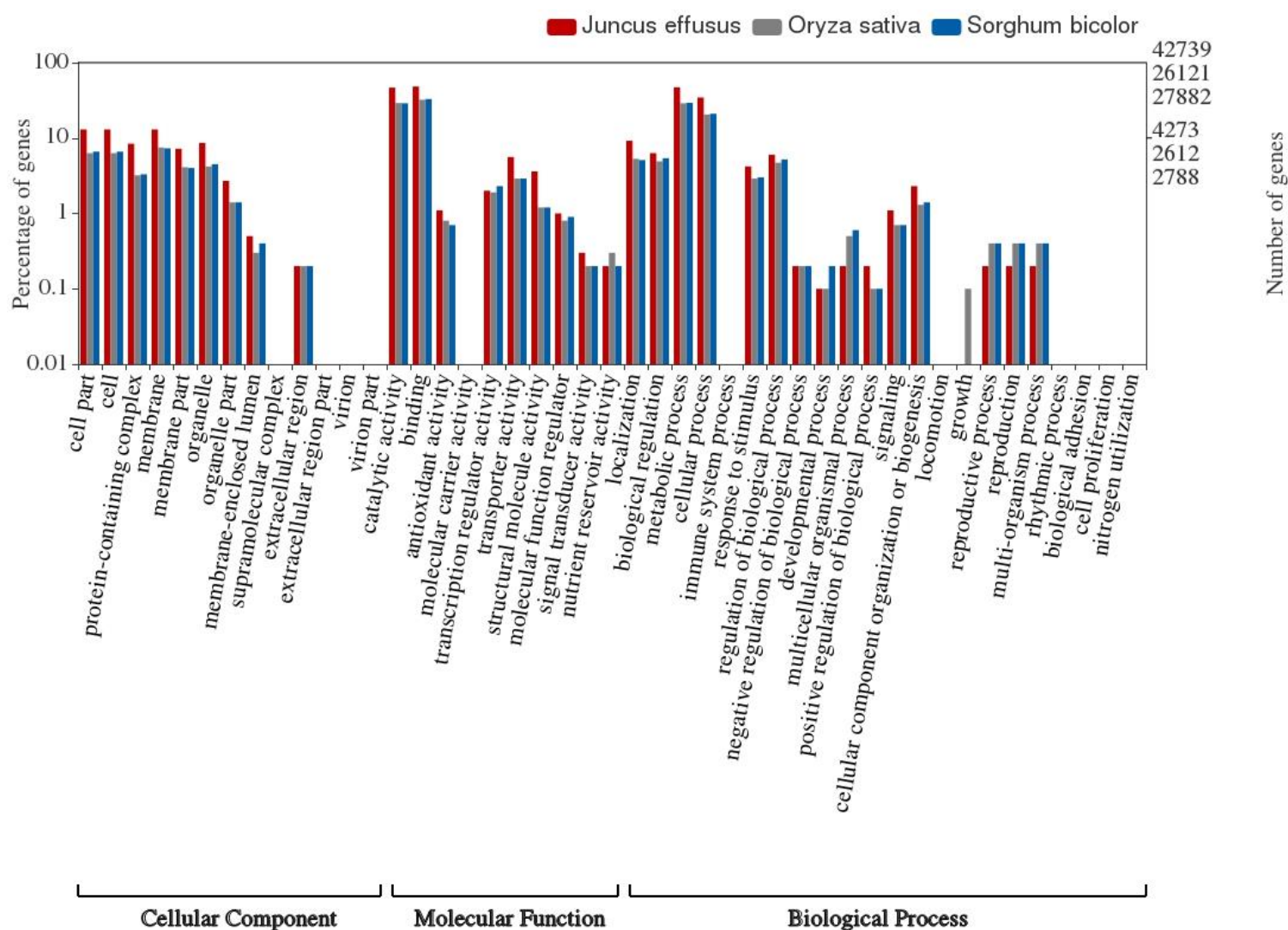
Figure 3.3: Histogram of level GO term assignments for *J. effusus*, *S. bicolor*, and *O. sativa* annotated gene models. The results are summarized for three GO categories, Cellular Component, Molecular Function, Biological Process. In all the processes, J. effusus shared significant similarities with its closer relatives.

The results revealed a similar functional distribution with both reference transcriptomes, suggesting similar gene complements between *J. effusus* and its relatives. Minor contributions of 'antioxidant activity' (GO:0016209), 'extracellular region' (GO:0005576), 'extracellular part' (GO:0044421), and 'viral reproduction' (GO:0016032) were observed for *J. effusus*, while those categories were missing for *S. bicolor* and *O. sativa*.

KEGG analysis assigned enzyme commission (EC) numbers to 7,036 protein sequences belonging to 380 different pathways. The KEGG category 'metabolic pathways' contained the majority of annotated

proteins (851 members, 12.1%), followed by 'biosynthesis of secondary metabolites' (395 members, 5.61%). To evaluate further the qualitative accuracy of the functional annotation, the completeness of the fundamental pathways was manually checked including photosynthesis, oxidative phosphorylation, glycolysis/gluconeogenesis, citrate cycle, pentose phosphate pathway, amino acid metabolism, and information processing. All of those pathways were mainly covered in the transcriptome.

Clusters of orthologous gene (COG) analysis of *J. effusus* revealed the presence of 21,931 clusters, out of which 10,296 were shared among *S. bicolor*, *O. sativa*, and *Z. mays* (Figure 3.4). These clusters involve proteins related to carboxylation and oxygenation, glycosylation, integral membrane components, nuclear mechanisms such as chromatin binding, cytoplasm, and chloroplast integrities, and several other putative uncharacterized proteins. Further analyses of GO terms illustrated a significant enrichment for the proteins related to electron carrier activities in the mitochondrial matrix (e.g., GO:0019243), photosystem II assembly (e.g., GO:0010207), transcription from plastid promoter (e.g., GO:0042793), regulation of protein dephosphorylation (e.g., GO:0035304), and hydrogen peroxide biosynthetic process (e.g., GO:0050665). The three members of the Poaceae had more similarities to each other than to *J. effusus*, which matches the topology of the phylogenetic tree based on plastome sequences (Givnish et al., 2010). Overall, 9,872 clusters were unique for *J. effusus*, and included proteins belonged to chloroplastic mechanisms, plasma membrane functioning, disease resistance, phytohormone productions for stress-ripening, and ion binding.

Orthologues are homologous genes which are diverged in different species from a common ancestral gene.

J. effusus showed highlight overlap for orthologous genes with S. bicolor
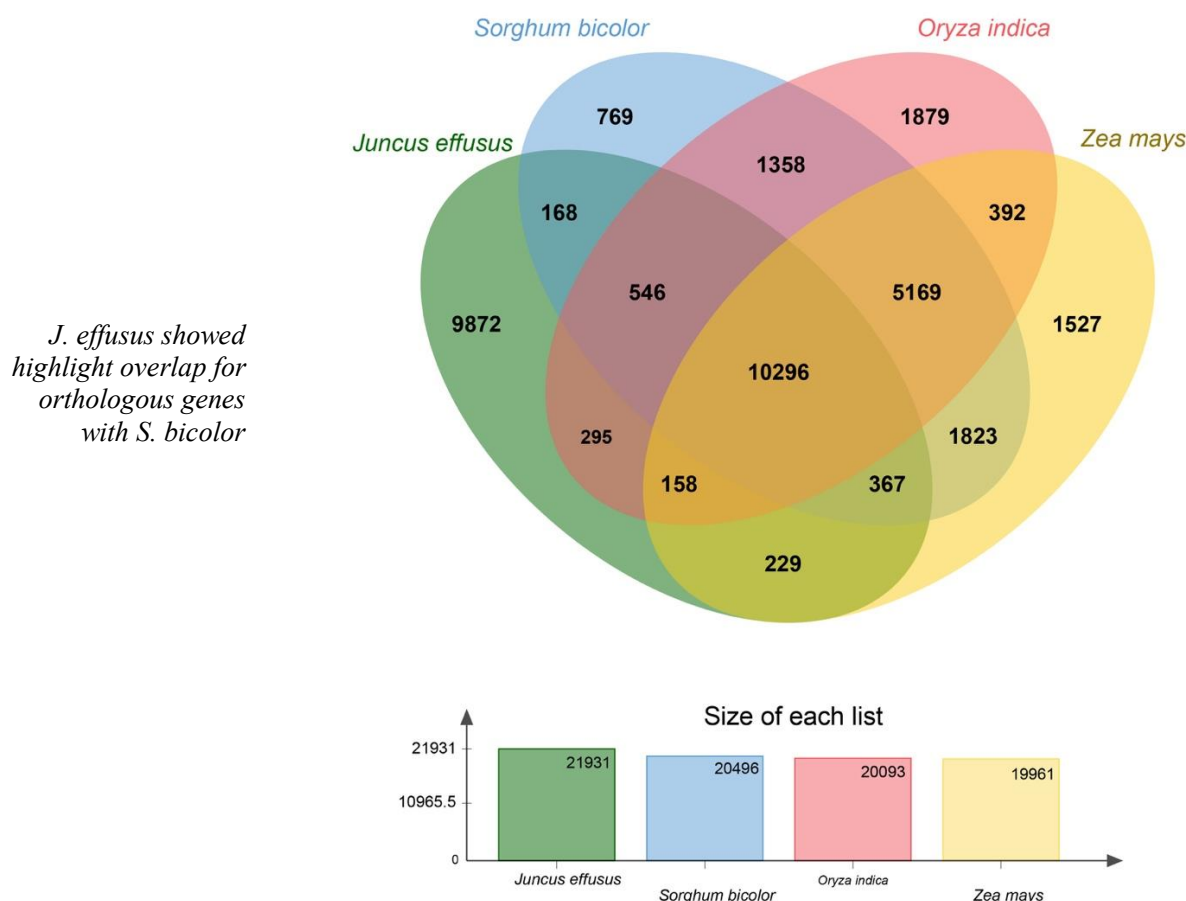
Figure 3.4: Comparisons of the core orthologous gene clusters among *J. effusus*, *O. sativa*, *Z. mays*, and *S. bicolor*. *J. effusus* exhibits the highest similarity with *S. bicolor* followed by *O. sativa* and *Z. mays*.

As a final quality control, Gene Set Enrichment Analysis (GSEA) with DAVID was carried out (Huang et al., 2008). Results of GSEA were consistent with the KEGG findings. A complete list of enriched sequences and number of KEGG orthology (KO) hits for *J. effusus*, *S. bicolor*, *O. sativa* and *Z. mays* are presented in Table 3.1. Sequences of *J. effusus* with redundant KO terms likely originating from paralogous genes and orthologues in the various genotypes were combined to a total of 30,932 gene sequences with matching hits to proteins (E < $1e^{-6}$). Among these sequences there were 3,185 enriched sequences (10.2%) of which most belonged to the sub-groups of metabolic pathways (1,407 sequences, 44.1%), biosynthesis of secondary metabolites (1140 sequences, 35.8%), biosynthesis of amino acids (156 sequences, 4.89%), oxidative phosphorylation (114 sequences, 3.57%),

amino sugar and nucleotide sugar metabolism (113 sequences, 3.54%). Sequences grouping into the category genetic information processing (GIP) accounted for 322 sequences (1.04%) and included the enriched categories ribosomes (276 sequences, 85.7%) and protein export (46 sequences, 14.2%). By contrast, environmental information processing (EIP) contained no enriched KEGG pathways for *J. effusus* (although the EIP pathways were complete as mentioned above). All pathways enriched for in *J. effusus* were also enriched for in *S. bicolor* except porphyrin and chlorophyll metabolism, which was only enriched in *J. effusus*.

Information on KEGG pathway maps representing knowledge on the molecular interaction, reaction and relation networks for **Metabolism.**

Table 3.1: Genes enriched for KEGG and number of KO hits for *J. effusus*, *S. bicolor*, *O. sativa*, and *Z. mays*

KEGG pathway	J. effusus		S. bicolor		O. sativa		Z. mays	
	KEGG	KO	KEGG	KO	KEGG	KO	KEGG	KO
Metabolism								
Global and overview maps								
Metabolic pathways	1407	855	1431	865	1369	817	1793	850
Biosynthesis of secondary metabolites	833	396	844	395	776	397	1033	400
Biosynthesis of antibiotics	307	193	312	194	352	192	462	194
Carbon metabolism	-	-	-	-	226	90	263	90
Biosynthesis of amino acids	156	98	157	98	189	97	-	-
Carbohydrate metabolism								
Glycolysis / Gluconeogenesis	92	33	94	33	112	32	134	33
Citrate cycle (TCA cycle)	-	-	-	-	49	20	-	-
Pentose phosphate pathway	-	-	-	-	46	17	-	-
Ascorbate and aldarate metabolism	-	-	-	-	37	16	-	-
Starch and sucrose metabolism	-	-	-	-	107	30	-	-
Amino sugar and nucleotide sugar metabolism	113	40	114	40	105	40	-	-
Pyruvate metabolism	-	-	-	-	73	27	-	-

Energy metabolism								
Oxidative phosphorylation	114	86	118	91	-	-	129	86
Photosynthesis	-	-	-	-	75	35	-	-
Carbon fixation in photosynthetic organisms	-	-	-	-	70	25	-	-
Lipid metabolism							-	-
Cutin, suberine and wax biosynthesis	-	-	-	-	-	-	28	8
Steroid biosynthesis	-	-	-	-	-	-	38	18
Linoleic acid metabolism	-	-	-	-	-	-	15	4
Amino acid metabolism								
Glycine, serine and threonine metabolism	52	34	52	34	-	-	-	-
Arginine and proline metabolism	-	-	-	-	-	-	62	24
Tyrosine metabolism	-	-	-	-	-	-	40	18
Metabolism of other amino acids								
Glutathione metabolism	98	18	98	18	-	-	-	-
Glycan biosynthesis and metabolism								
N-Glycan biosynthesis	-	-	-	-	-	-	44	31
Metabolism of cofactors and vitamins								
Thiamine metabolism	13	11	14	11	-	-	-	-
Pantothenate and CoA biosynthesis	-	-	-	-	-	-	30	16

Information on KEGG pathway maps representing knowledge on the molecular interaction, reaction and relation networks for **Genetic Information Processing and Environmental Information Processing** / **Information Processing**

Porphyrin and chlorophyll metabolism		41	33	36	33	50	33
Metabolism of terpenoids and polyketides							
Terpenoid backbone biosynthesis	-	-	-	-	-	-	58	30
Diterpenoid biosynthesis	-	-	-	-	27	18	-	-
Biosynthesis of other secondary metabolites							
Phenylpropanoid biosynthesis	-	-	-	-	114	17	-	-
<u>Genetic Information Processing</u>							
Transcription							
Spliceosome	-	-	-	-	-	-	194	102
Translation							
Ribosome	276	130	278	132	-	-	-	-
mRNA surveillance pathway	-	-	-	-	97	49		
Folding, sorting, and degradation							
Protein export	46	26	47	26	-	-	-	-
Sulfur relay system	-	-	-	-	-	-	14	10
<u>Environmental Information Processing</u>							
Signal transduction							
Plant hormone signal transduction	-	-	-	-	172	38	253	41

(Note: the value "33" also appears at the far left of the "Porphyrin and chlorophyll metabolism" row.)

Cellular Processes

Transport and catabolism

| Endocytosis | - | - | - | - | **117** | **58** | - | - |

3.3.3 Genes involved in plant defense

In total, 28 genes were identified to be involved in plant defense, i.e. KEGG pathway "plant-pathogen interaction" (KO04626) (Table 3.2; Figure 3.5). Four genes were found to be directly related with disease resistance and susceptibility (R-genes), one gene for pathogenicity, one identified as heat shock protein, and a few of them as kinases, oxidoreductase, nitric oxide synthase, transcription factors, or binding proteins (Table 3.2). Two genes encoding for FLS2 proteins were identified. Together, activation of these genes triggers MAPK signaling pathway and starts expression of defense genes. This completed the pathway to express "defense-related gene induction", "hypersensitive response", and "programmed cell death".

Table 3.2: Genes identified for the KEGG pathway "plant-pathogen interactions".

Entry	Name	Definition
K13457	RPM1, RPS3	disease resistance protein RPM1
K13459	RPS2	disease resistance protein RPS2
K13458	RAR1	disease resistance protein
K18875	EDS1	enhanced disease susceptibility 1 protein
K09487	HSP90B, TRA1	heat shock protein 90 kDa beta
K13449	PR1	pathogenesis-related protein 1
K13436	PTI1	pto-interacting protein 1
K13456	RIN4 (2)	RPM1-interacting protein 4
K05391	CNGCs	cyclic nucleotide gated channel, plant
K13420	FLS2 (2)	LRR receptor-like serine/threonine-protein kinase
K13473	CEBiP	chitin elicitor-binding protein
K13429	CERK1	chitin elicitor receptor kinase 1
K13412	CDPK	calcium-dependent protein kinase
K13447	Rboh	respiratory burst oxidase, oxidoreductase
K02183	CALM	calmodulin
K13427	NOA1 /NOS	nitric-oxide synthase, plant
K13414	MEKK1	mitogen-activated protein kinase kinase kinase 1
K13413	MKK4_5	mitogen-activated protein kinase kinase 4/5
K13423	WRKY25	WRKY transcription factor 25
K13426	WRKY29	WRKY transcription factor 29
K16224	FRK1	senescence-induced receptor-like serine/threonine-protein kinase
K00864	glpK, NHO1	glycerol kinase
K13430	PBS1	serine/threonine-protein kinase PBS1
K12795	SUGT1, SGT1 (2)	suppressor of G2 allele of SKP1
K18834	WRKY1	WRKY transcription factor 1
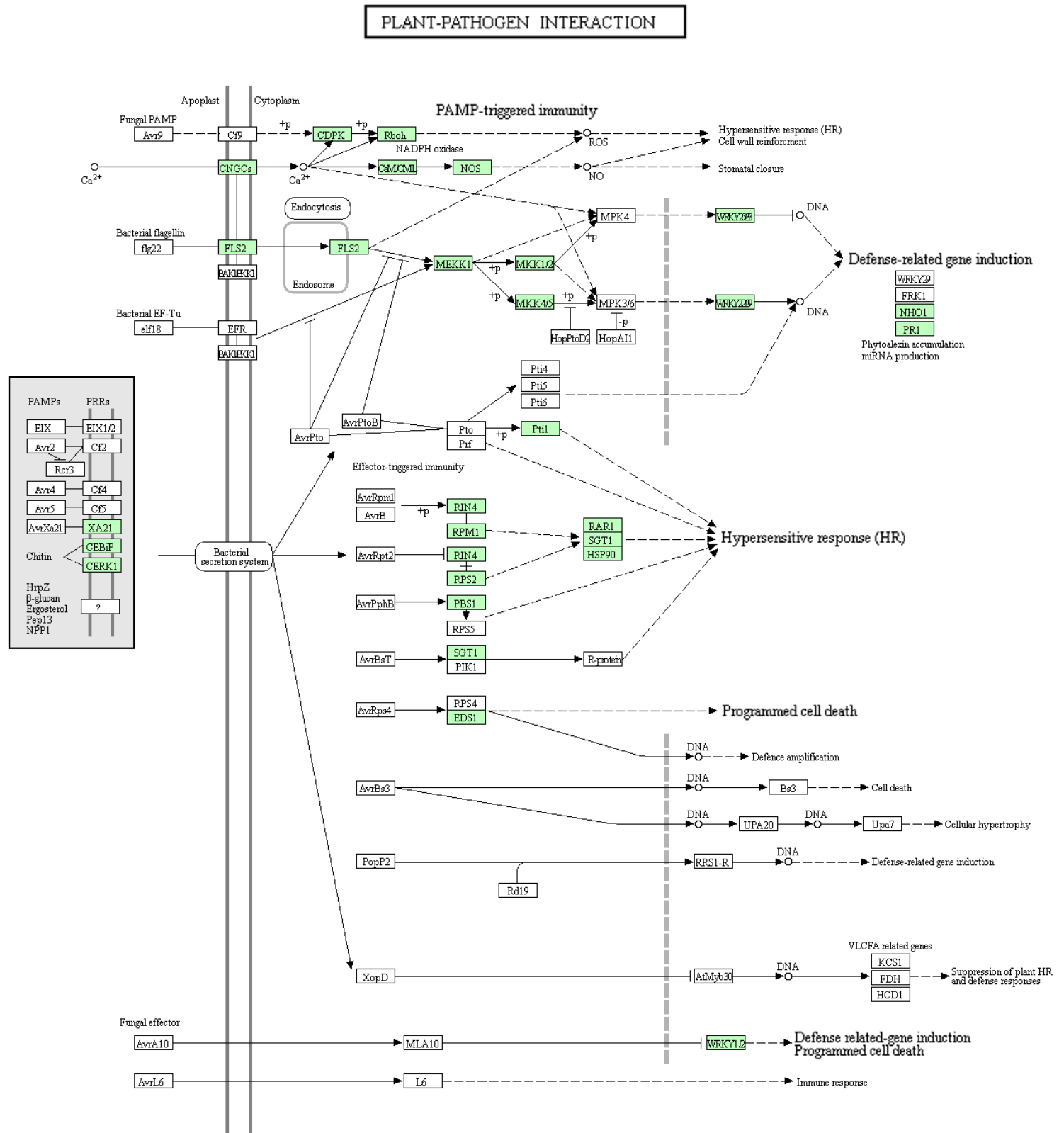
Figure 3.5: Genes predicted to be involved in plant-pathogen interaction pathway derived from KEGG pathway mapping. Green color indicates their presence in the database whereas white color means either they were missing or not being expressed.

Additionally, 280 Pfam entries of peroxidases and 72 for superoxide dismutases were found in the Pfam database of *J. effusus*. The complete KEGG pathway for plant-pathogen interactions is presented in Figure 3.5.

3.3.4 Response of *J. effusus* to cotrimoxazole exposure

Only 286 proteins were detected from the plant tissues, which suggested that protein extraction efficiency was not sufficient for a detailed analysis. Among the identified proteins, 113 matched to the database of *J. effusus* developed in this study, 168 were of bacterial origin, and 5 belonged to archaea (Supplementary Table B.1). No attempts were made to improve the protein extraction procedure since it was questionable whether a sufficient improvement could have been obtained during the timeframe of this Ph.D. Thus, data presented below of rather preliminary nature.

Plant proteins

In the un-exposed plant roots, proteins related to plant metabolic processes were identified.

In the sample from un-exposed roots, 75 proteins were identified among which some of them were related to the typical plant processes such as photosynthesis, acetylation, and biosynthesis of the polyphenol compounds. Additionally, there were proteins relating to general metabolic processes in plants such as glycolysis, citric acid cycle, cell division, and the oxidative pentose phosphate pathway. We also found peroxidases, heat shock proteins, catalases, ribosomal proteins, chaperons, and a few uncharacterized proteins. In the exposed roots, however, only 6 proteins were detected, which also highlighted the inefficiency of protein extraction. Among these proteins, 4 were annotated as uncharacterized proteins, 1 was peroxidase and the other one was predicted to be proline-rich protein (supplementary Table B.1).

In the exposed plant roots, protein extraction efficiency was not sufficient to make any opinion.

Likewise, in the un-exposed shoots, 44 plant proteins were detected including transketolase (a chloroplastic isoform), RuBisCO proteins, microtubules proteins, photosystem II proteins, ribosomal proteins, cell division control proteins, heat shock proteins, chaperons and histones, elongation factors, etc. These proteins, as explained earlier, are mainly related to plant metabolic processes. On the other hand, in the exposed shoots, 61 proteins were detected which were most similar to the proteins identified from un-exposed plant roots except that a few

peroxidases and catalases were also observed (Figure 3.5, Supplementary table B.1). While these proteins are involved in oxidative stress response, not too much emphasis should be placed on their detection gave the overall proteomic data paucity.

Bacterial proteins

Extraction of bacterial proteins appeared to be slightly better than that of plant proteins. In the un-exposed plant roots, 21 bacterial proteins were identified which were mostly related to metabolic pathways in rhizospheric bacteria or abundant prokaryotic proteins such as chaperons or flagellin. In the exposed roots, 109 bacterial proteins were detected. These proteins belonged to the compounds involved in C_1 pathway; for instance, methanol dehydrogenases, which strengthened our observations made at the genomics level (**Chapter 2**). Furthermore, there were ribosomal proteins, some chaperons, flagellin proteins, and others involved in growth and division of bacteria. In the un-exposed shoots, 58 bacterial proteins were detected. These proteins were ABC transporters and cell wall proteins, metal-binding proteins, membrane proteins, bacterial cytochrome proteins, and those involved in prokaryotic cell division and metabolism. In the exposed shoots, 51 bacterial proteins were identified which were similar to the proteins observed from the un-exposed shoots without any prominent differences relating to antimicrobial stress (Figure 3.5, Supplementary table B.1).

Archaeal proteins

Archaeal proteins (n = 5) were only detected in the exposed plant roots and shoots. Among them, 4 proteins were highly abundant in the exposed roots and 1 in the exposed shoots. These proteins were identified as ribosomal biogenesis proteins, urease subunit beta, or uncharacterized proteins with no specific information relating to the taxonomy.

_____

Although these results support the findings which were previously made at genomics level (chapter 2), further refinement in protein

The proportion of bacterial proteins was increased in the post-exposure plant roots.

Post-exposure bacterial proteins confirmed the results obtain at genomics level.

extraction procedures especially for the *J. effusus* post-exposure period is recommended.
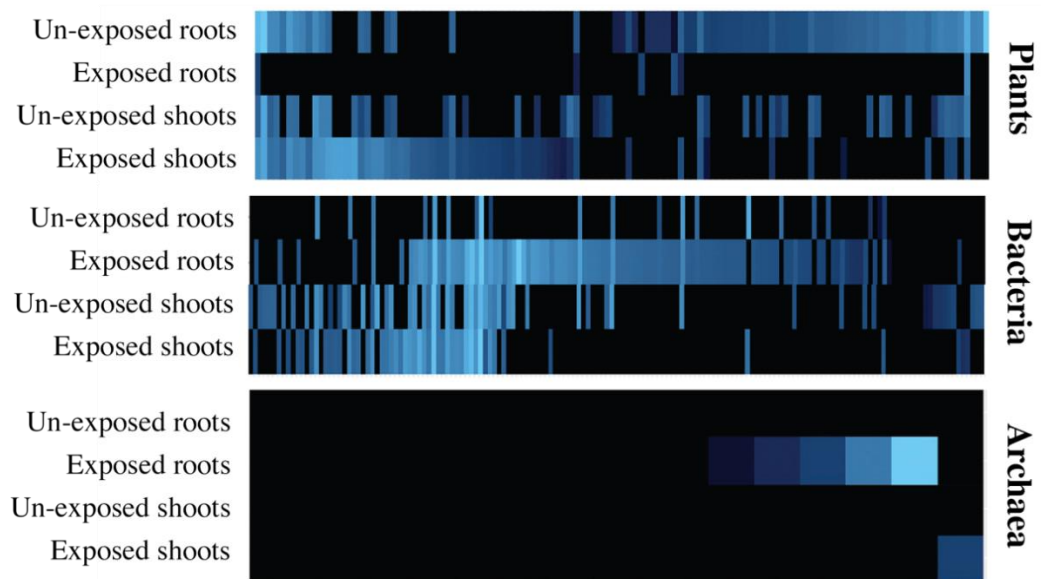
Figure 3.6: Heatmap plotting of identified proteins from exposed and un-exposed plant tissues. Plant proteins were not detected in the exposed roots but their abundance was increased in the exposed shoots. Bacterial proteins' abundance was increased in both roots and shoots after the exposure. Archaeal proteins were only observed in the exposed plant roots and shoots.

3.3 Discussion

The estimated genome size of *J. effusus* is approximately 270 Mbp which is in between the genome sizes of *Arabidopsis thaliana* (Arabidopsis Genome Initiative, 2000) and *O. sativa* (Goff et al., 2002; Yu et al., 2002). However, very few studies have been conducted to study the molecular genetics of this wetland plant. The available studies mostly focus on its intraspecific variability (Born and Michalski, 2017; Born and Michalski, 2019; Michalski and Durka, 2012).

In this study, RNA-Seq technology was used for the transcriptome profiling of 18 genotypes of *J. effusus*. As compared to the traditional large-scale expressed sequence tag (EST) sequencing, RNA-Seq is less costly as well as an efficient technology (Wang et al., 2009b). Furthermore, it gives the freedom to use a reference genome for the

assembly purposes, which was impossible with the previous assembly purposes, which was impossible with the previous transcriptome sequencing technologies (Nagalakshmi et al., 2010). As of today, RNA-Seq has been used for other members of the Poales, and particular of members of the family Poaceae, for various purposes such as *de novo* sequencing and assembly (rice, Tian et al., 2015), querying the transcriptome profiles of distinct tissues and at various development stages (wheat; Chu et al., 2017), characterization of genes involved in specific biochemical pathways (cordgrass, de Carvalho et al. 2012; pineapple, Ma et al., 2015), identification of novel transcriptome sequences (maize, Hansey et al., 2012) and isoforms (false-brome, Fox et al., 2013), SNP analysis (wheat, Fox et al., 2014), and simple sequence repeats (SSRs) detection (bamboo, Liu et al., 2012).

We conducted both single and paired-end sequencing runs to ensure high coverage. Previously, it was proposed that paired-end sequencing increases the depth of sequencing (Aronesty, 2013) and combining both single and paired-end reads even gives better efficiency in *de novo* assembly (Cahais et al., 2012). The quality analysis of the Trinity assembly (paired-end reads) with the software TransRate computed an optimized score of 0.34, which was better than the score for about 50% of 155 sampled *de novo* assembled transcriptomes (Gore et al., 2009). Subsequently, annotation was performed using the *dammit!* annotation pipeline. As of today, only two pipelines are available for transcriptome annotation: (1) *dammit!*, (prepared by Camille Scott https://github.com/dib-lab/dammit) and (2) annocript (Musacchia et al., 2015). However, annocript is in its earlier stage of development and it does not include information on at different levels of GO terms (Musacchia, F., personal communication, 2017); therefore, the *dammit!* annotation pipeline was used for our study (we were interested to look for the gene vocabulary at each level of GO terms for downstream analysis). Moreover, the *dammit!* annotation pipeline follows strict criteria of annotation, i.e., building gene models (Stein, 2001) and matching each transcript against several databases to search protein domains (Haas et al., 2013a), non-coding RNAs (Nawrocki et al., 2014), ortholog matches (Chevreux et al., 1999), and orthology assignments (Kriventseva et al., 2014). Together, this annotation process was successful because more than 27% of the annotation completed contigs were identified as unique genes. The remaining genes which had no significant matches may be lacking a known

conserved functional domain or they were very short to show significant sequence match (Wu et al., 2014). Nevertheless, the sequences that showed no hits might be of potential interests for future research on novel gene products, alternative splice variants, and differentially expressed genes. Additionally, *dammit!* comes with BUSCO orthologs analysis, which was previously suggested as ideal genomic features to assess assembly completeness (Simão et al., 2015). Our analysis suggested a high genome coverage of the assembly because the results were similar to its closer relatives *S. bicolor*, *O. sativa*, and *Z. mays*. Moreover, these results were also comparable to the previously well-finished genomes of other plants such as *A. thaliana* (Cheng et al., 2017, Triticum aestivum {Zimin, 2017 #367), *Helianthus annuus* (Badouin et al., 2017), *Olea europaea* (Cruz et al., 2016), *Malus domestica* (Daccord et al., 2017), etc. Hence, we concluded that *de novo* assembly obtained in this study was appropriate for the functional classification of genes.

Together, GO, KEGG, and COG analysis represented same findings that the quality of assembly was high and J. effusus had strikingly similar genomic features as of S. bicolor and O. sativa.

In this modern era of genome-scale biology, several tools are available to conduct functional analysis. Among them GO database (Gene Ontology Consortium, 2004), KEGG pathway mapping (Kanehisa and Goto, 2000), and COG comparison are well adopted (Chen et al., 2006). The GO database is an important genomic resource that provides structured and dynamically controlled vocabularies used for the annotation of genes, gene products, and sequences within an organism (Ashburner et al., 2000b). In this study, highly represented GO terms belonged to "Molecular Functions" category, which is consistent to the other plant transcriptome studies, e.g. *Phyllanthus amarus* (Bose Mazumdar and Chattopadhyay, 2016) and *Raphanus sativus* (Wu et al., 2015). Molecular function describes activities that occur at the molecular level, e.g. catalytic or binding activities. It is important to mention that the GO molecular function terms represent activities rather than the entities that perform a specific action (Consortium, 2004). In our case, the high similarity of GO terms with *S. bicolor* and *O. sativa* revealed similar functional distribution within these phylogenetic neighbours.

KEGG is a collection of databases that are used for the systematic analysis of gene functions and understanding of high-level functions and utilities of the biological system (Kanehisa and Goto, 2000). In

addition to the completeness of plant-specific KEGG pathways, high similarities for the enriched genes among the studied members of poales (*J. effusus*, *S. bicolor*, *O. sativa*, *Z. mays*) was most likely due to their close genetic relationship (Givnish et al., 2010). The second application of KEGG pathway analysis was to study the genes involved in "plant-pathogen interaction". In principle, plants lack adaptive immunity (Iriti and Faoro, 2007), hence, they have evolved different systems to defend against invading pathogens. The primary response is achieved via perception of pathogens by cell-surface pattern-recognition receptors (Zipfel, 2008), and is referred to as PAMP-triggered immunity (Zipfel, 2009). The presence of stress activates defense related genes whose upregulation is an indication of plant stress response (Ren et al., 2017). In our transcriptome, we found the presence of FLS2 genes in the KEGG pathway along with the activation of subsequent genes, i.e. stress-induced genes (Figure 3.4); previously, activation of FLS2 was reported to trigger MAPK signalling pathway that activates defence genes (Pitzschke et al., 2009). With this observation, we deduced the presence of primary stress response in our assembled transcriptome of *J. effusus*. It is further reported that some plants possess R genes (encoding for intracellular surveillance proteins), which monitor the presence of other pathogen virulence proteins (Houterman et al., 2009). This effector-triggered immunity occurs with localized programmed cell death to arrest pathogen growth (Coll et al., 2011). These genes were also present in our transcriptome assembly (cf. hypersensitive response genes, Figure 3.4). The presence of peroxidases and superoxide dismutases further supported the ability of *J. effusus* to respond to the presence of organismic stressors. Previously it was argued that enzymes such as catalase, superoxide dismutase, and peroxidase play an important role in the scavenging and/or detoxifying of reactive species, i.e. ROS and RNS (Shao et al., 2007).

In the KEGG pathway "plant-pathogen interaction" for J. effusus, genes involved in stress induction, and hypersensitive response were identified.

Metaproteomics is another powerful methodology to study plant stress response (Maron et al., 2007). As an attempted step-forward to the genomics study (Chapter 2), this methodology was used to study the response of *J. effusus* after cotrimoxazole exposure. However, low protein extraction prevented the gain of substantial further insights. This was particularly true for plant proteins whose relative proportion in the post-exposure root samples was extremely low. A most likely reason behind this low protein content is that the available method used

Extraction of protein efficiency should be improved for further investigations.

in this study was previously developed for soil samples and hence needs further modification to be used for plant tissues. Additionally, it could be that production of ROS and RNS might have resulted in degradation of plant proteins in the exposed roots (Davies, 1987; Russell et al., 2007). On the contrary, bacterial protein content after cotrimoxazole stress was increased in the exposed roots and most of the identified proteins were related to the bacteria involved in C_1 metabolism. This observation is in accordance with the observations made at genomics level, however, it remains unclear why extraction of bacterial proteins was better than plant proteins. Lastly, detection of archaeal proteins in the exposed plant tissues is in accordance to the PCR-observations made for total Archaea (+), methanogens (–), and ammonium oxidizing Archaea (+) [see section 2.3.10 of Chapter 2]. Presumably, degradation of plant tissues could have allowed some Archaea to enter and even proliferate within plant roots in the post-exposure period.

2.5 Concluding remarks and future outlook

Despite of the yet less successful metaproteomics attempt, this study provides the first genomic resource of *J. effusus* for future *omics* studies on this model wetland plant. Previously, only plastome sequence data was available for *J. effusus* (Bennett and Leitch, 2005), which was not sufficient to understand the complex microbiological interaction of this plant occurring in natural and engineered wetland ecosystems. A major strength of this work is the high quality of the database which shares extensive information on functional descriptions of several genetic features including genes involved in the plant-defense. In a nutshell, results obtained in this study are expected to open new opportunities for future *omics* studies on this plant. Further metaproteomics studies are recommended to decipher in-depth response of this plant to antimicrobials or other (a)biotic stressors.

References

Armengaud, J., Trapp, J., Pible, O., Geffard, O., Chaumot, A., Hartmann, E.M., 2014. Non-model organisms, a species endangered by proteogenomics. Journal of proteomics 105, 5-18.

Aronesty, E., 2013. Comparison of sequencing utility programs. The Open Bioinformatics Journal 7.

Ashburner, M., Ball, C.A., Blake, J.A., Botstein, D., Butler, H., Cherry, J.M., Davis, A.P., Dolinski, K., Dwight, S.S., Eppig, J.T., 2000a. Gene Ontology: tool for the unification of biology. Nature genetics 25, 25.

Ashburner, M., Ball, C.A., Blake, J.A., Botstein, D., Butler, H., Cherry, J.M., Davis, A.P., Dolinski, K., Dwight, S.S., Eppig, J.T., Harris, M.A., Hill, D.P., Issel-Tarver, L., Kasarskis, A., Lewis, S., Matese, J.C., Richardson, J.E., Ringwald, M., Rubin, G.M., Sherlock, G., 2000b. Gene Ontology: tool for the unification of biology. Nature genetics 25, 25.

Askari, H., Edqvist, J., Hajheidari, M., Kafi, M., Salekdeh, G.H., 2006. Effects of salinity levels on proteome of *Suaeda aegyptiaca* leaves. PROTEOMICS 6, 2542-2554.

Badouin, H., Gouzy, J., Grassa, C.J., Murat, F., Staton, S.E., Cottret, L., Lelandais-Brière, C., Owens, G.L., Carrère, S., Mayjonade, B., 2017. The sunflower genome provides insights into oil metabolism, flowering and Asterid evolution. Nature 546, 148.

Bennett, M.D., Leitch, I.J., 2005. Plant DNA C-values database. Royal Botanic Gardens, Kew.

Bhardwaj, A.R., Joshi, G., Kukreja, B., Malik, V., Arora, P., Pandey, R., Shukla, R.N., Bankar, K.G., Katiyar-Agarwal, S., Goel, S., 2015. Global insights into high temperature and drought stress regulated genes by RNA-Seq in economically important oilseed crop Brassica juncea. BMC plant biology 15, 9.

Born, J., Michalski, S.G., 2017. Strong divergence in quantitative traits and plastic behavior in response to nitrogen availability among provenances of a common wetland plant. Aquatic Botany 136, 138-145.

Born, J., Michalski, S.G., 2019. Trait expression and signatures of adaptation in response to nitrogen addition in the common wetland plant Juncus effusus. PLOS ONE 14, e0209886.

Bose Mazumdar, A., Chattopadhyay, S., 2016. Sequencing, de novo assembly, functional annotation and analysis of *Phyllanthus amarus* leaf transcriptome using the Illumina platform. Frontiers in Plant Science 6, 1199.

Cahais, V., Gayral, P., Tsagkogeorga, G., Melo-Ferreira, J., Ballenghien, M., Weinert, L., Chiari, Y., Belkhir, K., Ranwez, V., Galtier, N., 2012. Reference-free transcriptome assembly in non-model animals from next-generation sequencing data. Molecular ecology resources 12, 834-845.

Chen, F., Mackey, A.J., Stoeckert Jr, C.J., Roos, D.S., 2006. OrthoMCL-DB: querying a comprehensive multi-species collection of ortholog groups. Nucleic acids research 34, D363-D368.

Cheng, C.Y., Krishnakumar, V., Chan, A.P., Thibaud-Nissen, F., Schobel, S., Town, C.D., 2017. Araport11: a complete reannotation of the *Arabidopsis thaliana* reference genome. The Plant Journal 89, 789-804.

Chevreux, B., Pfisterer, T., Drescher, B., Driesel, A.J., Müller, W.E.G., Wetter, T., Suhai, S., 2004. Using the miraEST assembler for reliable and automated mRNA transcript assembly and SNP detection in sequenced ESTs. Genome research 14, 1147-1159.

Chevreux, B., Wetter, T., Suhai, S., 1999. Genome sequence assembly using trace signals and additional sequence information, German conference on bioinformatics. Citeseer, pp. 45-56.

Chu, Z., Chen, J., Sun, J., Dong, Z., Yang, X., Wang, Y., Xu, H., Zhang, X., Chen, F. and Cui, D., 2017. *De novo* assembly and comparative analysis of the transcriptome of embryogenic callus formation in bread wheat (*Triticum aestivum* L.). BMC plant biology, 17(1), p.244.

Coll, N.S., Epple, P., Dangl, J.L., 2011. Programmed cell death in the plant immune system. Cell Death And Differentiation 18, 1247.

Consortium, G.O., 2004. The Gene Ontology (GO) database and informatics resource. Nucleic acids research 32, D258-D261.

Cruz, F., Julca, I., Gómez-Garrido, J., Loska, D., Marcet-Houben, M., Cano, E., Galán, B., Frias, L., Ribeca, P., Derdak, S., 2016. Genome sequence of the olive tree, *Olea europaea*. Gigascience 5, 29.

Daccord, N., Celton, J.-M., Linsmith, G., Becker, C., Choisne, N., Schijlen, E., van de Geest, H., Bianco, L., Micheletti, D., Velasco, R., 2017. High-quality de novo assembly of the apple genome and methylome dynamics of early fruit development. Nature genetics 49, 1099.

Davies, K.J., 1987. Protein damage and degradation by oxygen radicals. I. general aspects. Journal of Biological Chemistry 262, 9895-9901.

De Carvalho, J.F., Poulain, J., Da Silva, C., Wincker, P., Michon-Coudouel, S., Dheilly, A., Naquin, D., Boutte, J., Salmon, A. and Ainouche, M., 2013. Transcriptome *de novo* assembly from next-generation sequencing and comparative analyses in the hexaploid salt marsh species *Spartina maritima* and *Spartina alterniflora* (Poaceae). Heredity, 110(2), p.181.

Debez, A., Braun, H.-P., Pich, A., Taamalli, W., Koyro, H.-W., Abdelly, C., Huchzermeyer, B., 2012. Proteomic and physiological responses of the halophyte Cakile maritima to moderate salinity at the germinative and vegetative stages. Journal of proteomics 75, 5667-5694.

Dugas, D.V., Monaco, M.K., Olson, A., Klein, R.R., Kumari, S., Ware, D., Klein, P.E., 2011. Functional annotation of the transcriptome of *Sorghum bicolor* in response to osmotic stress and abscisic acid. BMC genomics 12, 514.

Fan, P., Feng, J., Jiang, P., Chen, X., Bao, H., Nie, L., Jiang, D., Lv, S., Kuang, T., Li, Y., 2011. Coordination of carbon fixation and nitrogen metabolism in Salicornia europaea under salinity: Comparative proteomic analysis on chloroplast proteins. PROTEOMICS 11, 4346-4367.

Fox, S.E., Preece, J., Kimbrel, J.A., Marchini, G.L., Sage, A., Youens-Clark, K., Cruzan, M.B. and Jaiswal, P., 2013. Sequencing and de novo transcriptome assembly of *Brachypodium sylvaticum* (Poaceae). Applications in plant sciences, 1(3), p.1200011.

Fox, S.E., Geniza, M., Hanumappa, M., Naithani, S., Sullivan, C., Preece, J., Tiwari, V.K., Elser, J., Leonard, J.M., Sage, A. and Gresham, C., 2014. De novo transcriptome assembly and analyses of gene expression during photomorphogenesis in diploid wheat *Triticum monococcum*. PLoS One, 9(5), p.e96855.

Finn, R.D., Coggill, P., Eberhardt, R.Y., Eddy, S.R., Mistry, J., Mitchell, A.L., Potter, S.C., Punta, M., Qureshi, M., Sangrador-Vegas, A., 2016. The Pfam protein families database: towards a more sustainable future. Nucleic acids research 44, D279-D285.

Flowers, T.J., Colmer, T.D., 2008. Salinity tolerance in halophytes. New Phytologist 179, 945-963.

Fracasso, A., Trindade, L.M., Amaducci, S., 2016. Drought stress tolerance strategies revealed by RNA-Seq in two sorghum genotypes with contrasting WUE. BMC plant biology 16, 115.

Garg, R., Jain, M., 2013. RNA-Seq for transcriptome analysis in non-model plants, Legume Genomics. Springer, pp. 43-58.

Givnish, T.J., Ames, M., McNeal, J.R., McKain, M.R., Steele, P.R., Depamphilis, C.W., Graham, S.W., Pires, J.C., Stevenson, D.W., Zomlefer, W.B., 2010. Assembling the tree of the monocotyledons: plastome sequence phylogeny and evolution of Poales. Annals of the Missouri Botanical Garden 97, 584-616.

Goff, S.A., Ricke, D., Lan, T.-H., Presting, G., Wang, R., Dunn, M., Glazebrook, J., Sessions, A., Oeller, P., Varma, H., 2002. A draft sequence of the rice genome (*Oryza sativa* L. ssp. *japonica*). Science 296, 92-100.

Grabherr, M.G., Haas, B.J., Yassour, M., Levin, J.Z., Thompson, D.A., Amit, I., Adiconis, X., Fan, L., Raychowdhury, R., Zeng, Q., 2011. Trinity: reconstructing a full-length transcriptome without a genome from RNA-Seq data. Nature biotechnology 29, 644.

Haas, B.J., Papanicolaou, A., Yassour, M., Grabherr, M., Blood, P.D., Bowden, J., Couger, M.B., Eccles, D., Li, B., Lieber, M., 2013a. De novo transcript sequence reconstruction from RNA-seq using the Trinity platform for reference generation and analysis. Nature protocols 8, 1494-1512.

Haas, B.J., Papanicolaou, A., Yassour, M., Grabherr, M., Blood, P.D., Bowden, J., Couger, M.B., Eccles, D., Li, B., Lieber, M., 2013b. De novo transcript sequence reconstruction from RNA-seq using the Trinity platform for reference generation and analysis. Nature protocols 8, 1494.

Hansey, C.N., Vaillancourt, B., Sekhon, R.S., De Leon, N., Kaeppler, S.M. and Buell, C.R., 2012. Maize (*Zea mays* L.) genome diversity as revealed by RNA-sequencing. PloS one, 7(3), p.e33071.

He, F., Liu, Q., Zheng, L., Cui, Y., Shen, Z., Zheng, L., 2015. RNA-Seq analysis of rice roots reveals the involvement of post-transcriptional regulation in response to cadmium stress. Frontiers in Plant Science 6, 1136.

He, R., Kim, M.J., Nelson, W., Balbuena, T.S., Kim, R., Kramer, R., Crow, J.A., May, G.D., Thelen, J.J., Soderlund, C.A., 2012. Next-generation sequencing-based transcriptomic and proteomic analysis of the common reed, *Phragmites australis* (Poaceae), reveals genes involved in invasiveness and rhizome specificity. American Journal of Botany 99, 232-247.

Hirayama, T., Shinozaki, K., 2010. Research on plant abiotic stress responses in the post-genome era: past, present and future. The Plant Journal 61, 1041-1052.

Houterman, P.M., Ma, L., Van Ooijen, G., De Vroomen, M.J., Cornelissen, B.J.C., Takken, F.L.W., Rep, M., 2009. The effector protein Avr2 of the xylem-colonizing fungus Fusarium oxysporum activates the tomato resistance protein I-2 intracellularly. The Plant Journal 58, 970-978.

Huang, D.W., Sherman, B.T., Lempicki, R.A., 2008. Systematic and integrative analysis of large gene lists using DAVID bioinformatics resources. Nature protocols 4, 44.

Huang, D.W., Sherman, B.T., Tan, Q., Collins, J.R., Alvord, W.G., Roayaei, J., Stephens, R., Baseler, M.W., Lane, H.C., Lempicki, R.A., 2007. The DAVID Gene Functional Classification Tool: a novel biological module-centric algorithm to functionally analyze large gene lists. Genome biology 8, R183.

Iriti, M., Faoro, F., 2007. Review of innate and specific immunity in plants and animals. Mycopathologia 164, 57-64.

Kanehisa, M., Goto, S., 2000. KEGG: Kyoto Encyclopedia of Genes and Genomes. Nucleic acids research 28, 27-30.

Kreps, J.A., Wu, Y., Chang, H.-S., Zhu, T., Wang, X., Harper, J.F., 2002. Transcriptome changes for *Arabidopsis* in response to salt, osmotic, and cold stress. Plant Physiology 130, 2129-2141.

Kriventseva, E.V., Rahman, N., Espinosa, O., Zdobnov, E.M., 2007. OrthoDB: the hierarchical catalog of eukaryotic orthologs. Nucleic acids research 36, D271-D275.

Kriventseva, E.V., Tegenfeldt, F., Petty, T.J., Waterhouse, R.M., Simão, F.A., Pozdnyakov, I.A., Ioannidis, P., Zdobnov, E.M., 2014. OrthoDB v8: update of the hierarchical catalog of orthologs and the underlying free software. Nucleic acids research 43, D250-D256.

Liu, M., Qiao, G., Jiang, J., Yang, H., Xie, L., Xie, J. and Zhuo, R., 2012. Transcriptome sequencing and de novo analysis for ma bamboo (Dendrocalamus latiflorus Munro) using the Illumina platform. PloS one, 7(10), p.e46766.

Low, T.Y., Heck, A.J., 2016. Reconciling proteomics with next generation sequencing. Current opinion in chemical biology 30, 14-20.

Lünsmann, V., Kappelmeyer, U., Taubert, A., Nijenhuis, I., von Bergen, M., Heipieper, H.J., Müller, J.A., Jehmlich, N., 2016. Aerobic Toluene Degraders in the Rhizosphere of a Constructed Wetland Model Show Diurnal Polyhydroxyalkanoate Metabolism. Applied and Environmental Microbiology 82, 4126-4132.

Ma, J., Kanakala, S., He, Y., Zhang, J. and Zhong, X., 2015. Transcriptome sequence analysis of an ornamental plant, *Ananas comosus* var. *bracteatus*, revealed the potential unigenes involved in terpenoid and phenylpropanoid biosynthesis. PloS one, 10(3), p.e0119153.

Mahdavi Mashaki, K., Garg, V., Nasrollahnezhad Ghomi, A.A., Kudapa, H., Chitikineni, A., Zaynali Nezhad, K., Yamchi, A., Soltanloo, H., Varshney, R.K., Thudi, M., 2018. RNA-Seq analysis revealed genes associated with drought stress response in kabuli chickpea (Cicer arietinum L.). PLOS ONE 13, e0199774.

Maron, P.-A., Ranjard, L., Mougel, C., Lemanceau, P., 2007. Metaproteomics: A New Approach for Studying Functional Microbial Ecology. Microbial Ecology 53, 486-493.

Michalski, S.G., Durka, W., 2012. Identification and characterization of microsatellite loci in the rush *Juncus effusus* (Juncaceae) 1. American journal of botany 99, e53-e55.

Musacchia, F., Basu, S., Petrosino, G., Salvemini, M., Sanges, R., 2015. Annocript: a flexible pipeline for the annotation of transcriptomes able to identify putative long noncoding RNAs. Bioinformatics 31, 2199-2201.

Nagalakshmi, U., Waern, K., Snyder, M., 2010. RNA-Seq: A Method for Comprehensive Transcriptome Analysis. Current protocols in molecular biology 89, 4.11.11-14.11.13.

Nawrocki, E.P., Burge, S.W., Bateman, A., Daub, J., Eberhardt, R.Y., Eddy, S.R., Floden, E.W., Gardner, P.P., Jones, T.A., Tate, J., 2014. Rfam

12.0: updates to the RNA families database. Nucleic acids research 43, D130-D137.

Olson, A., Klein, R.R., Dugas, D.V., Lu, Z., Regulski, M., Klein, P.E., Ware, D., 2014. Expanding and vetting Sorghum bicolor gene annotations through transcriptome and methylome sequencing. The Plant Genome 7.

Pitzschke, A., Schikora, A., Hirt, H., 2009. MAPK cascade signalling networks in plant defence. Current Opinion in Plant Biology 12, 421-426.

Qiu, Q., Ma, T., Hu, Q., Liu, B., Wu, Y., Zhou, H., Wang, Q., Wang, J., Liu, J., 2011. Genome-scale transcriptome analysis of the desert poplar, *Populus euphratica*. Tree physiology 31, 452-461.

Ren, C.-G., Kong, C.-C., Yan, K., Zhang, H., Luo, Y.-M., Xie, Z.-H., 2017. Elucidation of the molecular responses to waterlogging in Sesbania cannabina roots by transcriptome profiling. Scientific Reports 7, 9256.

Russell, S.T., Eley, H., Tisdale, M.J., 2007. Role of reactive oxygen species in protein degradation in murine myotubes induced by proteolysis-inducing factor and angiotensin II. Cellular Signalling 19, 1797-1806.

Shao, H.-B., Chu, L.-Y., Lu, Z.-H., Kang, C.-M., 2007. Primary antioxidant free radical scavenging and redox signaling pathways in higher plant cells. International journal of biological sciences 4, 8-14.

Simão, F.A., Waterhouse, R.M., Ioannidis, P., Kriventseva, E.V., Zdobnov, E.M., 2015. BUSCO: assessing genome assembly and annotation completeness with single-copy orthologs. Bioinformatics 31, 3210-3212.

Smith-Unna, R., Boursnell, C., Patro, R., Hibberd, J.M., Kelly, S., 2016. TransRate: reference-free quality assessment of de novo transcriptome assemblies. Genome research.

Sobhanian, H., Motamed, N., Jazii, F.R., Nakamura, T., Komatsu, S., 2010. Salt Stress Induced Differential Proteome and Metabolome Response in the Shoots of *Aeluropus lagopoides* (Poaceae), a Halophyte C4 Plant. Journal of Proteome Research 9, 2882-2897.

Sonnhammer, E.L., Eddy, S.R., Durbin, R., 1997. Pfam: a comprehensive database of protein domain families based on seed alignments. Proteins: Structure, Function, and Bioinformatics 28, 405-420.

Stein, L., 2001. Genome annotation: from sequence to biology. Nature reviews genetics 2, 493.

Tian, X.J., Long, Y., Wang, J., Zhang, J.W., Wang, Y.Y., Li, W.M., Peng, Y.F., Yuan, Q.H. and Pei, X.W., 2015. De novo transcriptome assembly of common wild rice (*Oryza rufipogon* Griff.) and

discovery of drought-response genes in root tissue based on transcriptomic data. PLoS One, 10(7), p.e0131455.

Unamba, C.I., Nag, A., Sharma, R.K., 2015. Next generation sequencing technologies: the doorway to the unexplored genomics of non-model plants. Frontiers in Plant Science 6, 1074.

Vega-Arreguín, J.C., Ibarra-Laclette, E., Jiménez-Moraila, B., Martínez, O., Vielle-Calzada, J.P., Herrera-Estrella, L., Herrera-Estrella, A., 2009. Deep sampling of the Palomero maize transcriptome by a high throughput strategy of pyrosequencing. BMC genomics 10, 299.

Wang, J., Meng, Y., Li, B., Ma, X., Lai, Y., Si, E., Yang, K., Xu, X., Shang, X., Wang, H., 2015a. Physiological and proteomic analyses of salt stress response in the halophyte *Halogeton glomeratus*. Plant, cell & environment 38, 655-669.

Wang, X., Chang, L., Wang, B., Wang, D., Li, P., Wang, L., Yi, X., Huang, Q., Peng, M., Guo, A., 2013. Comparative Proteomics of *Thellungiella halophila* Leaves from Plants Subjected to Salinity Reveals the Importance of Chloroplastic Starch and Soluble Sugars in Halophyte Salt Tolerance. Molecular & Cellular Proteomics 12, 2174-2195.

Wang, X., Fan, P., Song, H., Chen, X., Li, X., Li, Y., 2009a. Comparative Proteomic Analysis of Differentially Expressed Proteins in Shoots of *Salicornia europaea* under Different Salinity. Journal of Proteome Research 8, 3331-3345.

Wang, Y., Coleman-Derr, D., Chen, G., Gu, Y.Q., 2015b. OrthoVenn: a web server for genome wide comparison and annotation of orthologous clusters across multiple species. Nucleic acids research 43, W78-W84.

Wang, Z., Gerstein, M., Snyder, M., 2009b. RNA-Seq: a revolutionary tool for transcriptomics. Nature reviews genetics 10, 57.

Wang, Z., Gerstein, M., Snyder, M., 2009c. RNA-Seq: a revolutionary tool for transcriptomics. Nature reviews genetics 10, 57.

Waterhouse, R.M., Zdobnov, E.M., Tegenfeldt, F., Li, J., Kriventseva, E.V., 2010. OrthoDB: the hierarchical catalog of eukaryotic orthologs in 2011. Nucleic acids research 39, D283-D288.

Wei, W., Qi, X., Wang, L., Zhang, Y., Hua, W., Li, D., Lv, H., Zhang, X., 2011. Characterization of the sesame (*Sesamum indicum* L.) global transcriptome using Illumina paired-end sequencing and development of EST-SSR markers. BMC genomics 12, 451.

Wu, G., Zhang, L., Yin, Y., Wu, J., Yu, L., Zhou, Y., Li, M., 2015. Sequencing, de novo assembly and comparative analysis of *Raphanus sativus* transcriptome. Frontiers in Plant Science 6, 198.

Wu, H.-x., Jia, H.-m., Ma, X.-w., Wang, S.-b., Yao, Q.-s., Xu, W.-t., Zhou, Y.-g., Gao, Z.-s., Zhan, R.-l., 2014. Transcriptome and proteomic analysis of mango (*Mangifera indica* Linn) fruits. Journal of proteomics 105, 19-30.

Yazawa, T., Kawahigashi, H., Matsumoto, T., Mizuno, H., 2013. Simultaneous transcriptome analysis of Sorghum and *Bipolaris sorghicola* by using RNA-seq in combination with de novo transcriptome assembly. PLOS ONE 8, e62460.

Ye, J., Zhang, Y., Cui, H., Liu, J., Wu, Y., Cheng, Y., Xu, H., Huang, X., Li, S., Zhou, A., 2018. WEGO 2.0: a web tool for analyzing and plotting GO annotations, 2018 update. Nucleic acids research.

Yu, J., Hu, S., Wang, J., Wong, G.K.-S., Li, S., Liu, B., Deng, Y., Dai, L., Zhou, Y., Zhang, X., 2002. A draft sequence of the rice genome (*Oryza sativa* L. ssp. *indica*). Science 296, 79-92.

Zhang, G., Guo, G., Hu, X., Zhang, Y., Li, Q., Li, R., Zhuang, R., Lu, Z., He, Z., Fang, X., 2010. Deep RNA sequencing at single base-pair resolution reveals high complexity of the rice transcriptome. Genome research.

Zhang, Y.-J., Ma, P.-F., Li, D.-Z., 2011. High-throughput sequencing of six bamboo chloroplast genomes: phylogenetic implications for temperate woody bamboos (Poaceae: Bambusoideae). PLOS ONE 6, e20596.

Zipfel, C., 2008. Pattern-recognition receptors in plant innate immunity. Current Opinion in Immunology 20, 10-16.

Zipfel, C., 2009. Early molecular events in PAMP-triggered immunity. Current Opinion in Plant Biology 12, 414-420.

Authors contribution statement:

Title: RNA-Seq analysis of soft rush (*Juncus effusus*): transcriptome sequencing, de novo assembly, annotation, and polymorphism identification. BMC Genomics.

Authors: Arslan, M., Devisetty, U.K., Porsch, M., Große, I., Müller, J.A., Michalski, S.G.

Muhammad Arslan
- Planned the study
- Checked the quality of previously prepared assembly through various computational and statistical analyses.
- Annotated the assembly.
- Performed functional analysis.
- Performed gene enrichment enrichment analysis.
- Performed orthologs comparisons.
- Wrote the chapter/manuscript.

Upendra K. Devisetty
- Helped in running several computational pipelines

Martin Porsche
- Prepared contigs assembly
- Performed SNPs analysis (not presented in the dissertation)

Ivo Große
- Planned the study
- Helped in analyzing data

Jochen A. Müller
- Planned / supervised the study.
- Helped in analyzing and interpretation of the data to extract biological information.
- Helped in writing the chapter.

Stefan G. Michalski
- Planned the study.
- Helped in analyzing data.

Nico Jehmlich (additional role)

- Performed proteomics analysis
- Helped in database searches

4

The response of plant-associated bacterial communities at low to moderate concentrations of antimicrobials could provide several opportunities to understand wetlands performance in this modern era of emerging pollutants. In this dissertation, disturbances in plant-bacteria interactions (i.e. plant endophytic and plant-rhizospheric bacteria) were studied during exposure of cotrimoxazole. It is a well-established fact that beneficial plant-associated bacterial communities play a key role in host growth and development by enhancing access to nutrients, alleviation of stress, and by strengthening immunity (Berendsen et al. 2012, Turner et al. 2013). This partnership is important in CWs because, in addition to supporting the host health, bacteria also carry out pollutant degradation, which is the primary objective for the operation of CWs. More specifically, a combination of physiological, microbiological (cultivation-dependent and cultivation-independent), and genomics tools were employed to elucidate changes in community diversity and to shed light on their function. Furthermore, a benchmarking database of *J. effusus* was developed and tested for metaproteomics analysis which will be a useful resource for future omics studies. This dissertation arrived at the following key findings:

i.   Multiple exposures of cotrimoxazole at low to moderate concentrations can affect the endophytic communities in the model wetland plant, *J. effusus,* particularly in the roots. This disturbance was a successional phenomenon that started with a decline in numbers of some members of the community and which was superseded by the appearance of an opportunistic community.

ii. Previously, it was argued that endophytic bacteria reside within plants without causing pathogenicity (Afzal et al. 2014); however, here we confront this classical definition and argue that various endophytic bacteria could be beneficial, opportunistic, or pathogenic in nature, taking any opportunity to proliferate within plants and feed upon the host nutrients.

iii.   A suspected plant pathogen was isolated from the exposed shoots. Likewise, a few members of family Xanthomonadales were also identified through 16S amplicon sequencing, which is previously recognized as the largest group of bacterial phytopathogens. Nevertheless, specific information on pathogenicity in *J. effusus* for the observed species/phylotypes remains uninvestigated in this study.

iv.   In this study, various observations of up to now unknown functional descriptions for endophytes were made. Firstly, the flux of C_1 compounds was increased upon exposure, which was most likely the result of plant material degradation maybe due to high ROS/RNS production. Secondly, there was a vigorous iron cycle in the exposed roots, which is not the case for root endophytes. Thirdly, sulfur oxidizers were highly abundant in the beginning but their absolute proportion decreased during the exposure. Together, these observations convey that the endophytic community was disturbed in terms of diversity, composition, and function.

v.   The imbalance in plant-endophytic community, particularly in the roots, was comparable to the animal gut dysbiosis because alpha diversity was decreased with the increase in cotrimoxazole concentrations. This observation is in accordance with the previous human microbiome studies, which reported that a decrease in alpha diversity results in impaired functioning affecting the growth and development of the host. In animals, this situation leads to several metabolic disorders; however, further research is necessary to establish such causality for plants.

vi.   In addition to the disturbances in plant-endophyte interactions, fitness of *J. effusus* declined upon exposure of cotrimoxazole. This observation was studied through plant physiological parameters such as monitoring of evapotranspiration, number of green shoots, and chlorophyll fluorescence, as well as visual inspections on plant tissues. Importantly, these plant fitness parameters declined after changes in the endophytic community occurred. These observations supported the hypothesis that

exposure with cotrimoxazole inhibited beneficial endophytes, and affecting the plant health afterward.

vii.   Targeted investigations on stress-related genes involved in "plant-pathogen defense" pathway illustrated that *J. effusus* has specific genes relating to primary immunity typically about hypersensitive response, defense-related gene induction, and programmed cell death. The database developed in this study was therefore deemed sufficient for monitoring the stress response for metaproteomics study.

viii.   Metaproteomics analysis during this study was hampered by an insufficient protein extraction method. However, the direct outcome of this dissertation is available for future *omics* studies in the form of genetic information of *J. effusus* (transcriptome-based database). The quality of developed database is considered reliable because the genomic features of *J. effusus* shared many similarities with its closer phylogenetic relatives, namely *S. bicolor* and *O. sativa.*

These findings may have several implications for further research on studying performance of CWs in the presence of antimicrobials. For example:

Function prediction through metagenomics and metaproteomics

In this study, 16S amplicon sequencing was carried out to reveal insights on the composition, diversity, and functions of bacterial communities in *J. effusus* during and before cotrimoxazole's exposure. Nevertheless, most of these observations were deduced based on the potential activities of many members of the community. However, further reporting on what actually these bacteria are doing is a subject of interest. Therefore, a follow-up study on metagenomics and metaproteomics would be of future interests (Kaul et al. 2016). An interesting aspect would be to look at how endophytic bacterial communities were responding when the diversity was significantly reduced (Phase IV). This is based on the argument that reduced diversity leads to impairment of ecosystem functioning. Previously, Sessitsch et al., (2012) performed metagenomics for the functional

characterization of root endophytes of rice which suggested a high potential of the endophyte community in terms of enhancement of plant stress resistance, biocontrol against pathogens, and bioremediation services. Furthermore, for metaproteomics studies, protocol development for increased efficiency of protein extraction is a crucial step.

Assessing the response of endophytic community from plant shoots

Most of the findings presented in this dissertation are related to the plant roots while less knowledge could be established regarding the plant shoots due to technical difficulties. A major issue was substantial contamination with chloroplasts-derived 16S. Thus, the number of bacterial 16S amplicon reads was too low to generate comprehensive insights. In our observations, cotrimoxazole was not accumulated in the plant tissue but an indirect effect of weakened plant health would be an interesting part to investigate especially in relation to the microbial community and metaproteomics analysis. Nevertheless, a pre-requisite in this part would be the adaption/development of improved methods for theses analysis in shoot tissue.

Evaluating the pathogenicity of newly developed endophytic bacteria in a pot experiment

In this study, pathogenicity due to opportunistic or latent phytopathogens was studied in the post-exposure period through ROS and RNS analysis. Furthermore, a suspected plant pathogen was isolated from the exposed roots; however, its actual potential to cause pathogenicity in healthy *J. effusus* plant is not investigated. According to the German physician and bacteriologist Robert Koch, a disease must be reproduced when a pure culture of the bacteria is inoculated into a healthy susceptible host (Koch 1890). Thus, a pot experiment could be of future interests in which previously isolated endophytic bacteria (from unhealthy plants) are inoculated to the healthy plant. This experiment would reveal if the endophytic bacteria in the post-exposure period are actually phytopathogens or simply potential opportunists that take advantage of the weakened system and start proliferating in *in planta*.

Application of antimicrobials contaminated wastewater, sludge, or manure in the agroecological environment

Land contamination with antimicrobials has gained less attention as compared to contamination with pesticides (Carvalho et al. 2014, Sauvé &Desrosiers 2014). Nevertheless, increasing usage of antimicrobials and their detection in wastewater treatment plants is raising further questions regarding the use of wastewater and sludge in agricultural practices (Drechsel &Scott 2010, Qadir et al. 2010, Singh et al. 2012). Thereon, deleterious effects of antimicrobials to the microbiome of crop plants could be a subject of interest. Moreover, if accumulated within plant tissues, their effects might be seen in the food chain. Recently, the concept of "One Health: Microbiome-Dependent Effects on Multitrophic Health" was proposed by the scientific community at the University of Bern, Switzerland, in which the effect of environmental chemicals is being studied through changes in the microbiome in the food chain; starting from soil to the plants, then to the ruminants, and finally to mice as model organisms for human health (One Health - Interfaculty Research Cooperation, 2018). Although the community is focusing on chemicals such as pesticides and plant secondary metabolites, similar research goals might be established for antimicrobials.

Can we recover the function after disturbed microbiome proliferates in planta?

In recent years, augmentation with beneficial bacteria has been extensively used to enhance the performance of CWs (Afzal et al. 2014, Ijaz et al. 2016, Saleem et al. 2018). These bacteria are typically isolated from healthy plants and possess several plant-growth promoting traits such as ACC-deaminase potential, IAA production, phosphorus solubilization, siderophore formation, etc. (Afzal et al. 2014, Glick 2014). By inoculating these bacteria, we aim to recover plant health (Kaminsky et al., 2018). A number of studies employing similar aspects have reported successful results in phytoremediation and increased crop yield. Thus, it is worthwhile to investigate if such a practice can be used to overcome a diseased state of the plant, not necessarily in terms of microbial diversity but also in terms of function, whose microbiome harbors already a non-beneficial community. This

practice might bring similar success as of faecal transplantation method in humans where dysbiosis is treated by transplanting faeces of a healthy donor to the diseased individual (Ferrere et al. 2017).

Field-scale wetlands: compromised or unaffected?

Field-scale application of CWs and their ecological variants have been seen in many parts of the world for the treatment of sewage and industrial wastewaters (Afzal et al. 2019, Vymazal 2010). Many of these studies claimed successful phytoremediation potential of the applied systems without looking at potential changes in the bacterial community during the operation of wetlands. As we know that sewage effluents are comprised of a variety of chemicals including antimicrobials, it may affect the performance of plants by disturbing its microbiota *in situ*. Hence, investigations on the response of microbial communities in such systems are crucial and will further help in improving the wetland performance towards increased phytoremediation. Likewise, it would be worthwhile to investigate the harmful effects in the scope of mixture toxicity which is more likely a phenomenon in a natural ecosystem.

References

Afzal M, Khan QM, Sessitsch A (2014): Endophytic bacteria: Prospects and applications for the phytoremediation of organic pollutants. Chemosphere 117, 232-242

Afzal M, Rehman K, Shabir G, Tahseen R, Ijaz A, Hashmat AJ, Brix H (2019): Large-scale remediation of oil-contaminated water using floating treatment wetlands. npj Clean Water 2, 3

Berendsen RL, Pieterse CM, Bakker PA (2012): The rhizosphere microbiome and plant health. Trends in plant science 17, 478-486

Carvalho PN, Basto MCP, Almeida CMR, Brix H (2014): A review of plant–pharmaceutical interactions: from uptake and effects in crop plants to phytoremediation in constructed wetlands. Environmental Science and Pollution Research 21, 11729-11763

Drechsel P, Scott CA (2010): Wastewater irrigation and health. International Development Research Centre

Ferrere G, Wrzosek L, Cailleux F, Turpin W, Puchois V, Spatz M, Ciocan D, Rainteau D, Humbert L, Hugot C (2017): Fecal microbiota

manipulation prevents dysbiosis and alcohol-induced liver injury in mice. Journal of hepatology 66, 806-815

Glick BR (2014): Bacteria with ACC deaminase can promote plant growth and help to feed the world. Microbiological Research 169, 30-39

Ijaz A, Imran A, Anwar ul Haq M, Khan QM, Afzal M (2016): Phytoremediation: recent advances in plant-endophytic synergistic interactions. Plant and Soil 405, 179-195

Kaul S, Sharma T, K. Dhar M (2016): "Omics" Tools for Better Understanding the Plant–Endophyte Interactions. Frontiers in Plant Science 7

Koch R (1890): Ueber bakteriologische forschung, Aus   Verhandlungen des X. Internationalen Medizinischen Kongresses, Berlin 1890.1891,Bd. I. Verlag von August Hirschwald, Berlin.

Qadir M, Wichelns D, Raschid-Sally L, McCornick PG, Drechsel P, Bahri A, Minhas P (2010): The challenges of wastewater irrigation in developing countries. Agricultural Water Management 97, 561-568

Saleem H, Arslan M, Rehman K, Tahseen R, Afzal M (2018): Phragmites australis—a helophytic grass—can establish successful partnership with phenol-degrading bacteria in a floating treatment wetland. Saudi Journal of Biological Sciences

Sauvé S, Desrosiers M (2014): A review of what is an emerging contaminant. Chemistry Central Journal 8, 15

Sessitsch A, Hardoim P, Döring J, Weilharter A, Krause A, Woyke T, Mitter B, Hauberg-Lotte L, Friedrich F, Rahalkar M (2012): Functional characteristics of an endophyte community colonizing rice roots as revealed by metagenomic analysis. Molecular Plant-Microbe Interactions 25, 28-36

Singh P, Deshbhratar P, Ramteke D (2012): Effects of sewage wastewater irrigation on soil properties, crop yield and environment. Agricultural Water Management 103, 100-104

Turner TR, James EK, Poole PS (2013): The plant microbiome. Genome biology 14, 209

Vymazal J (2010): Constructed wetlands for wastewater treatment: five decades of experience. Environmental Science & Technology 45, 61-69

A

Supplementary Table A.1: Volumes of 5M NaCl in 50 mL of washing buffer with corresponding formamide concentration in the hybridization buffer

Formamide in hybridization buffer (%)	5M NaCl (µL)
20	1350
25	950
30	640
35	420
40	270
45	160
50	90
55	30
60	0
65	0
70	0

The concentration of Na+ was calculated for stringent washing at 37 °C after hybridization at 35 °C

Supplementary Table A.2: Characteristics of the cotrimoxazole drug (i.e., SMX and TMP) and the HPLC-MS-MS method

	CAS-No./ logP*	Ion transitions (m/z)	HPLC- retention time (min)	SPE recovery (%), (n=4)	LOD$_i$ (ng/mL) ± SD (n=3)
Sulfamethoxazol **(SMX)**	723-46-6 0.89	254.2 → 92.0 254.2 → 65.0	9.9	111	0.5 ± 0.02
Trimethoprim **(TMP)**	738-70-5 0.91	290.9 → 230.1 290.9 → 261.0	8.5	109	0.5 ± 0.03

*logP from PubChem open chemical database

Supplementary Table A. 3: Summary Statistics and Mann-Whitney U test results. Bold values represent significant differences among un-exposed and exposed treatments.

		UE-R	E-R (1st PFR)	E-R (2nd PFR)	UE-S	E-S (1st PFR)	E-S (2nd PFR)
Gammaproteobacteria	Mean	58428248	574383693.6	3.73E+08	1799889	5479375	1079272
	Median	58345093	518872968.8	3.52E+08	1173919	5666400	1012693
	MU Test	**0 (0.000041) & 0 (0.000041)**			**9 (0.004)** & 42 (0.9314)		
	t test	-6.476 (0.00017) & -5.5937 (0.00044)			-4.069 (0.0015) & 0.8661 (0.4081)		
Firmicutes	Mean	75911111	224944444.4	3.21E+08	31840311	4660199	7970642
	Median	72500000	2.04E+08	2.53E+08	31809540	2991283	7506352
	MU Test	**0 (0.000041) & 0 (0.000041)**			**81 (0.000041) & 45 (0.0039)**		
	t test	-7.1939 (0.000014) & -6.242 (0.00016)			17.606 (0) & 65.49 (0)		
Actinobacteria	Mean	14226363	54737882.49	97135178	659109.2	1152167	5184581
	Median	17148015	55825688.48	72663809	116069.7	1065844	5583348
	MU Test	**0 (0.000042) / 0 (0.000040)**			**45 (0.0039) / 45 (0.0039)**		
	t test	-10.478 (0) & -4.618 (0.0016)			2.3393 (0.047) & 2.3393 (0.047)		
Total Endophytes	Mean	2.04E+08	1.72E+09	1.61E+09	5.16E+07	15005677	36106013
	Median	1.39E+08	1.77E+09	2.11E+09	5.08E+07	1.22E+07	4.31E+07
	MU Test	**0 (0.000042) / 9 (0.0039)**			54 (0.2581) / 48 (0.5457)		
	t test	-11.824 (0) & -4.023 (0.00325)			2.5078 (0.0356) & 0.9076 (0.3801)		

Supplementary Table A.4: Top twenty-five most abundant OTUs studied via 16S amplicon sequencing represents genus level taxonomy and abundance values for the endophytic community in the un-exposed and exposed plant roots.

Un-exposed roots			
UE-R (1st PFR)		UE-R (2nd PFR)	
Sulfuritalea	1499	Sulfuritalea	3812
Sulfuritalea	687	Sulfuritalea	1936
Dechloromonas	150	Methylosarcina	539
Sideroxydans	131	Sideroxydans	435
Staphylococcus	131	Dechloromonas	365
Rhizobacter	130	Sulfuricurvum	240
Lutimonas	126	Rhizobacter	237
Methylosarcina	123	Kineococcus	223
Streptococcus	109	Sulfuricurvum	212
Rothia	89	Lutimonas	208
Leptonema	74	Sulfurovum	204
Sulfurovum	74	Kineococcus	180
Sulfuricurvum	73	Pseudorhodoferax	161
Kineococcus	69	Staphylococcus	139
Flavobacterium	64	Flavobacterium	135
Sulfuricurvum	58	Leptonema	120
Leadbetterella	56	Rhizobacter	118
Pseudorhodoferax	52	Sulfuritalea	111
Sulfuritalea	45	Zoogloea	105

Rhizobacter	45	Sideroxydans	102
Sphaerochaeta	44	Leadbetterella	98
Hyalangium	44	Jahnella	96
Stigmatella	43	Sulfuricurvum	93
Gemella	38	Sphaerochaeta	90
Kineococcus	35	Zhangella	87

Exposed roots											
E-R1 (1st PFR)		E-R2 (1st PFR)		E-R3 (1st PFR)		E-R4 (2nd PFR)		E-R5 (2nd PFR)		E-R6 (2nd PFR)	
Methylocystis	4765	Curvibacter	5109	Dyella	8304	Methylocystis	12337	Curvibacter	15254	Dyella	6448
Bradyrhizobium	3063	Bradyrhizobium	4579	Methylocystis	7581	Ferritrophicum	8566	Bradyrhizobium	13117	Methylocystis	5675
Curvibacter	2275	Ferritrophicum	3964	Bradyrhizobium	6337	Bradyrhizobium	8366	Ferritrophicum	10624	Ferritrophicum	4795
Dyella	2170	Methylosinus	3128	Ferritrophicum	5942	Curvibacter	7783	Methylosinus	9203	Bradyrhizobium	4707
Methylosinus	2022	Thiobacillus	2542	Curvibacter	5386	Pandoraea	7251	Thiobacillus	7003	Curvibacter	4023
Bradyrhizobium	1991	Dyella	2088	Geothrix	5350	Dyella	5948	Dyella	5557	Geothrix	3926
Pandoraea	1928	Persicobacter	1907	Saccharibacteria_genera_incertae_sedis	4460	Bradyrhizobium	5200	Flavitalea	4244	Saccharibacteria_genera_incertae_sedis	3246
Ferritrophicum	1691	Flavitalea	1739	Flavisolibacter	3551	Methylosinus	4730	Persicobacter	4092	Flavisolibacter	2699
Geothrix	1462	Rhodomicrobium	1666	Methylosinus	3448	Geothrix	4095	Saccharibacteria_genera_incertae_sedis	4068	Methylosinus	2535
Saccharibacteria_genera_incertae_sedis	981	Saccharibacteria_genera_incertae_sedis	1657	Mucilaginibacter	3269	Saccharibacteria_genera_incertae_sedis	3219	Rhodomicrobium	3734	Mucilaginibacter	2215

Rhizobium	929	Methylocystis	1411	Rhodanobacter	2920	Rhizobium	2804	Methylocystis	3721	Rhodanobacter	2167
Rudaea	897	Bradyrhizobium	1129	Geothrix	2777	Ignavibacterium	2347	Bradyrhizobium	3223	Bradyrhizobium	2017
Rhodanobacter	822	Ignavibacterium	972	Bradyrhizobium	2704	Rudaea	2336	Rudaea	2694	Geothrix	1988
Ideonella	754	Pandoraea	846	Persicobacter	2641	Ideonella	2072	Pseudolabrys	2477	Persicobacter	1981
Azospira	661	Meniscus	826	Flavitalea	2519	Persicobacter	1960	Pandoraea	2403	Flavitalea	1868
Pseudolabrys	508	Kineococcus	792	Azospira	2312	Azospira	1902	Ignavibacterium	2147	Azospira	1780
Meniscus	483	Geothrix	776	Ignavibacterium	2245	Rhodanobacter	1885	Flavisolibacter	1995	Rudaea	1740
Persicobacter	463	Rudaea	773	Novosphingobium	2236	Pseudolabrys	1737	Geothrix	1971	Pseudolabrys	1662
Rhodomicrobium	450	Flavisolibacter	756	Thiobacillus	2206	Meniscus	1549	Caulobacter	1850	Novosphingobium	1651
Ignavibacterium	413	Mucilaginibacter	707	Bradyrhizobium	2155	Flavisolibacter	1519	Meniscus	1804	Thiobacillus	1620
Sideroxydans	386	Pseudolabrys	641	Rudaea	2103	Sideroxydans	1426	Kineococcus	1515	Ignavibacterium	1446
Constrictibacter	315	Caulobacter	620	Pseudolabrys	1990	Geothrix	1312	Mucilaginibacter	1333	Bradyrhizobium	1444
Rudaea	313	Terrimonas	590	Pandoraea	1777	Mucilaginibacter	1168	Terrimonas	1250	Pandoraea	1311
Beijerinckia	311	Flexithrix	511	Hyphomicrobium	1655	Rhodomicrobium	1135	Rhodanobacter	1205	Hyphomicrobium	1263
Bradyrhizobium	305	Perlucidibaca	496	Sulfuritalea	1635	Novosphingobium	1071	Perlucidibaca	1200	Sulfuritalea	1179

Color Key

- blue: methane/methanol oxidizers
- dark/light purple: iron oxidizers
- ochre: iron reducers
- dark yellow: sulfide/sulfide oxidizers
- light yellow: sulfide/sulfide oxidizers
- flesh: Dechloromonas, some strains can oxidize iron, some sulfur/sulfide

Table A.5: Analysis of Similarities (ANOSIM) for 16S amplicon sequencing data from 1st study.

One-Way - A

Resemblance worksheet
Name: Resem1
Data type: Similarity
Selection: All

Factors
Place　　Name　　　　Type　　　　Levels
A　　　　treatment　　Unordered　　4

treatment levels
UE–R
UE–S
E–R
E–S

Tests for differences between unordered treatment groups
Global Test
Sample statistic (R): 0,91
Significance level of sample statistic: 0,1%
Number of permutations: 999 (Random sample from 630630)
Number of permuted statistics greater than or equal to R: 0

Pairwise Tests

Pairwise Tests	R Statistic	Significance Level %	Possible Permutations	Actual Permutations	Number >= Observed
Groups					
UE-R, UE-S	0	66,7	3	3	2
UE-R, E-R	1	3,6	28	28	1
UE-R, E-S	1	6,7	15	15	1
UE-S, E-R	1	3,6	28	28	1
UE-S, E-S	1	6,7	15	15	1
E-R, E-S	1	0,5	210	210	1

Supplementary Table A.6: Analysis of Permutational multivariate analysis of variance (PERMANOVA) for 16S amplicon sequencing data from 1st study.

Resemblance worksheet
Name: Resem1
Data type: Similarity
Selection: All
Resemblance: S17 Bray-Curtis similarity

Sums of squares type: Type III (partial)
Fixed effects sum to zero for mixed terms
Permutation method: Unrestricted permutation of raw data
Number of permutations: 999

Factors

Name	Abbrev.	Type	Levels
treatment	tr	Fixed	4

PERMANOVA table of results

Source	df	SS	MS	Pseudo-F	P(perm)	Unique perms	P(MC)
tr	3	34587	11529	26,088	0,001	999	0,001
Res	10	4419,3	441,93				
Total	13	39007					

Details of the expected mean squares (EMS) for the model

Source	EMS
tr	1*V(Res) + 3,2381*S(tr)
Res	1*V(Res)

Construction of Pseudo-F ratio(s) from mean squares

Source	Numerator	Denominator	Num.df	Den.df
tr	1*tr	1*Res	3	10

Estimates of components of variation

Source	Estimate	Sq.root
S(tr)	3424	58,515
V(Res)	441,93	21,022

PERMANOVA
Permutational MANOVA

Resemblance worksheet
Name: Resem1
Data type: Similarity
Selection: All
Resemblance: S17 Bray-Curtis similarity

Sums of squares type: Type III (partial)
Fixed effects sum to zero for mixed terms
Permutation method: Unrestricted permutation of raw data
Number of permutations: 999

Factors

Name	Abbrev.	Type	Levels

treatment   tr   Fixed   4

PAIR-WISE TESTS

Term 'tr'

Groups	t	P(perm)	Unique perms	P(MC)
UE-R, UE-S	0,89485	0,67	3	0,492
UE-R, E-R	54,245	0,044	28	0,001
UE-R, E-S	59,822	0,063	15	0,002
UE-S, E-R	45,777	0,032	28	0,002
UE-S, E-S	52,633	0,079	15	0,002
E-R, E-S	55,462	0,008	207	0,001

Denominators

Groups	Denominator	Den.df
UE-R, UE-S	1*Res	2
UE-R, E-R	1*Res	6
UE-R, E-S	1*Res	4
UE-S, E-R	1*Res	6
UE-S, E-S	1*Res	4
E-R, E-S	1*Res	8

AvE-Rage Similarity between/within groups

	UE-R	UE-S	E-R	E-S
UE-R	80,61			
UE-S	78,254	70,804		
E-R	20,713	13,039	69,831	
E-S	0,76082	48,281	17,406	74,568

Supplementary Table A.7: Performance of 1st PFRs monitored monitored during the experiment.

	IC	TN	Acetat	Benzoat	pH (online)	rH(mV)	O2(µg/l)
1st PFR							
	mg/l	mg/l	mg/l	mg/l			
Phase 1	61.55	43.35	0	0	7.96	-210	0
	54.12	44.84	0	0	8.07	-191	0
	46.12	47.11	0	0	8.04	-203	0
	64.35	53.19	0	0	8.11	-211	0
	41.21	54.56	0	0	8.12	-211	28
	44.82	54.92	0	0	8.17	-207	40
Phase II	51.22	47.67	0	0	8.09	-208	NA
	46.35	51.55	0.5	0	8.14	-220	23
	63.86	54.94	0.8	0	8.19	-217	20
	73.41	59.63	0.8	0	8.23	-215	20
	42.08	58.16	0.5	0	8.28	-216	19
	72.95	60.31	0.9	0	8.22	-212	19
Phase III	79.57	57.28	0	0	8.25	-210	17
	52.39	48.68	0.8	0	8.24	-204	16
	67.53	49.7	0	0	8.27	-206	16
	57.13	44.89	0	0	8.28	-200	15
	39.87	36.06	0.5	0	8.30	-199	15
	39.17	34.23	0	0	8.36	-210	12
Phase IV	57.12	36.25	0	0	8.56	-214	18
	41.26	35.92	0	0	8.47	-215	14
	63.25	49.92	0.5	0	8.49	-210	14
	58.26	29.08	0.6	0	8.52	-203	14
	55.62	34.36	0	0	8.56	-206	15
	59.13	28.09	0.7	0	8.54	-204	17
Phase V	60.17	41.11	0.6	0	8.03	-235	22
	39.33	37.04	0	0	8.57	-199	17
	49.93	41.45	0	0	8.58	-199	13
	55.91	47.64	0.6	0	8.69	-205	15
	64.85	44.57	0.76	0	8.78	-208	14
	55.98	34.92	0	0	8.81	-205	16
Phase VI	57.67	38.74	0	0	8.93	-207	15
	47.88	30.96	0.54	0	8.98	-210	15
	50.51	36.03	0	0	9.07	-212	15
	40.35	31.2	0	0	9.10	-213	15
	63.42	40.78	0	0	9.40	-225	16

Different values in each phase were taken with interval of 1 week

Supplementary Table A.8: Performance of 1st PFRs monitored during the experiment.

	IC	TN	Acetat	Benzoat	pH	rH(mV)	O2(μg/l)
2nd PFR							
	mg/l	mg/l	mg/l	mg/l			
Phase 1	41.38	30.68	0	0	7.33	-421	132
	40.69	27.76	0	0	7.33	-421	0
	22.21	19.92	0	0	7.20	100	0
	8.8	15.56	0	0	6.73	162	0
	44.14	30.36	0	0	7.24	-406	150
	31.91	31.8	0.8	0	7.24	-414	0
Phase II	29.67	33.74	0.8	0	7.30	-423	0
	38.62	35.5	1.2	0	7.37	-426	0
	31.46	32.54	0	0	7.53	-382	0
	44.49	34.68	0	0	7.60	-398	0
	22.43	34.73	0	0	7.47	110	24
	24.12	31.72	0.4	0	7.64	-388	0
Phase III	43.91	36.6	0	0	7.68	-382	0
	44.06	34.39	0	0	7.73	-412	0
	42.55	31.39	0.8	0	7.67	-418	0
	37.07	33.57	0.5	0	7.74	-420	0
	30.61	21.71	0	0	7.57	-402	0
	30.36	20.03	0	0	7.62	-409	0
Phase IV	25.26	22.81	0	0	7.70	-424	13
	23.9	18.94	0	0	7.76	-436	19
	13.02	27.72	0	0	7.41	108	340
	26.06	26.54	0	0	7.87	-390	692
	42.66	33.46	0	0	7.94	-430	28
	38.98	23.78	0	0	7.97	-428	13
Phase V	43.01	22.97	0	0	7.97	-434	46
	49.32	35.54	0.5	0	8.05	-445	220
	42.02	24.83	0	0	8.58	-200	15
	29.13	29.84	0	0	8.10	-443	17
	39.83	34.29	0	0	8.14	-452	26
	42.74	42.71	0.46	0	8.25	-459	36
Phase VI	50.13	38.14	0	0	8.30	-455	30
	57.59	43.14	0	0	8.45	-464	32
	54.28	33.82	0	0	8.42	-461	193
	59.34	34.58	0	0	8.33	-458	297
	69.03	38.59	0	0	8.39	-460	18

Different values in each phase were taken with interval of 1 week
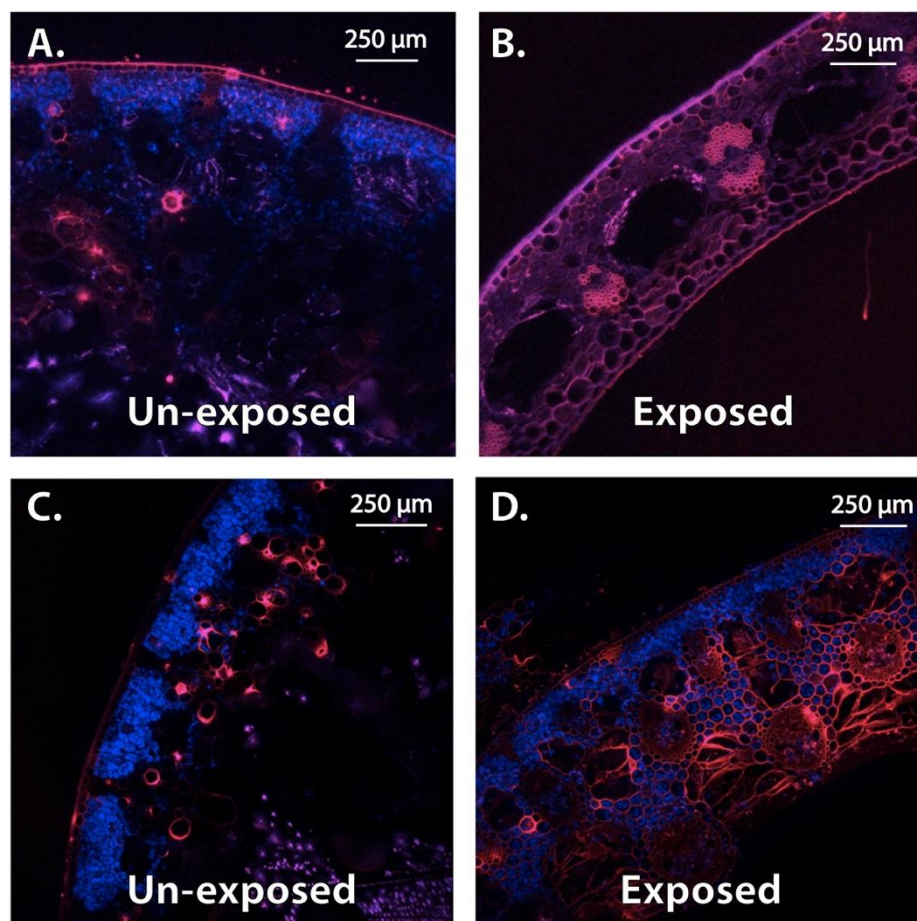
Supplementary Figure A.1: Micrographs representing the production of reactive oxygen species (ROS) in the plant shoots before and after the cotrimoxazole exposure. (A, C) un-exposed roots exhibit lower production of ROS and RNS, (B, D) exposed plant roots shows high production. [for anatomical descriptions, see figure 2.12]
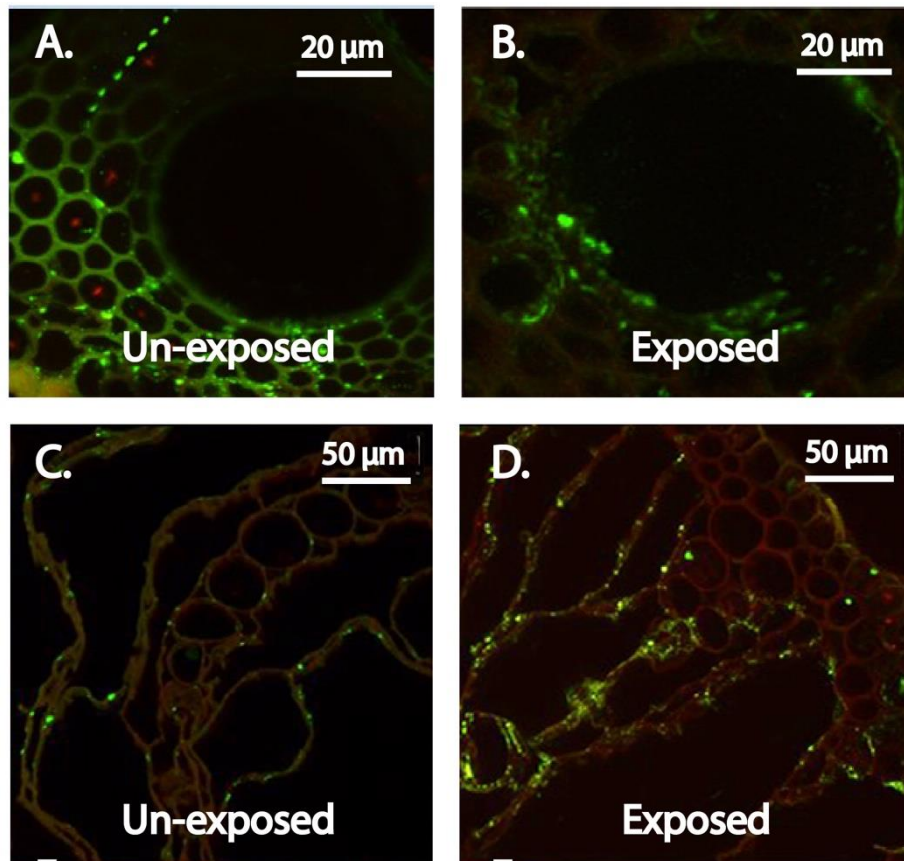
Supplementary Figure A.2: Colonization of *Firmicutes* in the phloem of the plant root before and after cotrimoxazole's exposure. Lesser colonization was observed in un-exposed root interior (A & C) as compared to exposed root interior (B & D).
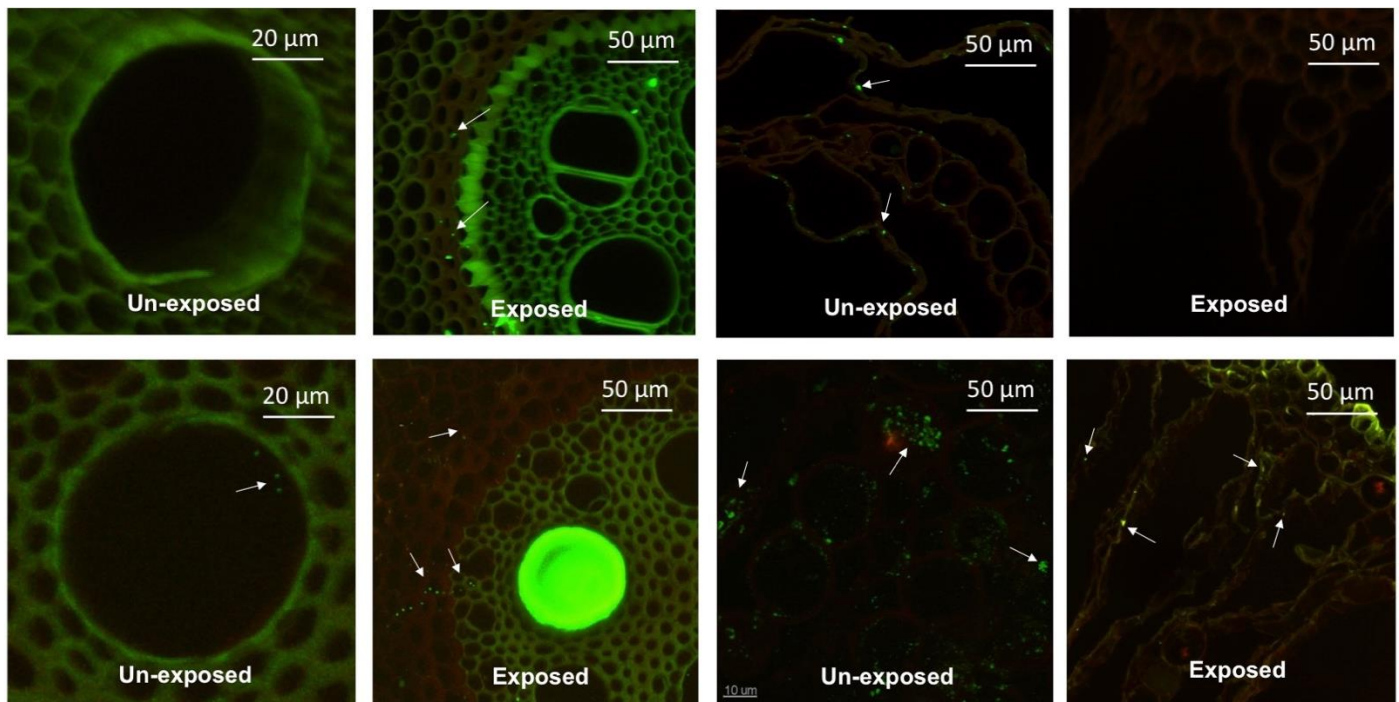
Supplementary Figure A.3: Colonization of *Actinobacteria* in the root interior of *J. effusus* before and after cotrimoxazole's exposure. *Actinobacteria* was the least colonized group among the studied taxa (*Gammaproteobacteria*, *Firmicutes*, and *Actinobacteria*). Slight or no differences were seen in the un-exposed roots and exposed roots for endodermis, pericycle, phloem, cortex and epidermis.
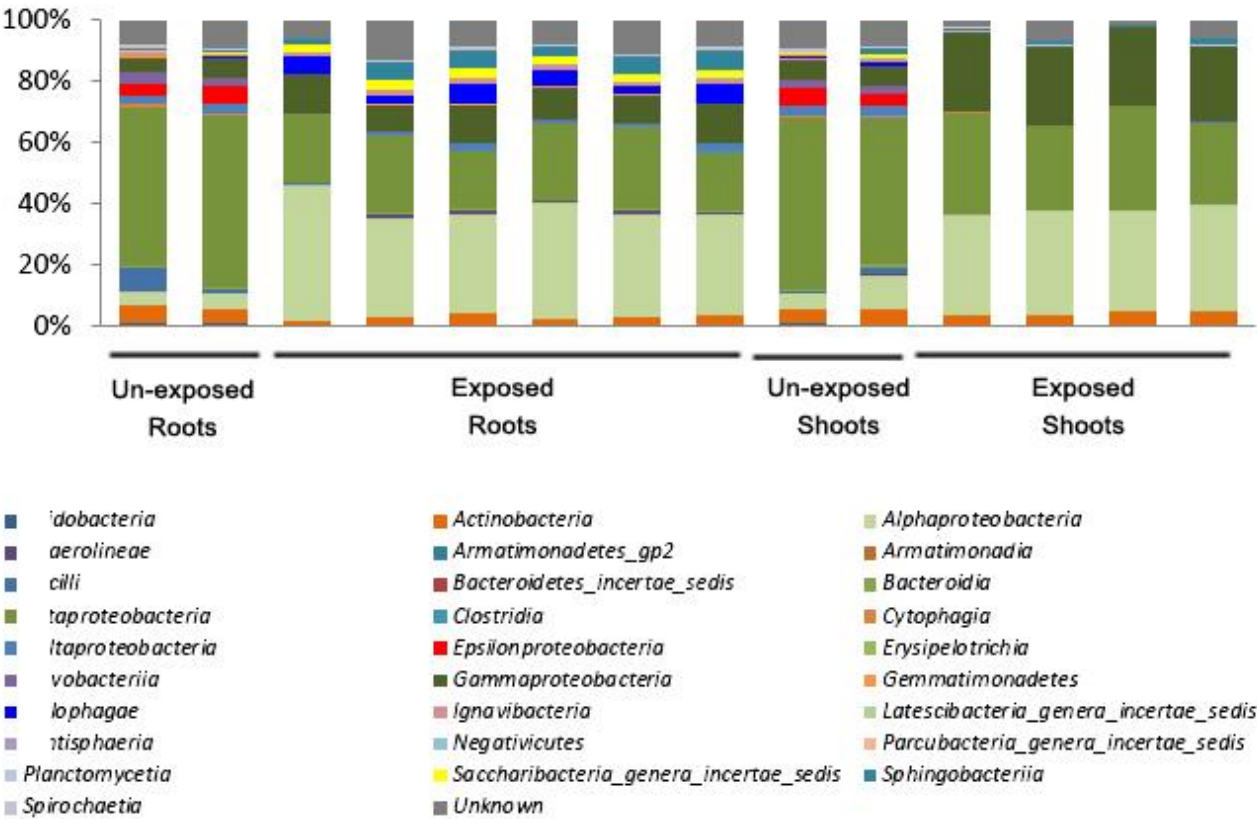
Supplementary Figure A.4: Relative distribution of endophytic bacteria in the roots of *J. effusus*. Major changes in community structure were seen for the phylum Proteobacteria.

Total endophytes (1st PFR)

Total endophytes (2nd PFR)
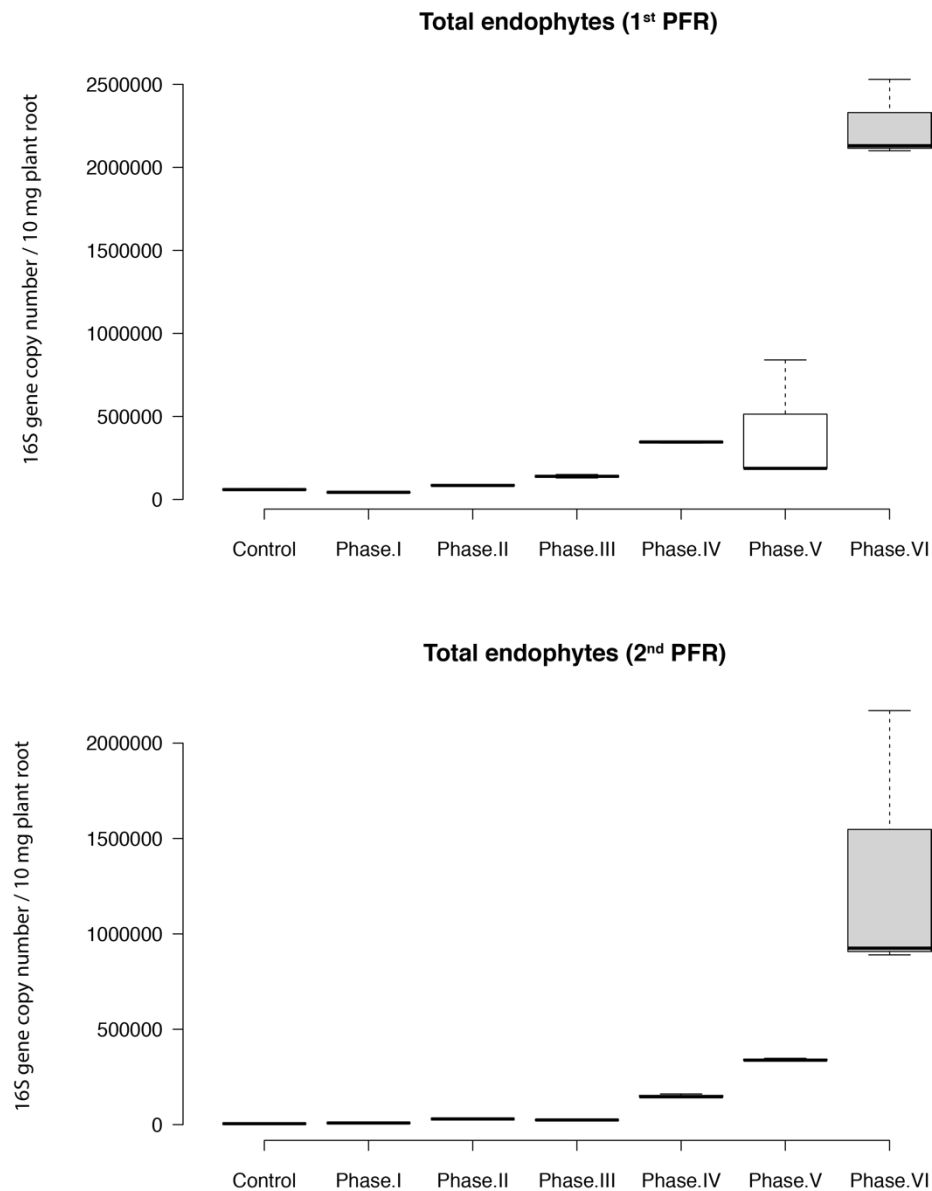
Supplementary Figure A.5: Absolute abundances of endophytic bacteria (16S) enumerated via qPCR for the second study. The abundance of endophytic bacteria increased along the exposure regime.

	Control	Phase I	Phase II	Phase III	Phase IV	Phase V	Phase VI
Proteobacteria; Sulfuritalea	39.1	12.8	22	13.6	0.3	4.5	4.2
Proteobacteria; Sulfuricurvum	3.4	16.5	11	9.8	3.1	1.8	3.8
Actinobacteria; Kineococcus	2.9	1.1	1.6	1.2	14.5	6.8	3.6
Proteobacteria; Methylocystis	0	0	0	0.1	7.9	4.4	5.3
Proteobacteria; Rhizobacter	3.4	1.6	1.9	2.6	4.8	8.7	4.7
Proteobacteria; Sideroxydans	2.9	1.8	2.1	9.1	0	0	3.2
Spirochaetes; Treponema	0.1	0	0.1	0.1	7.5	5.8	2.2
Proteobacteria; Bradyrhizobium	0.1	0.1	0.1	0	1	0.9	1.6
Acidobacteria; Geothrix	0.2	0.1	0.2	0.2	2.9	3.1	2.1
Proteobacteria; Ideonella	2.3	1.8	2.2	3.1	1.7	3.6	0.9
Proteobacteria; Curvibacter	0.6	0.3	0.4	1	2	0	1.5
Proteobacteria; Hydrogenophaga	1.2	0.7	0.8	1.6	2.8	1.8	1.9
Gemmatimonadetes; Gemmatimonas	0.7	4.9	3.9	3.2	0.1	0.4	0.2
Firmicutes; Anoxybacter	0.2	5.3	5.1	2.5	0	0.1	0.1
Proteobacteria; Sulfurisoma	0	0.1	0.1	0.1	0.5	3.3	2.8
Proteobacteria; Dechloromonas	2.8	2.6	2.5	0.3	0.4	0.3	1.3
Proteobacteria; Rhodomicrobium	0	0	0	0	1.4	2.6	1.6
Proteobacteria; Rudaea	0.1	0	0	0	0.2	0.4	2.8
Proteobacteria; Dyella	0	0	0	0	1.2	0	0.5
Proteobacteria; Methylosinus	0.1	0	0.1	0.2	1.4	1.3	0.4
Proteobacteria; Methylosarcina	2.6	1.3	2.2	2.8	0	0.4	0.1
Proteobacteria; Methylomonas	0.1	0	0.1	0.1	0.6	2.7	1.9
Bacteroidetes; Geofilum	0	0.1	0.1	0	1.2	0.9	1.5
Proteobacteria; Aquabacterium	1.3	0.6	0.8	3.2	0	0.7	0.6
Saccharibacteria_genera_incertae_sedis	0.6	1.4	1.3	0.1	0.4	0.5	0.4
Proteobacteria; Zoogloea	0.9	0.3	0.6	2.4	0.2	0.3	1.2
Proteobacteria; Undibacterium	0	0.1	0	0	0.1	0	3
Proteobacteria; Rhizomicrobium	0	0	0	0	1	1.8	1.1
Proteobacteria; Tepidamorphus	0	0	0	0	1.5	4.2	0.5
Proteobacteria; Ferritrophicum	0	0	0	0	0	0	0

Supplementary Figure A.6: Heatmap illustrating the phylotype abundances at genus level taxonomy. The members were Rhizobiales in Phase IV most likely came from the rhizosphere; whose abundance increased upon weakening of host health.

Supplementary Figure A.7: Heatmap illustrating the phylotype abundances at order level taxonomy. The members were Rhizobiales in Phase IV most likely came from the rhizosphere; whose abundance increased upon weakening of host health.
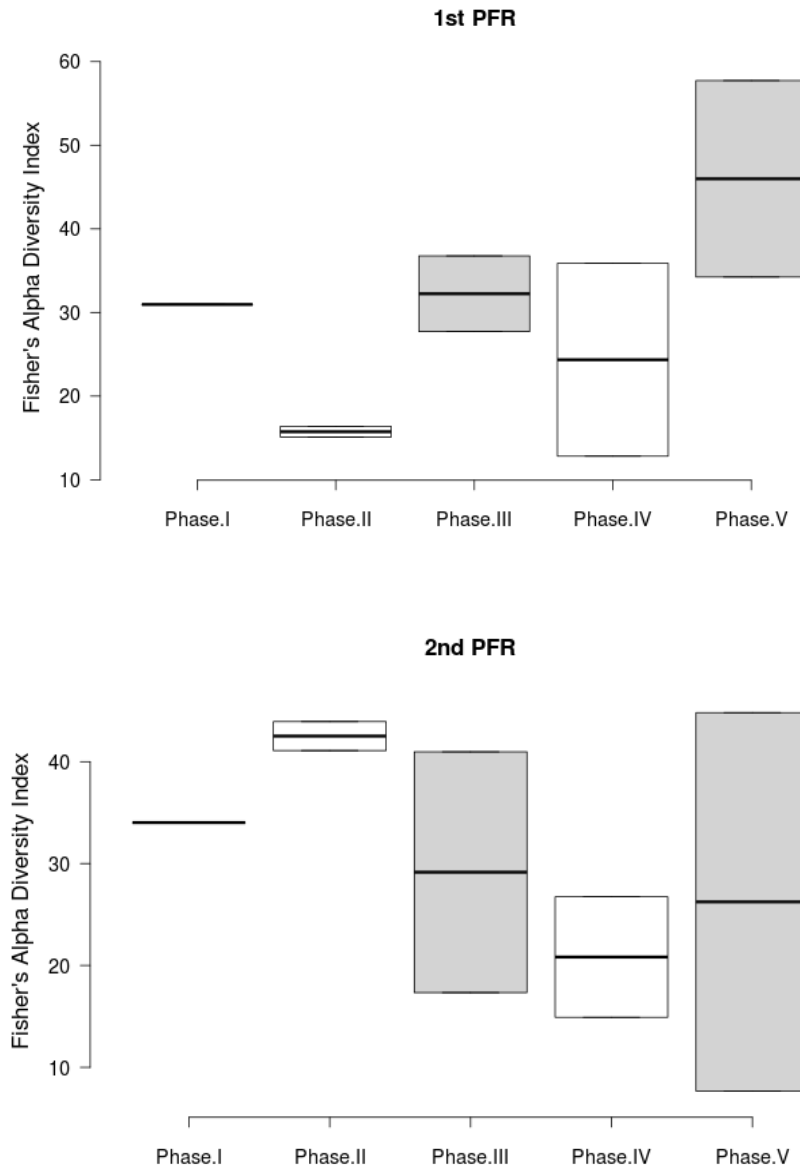
Supplementary Figure A.8: Fisher's alpha diversity index computed for the rhizospheric community in both PFRs. The community did not reveal any specific trend during the course of experiment.

B

SUPPLEMENTARY INFORMATION FOR CHAPTER 3
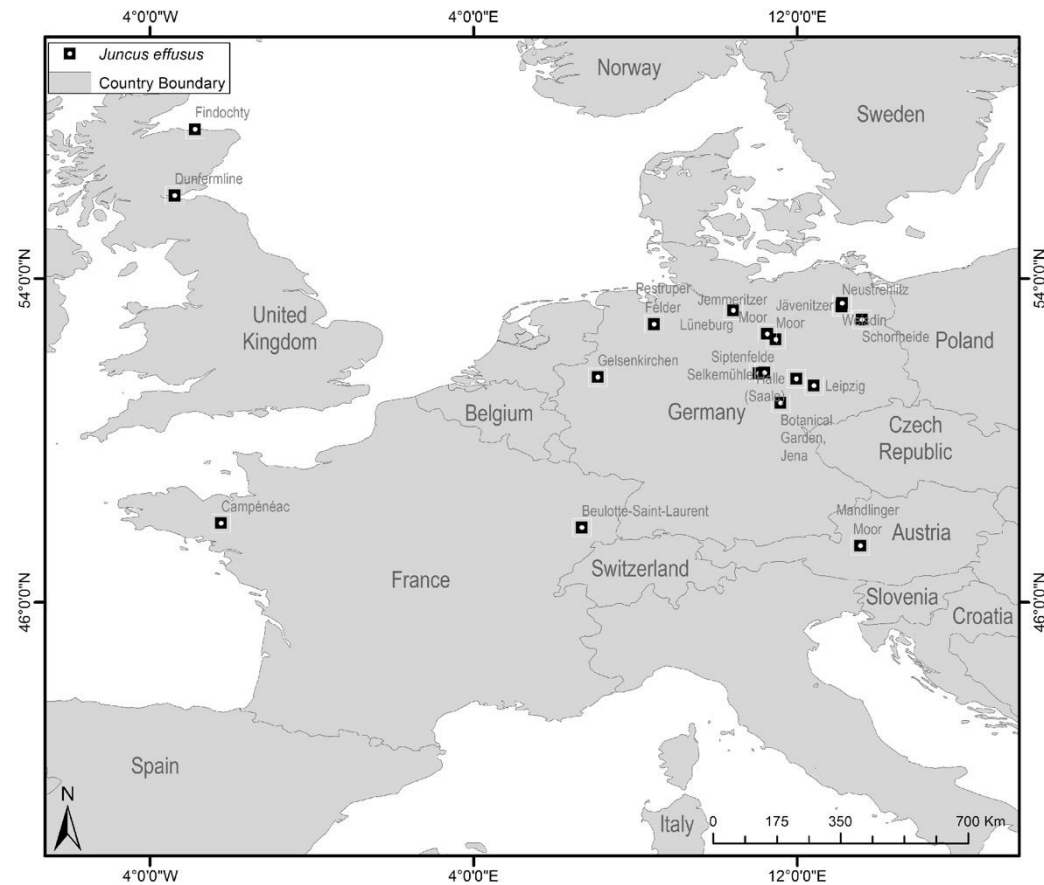
Accession	Country	Latitude	Longitude
Mandlinger Moor	Austria	47.40	13.56
Beulotte-Saint-Laurent	France	47.85	6.68
Campénéac	France	47.96	-2.24
Botanical Garden, Jena	Germany	50.93	11.59
Leipzig	Germany	51.36	12.41
Halle (Saale)	Germany	51.53	11.98
Gelsenkirchen	Germany	51.57	7.07
Siptenfelde	Germany	51.66	11.05
Selkemühle	Germany	51.68	11.19
Jävenitzer Moor	Germany	52.50	11.47
Jemmeritzer Moor	Germany	52.64	11.26
Pestruper Felder	Germany	52.88	8.46
Schorfheide	Germany	52.99	13.6
Lüneburg	Germany	53.22	10.42
Neustrehlitz	Germany	53.32	13.10
Weisdin	Germany	53.40	13.11
Dunfermline	Great Britain	56.06	-3.39
Findochty	Great Britain	57.70	-2.89

Supplementary Figure B.1: Overview map indicating sampling sites for *J. effusus* ecotypes analyzed in this study.

Supplementary Table B.1: List of proteins identified by proteomics analysis for J. effusus, endophytic bacteria, and archaea.

Accession	Description	Area UE-R	Area UE-S	Area E-R	Area E-S
A0A1Z5S8B3	Uncharacterized protein OS=*Juncus effusus* GN=SORBI_3001G302600 PE=4 SV=1 - [A0A1Z5S8B3_SORBI]	1.368E8	7.057E6	1.234E7	3.808E7
M5ELQ4	Glycerol-3-phosphate transporter subunit periplasmic-binding component of ABC superfamily OS=Mesorhizobium metallidurans STM 2683 GN=ugpB PE=4 SV=1 - [M5ELQ4_9RHIZ]	4.215E7	4.544E7	6.344E7	4.147E7
A0A1Z5R6T3	Uncharacterized protein OS=*Juncus effusus* GN=SORBI_3008G149200 PE=4 SV=1 - [A0A1Z5R6T3_SORBI]	7.784E6	0.000E0	0.000E0	3.230E7
A0A1B6QQS4	Catalase OS=*Juncus effusus* GN=SORBI_3001G517700 PE=3 SV=1 - [A0A1B6QQS4_SORBI]	1.028E7	1.806E7	0.000E0	6.108E7
Q98G39	sn-glycerol-3-phosphate transport system, periplasmic binding UgpB OS=*Rhizobium loti* (strain MAFF303099) GN=mll3503 PE=4 SV=1 - [Q98G39_RHILO]	0.000E0	2.298E7	3.895E7	2.744E7
C5Z2J6	Catalase OS=*Juncus effusus* GN=SORBI_3010G274500 PE=3 SV=1 - [C5Z2J6_SORBI]	1.892E7	2.307E7	1.160E6	4.111E7
V7FGC5	Phosphate-binding protein PstS OS=*Mesorhizobium* sp. LSHC420B00 GN=X759_24265 PE=3 SV=1 - [V7FGC5_9RHIZ]	7.743E7	5.288E7	8.786E7	9.691E7
A0A194YSW1	Uncharacterized protein OS=*Juncus effusus* GN=SORBI_3004G339700 PE=4 SV=1 - [A0A194YSW1_SORBI]	0.000E0	0.000E0	8.069E8	1.553E7
A0A194YGY2	Uncharacterized protein OS=*Juncus effusus* GN=SORBI_3010G027000 PE=3 SV=1 - [A0A194YGY2_SORBI]	1.614E7	7.621E6	0.000E0	2.128E7
Q98F26	Periplasmic binding protein of ABC transporter OS=*Rhizobium loti* (strain MAFF303099) GN=mll3970 PE=4 SV=1 - [Q98F26_RHILO]	9.144E6	2.128E7	2.631E7	0.000E0
C5YHF8	Uncharacterized protein OS=*Juncus effusus* GN=SORBI_3007G053300 PE=3 SV=1 - [C5YHF8_SORBI]	6.000E6	7.112E6	9.542E5	4.405E6
C5WZ25	Tubulin beta chain OS=*Juncus effusus* GN=SORBI_3001G069800 PE=3 SV=1 - [C5WZ25_SORBI]	2.426E7	2.647E6	0.000E0	0.000E0
A0A1B6Q328	Peroxidase OS=*Juncus effusus* GN=SORBI_3003G140200 PE=3 SV=1 - [A0A1B6Q328_SORBI]	1.344E7	0.000E0	3.259E7	4.802E6

R6TKL5	Uncharacterized protein OS=*Bacteroides coprophilus* CAG:333 GN=BN612_01068 PE=4 SV=1 - [R6TKL5_9BACE]	2.080E7	1.235E7	1.045E7	0.000E0
R5HIM5	Enolase OS=*Brachyspira* sp. CAG:484 GN=eno PE=3 SV=1 - [R5HIM5_9SPIR]	3.937E6	0.000E0	0.000E0	5.935E6
E8TK07	Short-chain dehydrogenase/reductase SDR OS=*Mesorhizobium ciceri* biovar biserrulae (strain HAMBI 2942 / LMG 23838 / WSM1271) GN=Mesci_1100 PE=4 SV=1 - [E8TK07_MESCW]	8.961E5	0.000E0	2.726E6	2.410E6
A0A136N6F9	10 kDa chaperonin OS=*Bacteroidetes bacterium* OLB11 GN=UZ11_BCD004001718 PE=3 SV=1 - [A0A136N6F9_9BACT]	1.606E7	1.856E7	2.826E7	0.000E0
C5XP45	Histone H2B OS=*Juncus effusus* GN=SORBI_3003G350100 PE=3 SV=1 - [C5XP45_SORBI]	2.997E7	0.000E0	0.000E0	0.000E0
C5XKU8	Uncharacterized protein OS=*Juncus effusus* GN=SORBI_3003G304600 PE=4 SV=1 - [C5XKU8_SORBI]	9.312E6	0.000E0	1.504E6	0.000E0
A0A1B6Q9E6	Uncharacterized protein OS=*Juncus effusus* GN=SORBI_3002G054000 PE=4 SV=1 - [A0A1B6Q9E6_SORBI]	1.089E7	7.604E6	0.000E0	6.410E6
A0A1B6QHK8	Uncharacterized protein OS=*Juncus effusus* GN=SORBI_3001G064500 PE=3 SV=1 - [A0A1B6QHK8_SORBI]	2.156E7	8.286E6	0.000E0	3.725E6
B2ICU4	60 kDa chaperonin OS=*Beijerinckia indica* subsp. indica (strain ATCC 9039 / DSM 1715 / NCIB 8712) GN=groL PE=3 SV=1 - [CH60_BEII9]	0.000E0	2.142E7	1.625E7	0.000E0
A0A084U6T6	ATP synthase subunit alpha OS=*Nitratireductor basaltis* GN=atpA PE=3 SV=1 - [A0A084U6T6_9RHIZ]	0.000E0	0.000E0	1.430E7	0.000E0
A0A1C2DFQ8	Phosphonate ABC transporter substrate-binding protein OS=Mesorhizobium sp. UASWS1009 GN=QV13_29470 PE=4 SV=1 - [A0A1C2DFQ8_9RHIZ]	0.000E0	1.978E6	2.556E6	0.000E0
W6VYU9	Methionine synthase OS=*Rhizobium* sp. CF080 GN=PMI07_001880 PE=4 SV=1 - [W6VYU9_9RHIZ]	0.000E0	1.019E7	1.853E7	1.801E7
G1Y0P1	Potassium-transporting ATPase ATP-binding subunit OS=Nitrospirillum amazonense Y2 GN=kdpB PE=3 SV=1 - [G1Y0P1_9PROT]	0.000E0	4.585E6	8.272E6	7.056E6
X6GHS3	Cytochrome b OS=Mesorhizobium sp. L48C026A00 GN=X737_16910 PE=3 SV=1 - [X6GHS3_9RHIZ]	0.000E0	2.971E6	7.080E6	0.000E0
E8TM02	D-amino acid dehydrogenase OS=*Mesorhizobium ciceri* biovar biserrulae (strain HAMBI 2942 / LMG 23838 / WSM1271) GN=dadA PE=3 SV=1 - [E8TM02_MESCW]	0.000E0	7.855E6	1.348E7	1.146E7
A6WWY9	Phosphate ABC transporter, phosphate-binding protein OS=*Ochrobactrum anthropi* (strain ATCC 49188 / DSM 6882 / JCM 21032 / NBRC 15819 / NCTC 12168)	0.000E0	1.978E6	1.970E6	0.000E0

	GN=Oant_0771 PE=4 SV=1 - [A6WWY9_OCHA4]				
A0A1W0VWQ0	Uncharacterized protein OS=*Juncus effusus* GN=SORBI_3003G105700 PE=4 SV=1 - [A0A1W0VWQ0_SORBI]	0.000E0	7.382E6	0.000E0	3.444E6
A0A021WYR6	CobW/P47K family protein OS=*Shinella* sp. DD12 GN=SHLA_42c000470 PE=4 SV=1 - [A0A021WYR6_9RHIZ]	0.000E0	0.000E0	1.192E7	1.326E7
A0A1A6FRC1	Phosphate-binding protein PstS OS=*Methylosinus* sp. 3S-1 GN=A8B73_06965 PE=3 SV=1 - [A0A1A6FRC1_9RHIZ]	0.000E0	0.000E0	1.975E7	3.680E7
A0A194YKF8	Uncharacterized protein OS=*Juncus effusus* GN=SORBI_3010G205600 PE=4 SV=1 - [A0A194YKF8_SORBI]	0.000E0	0.000E0	3.116E7	0.000E0
A1RA38	Transcriptional regulator for glyoxylate bypass, IclR family OS=*Paenarthrobacter aurescens* (strain TC1) GN=iclR PE=4 SV=1 - [A1RA38_PAEAT]	3.745E7	0.000E0	0.000E0	5.360E6
A0A0C3RLN5	Uncharacterized protein (Fragment) OS=*Nitrosospira* sp. NpAV GN=SQ11_16095 PE=4 SV=1 - [A0A0C3RLN5_9PROT]	6.503E6	5.383E6	0.000E0	0.000E0
A0A0G1FEU3	Enolase OS=*Parcubacteria* group bacterium GW2011_GWB1_43_8 GN=eno PE=3 SV=1 - [A0A0G1FEU3_9BACT]	1.117E7	4.684E6	0.000E0	0.000E0
A0A0K1JJJ2	FO synthase OS=*Luteipulveratus mongoliensis* GN=fbiC PE=3 SV=1 - [A0A0K1JJJ2_9MICO]	9.874E7	0.000E0	9.823E7	0.000E0
A0A1B3MBM6	ABC transporter, substrate binding protein OS=*Sinorhizobium* sp. RAC02 GN=BSY16_108 PE=4 SV=1 - [A0A1B3MBM6_9RHIZ]	4.276E6	0.000E0	3.218E6	0.000E0
B9VAS9	Sucrose synthase OS=*Juncus effusus* GN=SUSY2 PE=3 SV=1 - [B9VAS9_SORBI]	1.929E7	1.473E6	0.000E0	0.000E0
C5YSP7	Fructose-bisphosphate aldolase OS=*Juncus effusus* GN=SORBI_3008G053200 PE=3 SV=1 - [C5YSP7_SORBI]	1.349E7	0.000E0	0.000E0	1.047E7
C5Y3N7	Uncharacterized protein OS=*Juncus effusus* GN=SORBI_3005G019700 PE=3 SV=1 - [C5Y3N7_SORBI]	1.533E7	0.000E0	0.000E0	1.046E7
A0A1B6Q0Z3	Uncharacterized protein OS=*Juncus effusus* GN=SORBI_3003G025200 PE=3 SV=2 - [A0A1B6Q0Z3_SORBI]	4.712E6	0.000E0	0.000E0	5.763E6
A0A194YR04	Uncharacterized protein OS=Juncus effusus GN=SORBI_3004G220000 PE=4 SV=1 - [A0A194YR04_SORBI]	3.569E6	0.000E0	0.000E0	5.805E5
A0A194YM06	Uncharacterized protein OS=Juncus effusus GN=SORBI_3010G230600 PE=3 SV=1 - [A0A194YM06_SORBI]	1.233E7	0.000E0	0.000E0	0.000E0
A0A1B6PS42	Uncharacterized protein (Fragment) OS=Juncus effusus GN=SORBI_3005G128800	7.382E6	0.000E0	0.000E0	4.031E6

	PE=3 SV=1 - [A0A1B6PS42_SORBI]				
A0A1B6PAA3	Uncharacterized protein OS=Juncus effusus GN=SORBI_3009G233700 PE=3 SV=1 - [A0A1B6PAA3_SORBI]	4.749E6	4.557E6	0.000E0	0.000E0
A0A1B6PLD6	Uncharacterized protein OS=Juncus effusus GN=SORBI_3006G109500 PE=3 SV=1 - [A0A1B6PLD6_SORBI]	3.469E6	0.000E0	4.324E6	0.000E0
A0A1B6Q3J2	Uncharacterized protein OS=Juncus effusus GN=SORBI_3003G161300 PE=4 SV=1 - [A0A1B6Q3J2_SORBI]	5.073E6	0.000E0	0.000E0	0.000E0
P0A910	Outer membrane protein A OS=Escherichia coli (strain K12) GN=ompA PE=1 SV=1 - [OMPA_ECOLI]	0.000E0	1.847E6	0.000E0	1.737E6
V7FP03	Cell envelope biogenesis protein OmpA OS=Mesorhizobium sp. LSHC420B00 GN=X759_05480 PE=3 SV=1 - [V7FP03_9RHIZ]	0.000E0	1.163E6	0.000E0	2.550E6
A0A011UDS3	30S ribosomal protein S2 OS=Aquamicrobium defluvii GN=rpsB PE=3 SV=1 - [A0A011UDS3_9RHIZ]	0.000E0	0.000E0	0.000E0	4.848E6
A0A090EXN5	Ureidoglycolate lyase OS=Mesorhizobium sp. SOD10 GN=MPLSOD_190001 PE=4 SV=1 - [A0A090EXN5_9RHIZ]	0.000E0	8.202E5	0.000E0	1.962E6
E8TML5	Extracellular ligand-binding receptor OS=Mesorhizobium ciceri biovar biserrulae (strain HAMBI 2942 / LMG 23838 / WSM1271) GN=Mesci_4851 PE=4 SV=1 - [E8TML5_MESCW]	0.000E0	4.517E6	0.000E0	0.000E0
B2IBE5	3-hydroxybutyrate dehydrogenase OS=Beijerinckia indica subsp. indica (strain ATCC 9039 / DSM 1715 / NCIB 8712) GN=Bind_3009 PE=4 SV=1 - [B2IBE5_BEII9]	0.000E0	0.000E0	5.714E6	0.000E0
A0A0Q7WLY2	Uncharacterized protein OS=Mesorhizobium sp. Root554 GN=ASD44_02975 PE=4 SV=1 - [A0A0Q7WLY2_9RHIZ]	0.000E0	5.060E6	0.000E0	6.069E6
A0A126RQY4	Uncharacterized protein OS=Sphingobium sp. TKS GN=K426_17745 PE=4 SV=1 - [A0A126RQY4_9SPHN]	0.000E0	1.685E6	1.421E6	0.000E0
A0A176HPB8	ABC transporter ATP-binding protein (Fragment) OS=Oceanobacter sp. HI0075 GN=A3746_20960 PE=4 SV=1 - [A0A176HPB8_9GAMM]	0.000E0	3.370E6	5.922E6	0.000E0
C5Y9U0	Uncharacterized protein OS=Juncus effusus GN=SORBI_3006G106100 PE=3 SV=1 - [C5Y9U0_SORBI]	0.000E0	2.262E6	0.000E0	3.641E6
C5Z2S4	Uncharacterized protein OS=Juncus effusus GN=SORBI_3010G011200 PE=3 SV=1 - [C5Z2S4_SORBI]	0.000E0	2.531E6	0.000E0	8.835E5
C5YAK0	Uncharacterized protein OS=Juncus effusus GN=SORBI_3006G268200 PE=4 SV=1	0.000E0	1.437E7	0.000E0	1.640E6

	- [C5YAK0_SORBI]				
A0A1B6PLC6	Glyceraldehyde-3-phosphate dehydrogenase OS=Juncus effusus GN=SORBI_3006G105900 PE=3 SV=1 - [A0A1B6PLC6_SORBI]	0.000E0	2.548E7	0.000E0	9.592E6
A0A1Z5RKF8	Catalase OS=Juncus effusus GN=SORBI_3004G011566 PE=3 SV=1 - [A0A1Z5RKF8_SORBI]	0.000E0	1.436E7	0.000E0	0.000E0
Q8AAP6	Outer membrane porin F OS=Bacteroides thetaiotaomicron (strain ATCC 29148 / DSM 2079 / NCTC 10582 / E50 / VPI-5482) GN=BT_0418 PE=4 SV=1 - [Q8AAP6_BACTN]	0.000E0	0.000E0	1.054E7	1.124E7
B8HTV9	DNA-directed RNA polymerase subunit gamma OS=Cyanothece sp. (strain PCC 7425 / ATCC 29141) GN=rpoC1 PE=3 SV=1 - [RPOC1_CYAP4]	0.000E0	0.000E0	8.531E6	1.901E6
A0A090EMC1	Putative protease, membrane anchored OS=Mesorhizobium sp. SOD10 GN=ybbK PE=4 SV=1 - [A0A090EMC1_9RHIZ]	0.000E0	0.000E0	3.973E6	6.247E6
Q98BB2	O-succinylhomoserine sulfhydrylase OS=Rhizobium loti (strain MAFF303099) GN=metZ PE=3 SV=1 - [Q98BB2_RHILO]	0.000E0	0.000E0	2.004E6	1.916E6
E8TDV3	Extracellular solute-binding protein family 1 OS=Mesorhizobium ciceri biovar biserrulae (strain HAMBI 2942 / LMG 23838 / WSM1271) GN=Mesci_1842 PE=4 SV=1 - [E8TDV3_MESCW]	0.000E0	0.000E0	1.280E7	1.416E7
A0A1A6FKZ1	Methanol dehydrogenase OS=Methylosinus sp. 3S-1 GN=A8B73_11760 PE=4 SV=1 - [A0A1A6FKZ1_9RHIZ]	0.000E0	0.000E0	9.901E6	0.000E0
A0A101KSC6	Nitrate ABC transporter substrate-binding protein OS=Rhizobium loti GN=AU467_03165 PE=4 SV=1 - [A0A101KSC6_RHILI]	0.000E0	0.000E0	2.778E6	3.757E6
A0A177PMX2	Methanol dehydrogenase OS=Methylosinus sp. R-45379 GN=A1351_08275 PE=4 SV=1 - [A0A177PMX2_9RHIZ]	0.000E0	0.000E0	3.087E6	0.000E0
A0A1Z5R3M0	Uncharacterized protein OS=Juncus effusus GN=SORBI_3009G210000 PE=4 SV=1 - [A0A1Z5R3M0_SORBI]	0.000E0	0.000E0	3.892E6	2.384E6
R5T283	50S ribosomal protein L29 OS=Clostridium sp. CAG:75 GN=rpmC PE=3 SV=1 - [R5T283_9CLOT]	9.944E5	0.000E0	0.000E0	0.000E0
B4WMT0	60 kDa chaperonin OS=Synechococcus sp. (strain ATCC 29403 / PCC 7335) GN=groL PE=3 SV=1 - [B4WMT0_SYNS7]	1.979E6	0.000E0	0.000E0	0.000E0
A0A0D6KPX4	C-phycoerythrin beta subunit OS=Tolypothrix sp. PCC 7601 GN=FDUTEX481_07654 PE=3 SV=1 - [A0A0D6KPX4_9CYAN]	6.190E5	0.000E0	0.000E0	0.000E0
A0A0D8QAG	4-hydroxy-tetrahydrodipicolinate reductase (Fragment) OS=Raoultella planticola	7.592E6	0.000E0	0.000E0	0.000E0

6	GN=UA70_16265 PE=3 SV=1 - [A0A0D8QAG6_RAOPL]				
A0A099JP40	Uncharacterized protein OS=Cryobacterium roopkundense GN=GY21_03325 PE=4 SV=1 - [A0A099JP40_9MICO]	0.000E0	0.000E0	0.000E0	0.000E0
R9KCJ2	Uncharacterized protein OS=Lachnospiraceae bacterium A2 GN=C810_03348 PE=4 SV=1 - [R9KCJ2_9FIRM]	5.035E6	0.000E0	0.000E0	0.000E0
A0A098RHM 6	ABC transporter permease OS=Halomonas salina GN=FP66_11745 PE=4 SV=1 - [A0A098RHM6_9GAMM]	3.456E7	0.000E0	0.000E0	0.000E0
C6WBA0	Metallophosphoesterase OS=Actinosynnema mirum (strain ATCC 29888 / DSM 43827 / NBRC 14064 / IMRU 3971) GN=Amir_5573 PE=4 SV=1 - [C6WBA0_ACTMD]	0.000E0	0.000E0	0.000E0	0.000E0
A0A0F3R0J0	Hsp90 family protein OS=Orientia tsutsugamushi str. UT76 GN=OTSUT76_0191 PE=4 SV=1 - [A0A0F3R0J0_ORITS]	4.326E6	0.000E0	0.000E0	0.000E0
A0A0Q6Q0W 5	Lysine--tRNA ligase OS=Leifsonia sp. Root112D2 GN=lysS PE=3 SV=1 - [A0A0Q6Q0W5_9MICO]	4.692E6	0.000E0	0.000E0	0.000E0
A0A0Q4V5X2	Photosystem reaction center subunit H OS=Curtobacterium sp. Leaf261 GN=ASF23_06895 PE=4 SV=1 - [A0A0Q4V5X2_9MICO]	0.000E0	0.000E0	0.000E0	0.000E0
A0A0P8C8W 7	Transposase OS=Algoriphagus marincola HL-49 GN=HLUCCX10_03030 PE=4 SV=1 - [A0A0P8C8W7_9BACT]	4.505E6	0.000E0	0.000E0	0.000E0
A0A161GLS9	Heat shock protein DnaJ domain-containing protein OS=Defluviimonas alba GN=AKL17_1217 PE=4 SV=1 - [A0A161GLS9_9RHOB]	0.000E0	0.000E0	0.000E0	0.000E0
A0A1E4IKV4	Uncharacterized protein OS=Rubrivivax sp. SCN 71-131 GN=ABS84_03095 PE=4 SV=1 - [A0A1E4IKV4_9BURK]	2.316E6	0.000E0	0.000E0	0.000E0
C5X163	40S ribosomal protein S27 OS=Juncus effusus GN=SORBI_3001G091801 PE=3 SV=1 - [C5X163_SORBI]	3.116E6	0.000E0	0.000E0	0.000E0
C5WY08	Uncharacterized protein OS=Juncus effusus GN=SORBI_3001G058900 PE=3 SV=1 - [C5WY08_SORBI]	1.348E7	0.000E0	0.000E0	0.000E0
A0A194YJS5	Uncharacterized protein OS=Juncus effusus GN=SORBI_3010G172500 PE=3 SV=1 - [A0A194YJS5_SORBI]	7.181E5	0.000E0	0.000E0	0.000E0
C5XW73	Uncharacterized protein OS=Juncus effusus GN=SORBI_3004G060100 PE=3 SV=1 - [C5XW73_SORBI]	4.764E5	0.000E0	0.000E0	0.000E0
C5X389	Uncharacterized protein OS=Juncus effusus GN=SORBI_3002G387500 PE=3 SV=1 - [C5X389_SORBI]	2.691E6	0.000E0	0.000E0	0.000E0

C5XFY9	Uncharacterized protein OS=Juncus effusus GN=SORBI_3003G248600 PE=3 SV=1 - [C5XFY9_SORBI]	5.639E6	0.000E0	0.000E0	0.000E0
C5XJD6	Uncharacterized protein OS=Juncus effusus GN=SORBI_3003G443300 PE=3 SV=1 - [C5XJD6_SORBI]	7.648E6	0.000E0	0.000E0	0.000E0
C5WSU8	Uncharacterized protein OS=Juncus effusus GN=SORBI_3001G458800 PE=3 SV=1 - [C5WSU8_SORBI]	2.673E6	0.000E0	0.000E0	0.000E0
C5Z475	Peroxidase OS=Juncus effusus GN=SORBI_3010G162000 PE=3 SV=1 - [C5Z475_SORBI]	3.663E5	0.000E0	0.000E0	0.000E0
C5XUM2	Uncharacterized protein OS=Juncus effusus GN=SORBI_3004G039400 PE=3 SV=1 - [C5XUM2_SORBI]	1.619E6	0.000E0	0.000E0	0.000E0
C5XKC8	Uncharacterized protein OS=Juncus effusus GN=SORBI_3003G013700 PE=3 SV=1 - [C5XKC8_SORBI]	2.094E6	0.000E0	0.000E0	0.000E0
C5WT04	Uncharacterized protein OS=Juncus effusus GN=SORBI_3001G016500 PE=3 SV=1 - [C5WT04_SORBI]	3.726E6	0.000E0	0.000E0	0.000E0
C5WZL1	Uncharacterized protein OS=Juncus effusus GN=SORBI_3001G364500 PE=4 SV=1 - [C5WZL1_SORBI]	3.768E7	0.000E0	0.000E0	0.000E0
C5X897	Uncharacterized protein OS=Juncus effusus GN=SORBI_3002G155500 PE=3 SV=1 - [C5X897_SORBI]	2.780E6	0.000E0	0.000E0	0.000E0
C5X1K7	Uncharacterized protein OS=Juncus effusus GN=SORBI_3001G247600 PE=4 SV=1 - [C5X1K7_SORBI]	9.963E6	0.000E0	0.000E0	0.000E0
C5Z3D2	Uncharacterized protein OS=Juncus effusus GN=SORBI_3010G023900 PE=3 SV=1 - [C5Z3D2_SORBI]	8.375E6	0.000E0	0.000E0	0.000E0
C5XMD2	Uncharacterized protein OS=Juncus effusus GN=SORBI_3003G322400 PE=4 SV=1 - [C5XMD2_SORBI]	6.793E6	0.000E0	0.000E0	0.000E0
C5X5D7	Uncharacterized protein OS=Juncus effusus GN=SORBI_3002G263100 PE=4 SV=1 - [C5X5D7_SORBI]	3.938E6	0.000E0	0.000E0	0.000E0
C5XYN8	Uncharacterized protein OS=Juncus effusus GN=SORBI_3004G232700 PE=4 SV=1 - [C5XYN8_SORBI]	7.498E6	0.000E0	0.000E0	0.000E0
A0A1B6Q8L9	Eukaryotic translation initiation factor 5A OS=Juncus effusus GN=SORBI_3002G007100 PE=3 SV=1 - [A0A1B6Q8L9_SORBI]	1.316E7	0.000E0	0.000E0	0.000E0
A0A1B6Q3C2	Uncharacterized protein OS=Juncus effusus GN=SORBI_3003G143700 PE=4 SV=1 - [A0A1B6Q3C2_SORBI]	1.678E6	0.000E0	0.000E0	0.000E0

A0A1B6QPA5	Uncharacterized protein OS=Juncus effusus GN=SORBI_3001G432800 PE=3 SV=1 - [A0A1B6QPA5_SORBI]	4.518E6	0.000E0	0.000E0	0.000E0
A0A1Z5S4X0	Uncharacterized protein OS=Juncus effusus GN=SORBI_3001G047400 PE=3 SV=1 - [A0A1Z5S4X0_SORBI]	2.914E6	0.000E0	0.000E0	0.000E0
A0A1B6P733	Uncharacterized protein OS=Juncus effusus GN=SORBI_3009G062800 PE=4 SV=1 - [A0A1B6P733_SORBI]	1.176E7	0.000E0	0.000E0	0.000E0
C5Y2Y8	Clathrin heavy chain OS=Juncus effusus GN=SORBI_3005G003300 PE=3 SV=3 - [C5Y2Y8_SORBI]	9.444E5	0.000E0	0.000E0	0.000E0
A0A1B6Q846	Uncharacterized protein OS=Juncus effusus GN=SORBI_3003G418600 PE=4 SV=1 - [A0A1B6Q846_SORBI]	1.615E7	0.000E0	0.000E0	0.000E0
A0A1B6Q7X7	Uncharacterized protein OS=Juncus effusus GN=SORBI_3003G410500 PE=3 SV=1 - [A0A1B6Q7X7_SORBI]	6.832E6	0.000E0	0.000E0	0.000E0
A0A1B6Q8Y2	Succinate dehydrogenase [ubiquinone] flavoprotein subunit, mitochondrial OS=Juncus effusus GN=SORBI_3002G028700 PE=3 SV=1 - [A0A1B6Q8Y2_SORBI]	1.642E6	0.000E0	0.000E0	0.000E0
A0A1B6PIG1	Uncharacterized protein OS=Juncus effusus GN=SORBI_3007G171500 PE=4 SV=1 - [A0A1B6PIG1_SORBI]	9.344E6	0.000E0	0.000E0	0.000E0
A0A1B6PIJ8	Pyruvate dehydrogenase E1 component subunit beta OS=Juncus effusus GN=SORBI_3007G190100 PE=4 SV=1 - [A0A1B6PIJ8_SORBI]	3.737E6	0.000E0	0.000E0	0.000E0
A0A1Z5S6W9	Uncharacterized protein OS=Juncus effusus GN=SORBI_3001G206900 PE=4 SV=1 - [A0A1Z5S6W9_SORBI]	1.726E7	0.000E0	0.000E0	0.000E0
A0A1B6PN81	Uncharacterized protein OS=Juncus effusus GN=SORBI_3006G218400 PE=4 SV=1 - [A0A1B6PN81_SORBI]	1.698E5	0.000E0	0.000E0	0.000E0
A0A1W0VWV3	Uncharacterized protein OS=Juncus effusus GN=SORBI_3003G109600 PE=3 SV=1 - [A0A1W0VWV3_SORBI]	1.597E6	0.000E0	0.000E0	0.000E0
A0A1Z5S482	40S ribosomal protein S26 OS=Juncus effusus GN=SORBI_3001G039400 PE=3 SV=1 - [A0A1Z5S482_SORBI]	9.375E7	0.000E0	0.000E0	0.000E0
D4YZF8	Putative outer membrane protein OS=Sphingobium japonicum (strain NBRC 101211 / UT26S) GN=SJA_C1-09060 PE=4 SV=1 - [D4YZF8_SPHJU]	0.000E0	1.833E6	0.000E0	0.000E0
R5F7Y3	Uncharacterized protein OS=Clostridium bolteae CAG:59 GN=BN723_04419 PE=4 SV=1 - [R5F7Y3_9CLOT]	0.000E0	3.578E6	0.000E0	0.000E0
S3P2N4	Uncharacterized protein OS=Acinetobacter rudis CIP 110305 GN=F945_00417 PE=4	0.000E0	0.000E0	0.000E0	0.000E0

SV=1 - [S3P2N4_9GAMM]

C6RMX7	DNA polymerase III, subunit gamma and tau OS=Acinetobacter radioresistens SK82 GN=dnaX PE=4 SV=1 - [C6RMX7_ACIRA]	0.000E0	1.090E7	0.000E0	0.000E0
D4INB7	Uncharacterized protein OS=Alistipes shahii WAL 8301 GN=AL1_21250 PE=4 SV=1 - [D4INB7_9BACT]	0.000E0	0.000E0	0.000E0	0.000E0
Q1JXS2	60 kDa chaperonin OS=Desulfuromonas acetoxidans DSM 684 GN=groL PE=3 SV=1 - [Q1JXS2_DESAC]	0.000E0	2.819E6	0.000E0	0.000E0
M5EXE0	Ubiquinol-cytochrome c reductase iron-sulfur subunit OS=Mesorhizobium metallidurans STM 2683 GN=petA PE=4 SV=1 - [M5EXE0_9RHIZ]	0.000E0	8.513E6	0.000E0	0.000E0
G6YDB9	2-isopropylmalate synthase OS=Mesorhizobium amorphae CCNWGS0123 GN=leuA PE=3 SV=1 - [G6YDB9_9RHIZ]	0.000E0	3.521E6	0.000E0	0.000E0
J1RUK1	Ferrochelatase OS=Streptomyces auratus AGR0001 GN=hemH PE=3 SV=1 - [J1RUK1_9ACTN]	0.000E0	2.754E7	0.000E0	0.000E0
A9CJ78	3-oxoacyl-(Acyl carrier protein) reductase OS=Agrobacterium fabrum (strain C58 / ATCC 33970) GN=fabG PE=4 SV=1 - [A9CJ78_AGRFC]	0.000E0	1.032E6	0.000E0	0.000E0
J3HM81	Putative phosphatase OS=Phyllobacterium sp. YR531 GN=PMI41_04031 PE=4 SV=1 - [J3HM81_9RHIZ]	0.000E0	4.590E6	0.000E0	0.000E0
M5EHQ5	Uncharacterized protein OS=Mesorhizobium metallidurans STM 2683 GN=MESS2_1160008 PE=4 SV=1 - [M5EHQ5_9RHIZ]	0.000E0	1.313E6	0.000E0	0.000E0
M5EGZ4	Phosphonate metabolism protein OS=Mesorhizobium metallidurans STM 2683 GN=MESS2_1140024 PE=4 SV=1 - [M5EGZ4_9RHIZ]	0.000E0	2.126E6	0.000E0	0.000E0
M5ETV5	Multiple sugar-binding periplasmic receptor chvE OS=Mesorhizobium metallidurans STM 2683 GN=chvE PE=4 SV=1 - [M5ETV5_9RHIZ]	0.000E0	7.185E6	0.000E0	0.000E0
A0A090EW20	Fructose-bisphosphate aldolase 2 OS=Mesorhizobium sp. SOD10 GN=cfxB PE=3 SV=1 - [A0A090EW20_9RHIZ]	0.000E0	6.917E5	0.000E0	0.000E0
Q98KQ2	Cobalamin synthesis protein CobW OS=Rhizobium loti (strain MAFF303099) GN=mlr1375 PE=4 SV=1 - [Q98KQ2_RHILO]	0.000E0	1.546E6	0.000E0	0.000E0
A0A0M9GIR7	YMGG-like Gly-zipper OS=Pseudomonas fuscovaginae GN=PF66_00973 PE=4 SV=1 - [A0A0M9GIR7_9PSED]	0.000E0	0.000E0	0.000E0	0.000E0
A0A0H1A5G8	Calcium-binding protein OS=Mesorhizobium sp. LC103 GN=XW59_10665 PE=4 SV=1 - [A0A0H1A5G8_9RHIZ]	0.000E0	6.920E5	0.000E0	0.000E0

A0A0R2U1F3	Transketolase (Fragment) OS=cyanobacterium BACL30 MAG-120619-bin27 GN=ABR96_05030 PE=3 SV=1 - [A0A0R2U1F3_9CYAN]	0.000E0	1.519E6	0.000E0	0.000E0
A0A101KUX2	Putrescine-binding periplasmic protein OS=Rhizobium loti GN=AU467_02860 PE=3 SV=1 - [A0A101KUX2_RHILI]	0.000E0	2.506E6	0.000E0	0.000E0
A0A1B2EZJ9	Glycerol-3-phosphate ABC transporter substrate-binding protein OS=Microvirga sp. V5/3M GN=BB934_44265 PE=4 SV=1 - [A0A1B2EZJ9_9RHIZ]	0.000E0	1.349E7	0.000E0	0.000E0
A0A1E4CLN2	6-phosphofructokinase (Fragment) OS=Kaistia sp. SCN 65-12 GN=ABS35_09660 PE=4 SV=1 - [A0A1E4CLN2_9RHIZ]	0.000E0	8.511E6	0.000E0	0.000E0
C5WTN6	T-complex protein 1 subunit gamma OS=Juncus effusus GN=SORBI_3001G460500 PE=3 SV=1 - [C5WTN6_SORBI]	0.000E0	2.730E6	0.000E0	0.000E0
A0A1B6PEC9	Uncharacterized protein OS=Juncus effusus GN=SORBI_3008G178800 PE=3 SV=1 - [A0A1B6PEC9_SORBI]	0.000E0	3.100E7	0.000E0	0.000E0
A0A1B6QCC 4	Uncharacterized protein OS=Juncus effusus GN=SORBI_3002G193000 PE=4 SV=1 - [A0A1B6QCC4_SORBI]	0.000E0	3.373E8	0.000E0	0.000E0
A0A194YLP4	Uncharacterized protein OS=Juncus effusus GN=SORBI_3010G267400 PE=3 SV=1 - [A0A194YLP4_SORBI]	0.000E0	1.176E6	0.000E0	0.000E0
B8F565	Integral membrane protein OS=Haemophilus parasuis serovar 5 (strain SH0165) GN=HAPS_0835 PE=4 SV=1 - [B8F565_HAEPS]	0.000E0	0.000E0	0.000E0	0.000E0
W4PU10	RteB, two-component system response regulator OS=Bacteroides pyogenes JCM 10003 GN=JCM10003_3102 PE=3 SV=1 - [W4PU10_9BACE]	0.000E0	0.000E0	2.479E6	0.000E0
W7YXJ9	Uncharacterized protein OS=Bacillus sp. JCM 19045 GN=JCM19045_1209 PE=4 SV=1 - [W7YXJ9_9BACI]	0.000E0	0.000E0	0.000E0	0.000E0
P42475	Elongation factor Tu OS=Fibrobacter succinogenes (strain ATCC 19169 / S85) GN=tuf1 PE=3 SV=2 - [EFTU_FIBSS]	0.000E0	0.000E0	3.633E6	0.000E0
A0A0A2U0G9	ATP-dependent protease ATPase subunit HslU OS=Desulfosporosinus sp. Tol-M GN=hslU PE=3 SV=1 - [A0A0A2U0G9_9FIRM]	0.000E0	0.000E0	3.200E6	0.000E0
B9K3G0	Uncharacterized protein OS=Agrobacterium vitis (strain S4 / ATCC BAA-846) GN=Avi_9075 PE=4 SV=1 - [B9K3G0_AGRVS]	0.000E0	0.000E0	2.915E6	0.000E0
W7WQG4	Formate dehydrogenase subunit alpha OS=Hydrogenophaga sp. T4 GN=fdhA PE=4 SV=1 - [W7WQG4_9BURK]	0.000E0	0.000E0	1.520E6	0.000E0
A0A080LUE8	3-hydroxylaminophenol mutase OS=Candidatus Accumulibacter sp. BA-91 GN=AW09_002596 PE=3 SV=1 - [A0A080LUE8_9PROT]	0.000E0	0.000E0	4.353E6	0.000E0

A0A0E7U1W4	Amino acid ABC transporter substrate-binding protein OS=Bordetella pertussis GN=peb1A_2 PE=3 SV=1 - [A0A0E7U1W4_BORPT]	0.000E0	0.000E0	6.503E6	0.000E0
V5SEY8	Glutamine synthetase OS=Hyphomicrobium nitrativorans NL23 GN=glnA PE=3 SV=1 - [V5SEY8_9RHIZ]	0.000E0	0.000E0	1.885E6	0.000E0
U3TMR2	Aspartate 1-decarboxylase OS=Plautia stali symbiont GN=panD PE=3 SV=1 - [U3TMR2_9ENTR]	0.000E0	0.000E0	1.324E7	0.000E0
X6DAF6	Malate dehydrogenase OS=Mesorhizobium sp. LNHC252B00 GN=mdh PE=3 SV=1 - [X6DAF6_9RHIZ]	0.000E0	0.000E0	4.005E6	0.000E0
G6YI93	Family 5 extracellular solute-binding protein (Fragment) OS=Mesorhizobium amorphae CCNWGS0123 GN=MEA186_28567 PE=4 SV=1 - [G6YI93_9RHIZ]	0.000E0	0.000E0	1.958E6	0.000E0
G6Y315	Cytochrome c prime OS=Mesorhizobium amorphae CCNWGS0123 GN=MEA186_01553 PE=4 SV=1 - [G6Y315_9RHIZ]	0.000E0	0.000E0	2.586E6	0.000E0
E2CEI8	Phosphoenolpyruvate carboxykinase (ATP) OS=Roseibium sp. TrichSKD4 GN=pckA PE=3 SV=1 - [E2CEI8_9RHOB]	0.000E0	0.000E0	2.361E6	0.000E0
M5F3K7	Serine hydroxymethyltransferase OS=Mesorhizobium metallidurans STM 2683 GN=glyA PE=3 SV=1 - [M5F3K7_9RHIZ]	0.000E0	0.000E0	1.962E6	0.000E0
A0A090FMJ6	ATP synthase subunit delta OS=Mesorhizobium sp. SOD10 GN=atpH PE=3 SV=1 - [A0A090FMJ6_9RHIZ]	0.000E0	0.000E0	3.076E6	0.000E0
A0A090GRC2	Cystine transporter subunit periplasmic-binding component of ABC superfamily OS=Mesorhizobium sp. SOD10 GN=fliY PE=3 SV=1 - [A0A090GRC2_9RHIZ]	0.000E0	0.000E0	3.397E6	0.000E0
A0A090EZL9	Phosphate import ATP-binding protein PstB OS=Mesorhizobium sp. SOD10 GN=pstB PE=3 SV=1 - [A0A090EZL9_9RHIZ]	0.000E0	0.000E0	7.572E6	0.000E0
A0A090EQB5	26 kDa periplasmic immunogenic protein OS=Mesorhizobium sp. SOD10 GN=bp PE=4 SV=1 - [A0A090EQB5_9RHIZ]	0.000E0	0.000E0	1.026E6	0.000E0
U6B4V0	HflK protein OS=Candidatus Liberibacter americanus str. Sao Paulo GN=hflK PE=4 SV=1 - [U6B4V0_9RHIZ]	0.000E0	0.000E0	2.560E6	0.000E0
K9U657	Sorbitol ABC transporter membrane protein OS=Chroococcidiopsis thermalis PCC 7203 GN=Chro_4737 PE=3 SV=1 - [K9U657_9CYAN]	0.000E0	0.000E0	0.000E0	0.000E0
Q1QHX1	Respiratory nitrate reductase beta subunit OS=Nitrobacter hamburgensis (strain DSM 10229 / NCIMB 13809 / X14) GN=Nham_3447 PE=4 SV=1 - [Q1QHX1_NITHX]	0.000E0	0.000E0	2.768E6	0.000E0
A0A0F2Q1I8	Inosine-5'-monophosphate dehydrogenase OS=Hoeflea sp. BRH_c9 GN=guaB PE=3 SV=1 - [A0A0F2Q1I8_9RHIZ]	0.000E0	0.000E0	3.667E6	0.000E0

A0A177P4M2	30S ribosomal protein S13 OS=Methylosinus sp. R-45379 GN=rpsM PE=3 SV=1 - [A0A177P4M2_9RHIZ]	0.000E0	0.000E0	2.822E6	0.000E0
A0A0F3M9V5	FAD binding domain protein OS=Orientia tsutsugamushi str. Gilliam GN=OTSGILL_2314 PE=4 SV=1 - [A0A0F3M9V5_ORITS]	0.000E0	0.000E0	3.511E6	0.000E0
A0A177PIQ4	Methane monooxygenase OS=Methylosinus sp. R-45379 GN=A1351_00950 PE=4 SV=1 - [A0A177PIQ4_9RHIZ]	0.000E0	0.000E0	1.441E7	0.000E0
A0A0S8FY34	Glutamate dehydrogenase OS=Gemmatimonas sp. SG8_38_2 GN=AMS21_04190 PE=3 SV=1 - [A0A0S8FY34_9BACT]	0.000E0	0.000E0	2.951E6	0.000E0
A0A136JVT1	Nitrate oxidoreductase subunit alpha OS=Nitrospira sp. OLB3 GN=nxrA_1 PE=4 SV=1 - [A0A136JVT1_9BACT]	0.000E0	0.000E0	7.206E6	0.000E0
A0A0Q3SZH9	Amino acid ABC transporter substrate-binding protein OS=Bosea thiooxidans GN=ARD30_12690 PE=4 SV=1 - [A0A0Q3SZH9_9BRAD]	0.000E0	0.000E0	4.452E6	0.000E0
A0A101VM04	Uncharacterized protein OS=Alphaproteobacteria bacterium BRH_c36 GN=APF80_11355 PE=4 SV=1 - [A0A101VM04_9PROT]	0.000E0	0.000E0	2.641E6	0.000E0
A0A1C2E8X1	ABC transporter substrate-binding protein OS=Mesorhizobium sp. UASWS1009 GN=QV13_04145 PE=4 SV=1 - [A0A1C2E8X1_9RHIZ]	0.000E0	0.000E0	2.602E6	0.000E0
A0A1A6C7A9	Tryptophan--tRNA ligase OS=Acidihalobacter prosperus GN=trpS PE=3 SV=1 - [A0A1A6C7A9_9GAMM]	0.000E0	0.000E0	4.123E6	0.000E0
A0A178MHJ6	Phasin OS=Magnetospirillum marisnigri GN=A6A04_05165 PE=4 SV=1 - [A0A178MHJ6_9PROT]	0.000E0	0.000E0	1.133E6	0.000E0
A0A161SMR1	Flagellin OS=Tardiphaga sp. Vaf07 GN=A4A58_11335 PE=3 SV=1 - [A0A161SMR1_9BRAD]	0.000E0	0.000E0	2.276E6	0.000E0
C5WZZ8	Uncharacterized protein OS=Juncus effusus GN=SORBI_3001G522000 PE=3 SV=1 - [C5WZZ8_SORBI]	0.000E0	0.000E0	3.221E6	0.000E0
C5XY65	Glycosyltransferase OS=Juncus effusus GN=SORBI_3004G224400 PE=3 SV=1 - [C5XY65_SORBI]	0.000E0	0.000E0	0.000E0	0.000E0
A0A1Z5R4Z3	Uncharacterized protein OS=Juncus effusus GN=SORBI_3008G010400 PE=3 SV=1 - [A0A1Z5R4Z3_SORBI]	0.000E0	0.000E0	8.804E6	0.000E0
A0A1Z5S6X9	Alpha-galactosidase OS=Juncus effusus GN=SORBI_3001G208200 PE=3 SV=1 - [A0A1Z5S6X9_SORBI]	0.000E0	0.000E0	6.399E6	0.000E0
A0A194YLW8	4-hydroxy-4-methyl-2-oxoglutarate aldolase OS=Juncus effusus GN=SORBI_3010G277100 PE=3 SV=1 - [A0A194YLW8_SORBI]	0.000E0	0.000E0	1.023E6	0.000E0

Q1NE58	Ribosomal protein S7 (Fragment) OS=Sphingomonas sp. (strain SKA58) GN=SKA58_04230 PE=3 SV=1 - [Q1NE58_SPHSS]	0.000E0	0.000E0	0.000E0	2.844E6
P08660	Lysine-sensitive aspartokinase 3 OS=Escherichia coli (strain K12) GN=lysC PE=1 SV=2 - [AK3_ECOLI]	0.000E0	0.000E0	0.000E0	0.000E0
N4W783	Phosphatase YhfR OS=Gracilibacillus halophilus YIM-C55.5 GN=J416_12849 PE=3 SV=1 - [N4W783_9BACI]	0.000E0	0.000E0	0.000E0	0.000E0
A0A0D6WW23	Peptidyl-prolyl cis-trans isomerase OS=Streptomyces sp. MBRL 601 GN=SF12_05580 PE=3 SV=1 - [A0A0D6WW23_9ACTN]	0.000E0	0.000E0	0.000E0	2.349E7
E8T720	Extracellular solute-binding protein family 5 OS=Mesorhizobium ciceri biovar biserrulae (strain HAMBI 2942 / LMG 23838 / WSM1271) GN=Mesci_0121 PE=4 SV=1 - [E8T720_MESCW]	0.000E0	0.000E0	0.000E0	5.936E6
X6DAZ4	2-dehydro-3-deoxyphosphooctonate aldolase OS=Mesorhizobium sp. LNHC252B00 GN=kdsA PE=3 SV=1 - [X6DAZ4_9RHIZ]	0.000E0	0.000E0	0.000E0	4.666E6
G6Y2C9	Homospermidine synthase OS=Mesorhizobium amorphae CCNWGS0123 GN=MEA186_00335 PE=4 SV=1 - [G6Y2C9_9RHIZ]	0.000E0	0.000E0	0.000E0	4.959E6
W9BYR1	Flagellin OS=Blastomonas sp. CACIA14H2 GN=Q27BB25_08260 PE=3 SV=1 - [W9BYR1_9SPHN]	0.000E0	0.000E0	0.000E0	7.140E5
A9DS80	Putrescine-binding periplasmic protein OS=Oceanibulbus indolifex HEL-45 GN=OIHEL45_02350 PE=3 SV=1 - [A9DS80_9RHOB]	0.000E0	0.000E0	0.000E0	2.956E6
E8TM73	Phasin OS=Mesorhizobium ciceri biovar biserrulae (strain HAMBI 2942 / LMG 23838 / WSM1271) GN=Mesci_2426 PE=4 SV=1 - [E8TM73_MESCW]	0.000E0	0.000E0	0.000E0	1.296E7
A0A021X1K2	Uncharacterized protein OS=Shinella sp. DD12 GN=SHLA_42c000530 PE=4 SV=1 - [A0A021X1K2_9RHIZ]	0.000E0	0.000E0	0.000E0	1.402E7
A0A090FK79	Putative peptidase TldD OS=Mesorhizobium sp. SOD10 GN=tldD PE=4 SV=1 - [A0A090FK79_9RHIZ]	0.000E0	0.000E0	0.000E0	1.061E6
E8TDS0	Tetratricopeptide TPR_1 repeat-containing protein OS=Mesorhizobium ciceri biovar biserrulae (strain HAMBI 2942 / LMG 23838 / WSM1271) GN=Mesci_1809 PE=4 SV=1 - [E8TDS0_MESCW]	0.000E0	0.000E0	0.000E0	5.558E5
L0G2Q9	Uncharacterized protein OS=Echinicola vietnamensis (strain DSM 17526 / LMG 23754 / KMM 6221) GN=Echvi_3048 PE=4 SV=1 - [L0G2Q9_ECHVK]	0.000E0	0.000E0	0.000E0	0.000E0
D4Z3W6	Uncharacterized protein OS=Sphingobium japonicum (strain NBRC 101211 / UT26S) GN=SJA_C1-24640 PE=4 SV=1 - [D4Z3W6_SPHJU]	0.000E0	0.000E0	0.000E0	2.256E6

A0A0Q4B945	Elongation factor Tu (Fragment) OS=Candidatus Bacteroides periocalifornicus GN=tuf PE=4 SV=1 - [A0A0Q4B945_9BACE]	0.000E0	0.000E0	0.000E0	4.571E6
A0A0Q8AN16	Histidine phosphotransferase OS=Mesorhizobium sp. Root157 GN=ASD64_06165 PE=4 SV=1 - [A0A0Q8AN16_9RHIZ]	0.000E0	0.000E0	0.000E0	1.622E6
A0A0Q8BF73	Carbon monoxide dehydrogenase OS=Mesorhizobium sp. Root157 GN=ASD64_15940 PE=4 SV=1 - [A0A0Q8BF73_9RHIZ]	0.000E0	0.000E0	0.000E0	0.000E0
A0A0J7HPG8	Serine protein kinase PrkA OS=Chitinispirillum alkaliphilum GN=CHISP_2834 PE=4 SV=1 - [A0A0J7HPG8_9BACT]	0.000E0	0.000E0	0.000E0	0.000E0
A1E9Q9	Photosystem II D2 protein OS=Juncus effusus GN=psbD PE=3 SV=1 - [PSBD_SORBI]	0.000E0	0.000E0	0.000E0	5.107E6
A1E9Q4	Photosystem II protein D1 OS=Juncus effusus GN=psbA PE=3 SV=1 - [PSBA_SORBI]	0.000E0	0.000E0	0.000E0	1.878E6
C5XR87	Uncharacterized protein OS=Juncus effusus GN=SORBI_3003G370000 PE=4 SV=1 - [C5XR87_SORBI]	0.000E0	0.000E0	0.000E0	7.579E6
C6JS29	Uncharacterized protein OS=Juncus effusus GN=Sb0019s004410 PE=4 SV=1 - [C6JS29_SORBI]	0.000E0	0.000E0	0.000E0	1.196E6
C5Z8A4	Uncharacterized protein OS=Juncus effusus GN=SORBI_3010G236200 PE=4 SV=1 - [C5Z8A4_SORBI]	0.000E0	0.000E0	0.000E0	0.000E0
C5Z0N4	Dihydrolipoyl dehydrogenase OS=Juncus effusus GN=SORBI_3009G054600 PE=3 SV=1 - [C5Z0N4_SORBI]	0.000E0	0.000E0	0.000E0	2.584E6
C5YZV7	Uncharacterized protein OS=Juncus effusus GN=SORBI_3009G176900 PE=4 SV=1 - [C5YZV7_SORBI]	0.000E0	0.000E0	0.000E0	0.000E0
C5XX72	Uncharacterized protein OS=Juncus effusus GN=SORBI_3004G207400 PE=3 SV=1 - [C5XX72_SORBI]	0.000E0	0.000E0	0.000E0	1.113E6
C5YW21	Malate dehydrogenase OS=Juncus effusus GN=SORBI_3009G240700 PE=3 SV=1 - [C5YW21_SORBI]	0.000E0	0.000E0	0.000E0	2.650E6
C5Y7U2	Chlorophyll a-b binding protein, chloroplastic OS=Juncus effusus GN=SORBI_3005G087000 PE=3 SV=1 - [C5Y7U2_SORBI]	0.000E0	0.000E0	0.000E0	2.429E6
C5YLK6	Uncharacterized protein OS=Juncus effusus GN=SORBI_3007G140700 PE=3 SV=1 - [C5YLK6_SORBI]	0.000E0	0.000E0	0.000E0	3.267E6
A0A1W0VUV9	Peptidyl-prolyl cis-trans isomerase OS=Juncus effusus GN=SORBI_3010G258000 PE=3 SV=1 - [A0A1W0VUV9_SORBI]	0.000E0	0.000E0	0.000E0	1.330E7

A0A1W0VYB5	Chlorophyll a-b binding protein, chloroplastic OS=Juncus effusus GN=SORBI_3003G209800 PE=3 SV=1 - [A0A1W0VYB5_SORBI]	0.000E0	0.000E0	0.000E0	2.044E6
A0A1B6PRF2	Uncharacterized protein OS=Juncus effusus GN=SORBI_3005G103500 PE=4 SV=1 - [A0A1B6PRF2_SORBI]	0.000E0	0.000E0	0.000E0	1.401E7
A0A1Z5R5X6	Uncharacterized protein OS=Juncus effusus GN=SORBI_3008G063500 PE=4 SV=1 - [A0A1Z5R5X6_SORBI]	0.000E0	0.000E0	0.000E0	1.153E7
P50002	ATP synthase subunit beta, sodium ion specific OS=Acetobacterium woodii (strain ATCC 29683 / DSM 1030 / JCM 2381 / KCTC 1655 / WB1) GN=atpD PE=1 SV=3 - [ATPB_ACEWD]	7.769E6	2.707E6	6.014E6	1.444E7
A0A085H8H4	Lpp family major outer membrane lipoprotein (Fragment) OS=Kluyvera ascorbata ATCC 33433 GN=lpp PE=4 SV=1 - [A0A085H8H4_9ENTR]	1.251E7	2.470E7	2.798E7	2.473E7
A0A1B6QNF2	Uncharacterized protein OS=Juncus effusus GN=SORBI_3001G383000 PE=4 SV=1 - [A0A1B6QNF2_SORBI]	3.167E7	4.151E7	0.000E0	3.732E7
C5WTL6	Histone H4 OS=Juncus effusus GN=SORBI_3001G313200 PE=3 SV=1 - [C5WTL6_SORBI]	3.114E7	1.225E7	1.502E7	1.539E7
T0ICN3	Uncharacterized protein (Fragment) OS=Sphingobium quisquiliarum P25 GN=L288_09620 PE=3 SV=1 - [T0ICN3_9SPHN]	1.549E7	1.494E7	0.000E0	1.520E7
A0A175RNG4	S-adenosyl-L-homocysteine hydrolase (Fragment) OS=Aureimonas ureilytica GN=NS365_14925 PE=4 SV=1 - [A0A175RNG4_9RHIZ]	7.615E6	2.330E7	2.141E7	2.773E7
C5XT06	Peptidyl-prolyl cis-trans isomerase OS=Juncus effusus GN=SORBI_3004G018400 PE=3 SV=1 - [C5XT06_SORBI]	2.452E7	2.713E7	0.000E0	2.504E7
A0A1B6Q2X9	Tubulin beta chain OS=Juncus effusus GN=SORBI_3003G135400 PE=3 SV=1 - [A0A1B6Q2X9_SORBI]	1.315E7	2.647E6	0.000E0	0.000E0
I5C7U7	Xanthine dehydrogenase, molybdenum binding subunit apoprotein OS=Nitratireductor aquibiodomus RA22 GN=A33O_00930 PE=4 SV=1 - [I5C7U7_9RHIZ]	0.000E0	1.397E6	4.292E6	3.179E6
E8TMH7	Alanine dehydrogenase OS=Mesorhizobium ciceri biovar biserrulae (strain HAMBI 2942 / LMG 23838 / WSM1271) GN=Mesci_3679 PE=3 SV=1 - [E8TMH7_MESCW]	0.000E0	1.590E7	1.468E7	1.353E7
A0A1C2EBS2	Peptide ABC transporter substrate-binding protein OS=Mesorhizobium sp. UASWS1009 GN=QV13_01920 PE=4 SV=1 - [A0A1C2EBS2_9RHIZ]	0.000E0	6.876E6	9.289E6	7.062E6
D4AHW5	Haloalkane dehalogenase OS=Sphingomonas sp. MM-1 GN=linB PE=3 SV=1 - [D4AHW5_9SPHN]	7.228E6	8.167E6	0.000E0	1.322E7

A0A124GFC6	Glyceraldehyde-3-phosphate dehydrogenase OS=Rhizobium loti GN=gapA PE=3 SV=1 - [A0A124GFC6_RHILI]	1.031E7	1.592E7	0.000E0	8.648E6
C5WYF2	Malate dehydrogenase OS=Juncus effusus GN=SORBI_3001G219300 PE=3 SV=1 - [C5WYF2_SORBI]	1.009E7	0.000E0	0.000E0	1.186E7
A0A1B6Q4Z8	GTP-binding nuclear protein OS=Juncus effusus GN=SORBI_3003G238000 PE=3 SV=1 - [A0A1B6Q4Z8_SORBI]	2.848E7	1.251E7	0.000E0	5.606E6
A0A0Q6SQH 2	Uncharacterized protein OS=Rhizobium sp. Root1212 GN=ASC86_08470 PE=4 SV=1 - [A0A0Q6SQH2_9RHIZ]	0.000E0	7.607E6	1.369E7	6.621E6
Q98FL6	Phosphate-specific transport system accessory protein PhoU OS=Rhizobium loti (strain MAFF303099) GN=mll3718 PE=3 SV=1 - [Q98FL6_RHILO]	0.000E0	0.000E0	7.190E6	6.659E6
C5XS48	Uncharacterized protein OS=Juncus effusus GN=SORBI_3004G301700 PE=4 SV=1 - [C5XS48_SORBI]	8.399E6	0.000E0	0.000E0	0.000E0
A0A1B6PCG3	Uncharacterized protein OS=Juncus effusus GN=SORBI_3008G081900 PE=3 SV=1 - [A0A1B6PCG3_SORBI]	4.117E6	3.921E6	0.000E0	0.000E0
A0A1C7GDR 7	Flagellin OS=Lachnoclostridium sp. YL32 GN=A4V08_30970 PE=3 SV=1 - [A0A1C7GDR7_9FIRM]	0.000E0	3.304E6	0.000E0	0.000E0
W9BRB9	Flagellar motor protein MotB OS=Blastomonas sp. CACIA14H2 GN=Q27BB25_19495 PE=3 SV=1 - [W9BRB9_9SPHN]	0.000E0	0.000E0	3.214E6	0.000E0
Q70EF2	Particulate Methane Monooxygenase subunit B OS=Methylocystis sp. (strain SC2) GN=pmoB PE=4 SV=1 - [Q70EF2_METSZ]	0.000E0	0.000E0	3.340E7	0.000E0
C5Z0B5	Phosphoglycerate kinase OS=Juncus effusus GN=SORBI_3009G183700 PE=3 SV=1 - [C5Z0B5_SORBI]	0.000E0	0.000E0	0.000E0	3.439E6
C5WTC1	Chlorophyll a-b binding protein, chloroplastic OS=Juncus effusus GN=SORBI_3001G177000 PE=3 SV=1 - [C5WTC1_SORBI]	0.000E0	0.000E0	0.000E0	1.596E7
Q981F7	Elongation factor Tu OS=Rhizobium loti (strain MAFF303099) GN=tufA PE=3 SV=1 - [EFTU_RHILO]	1.241E6	9.579E6	2.399E7	1.587E7
A0A194YJY9	Elongation factor 1-alpha OS=Juncus effusus GN=SORBI_3010G182100 PE=3 SV=1 - [A0A194YJY9_SORBI]	1.326E8	6.811E7	2.347E7	7.745E7
A0A194YMM 6	Glyceraldehyde-3-phosphate dehydrogenase OS=Juncus effusus GN=SORBI_3010G262500 PE=3 SV=1 - [A0A194YMM6_SORBI]	2.963E7	1.848E7	1.836E6	2.204E7
A0A1B6PA67	ATP synthase subunit beta OS=Juncus effusus GN=SORBI_3009G224400 PE=3 SV=1 - [A0A1B6PA67_SORBI]	1.200E7	0.000E0	2.185E7	1.360E7

C5XIY6	Uncharacterized protein OS=Juncus effusus GN=SORBI_3003G152600 PE=4 SV=1 - [C5XIY6_SORBI]	2.671E7	1.461E7	0.000E0	0.000E0
A0A1B6QF50	Tubulin alpha chain OS=Juncus effusus GN=SORBI_3002G350400 PE=3 SV=1 - [A0A1B6QF50_SORBI]	4.228E7	2.809E7	0.000E0	0.000E0
C5YJ75	Uncharacterized protein OS=Juncus effusus GN=SORBI_3007G216300 PE=3 SV=1 - [C5YJ75_SORBI]	8.343E6	3.953E6	0.000E0	4.689E6
A0A090GMX8	60 kDa chaperonin OS=Mesorhizobium sp. SOD10 GN=groL PE=3 SV=1 - [A0A090GMX8_9RHIZ]	0.000E0	2.142E7	2.936E7	2.291E6
A0A117N509	ABC transporter substrate-binding protein OS=Rhizobium loti GN=AU467_10850 PE=4 SV=1 - [A0A117N509_RHILI]	4.252E5	1.522E6	0.000E0	2.774E6
C5WXV4	Uncharacterized protein OS=Juncus effusus GN=SORBI_3001G501300 PE=4 SV=1 - [C5WXV4_SORBI]	9.373E6	5.279E6	0.000E0	0.000E0
A0A1B6PT78	Uncharacterized protein OS=Juncus effusus GN=SORBI_3005G175100 PE=4 SV=1 - [A0A1B6PT78_SORBI]	3.633E6	0.000E0	0.000E0	0.000E0
Q98FL2	Phosphate-binding protein PstS OS=Rhizobium loti (strain MAFF303099) GN=pstS PE=3 SV=1 - [PSTS_RHILO]	2.959E7	7.211E7	6.954E7	7.192E7
A0A090FQN2	Phosphonate ABC transporter, periplasmic phosphonate binding protein OS=Mesorhizobium sp. SOD10 GN=MPLSOD_60051 PE=4 SV=1 - [A0A090FQN2_9RHIZ]	5.259E6	1.320E7	1.404E7	1.532E7
A0A1C2EA77	Flagellin OS=Mesorhizobium sp. UASWS1009 GN=QV13_03310 PE=3 SV=1 - [A0A1C2EA77_9RHIZ]	2.651E6	1.211E7	2.278E7	1.741E7
C5XFH6	Fructose-bisphosphate aldolase OS=Juncus effusus GN=SORBI_3003G393900 PE=3 SV=1 - [C5XFH6_SORBI]	1.391E7	1.603E6	0.000E0	8.164E6
C5XPN2	Uncharacterized protein OS=Juncus effusus GN=SORBI_3003G350700 PE=3 SV=1 - [C5XPN2_SORBI]	9.453E6	8.881E6	0.000E0	0.000E0
A0A1W0W7G1	Uncharacterized protein OS=Juncus effusus GN=SORBI_3002G379500 PE=3 SV=1 - [A0A1W0W7G1_SORBI]	1.187E7	4.884E7	0.000E0	2.350E7
A0A1B6PBJ7	Uncharacterized protein OS=Juncus effusus GN=SORBI_3008G047000 PE=3 SV=1 - [A0A1B6PBJ7_SORBI]	8.897E7	1.237E7	2.599E7	6.768E6
A1E9T2	Ribulose bisphosphate carboxylase large chain OS=Juncus effusus GN=rbcL PE=3 SV=1 - [RBL_SORBI]	0.000E0	1.498E7	0.000E0	6.825E7

ERKLÄRUNG

Die vorliegende Dissertation wurde im Department Umweltbiotechnologie vom UFZ – Helmholtz-Zentrum für Umweltforschung in Zusammenarbeit mit dem Lehr- und Forschungsgebiet für Instituts für Umweltforschung (Biologie V) der RWTH Aachen University unter Betreuung von Herrn Prof. Dr. Rolf Altenburger und Herrn Prof. Dr. Henner Hollert angefertigt.

Hiermit versichere ich, dass ich die vorliegende Doktorarbeit selbstständig verfasst und keine anderen als die angegebenen Hilfsmittel verwendet habe. Alle Textauszuge und Grafiken, die sinngemäß oder wörtliche aus veröffentlichten Schriften entnommen wurden, sind durch Referenzen gekennzeichnet.

Muhammad Arslan   Aachen, den 05.07.2019

ACKNOWLEDGEMENTS

Arizona, USA) who guided me regularly to RNA-Seq analyses via online discussions and chatting.

I am enormously thankful to Dr. Muhammad Afzal (NIBGE, Pakistan) for his unconditional support throughout my academic career. He is the person among those first people who trusted upon my scientific skills. In this doctoral journey, he allowed me to work on several of his projects. He trusted me selflessly and whenever I went for help or advice, he provided it beyond my expectations. I am also thankful to the team "Soil and Environmental Biotechnology Division" for always showing eagerness to collaborate with me.

I am grateful to all my friends and colleagues especially Naeem Shahid, Arslan Kamal Hashmi, and Muhammad Nassir for sharing many cheerful memories, weekend sittings and little celebrations. Additionally, I acknowledge the moral support I always received from Dr. Saddam A. Abbasi, Dr. Muhammad Riaz, Rashid Mehmood, Mehtab Gul, Inaam Ullah, Imran Sohail, Muhammad Waqas, and Jamrod Khan during my doctoral work.

I am also greatly thankful to my parents, Mr. and Mrs. Muhammad Amin, my wife Hamna Saleem, and my son Aez M. Arslan (former name A'ez Amin Muhammad). They have been the ultimate source of inspiration and strength in my journey of life. They have always assured me of the trust I need to nourish and develop independent thinking. In my whole life, the role of my father is more than I can ever admire. Prophet Muhammad (ﷺ) said "There is no more virtuous gift a father can give to his children than good manners and education", and I have no doubt that my father is an embodiment of this noble saying. In the end, I believe that if there is anything good in me, I owe it to adopting the ways and manners of the holy prophet Muhammad (ﷺ). With all my belief, I am indebted to his message of equality, tolerance, and harmony that has been the essence of and been echoed ever since its inception, in every human rights charter. From the early days of my life till today, his teachings and core of philosophy is the only source for me to reach the creator of this universe, Allah Almighty. I cannot complete anything without appreciating what He has given me. I am thankful that I have received every blessing in plenty.

CURRICULUM VITAE

Name: Muhammad Arslan
Date of Birth: 11.05.1989
Place of Birth: Kasur, Pakistan

Education

2016 – 2019	**Dr. rer. nat.** **RWTH Aachen University, Aachen, Germany (External doctoral student)** Institute for Environmental Research Environmental Biotechnology Department, Helmholtz Center for Environmental Research – UFZ, Leipzig, Germany Thesis: "Antimicrobials in constructed wetlands can cause *in planta* dysbiosis".
2013 – 2015	**M.Sc. in Environmental Sciences - CGPA: 3.78 / 4.00** **Earth Sciences Department** King Fahd University of Petroleum & Minerals Thesis: "Benthic foraminifera in the Arabian Gulf: Effects of seasonal dynamics, environmental parameters, and marine pollution on their distribution and behaviors".
2011 – 2013	**M.Phil. in Environmental Biotechnology - CGPA: 3.84 / 4.00** **National Institute for Biotechnology and Genetic Engineering (NIBGE)** Pakistan Institute of Engineering and Applied Sciences (PIEAS), Pakistan Thesis: "Plant-Bacteria Partnership for Remediation of Petroleum Hydrocarbons".
2007 – 2011	**B.Sc. in Environmental Sciences CGPA: 3.66 / 4.00** **University of the Punjab** College of Earth and Environmental Sciences.

Work Experience

Currently	**External PhD student** **Helmholtz Center for Environmental Research, Leipzig, Germany** Environmental Biotechnology Department Working at UFZ while being enrolled as an external doctoral student at RWTH University
2013 – 2014	**Lecturer / Laboratory Instructor (Part-Time)** **King Fahd University of Petroleum and Minerals, Dhahran, Saudi Arabia** Biology Department Teaching undergraduate level biology courses – Biology for Engineers

2013 – 2015	**Environmental Officer (Part-Time)**
	King Fahd University of Petroleum and Minerals, Dhahran, Saudi Arabia
	Environmental Health and Safety Department
	Environmental awareness, environmental monitoring, and web maintenance

Publications

* affiliation with RWTH Aachen University

1. ***Arslan, M.,** Devisetty, U. K., Porsch, M., Große, I., Müller, J. A., & Michalski, S. G. (2019). RNA-Seq analysis of soft rush (*Juncus effusus*): transcriptome sequencing, de novo assembly, annotation, and polymorphism identification. BMC genomics, 20(1), 489.

2. ***Arslan, M.,*** Ullah, I., Shahid, N., Müller, J.A, Afzal, M. (2017). Organic micropollutants in the environment: ecotoxicity potential and methods for remediation, In: Anjum, N.A., Ahmad, I., Pereira, M.E., Duarte, A.C., Umar, S., Khan, N.A. (eds), "Enhancing Remediation of Environmental Pollutants - Biological and Non-Biological Approaches", *Springer Science+Business Media*.

3. ***Afzal, M., Arslan, M.,** Müller, J. A., Shabir, G., Islam, E., Tahseen, R., Anwar-ul-Haq, M., Hashmat, A., Iqbal, S., Khan, Q. Floating treatment wetlands as a suitable option for large-scale wastewater treatment. Nature Sustainability (accepted).

4. ***Tara, N., Arslan, M.,** Hussain, Z., Iqbal, M., Khan, Q. M., & Afzal, M. (2019). On-site performance of floating treatment wetland macrocosms augmented with dye-degrading bacteria for the remediation of textile industry wastewater. Journal of Cleaner Production, 217, 541-548.

5. ***Rehman, R., Ijaz, A., Arslan, M.,** Afzal, M., (2019). Floating treatment wetlands as biological buoyant filters for wastewater reclamation, International Journal of Phytoremediation, DOI: 10.1080/15226514.2019.1633253

6. Shahid, M. J., **Arslan, M.,** Siddique, M., Ali, S., Tahseen, R., & Afzal, M. (2019). Potentialities of floating wetlands for the treatment of polluted water of river Ravi, Pakistan. Ecological Engineering, 133, 167-176.

7. Hussain, Z., **Arslan, M.,** Shabir, G., Malik, M. H., Mohsin, M., Iqbal, S., & Afzal, M. (2019). Remediation of textile bleaching effluent by bacterial augmented horizontal flow and vertical flow constructed wetlands: A comparison at pilot scale. The Science of the total environment, 685, 370-379.

8. Nguyen, P. M., Afzal, M., Ullah, I., Shahid, N., Baqar, M., & **Arslan, M.** (2019). Removal of pharmaceuticals and personal care products using constructed wetlands: effective plant-bacteria synergism may enhance degradation efficiency. Environmental Science and Pollution Research, 1-18.

9. Tahseen, R., **Arslan, M.,** Iqbal, S., Khalid, Z.M. and Afzal, M., (2019). Enhanced degradation of hydrocarbons by gamma ray induced mutant strain of *Pseudomonas putida*. *Biotechnology Letters*, pp.1-9.

10. Ashraf, U., Chaudhry, M.N., Ahmad, S.R., Ashraf, I., **Arslan, M.,** Noor, H. and Jabbar, M., (2018). Impacts of climate change on *Capparis spinosa* L. based on ecological niche modeling. *PeerJ*, 6, p.e5792.

11. Hussain, Z., **Arslan, M.,*** Malik, M.H., Mohsin, M., Iqbal, S., Afzal, M., (2018). "Treatment of the textile industry effluent in a pilot-scale vertical flow constructed wetland system augmented with bacterial endophytes", *Science of The Total Environment*.

12. Hussain, Z., **Arslan, M.,*** Malik, M.H., Mohsin, M., Iqbal, S., Afzal, M., (2018). "Integrated perspectives on the use of bacterial endophytes in horizontal flow constructed wetlands for the

treatment of liquid textile effluent: Phytoremediation advances in the field", *Journal of Environmental Management*

13. Shahid, M.J., **Arslan, M.,** Ali, S., Siddique, M. and Afzal, M., (2018). Floating Wetlands: A Sustainable Tool for Wastewater Treatment. *CLEAN–Soil, Air, Water*, 46(10), p.1800120.

14. Khalil, A., Sivakumar, N., **Arslan, M**, Slaeem, H., Qarawi, S., (2018). Insights into *Brevibacillus borstelensis* AK1 through whole genome sequencing: a thermophilic bacterium isolated from a hot spring in Saudi Arabia. *Biomed Research International:* DOI: 10.1155/2018/5862437

15. Saleem, H., Rehman, K., **Arslan, M.,*** Afzal, M., (2018). Enhanced degradation of phenol in floating treatment wetlands by plant-bacterial synergism. *International Journal of Phytoremediation*.

16. Saleem, H., **Arslan, M.,*** Rehman, K., Tehseen, R., Afzal, M., (2018). *Phragmites australis* — a helophytic grass — can establish successful partnership with phenol-degrading bacteria in a floating treatment wetland. *Saudi Journal of Biological Sciences*.

17. **Arslan, M.**, Afzal, M.,* Khan, Q.M., (2017). Plant-bacteria partnerships for the remediation of persistent organic pollutants. *Environmental Science and Pollution Research*, 24(5), p. 4322–4336.

18. **Arslan**, **M***, Kaminski, M.A., Khalil, A.B., Ilyas, M., Tawabini, B.T. (2017). Benthic foraminifera in eastern Bahrain: relationship to local pollution sources. *Polish Journal of Environmental Studies*

19. **Arslan, M.,*** Kaminski, M.A., Tawabini, B.S., Ilyas, M., Frontalini, F. (2016) Benthic foraminifera in sandy (siliciclastic) coastal sediments of the Arabian Gulf (Saudi Arabia): a technical report. *Arabian Journal of Geosciences*; DOI:10.1007/s12517-016-2436-4

20. **Arslan**, **M***, Kaminski, M.A., Tawabini, B.A., Ilyas, M., Babalola, L., Frontalini, F. (2016). "Seasonal variations, environmental parameters, and standing crop assessment of benthic foraminifera in western Bahrain, Arabian Gulf". *Geological Quarterly*

21. Baqar, M., **Arslan, M.,*** Sadef, Y., Mahmood, A., Qadir, A., Rashid, S., (2017). Persistent organic pollutants: potential threat to ecological integrities in term of geno-toxicity and oxidative stress. *Human and Ecological Risk Assessment: An International Journal*

22. Khalil, A., Sivakumar, N., **Arslan**, **M***, Qarawi, S., (2017). Novel *Anoxybacillus flavithermus* AK1: A Thermophile Isolated from a Hot Spring in Saudi Arabia. *Arabian Journal for Science and Engineering*;

23. Sanaullah, M*., Ahmad, I., **Arslan**, **M**, Ahmad, S.R., Zeeshan, M. (2017). Evaluation of morphometric parameters of Haro river drainage basin in northern Pakistan. *Polish Journal of Environmental Studies*

24. Jamil, N., Baqar, M., Ilyas, S., Qadir, A., **Arslan, M.,** Salman, M., Ahsan, N., Zahid, H., (2016) "Use of mercury in dental silver amalgam: an occupational and environmental assessment," *BioMed Research International*, vol. 2016, Article ID 6126385,. doi:10.1155/2016/6126385

25. Shabir, G., **Arslan, M.,** Amin. I., Fatima, K., Khan, Q.M., Afzal, M.* (2016) Effects of inoculum density on plant growth and hydrocarbon degradation. *Pedosphere*, 26(5), p. 774-778

26. Tabassum, S., Shahid, N., Shafiq, M., Mumtaz, M., **Arslan, M.,** (2016). An oxidative stress response of *Mirabilis jalapa* to exhausted engine oil (EEO) during phytoremediation. *Polish Journal of Environmental Studies*, 25(6), p. 2581-2587.

27. Khan, M. U., Sessitsch, A., Haris, M., **Arslan, M**., Imran, A., Shabir, G., Khan, Q. M., Afzal, M.*, (2014). Cr-resistant rhizo- and endophytic bacteria associated with *Prosopis juliflora* and their potential as phytoremediation enhancing agents in metal-degraded soils. *Frontiers in Plant Science*.

28. **Arslan, M.,** Kaminski, M.A., Tawabini, B.S., Ilyas, M., Babalola, L.O. and Frontalini, F., (2015). Seasonal variations, environmental parameters, and standing crop assessment of benthic foraminifera in eastern Bahrain, Arabian Gulf. *Geological Quarterly*, 60(1), pp.26-37.

29. **Arslan, M.,*** Afzal, M., Amin. I., Iqbal, S., Khan, Q.M., (2014). Nutrients can enhance the abundance and expression of alkane hydroxylase *CYP153* gene in the rhizosphere of ryegrass planted in diesel-contaminated soil. *PLoS ONE,* 9(10) DOI: 10.1371/journal.pone.0111208,

30. Ullah, I., Asif, M., **Arslan, M.,** Ashfaq, M., (2014). Temporal expression of Cry1Ab/c protein in Bt-Cotton varieties, their efficacy against *Helicoverpa armigera* (Lepidoptera: Noctuidae) and population dynamics of sucking arthropods on them, *International Journal of Agriculture and Biology.* 16(5), 879-885. DOI: 13–1001/2014/16–5–879–885

Conference Presentations

1. Arslan M., Santoni M., Wiessner, A., Neu, T., Piper, D., Müller J.A., (2019). "Decline of fitness of *Juncus effesus* during low dose exposures with antimicrobials coincides with major changes of the endophytic bacterial community", WETPOL-2019: Aarhaus, (Denmark).

2. Arslan M., Santoni M., Wiessner, A., Neu, T., Piper, D., Müller J.A., (2018). "Repeated exposures of low-dose antimicrobials can cause dysbiosis in plant-endophyte interplay", ISME-17: Leipzig, (Germany).

3. Arslan M., Santoni M., Wiessner, A., Neu, T., Piper, D., Müller J.A., (2017). "Dysbiosis in plant-endophyte partnership: repeated short exposures of sulfamethoxazole and trimethoprim at micro-concentrations can disturb the microbial community in soft rush, Juncus effusus", EcotoxicoMic 2017: First International Conference on Microbial Ecotoxicology 21-24 Nov 2017 Lyon (France).

4. Arslan M., Santoni M., Wiessner, A., Neu, T., Müller J.A., (2017). "Effect of antibiotics in the environment: disturbances of plant-bacterial endophyte interactions in soft rush, Juncus effusus, after repeated exposure to sulfamethoxazole and trimethoprim", Microbiology and Infection 2017 – 5th Joint Conference of the VAAM & DGHM 2017 in Würzburg, Germany, March 6th, 2017.

Professional Trainings

Workshops/courses offered by Helmholtz Interdisciplinary GRADuate School for Environmental Research (HIGRADE), Helmholtz Centre for Environmental Research (UFZ), Leipzig, Germany

- Metagenomics with the Galaxy Server
- Genome Assembly with the Galaxy Server
- Introduction to the Galaxy Server" / "Transcriptomics with the Galaxy Server
- Laser Scanning Microscopy
- Meta-analysis in Biological and Environmental Sciences
- Modern Methods and Applications for Isotope Analysis of Light Elements
- Introduction to ProVIS
- Introduction to Systems Biology: From OMICS data analysis to metabolic network modeling
- Introduction to Statistics for Ecologists and Environmental Scientists
- Introduction to Environmental Toxicology and Chemistry
- Introduction to R for Ecologists and Environmental Scientists
- Introduction to Handling Spatial Data with R
- Biotechnology of Conversion: Fundamentals of (Bio)Electrochemistry

- Biodiversity and Niche Theory
- Introduction to Solution-oriented Environmental Research
- Understanding Chemical Partition Equilibria
- Which regulation do we need for bioaccumulation and toxicity assessment?
- Good Scientific Practice
- Proposal Writing
- Editors Workshop
- "UBA" Excursion - Federal Environment Agency
- Business Model You - Replace Career Uncertainty with Career Confidence

DZIF bioinformatics workshop: 16S Community Profiling with QIIME 2.
Dec. 19, 2017 - Dec. 22, 2017. BRICS, Braunschweig, Germany

Fluorescence Microscopy" - FluoMicro@ICGEB – International Centre for Genetic Engineering and Biotechnology – ICGEB, in collaboration with Nikon.
2 - 4 May 2016

Theoretical and Practical Course on "Bioinformatics: Computer Methods in Molecular and Systems Biology – International Centre for Genetic Engineering and Biotechnology (ICGEB), Trieste, Italy**.** 23 - 28 June 2014.

Experimental Skills

Biotechnology: 16S amplicon sequencing, Confocal Laser Scanning Electron Microscopy (CLSM), Fluorescent *in situ* hybridization (FISH), Polymerase Chain Reaction (PCR), Quantitative PCR (qPCR), DNA/RNA Extraction, Restriction Fragment Length Polymorphism (RFPL), Bacterial Isolation and Cultivation, Culture Dependent Characterization, Ion Chromatography, Sediment Substrate Analysis.

Bioinformatics: NGS Data Analysis, Genome Annotation (Plants), Transcriptome Annotation, Functional Genomics, Sequence Phylogeny, Genome and Proteome Databases Analyses, WWW-based services, Functional Genomics, and *in silico* cloning, and Meta-analysis.
Tools in bioinformatics: R-language, QIIME, WQ-Maker, Phyloseq, Annocript and Dammit pipeline for transcriptome annotation, Functional Annotation of Prokaryotic Taxa (FAPROTAX), Parallel-Meta3, TotalLab Quant, Gene Designer by DNA2.0, GIS)